Technical Report Documentation Page

1. Report No.	2. Government Accession No.	3. Recipient's Catalog No.
FHWA/TX-03/4126–1		

4. Title and Subtitle	5. Report Date
USING INFRARED IMAGING AND GROUND-PENETRATING RADAR TO DETECT SEGREGATION IN HOT-MIX OVERLAYS	May 2002 Resubmitted: September 2002
	6. Performing Organization Code

7. Author(s)	8. Performing Organization Report No.
Stephen Sebesta and Tom Scullion	Report 4126-1

9. Performing Organization Name and Address	10. Work Unit No. (TRAIS)
Texas Transportation Institute The Texas A&M University System College Station, Texas 77843-3135	11. Contract or Grant No. Project No. 0-4126

12. Sponsoring Agency Name and Address	13. Type of Report and Period Covered
Texas Department of Transportation Research and Technology Implementation Office P. O. Box 5080 Austin, Texas 78763-5080	Research: September 2000–April 2002
	14. Sponsoring Agency Code

15. Supplementary Notes

Research performed in cooperation with the Texas Department of Transportation and the U.S. Department of Transportation.

Research Project Title: Development of Infrared Photography and GPR Procedures for Identifying Mixture Segregation

16. Abstract

Segregation of any type is a serious problem in hot-mix asphalt and typically leads to poor performance, poor durability, shorter life, and higher maintenance costs. This project focused on using both infrared (IR) imaging and ground-penetrating radar (GPR) to evaluate the uniformity of newly placed hot-mix overlays. Both techniques provide a distinct advantage over existing nuclear techniques in that they provide 100 percent coverage of the new surface. In this project IR and GPR measurements were made in test sections on four newly placed asphalt overlays. Cores were taken where anomalies were detected in the mat. These cores were returned to the laboratory to identify changes in both the volumetric and engineering properties.

Analysis showed that significant changes in both IR and GPR values are related to changes in hot-mix properties, primarily air void content. Based upon current Texas Department of Transportation (TxDOT) specifications significant changes in the hot-mix asphalt are expected if temperature changes of greater than 25 °F are measured in the field. If the surface dielectric changes by more than 0.8 for coarse-graded mixes and 0.4 for dense-graded materials, significant changes in mix properties are expected. The approach used in Finland to use a calibration core to convert GPR surface dielectric to mat air void contents worked well.

TxDOT should consider future implementation of these technologies. Neither of the devices used in this project was thought optimal for full implementation. The research team has provided schematics and recommendations for future implementation efforts.

17. Key Words	18. Distribution Statement
Segregation, Infrared, Ground-Penetrating Radar, Paving, Quality Control, Quality Assurance	No restrictions. This document is available to the public through NTIS: National Technical Information Service 5285 Port Royal Road Springfield, Virginia 22161

19. Security Classif.(of this report)	20. Security Classif.(of this page)	21. No. of Pages	22. Price
Unclassified	Unclassified	176	

USING INFRARED IMAGING AND GROUND-PENETRATING RADAR TO DETECT SEGREGATION IN HOT-MIX OVERLAYS

by

Stephen Sebesta
Assistant Transportation Researcher
Texas Transportation Institute

and

Tom Scullion
Research Engineer
Texas Transportation Institute

Report 4126-1
Project Number 0-4126
Research Project Title: Development of Infrared Photography and GPR Procedures for Identifying Mixture Segregation

Sponsored by the
Texas Department of Transportation
in cooperation with the
U.S. Department of Transportation

May 2002
Resubmitted: September 2002

TEXAS TRANSPORTATION INSTITUTE
The Texas A&M University System
College Station, Texas 77843-3135

DISCLAIMER

The contents of this report reflect the views of the authors, who are responsible for the facts and the accuracy of the data presented herein. The contents do not necessarily reflect the official view or policies of the Texas Department of Transportation (TxDOT) or the Federal Highway Administration (FHWA). This report does not constitute a standard, specification, or regulation. The engineer in charge was Tom Scullion, P.E. (Texas, # 62683).

ACKNOWLEDGMENTS

This project was made possible by the Texas Department of Transportation in cooperation with the Federal Highway Administration. Numerous persons have made the accomplishment of this project possible. First, the personnel of the Texas Department of Transportation who have worked to facilitate project needs: Magdy Mikhail P.E., the project director, was instrumental in providing project oversight. The project also would not have been possible without the assistance of district personnel who assisted with coordinating test sections:

- Catherine Hejl, P.E., Bryan District
- Darlene Goehl, P.E, Bryan District
- Zyna Polansky, Bryan District
- P.J. Vargas, Bryan District
- Darla Walton, Bryan District
- Gerald Freytag, P.E., Yoakum District
- James Ivy P.E., Yoakum District
- Tony Yrigoyen, P.E., Houston District

Gary Strahan of Texas Infrared provided technical guidance on the usage of the infrared products, and Rob Raymer of FLIR Systems provided a ThermaCam PM 695 for trial at one of the test sites. Field data collection would not have been possible without the assistance of Lee Gustavus, Pat Harris, and Spencer Guthrie of the Texas Transportation Institute (TTI) coming out and braving the summer heat. Sydney Greer assisted by providing guidance on the laboratory testing of the asphalt cores.

TABLE OF CONTENTS

Page

List of Figures x
List of Tables xiii
Executive Summary 1
Chapter 1 Introduction 3
I. Background 3
II. Objectives 3
III. Work Plan 4
Chapter 2 Literature Review 5
I. Summary 5
II. Kansas Department of Transportation (KDOT) 5
III. Texas Department of Transportation (TxDOT) 7
IV. Connecticut Department of Transportation (CDOT) 8
V. Washington Department of Transportation (WSDOT) 8
VI. National Center for Asphalt Technology (NCAT) 11
VII. Michigan Department of Transportation (MDOT) 14
VIII. Infrared Imaging 15
IX. Ground-Penetrating Radar 18
Chapter 3 Laboratory Verification of Infrared Equipment 23
I. Summary 23
II. Emissivity Determination of Hot Plate Surface 24
III. Laboratory Verification of Infrared Camera Temperatures under Windless Conditions 26
IV. Laboratory Investigation of Wind Effects on Infrared-Determined Temperatures 31
V. Implications for Field Testing 34
Chapter 4 Field Data Collection and Analysis Procedures 37
I. Protocol Development 37
II. Field Testing Protocol for Data Collection 37
Chapter 5 SH 6 Investigation 41

I. Summary 41
II. Paving Parameters and Environmental Conditions 42
III. Infrared Imaging Settings 42
IV. Results from Infrared Imaging 42
V. Results from Ground-Penetrating Radar 45
VI. Results from Cores 48
VII. Relationships between Changes in Temperature and Dielectric and Changes in Mix Parameters 50
VIII. Conclusions 53
Chapter 6 US 79 Investigation 55
I. Summary 55
II. Paving Parameters and Environmental Conditions 56
III. Infrared Imaging Settings 56
IV. Results from Infrared Imaging 56
V. Results from Ground-Penetrating Radar 61
VI. Results from Cores 65
VII. Relationships between Changes in Temperature and Dielectric and Changes in Mix Parameters 66
VIII. Conclusions 69
Chapter 7 IH 10 Investigation 71
I. Summary 71
II. Paving Parameters and Environmental Conditions 71
III. Infrared Imaging Settings 72
IV. Results from Infrared Imaging 72
V. Results from Ground-Penetrating Radar 75
VI. Results from Cores 78
VII. Relationships between Changes in Temperature and Dielectric and Changes in Mix Parameters 82
VIII. Conclusions 85
Chapter 8 US 290 Investigation 87
I. Summary 87

II. Paving Parameters and Environmental Conditions 87
III. Infrared Imaging Settings 88
IV. Results from Infrared Imaging 88
V. Results from Ground-Penetrating Radar 93
VI. Results from Cores 96
VII. Relationships between Changes in Temperature and Dielectric and Changes in Mix Parameters 97
VIII. Conclusions 99
Chapter 9 Conclusions and Recommendations 101
I. Summary 101
II. Recommendation for Calibration Tests and Accuracy of NDT Equipment 104
III. Recommendation on Effectiveness of Infrared Equipment for Detecting Segregation 105
IV. Recommendation on Effectiveness of GPR for Detecting Segregation 106
V. Recommendations on Material Acceptability Limits 107
VI. Recommendations for Use of NDT Devices as QC/QA 107
VII. Recommendation for Implementation 108
References 113
Appendix A SH 6 Correlation Matrices and Regression Equations 115
Appendix B US 79 Correlation Matrices and Regressions 121
Appendix C IH 10 Correlation Matrices and Regressions 127
Appendix D US 290 Correlation Matrices and Regressions 143
Appendix E Ground-Penetrating Radar Specifications 149
Appendix F Pavetracker Evaluation 155

LIST OF FIGURES

Figure **Page**

1. Kansas DOT Segregation Profile Locations 6
2. Example of Washington DOT Infrared Data 9
3. Washington DOT Data of Temperature Differentials vs. Range of Average to Lowest Measured Mat Density 10
4. Example Analysis Sheet for Segregation Detection from MDOT 15
5. Surface Plot of Voids for Airport Survey from Roadscanners Oy 20
6. Relationship between Surface Dielectric from GPR and Lab Density 21
7. Equipment for Lab Verification of Infrared Equipment 23
8. Thermal Image for Emissivity Determination of Aluminum Hot Plate 25
9. Thermal Image for Emissivity Determination of Painted Aluminum Surface 25
10. Thermal Image to Verify Emissivity of Painted Aluminum Surface 26
11. Hot Plate from 90° with Camera Height of 6 Feet 27
12. Hot Plate from 60° with Camera Height of 6 Feet 27
13. Hot Plate from 45° with Camera Height of 6 Feet 28
14. Hot Plate from 30° with Camera Height of 6 Feet 28
15. Hot Plate from 90° with Camera Height of 8 Feet 29
16. Hot Plate from 60° with Camera Height of 8 Feet 29
17. Hot Plate from 45° with Camera Height of 8 Feet 30
18. Hot Plate from 30° with Camera Height of 8 Feet 30
19. Setup and Wind Speed Being Measured for Lab Testing with Wind 31
20. Two Hot Plates with No Wind 32
21. Verification of Temperature Differentials on Second Hot Plate 32
22. Image of Hot Plates with Low Wind Speed 33
23. Image of Hot Plates with Medium Wind Speed 33
24. Image of Hot Plates with High Wind Speed 34
25. Infrared Imaging in Progress 38
26. SH 6 Test Site Starting at RM 602 41
27. Temperature Differentials of 20 °F 319 Feet into SH 6 Test Site 43

28. Temperature Differentials of 20 °F in Centerline at 679 Feet in SH 6 Test Section 43
29. Temperature Differentials of 25 °F at 797 Feet into SH 6 Test Site 44
30. Representative Image of Uniform Pavement Mat on SH 6 44
31. Distribution of Air Voids for SH 6 Test Section 46
32. Surface Plot of Air Voids for SH 6 Test Section 47
33. Gradation Results from SH 6 Test Section 49
34. Number of Sieves with Greater than 3% Change in Percent Retained for SH 6 50
35. US 79 Test Site Location 55
36. Paving Train on US 79 56
37. Cool Centerline at 200 Feet on US 79 with Temperature Drop of 20 °F 57
38. Temperature Drop of 27 °F 220 Feet into US 79 Test Section 58
39. Location of Paver Being Stopped at 360 Feet on US 79 58
40. IR Image at 620 Feet into US 79 Test Section 59
41. Temperatures from 270 °F to 295 °F at 790 Feet on US 79 59
42. Contrast in Mat Temperatures Where Paver Stopped (Aqua Region) and Typical Mat on US 79 60
43. Temperature Drops of 25 °F at 895 Feet on US 79 60
44. Normal Section at 500 Feet into US 79 Test Section 61
45. Air Voids Cumulative Probability Distribution for US 79 62
46. Surface Plot of US 79 Air Voids 64
47. Gradation Results from US 79 Test Section 66
48. Number of Sieves with Greater than 3% Change in Percent Retained vs. Change in Temperature for US 79 68
49. Number of Sieves with Greater than 3% Change in Percent Retained vs. Change in GPR Dielectric for US 79 68
50. Paving Operation on IH 10 WB 72
51. IR Image of Core Locations 1-4 on IH 10 73
52. Temperature Drop of 52 °F on IH 10 73
53. Close-up of Cold Streak Shown in Figure 52 74
54. IR Image of Core Locations 5-10 on IH 10 74
55. IR Image of Core Locations 11 and 12 on IH 10 75

56. Percent Voids vs. GPR Dielectric for IH 10 76
57. Predicted Air Void Distribution for IH 10 Test Section 76
58. Surface Plot of IH 10 Predicted Air Voids 77
59. Locations of Cores 1-4 on IH 10 Test Section 78
60. Locations of Cores 5-10 on IH 10 Test Section 79
61. Locations of Cores 11 and 12 on IH 10 Test Section 79
62. Gradation Graph for IH 10 Cores 1 through 4 81
63. Gradation Graph for IH 10 Cores 5 through 10 81
64. Gradation Graph for IH 10 Cores 11 and 12 82
65. Change in Voids vs. Change in Temp for All IH 10 Data 83
66. Change in Voids vs. Change in Temp for Grouped IH 10 Data 84
67. Recycling Machine on US 290 88
68. Temp Drop of 20 °F at 130 Feet into US 290 Test Section 89
69. Center of Mat 25 °F Hotter at 530 Feet into US 290 Test Section 89
70. Temperature Drops of 40 °F at 850 Feet into US 290 Test Section 90
71. Temperature Drops of 40 °F at 900 Feet into US 290 Test Section 91
72. Temperature Drop of 30 °F at 980 Feet into US 290 Test Section 92
73. Distribution of Air Voids for US 290 Test Section 94
74. Surface Plot of Air Voids for US 290 Test Section 95
75. Gradation Results from US 290 Test Section 97
76. Expected Distributions of Mat Air Voids for Test Locations 103
77. IR Image with Corresponding Void Predictions 104
78. Example GPR Data Showing Significant Drop in Dielectric 106
79. Example Surface Plot of Air Voids from GPR Data 107
80. Concept Infrared Sensor Bar for Quality Control 110
81. Schematic of Concept Infrared Sensor Bar 111
82. Concept GPR Systems for Quality Assurance and Rapid Non-Contact Density Measurement 112
F1. Nuclear Gauge (left) vs. Pavetracker (right) 157
F2. Slope Factor Problems with Pavetracker 158
F3. Dispersion of Nuclear Densities around the Perfect Fit Line 159

LIST OF TABLES

Tables **Page**

1. Texas DOT Specifications for Density Profile Acceptance 7
2. Specification Limits and Expected Mix Property Changes from Segregation 13
3. Current Available Infrared Cameras and Their Features 17
4. Finland Penalty Schedule for Air Voids Higher Than Specifications 19
5. Finland Penalty Schedule for Air Voids Out of Specification Limits 19
6. Predicted Mat Statistics for SH 6 from GPR Data 45
7. Core Results from SH 6 Test Section 48
8. Gradations for SH 6 Cores 48
9. Selected Significant Correlations between Data for SH 6 51
10. Limits on Changes in Temperature and Dielectric before Mix Parameter Changes Are at Tolerance Limit 52
11. Predicted Mat Statistics for US 79 from GPR 62
12. Core Results from US 79 Test Section 65
13. Gradations for US 79 Cores 65
14. Selected Significant Correlations between Data for US 79 67
15. Limits on Changes of NDT Data before Mix Parameter Changes Are at Tolerance Limit for US 79 67
16. Core Results from IH 10 Test Section 80
17. Gradations for IH 10 Cores 80
18. Selected Significant Correlations between Data for IH 10 83
19. Limits on Changes of NDT Data before Mix Parameter Changes Are at Tolerance Limit for IH 10 84
20. Predicted Mat Statistics for US 290 Test Section 93
21. Core Results from US 290 Test Section 96
22. Gradations for US 290 Cores 96
23. Selected Significant Correlations between Data for US 290 98
24. Limits on Changes of NDT Data before Mix Parameters Changes Are at Tolerance Limit for US 290 98
25. Summary of Test Sites Investigated 102

A1. Significant Correlations between Data for SH 6 117
A2. Complete Correlation Matrix between Differences of Data for SH 6 118
A3. Correlation Coefficient t-values for SH 6 119
A4. Regressions between Changes in NDT Data and Changes in Mix Parameters for SH 6 120
B1. Significant Correlations between Data for US 79 123
B2. Complete Correlation Matrix between Differences of Data for US 79 124
B3. Correlation Coefficient t-values for US 79 125
B4. Regressions between Changes in NDT Data and Changes in Mix Parameters for US 79 126
C1. Significant Correlations between Data from IH 10 129
C2. Limits on Changes of NDT Data before Mix Parameter Changes Are at Tolerance Limit for IH 10 130
C3. Complete Correlation Matrix between Differences of Data for IH 10 Pooled Data 131
C4. Correlation Coefficient t-values for IH 10 Pooled Data 132
C5. Regressions between Changes in Temperature and Changes in Mix Parameters for IH 10 Pooled Data 133
C6. Complete Correlation Matrix between Differences of Data for IH 10 Pooled Data without Core 10 134
C7. Correlation Coefficient t-values for IH 10 Pooled Data without Core 10 135
C8. Regressions between Changes in GPR Dielectric and Changes in Mix Parameters for IH 10 Pooled Data without Core 10 136
C9. Complete Correlation Matrix between Differences of Data for IH 10 Grouped Data 137
C10. Correlation Coefficient t-values for IH 10 Grouped Data 138
C11. Regressions between Changes in Temperature and Changes in Mix Parameters for IH 10 Grouped Data 139
C12. Complete Correlation Matrix between Differences of Data for IH 10 Grouped Data without Core 10 140
C13. Correlation Coefficient t-values for IH 10 Grouped Data without Core 10 141
C14. Regressions between Changes in GPR Dielectric and Changes in Mix Parameters for IH 10 Grouped Data without Core 10 142

D1. Significant Correlations between Data for US 290 145
D2. Complete Correlation Matrix between Differences of Data for US 290 146
D3. Correlation Coefficient t-values for US 290 147
D4. Regressions between Changes in NDT Data and Changes in Mix Parameters for US 290 148
F1. Prediction Statistics for Density Gauges 158

EXECUTIVE SUMMARY

Segregation of any type is a serious problem in hot-mix asphalt and typically leads to poor performance, poor durability, shorter life, and higher maintenance costs. There are obvious performance and financial benefits from developing techniques to minimize segregation. Currently, longitudinal density measurements are being used in attempts to measure segregation. However, this method of quality control is considered quite labor intensive and may not always accurately identify problem areas. Clearly, new and innovative techniques for detecting segregation are needed.

This project focused on using two non-destructive testing (NDT) technologies, infrared imaging (IR), and ground-penetrating radar (GPR), to evaluate the uniformity of newly placed hot mix overlays. Four sections were tested and cores were taken where anomalies were identified in either of the NDT readings. Researchers returned the cores to Texas Transportation Institute (TTI) laboratories and conducted a range of tests to measure important materials properties such as air void content, percentage asphalt, and gradation. The primary objectives of the project were to determine:

- What do the devices measure, and what are their limitations?
- How can the Texas Department of Transportation (TxDOT) use these technologies for both quality control (QC) and quality assurance (QA) applications?
- What steps are necessary for eventual statewide implementation?

Analysis of data collected in the study showed that data from both infrared imaging and ground penetrating radar are relatable to changes in hot-mix properties. Changes in temperature were significantly related to changes in surface dielectric (all test sites), air voids (three test sites), asphalt content (two test sites), and gradation (two test sites). From the radar data, researchers found a strong relationship between changes in surface dielectric and changes in air voids (all test sites), asphalt content (one test site), and gradation (one test site). Based upon TxDOT specifications for allowable operational tolerances and the relationship between changes in non-destructive testing data and changes in mix properties, researchers propose the following material acceptability limits:

- Significant changes in mix properties will occur if changes in surface temperature of more than 25 °F are measured in the field.
- Significant changes in mix properties will occur if the surface dielectric changes by more than 0.8 for coarse graded mixes and 0.4 for dense graded materials.

Additionally, the surface dielectric from the radar data appears to be the best indicator of mix density. A new capacitance-based density device was tried as part of this project, but several problems occurred with it, and at this time TxDOT should not replace the nuclear gauges with this type of instrument. A discussion of this device is included as Appendix F in this report. In contrast to typical density gauges, ground-penetrating radar is a non-contact measurement, so it is not impacted by surface texture. If density variations are the primary irregularities occurring

in the hot-mix mat, radar is likely the best tool for assessing mat uniformity. Infrared imaging worked well as an early screening tool for locating potential problem areas, and both infrared and ground-penetrating radar technologies could be considered effective as quality control (infrared) or quality assurance (radar) methods. Infrared imaging provides a means of assessing mat quality and identifying potential problems as placement is taking place, thus allowing the opportunity for corrective action, and radar provides a rapid and reliable means of obtaining density data.

TxDOT should consider future implementation of these technologies. However, neither of the two devices used in this study were thought optimum for full implementation. The infrared cameras are expensive, in the range of $20,000 to $50,000, and the angle of operation and limited field of view make development of a field test and acceptance protocol difficult. A typical image covers about 20 to 30 feet of pavement; therefore, multiple images need to be collected and merged as the paving train passes along the highway. Coming back to an exact location is nearly impossible unless the area is marked immediately upon imaging. The 1 GHz radar system used is relatively large and bulky. A slightly higher operating frequency system, such as 2 GHz, would have the advances of smaller size (factor of 2) and greater near surface accuracy. With recent advances in GPR systems it should be possible to build a handheld unit for spot-specific measurement. This system could potentially replace the nuclear density gauge and would have significant advances over alternative density measurement systems in that it would be non-contact and therefore not impacted by surface texture.

Ideas on achieving an effective implementation of these technologies for detecting segregation are:

Infrared: A bar with spot infrared sensors at known transverse offsets could be pulled behind the paver. A distance-measuring instrument would trigger data acquisitions at pre-set intervals. This process would create a data file of mat temperatures at known locations, eliminating the uncertainty with accurately locating a location on the mat when an infrared camera is used. Surface mapping software could be used to plot the data, and anomalous areas could be identified, located, and investigated. Overall temperature variability of the entire section could easily be investigated.

Ground-Penetrating Radar: A small, high frequency handheld unit could be developed to replace the nuclear density and capacitance-based gauges. The system would be non-contact and thus not impacted by surface texture. In addition, multiple antennas of a high frequency system could be mounted across the front of a vehicle, and a single pass could collect all the data necessary to generate a surface plot of the air voids for the entire mat. High void areas could be located, and the data could be used to generate the distribution of voids in the section. This implementation method would provide a means of examining mat uniformity and could also be used for assessing bonuses and/or penalties.

CHAPTER 1

INTRODUCTION

I. BACKGROUND

Past definitions of segregation in hot-mix asphalt (HMA) have been focused on concentrations of either coarse or fine materials in a portion of the mat. Extensive work by Stroup-Gardiner and Brown has led to a more recent definition of segregation: "the lack of homogeneity in the hot-mix asphalt constituents of the in-place mat of such a magnitude that there is a reasonable expectation of accelerated pavement distress(es)" (*1*). This new definition of segregation encompasses all types of segregation. Specifically, a new definition of segregation was necessary when Read suggested that problems in HMA such as lower compaction, stripping, and raveling, were being caused by cool spots in the mat rather than gradation segregation (*2*). Thus, the concept of temperature segregation began.

Segregation of any type is a serious problem in HMA, as segregation typically leads to poor performance, poor durability, shorter life, and higher maintenance costs (*3*). Pavement life can be shortened substantially due to segregation resulting in increased air voids, increased permeability, decreased resilient and dynamic modulus, decreased tensile strength, increased rutting potential, increased raveling, increased longitudinal and fatigue cracking, and decreased density (*1*).

There are obvious performance and financial benefits from developing techniques to minimize segregation. Currently, longitudinal density measurements are being used in attempts to measure segregation (*4*). However, this method of quality control is considered quite labor intensive and may not always accurately identify problem areas.

Clearly, new and innovative techniques for detecting segregation are needed. One often cited candidate for this task is infrared imaging. In addition, GPR has been used to successfully detect areas of low density in HMA (*5*, *6*). This project aims to incorporate these two technologies together in order to identify segregation.

II. OBJECTIVES

The primary objectives of the project were to determine:

- What do the devices measure, and what there are limitations?
- How can TxDOT use these technologies for both QC and QA applications?
- What steps are necessary for eventual statewide implementation; i.e., data collection protocols, training requirements, and equipment specifications?

III. WORK PLAN

In order to gain further understanding about how these technologies can be used to detect segregation, how the technologies can be used in the field, and how infrared and GPR data obtained in the field relate to laboratory-measured properties of the HMA, the following basic work plan was made:

Task 1: Literature Review

Search published research from the past three years and contact Departments of Transportation (DOTs), research organizations, and industry organizations, to determine the current status and approaches to segregation.

Task 2: Accuracy and Repeatability of Testing Equipment

In the laboratory, investigate the repeatability and accuracy of infrared imaging using a calibration pad and different angles to the pad from the camera. Use calibrated thermocouples to compare with infrared images. Investigate wind effects on the infrared images.

Task 3: Field Evaluation

On several upcoming overlay projects, collect infrared images as the mat is being placed and mark areas of potential segregation. Collect GPR data as soon as possible after compaction. Also collect density data both with a nuclear density gauge and with the Pavetracker non-nuclear surface density instrument. With the infrared and GPR data, determine areas to core. Also take cores of non-segregated areas for comparison.

Task 4: Effects of Segregation on Material Properties

From the field cores, perform the following tests:

- Laboratory dielectric
- Density
- Surface texture depth
- Permeability
- Wheel tracking performance in the Asphalt Pavement Analyzer
- Rice gravity
- Percent air voids
- Percent asphalt
- Gradation
- Laboratory dielectric

Task 5: Research Report

Consolidate the research into a report detailing the work and the results.

CHAPTER 2

LITERATURE REVIEW

I. SUMMARY

From the literature, it is clear that controlling segregation is an important item on the agenda of many organizations. Studies show that segregation causes, among other things, lower densities, rutting, raveling, fatigue cracking, and thus shorter pavement life. DOTs have been implementing methods aimed at checking for and quantifying segregation. The most prevalent method is through longitudinal density measurements, where criteria for the maximum allowable variation in density must be met. However, this method is quite labor intensive and time consuming, and there is some evidence to suggest this method is not very effective.

Other research has focused on profiling, infrared imaging, and ground-penetrating radar as methods to check for segregation. Current research has concluded that all three of these technologies have potential to reliably identify and quantify segregation.

II. KANSAS DEPARTMENT OF TRANSPORTATION (KDOT)

KDOT has performed testing to evaluate the effects of segregation. Significant conclusions were that segregation causes a drop in unit weight, higher porosity, a decrease in indirect tensile strength, an increase in moisture susceptibility, and a reduction in fatigue life (*7*). The research also found a correlation between unit weight and permeability, tensile strength, moisture susceptibility, and fatigue life.

KDOT has since developed procedures for dealing with segregation. One such item is "Segregation Check Points," available from the KDOT Bureau of Construction and Maintenance. This document highlights control points, ranging from stockpiling through the laydown operation, that one should check to help eliminate segregation problems in the production and placement of hot mix. Numerous checks are suggested for each of the following (*8*):

- Stockpiling
- Loading cold bins
- Cold bin operation
- Cold feed conveyors
- Drum mixer of dryer
- Hot conveyors (drum mixer)
- Slat conveyor (drum mixer)
- Gob hopper (drum mixer)
- Hot bins (batch plant)
- Hot conveyor and gob hopper (batch plant)
- Surge bin
- Truck loading
- Truck to laydown machine
- Laydown machine

KDOT has also implemented procedures checking for segregation by taking longitudinal density readings. The procedure, "Segregation Check Using the Nuclear Density Gauge," is essentially as follows (9):

1. Allow the paving unit 1000 feet of progress before starting a density profile.
2. Select a "zero" point at the location where the screed stops, or, if the paving unit progresses without any stops, the engineer determines a starting point for the profile.
3. Select measurement locations. If checking for truck load segregation, use a fixed transverse distance of at least 2 feet from either edge of the mat. If checking for longitudinal streaking, start the profile with a transverse offset of approximately 2 feet from the center of the longitudinal streak, and end the profile with a transverse offset of approximately two feet on the opposite side of the streak. When checking for longitudinal segregation, each end of the profile must be at least 1 foot from the edge of the mat. See Figure 1.

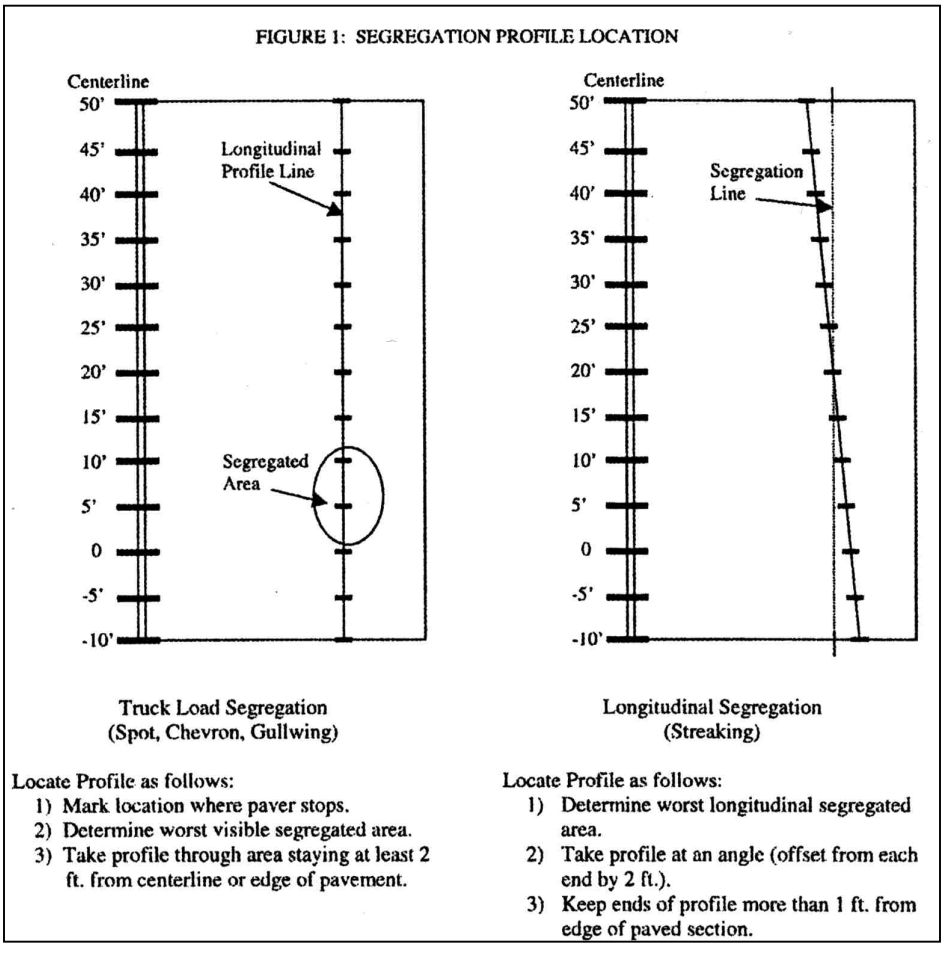

Figure 1. Kansas DOT Segregation Profile Locations (9).

4. Take density readings approximately every 5 feet in the transverse direction, with the first reading being approximately 10 feet behind the zero point. Use minus #40

aggregate from the mix to fill any voids in the surface. In the backscatter mode, take three 1 minute readings and average them. If one of the readings varies by more than 1 lb/ft^3, discard the reading and take a new one. Test a minimum of 10 locations along the profile section.

5. Initially perform four segregation checks for each mix. When four consecutive profile evaluations meet the specifications in KDOT 90M-198, the frequency of the checks may be reduced by the district materials engineer.

The acceptable criteria for the uniformity of the density readings in each profile is (*10*):

- Maximum range of highest to lowest density ..... 5 lb/ft^3
- Maximum range of average to lowest density ..... 2.5 lb/ft^3

In addition to specifying the maximum allowable density ranges, this KDOT special provision also requires material transferred from the hauling truck to be remixed prior to being placed. Remixing is required prior to placement to help reduce gradation and temperature irregularities in the mix.

III. TEXAS DEPARTMENT OF TRANSPORTATION (TxDOT)

TxDOT has adopted procedures patterned from the Kansas procedure to deal with segregation. In a Special Provision, TxDOT may require for the hauled material to be re-mixed prior to placement if segregation problems cannot be corrected through plant or process adjustment (*11*). In addition, longitudinal density measurements of the mat are to be made after it is placed. The density measurements are to be every 5 feet in a 50-foot section at a certain transverse distance (at least 2 feet) from the paving edge (*12*). At least four segregation checks are to be made per day for each mix type used on the project, and Texas specifications require four consecutive longitudinal density profiles to meet the criteria shown in Table 1.

Table 1. Texas DOT Specifications for Density Profile Acceptance (*13*).

Nominal Max Aggregate Size	Maximum Allowable Density Range (highest to lowest)	Maximum Allowable Density Range (average to lowest)
5/8” or less	6.0 lb/ft^3	3.0 lb/ft^3
5/8” or greater	8.0 lb/ft^3	4.0 lb/ft^3

In October of 1999, TxDOT held a material transfer device (MTD) “showcase” in El Paso, Texas, in which five MTDs were tested and evaluated using in-place density, infrared imaging, visual rating, and profiling. Key significant findings and conclusions from this study were (*14*):

- None of the MTDs eliminated all segregation-related problems.
- The proposed test method for identifying segregation by establishing density profiles does not appear to be a very effective tool.

- The infrared thermal imaging technique was found to be an excellent quality control tool.
- Ground-penetrating radar has the potential to identify and quantify segregation.
- MTDs alone cannot cure all problems related to segregation.

IV. CONNECTICUT DEPARTMENT OF TRANSPORTATION (CDOT)

In 1999, CDOT published a study in which thermal imaging was used to try to identify areas of segregation in freshly placed asphalt. Areas of varying temperature were identified, then density and percent air voids were measured with a nuclear density gauge. Selected areas showing large differences in temperature (normally greater than 36 °F) were then cored and tested in the laboratory for air voids, asphalt content, and gradation.

This project concluded that segregation did not occur in the areas identified as having large temperature differentials. In general, average density tended to be lower with lower hot-mix temperature, but no significant correlation between temperature differentials and changes in density was found. The author further concluded that there was no significant correlation between temperature differentials and asphalt content, or any correlation between temperature differentials and gradation, and that "cyclic" segregation was not the result of temperature differences in the hot mix (*15*).

The Connecticut study concluded that the use of material transfer devices resulted in substantially lower temperature differentials in the pavement mat. Therefore, the researcher recommended that some type of remixing equipment be used on paving projects, noting that HMA that was well mixed for temperature uniformity should likewise have been well mixed for particle size distribution (*15*).

V. WASHINGTON DEPARTMENT OF TRANSPORTATION (WSDOT)

WSDOT has done substantial work with infrared imaging of hot-mix asphalt. WSDOT is taking thermal images of paving operations and noting where the location is, what the weather conditions are, what type of equipment is being used to produce, haul, lay, and compact the surface, the thickness of the surface, and the type of asphalt being used. Thermal images are available online, and some images have associated longitudinal density data. An example of some of the Washington data is in Figure 2. This figure shows a thermal image of a section of the pavement mat, two spot temperature readings, the longitudinal line of temperature and density measurements, and the density ranges.

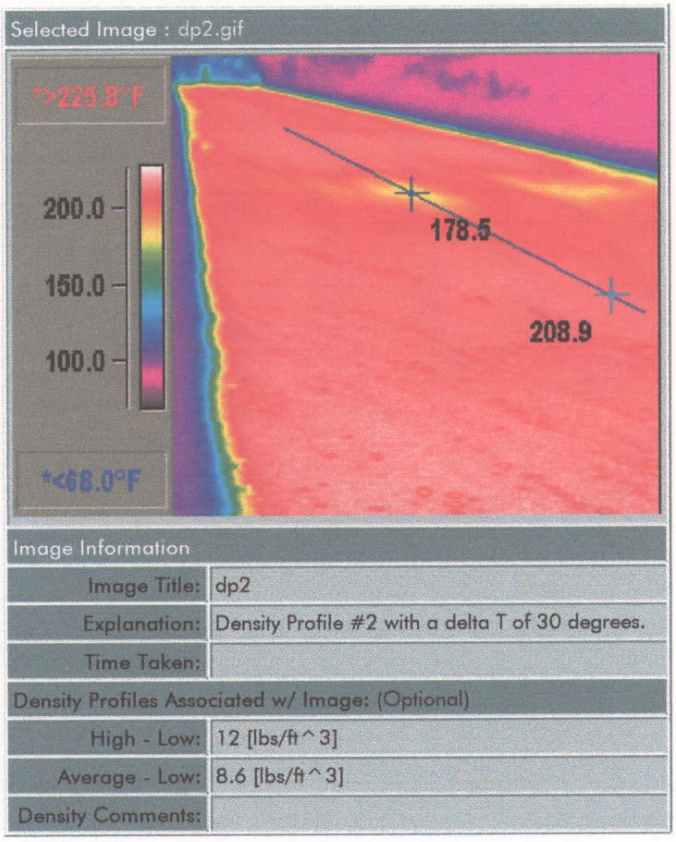

Figure 2. Example of Washington DOT Infrared Data (*16*).

Figure 3 is a scatter plot of the Washington data showing longitudinal temperature differences versus the difference between the average and lowest mat measured mat density, as taken in a longitudinal density profile. This data exhibits a noticeable trend, which can be estimated with the following:

$$\text{Ln(AVG to low Density)} = 0.579 + 0.0240*(\text{Delta T}) \qquad R^2 = 0.55$$
$$(0.068)\ \ (0.0028) \qquad \text{(s.e.)} \qquad \hat{\sigma} = 0.33$$

A logarithmic relationship was used instead of a quadratic in order to address the obvious heteroskedasticity (increasing or decreasing errors with increasing or decreasing X values) in the data. The important point is the Washington data show a statistically significant positive relationship between temperature differentials and the range of average mat density to the lowest mat density. The P-Values for both the estimated intercept and slope in the relationship above are both essentially zero. The Washington data result in a correlation coefficient of 0.74 between the natural log of the average to low density range and temperature differentials.

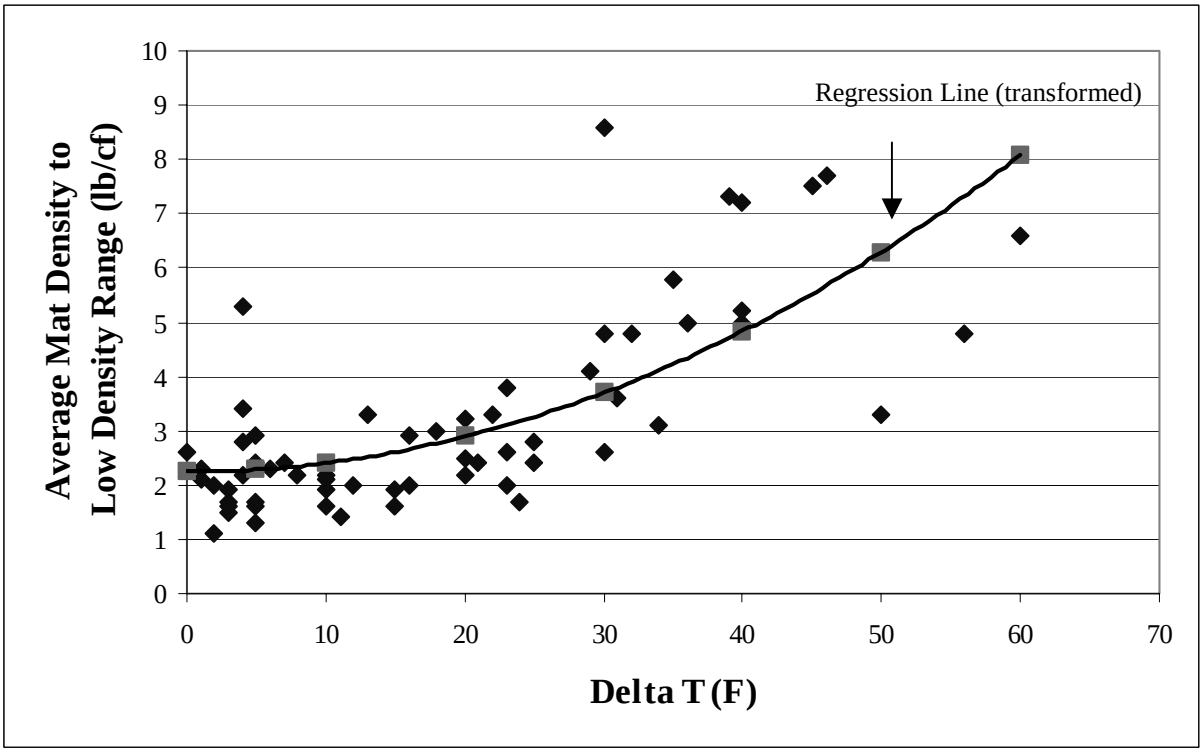

Figure 3. Washington DOT Data of Temperature Differentials vs. Range of Average to Lowest Measured Mat Density (*16*).

WSDOT recently compiled results from testing performed from 1998 through 2000 on segregation (*17*). From the work in 1998, projects seen with significant temperature drops showed higher air voids in the cooler portions of the mat, but did not exhibit significant aggregate segregation. Some significant findings from the 1999 work include:

- 87 percent of observations with temperature differentials of less than 25 °F had air void differentials of 2 percent or less. With temperature differentials greater than 25 °F, only 35 percent of observations had void differentials of 2 percent or less.
- End dump operations accounted for over half of the data points with voids changes of more than ±2 percent.

The work performed in 2000 focused on evaluating the density profile technique for locating segregation, where a maximum density range of 6.0 lb/cf and a maximum density drop (average to low) of 3.0 lb/cf was allowed. In areas with temperature drops of more than 25 °F, 89 percent of the profiles failed to meet the criteria. Also significant is that, when a density profile failed both the range and drop criteria, in-place densities were lower than the minimum allowed for QA in over 80 percent of the cases. The authors suggest that this implies the density profile may also be able to capture densities below the in-place density specification. Researchers concluded that the quality assurance program used by WSDOT does not capture the significance of low-density areas, but the density profile procedure could locate potential problem areas and provide results to determine the extent of the problem (*17*).

Based on this work, WSDOT decided to perform density and temperature profiles as a shadow specification for the 2001 construction season (*18*). At least two density profiles were to be taken each day in areas with temperature differentials of more than 25 °F, and at least one per day in an area with a temperature differential of less than 25 °F. Based upon these results, full implementation was considered. However, WSDOT concluded the density profile was too labor intensive and instead has adopted a specification into five projects for the summer 2002 paving season that imposes a 15 percent penalty on a lot if four or more spots or streaks in a lot are less than 89.0 percent of maximum theoretical density (*19*). Areas to be tested can be identified visually or through temperature differentials. The complete specification is as follows (*20*):

> In addition to the random acceptance density testing, the Engineer may also evaluate the mixture for low cyclic density of the pavement. Low cyclic density areas are defined as spots or streaks in the pavement that are less than 89.0 percent of maximum theoretical density. If four or more low cyclic density areas are identified in a lot, a cyclic density price adjustment will be assessed for that lot. The price adjustment will be calculated as 15% of the unit bid price for the quantity of ACP represented by that lot. In any 100 feet of paving only one area will be counted toward the number of infractions. The outside 1.5 feet of pavement will be excluded from this analysis.

VI. NATIONAL CENTER FOR ASPHALT TECHNOLOGY (NCAT)

Stroup-Gardiner and Brown at Auburn University have recently concluded a study identifying the effects of segregation on pavement properties, testing various techniques for identifying segregation, and defining levels of segregation.

In order to perform these tasks, the researchers conducted field surveys of existing pavements, as well as density measurements, infrared imaging, and $ROSAN_v$ surface texture measurements, on freshly placed hot-mix mats. They also performed laboratory tests of field cores.

In the field, surveys of pavements in Alabama, Washington, Minnesota, Georgia, Texas, and Connecticut were conducted. Key conclusions drawn from these surveys were (*1*):

- Temperature segregation results in an area of low density and thus periodic rutting. Also seen in areas with this type of segregation are increased longitudinal and fatigue cracking.
- Gradation segregation results in increased raveling and longitudinal and fatigue cracking. However, in contrast to areas with temperature segregation, no significant depressions caused by traffic densification were seen.
- Depending on the severity of the problem, segregation reduces a pavement life by 20 percent to 58 percent.

The researchers also evaluated several technologies to try to identify segregation in freshly placed pavement mats. Gardiner and Brown's conclusions as to the effectiveness of these technologies for detecting and measuring segregation are as follows (*1*):

- Nuclear Density Measurements:
    - Changes in density tended to be statistically significant at only high levels of segregation.
    - Technologies that measure only density will have difficulty distinguishing between levels of segregation.
    - Density measurements are very effective at identifying a specific type of temperature segregation. Density measurements effectively locate transverse strips of low density that occur when the paver stops.

- Infrared Thermography:
    - Infrared imaging can detect and measure each level of segregation.
    - Infrared imaging cannot distinguish between gradation and temperature segregation; it sees both as cold spots.
    - Infrared imaging can be used to estimate the percent of segregation in a certain area of the mat.
    - Infrared imaging shows immediate promise for use in inspection of the mat behind the paver as the mat is being placed. This inspection process can be used to identify areas of non-uniformity and to check for segregation.

- $ROSAN_v$ Surface Texture Measurements:
    - Surface texture measurements are effective for detecting and measuring each level of gradation segregation.
    - Surface texture measurements cannot detect temperature segregation.
    - Surface texture measurements can be used to estimate the percentage of the mat with each level of gradation segregation.

The other major area of the NCAT study was defining levels of segregation and the impacts of segregation on the mix properties. The researchers defined levels of segregation as none, low, medium, and high, identified these levels according to differences in surface temperatures and surface texture ratios, and outlined the expected effect on mix properties from the segregation. Table 2 presents this information.

Table 2. Specification Limits and Expected Mix Property Changes from Segregation (*1*).

Mix Property	Percent of Non-Segregated Mix Property by Level of Segregation			
	None	Low	Medium	High
Temp. Difference (°F)	<18	18 – 28.8	30.6 – 37.8	>37.8
Surface Texture Ratios	<1.16	1.16 – 1.56	1.57 – 2.09	>2.09
Mix Properties as Percent of Non-Segregated Areas				
Permeability	Slightly increased	Increased with coarse level of segregation		
Resilient Modulus	Little or slightly increasing stiffness	70 – 90%	50 – 70%	<50%
Dynamic Modulus	Little or slightly increasing stiffness	80 – 90%	70 – 80%	50 – 70%
Dry Tensile Strength	110%	90 – 100%	50 – 80%	30 – 50%
Wet Tensile Strength	80 – 90%	75%	50%	30%
Loss of Fatigue Life when Segregation in Upper Lifts, %	Not Estimated	38%	80%	99%
Rutting Potential	Not heavily influenced by gradation segregation until a high level of segregation is seen			
Difference in Values between Segregated and Non-Segregated Areas				
Minimum # of Sieve Sizes that are Given % Coarser	NA	1 sieve > 5% coarser	2 sieves > 10% coarser	4 sieves > 15% coarser
Change in Air Voids	NA	2.5 – 4.5% higher	4.5 – 6.5% higher	>6.5% higher
Change in Asphalt Content	NA	0.3 – 0.75% decrease	0.75 – 1.3% decrease	>1.3% decrease

VII. MICHIGAN DEPARTMENT OF TRANSPORTATION (MDOT)

MDOT recently conducted a study using one-minute nuclear density readings to rapidly confirm or deny the existence of segregation (*21*). The basic procedure is to perform multiple density readings on areas that visually appear segregated and compare them, using automated statistical procedures, to density readings from areas that appear non-segregated.

After comparing density measurements from areas visually identified as non-segregated and heavily segregated (stone on stone with little or no matrix), the probability of the average densities being significantly different at the 99 percent confidence level was 81 percent. For non-segregated vs. medium-segregated (significantly more stone than surrounding mat), this probability drops to 69 percent. It was concluded that lightly segregated areas (more stone than surrounding mat) were generally not differentiable from non-segregated areas. Gradation analysis of changes in percent passing the 3/8 inch, #4, and #8 sieves was performed as a follow up to investigate how significantly different average densities may relate to significant changes in gradation. When the average densities were significantly different at the 99 percent confidence level, the probability of observing a significant difference in gradation (at the 90 percent confidence level) was 77 percent (*21*). The researchers further found (*21*):

> If segregated and non-segregated areas are visually identified on the pavement surface and if a t-test between the one-minute nuclear density readings taken in both areas result in a p-value of 10^{-3} or less, then the probabilities that segregation will also be confirmed by aggregate gradation difference (percent passing the No. 4 sieve) with p-value of 10^{-2} or less are:
>
> For light degree of segregation-57 percent
> For light to medium degree of segregation-50 percent
> For medium degree of segregation-88 percent
> For medium to heavy degree of segregation-86 percent
> For heavy degree of segregation-85 percent
>
> Thus the research indicated:
>
> - if an area was visually identified as medium or severely segregated, and
> - if the average of multiple density readings in the visually identified segregated area were significantly different from the average density values in visually appearing non-segregated areas, then
> - there was approximately an 88 percent chance of a statistically significant difference in gradation between the segregated and non-segregated areas at the 90 percent confidence level.

Based upon these results, a spreadsheet program to verify segregation by comparison of average densities between visually identified non-segregated and segregated areas was developed and adopted by MDOT, the Michigan Asphalt Paving Association (MAPA), and the asphalt industry (*21*). Figure 4 shows an example of this program.

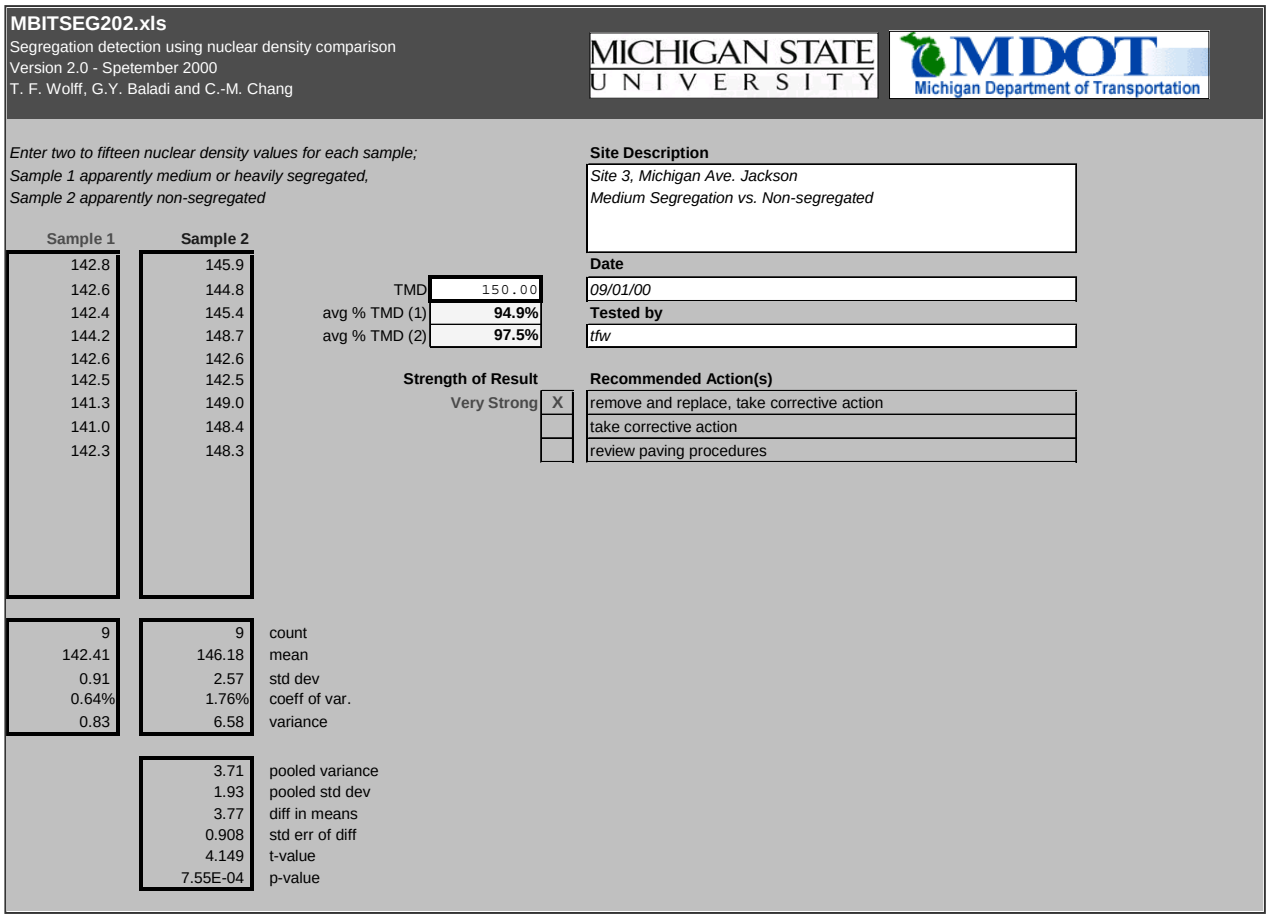

MBITSEG202.xls
Segregation detection using nuclear density comparison
Version 2.0 - September 2000
T. F. Wolff, G.Y. Baladi and C.-M. Chang

MICHIGAN STATE UNIVERSITY

MDOT Michigan Department of Transportation

Enter two to fifteen nuclear density values for each sample;
Sample 1 apparently medium or heavily segregated,
Sample 2 apparently non-segregated

Site Description
Site 3, Michigan Ave. Jackson
Medium Segregation vs. Non-segregated

Sample 1	Sample 2
142.8	145.9
142.6	144.8
142.4	145.4
144.2	148.7
142.6	142.6
142.5	142.5
141.3	149.0
141.0	148.4
142.3	148.3

TMD 150.00
avg % TMD (1) 94.9%
avg % TMD (2) 97.5%

Date
09/01/00
Tested by
tfw

Strength of Result		Recommended Action(s)
Very Strong	X	remove and replace, take corrective action
		take corrective action
		review paving procedures

Sample 1	Sample 2	
9	9	count
142.41	146.18	mean
0.91	2.57	std dev
0.64%	1.76%	coeff of var.
0.83	6.58	variance
	3.71	pooled variance
	1.93	pooled std dev
	3.77	diff in means
	0.908	std err of diff
	4.149	t-value
	7.55E-04	p-value

Figure 4. Example Analysis Sheet for Segregation Detection from MDOT.

VIII. INFRARED IMAGING

Previous research has identified infrared imaging as an immediate candidate for use as an inspection/quality control tool for freshly placed HMA (*1*, *14*, *15*). Clearly, WSDOT has found infrared imaging to have substantial promise in this area, which is evidenced by its large image base combining thermal images with density profiles. It has also been suggested that infrared imaging could be used to determine the percent uniformity of a mat and the proportion of the mat that has no, low, medium, and high levels of segregation (*1*).

Before examining some issues specific to thermal imaging of HMA, it is important to understand some basics about infrared thermography. The total amount of infrared radiation seen from an object is composed of reflected, transmitted, and emitted radiation. For any opaque material, there is no transmitted radiation seen (*22*). Thus, for materials such as a HMA surfacing, the total amount of infrared radiation seen by the infrared camera is made up of emitted and reflected radiation. The emitted radiation represents the portion attributable to heat from the object of interest (*22*). For a HMA surface, between 90 percent and 98 percent of the measured infrared radiation is emitted (*23*). This proportion of infrared radiation that is emitted from an object is termed the emissivity. Based upon the total amount of infrared radiation detected from an object and the object's emissivity, the surface temperature of the object can be

determined. The depth of temperature measurement with infrared equipment is only about two thousandths of an inch deep (*24*).

Some commonly cited concerns with infrared imaging are the effects of shade and wind on infrared images. According to Strahan, a Level I and Level II instructor with over 20 years experience in infrared thermography, solar loading will make little difference when imaging freshly placed hot mix because the mix is radiating more energy than the surrounding area loaded with thermal energy from the sun (*24*). Shade, if present, will not be an issue until after quite some time has elapsed since the placing of the HMA (*24*). However, as pointed out by Gardiner and Brown (*1*), imaging of the mat should take place just after placement as compaction will alter the thermal characteristics of the surface. Thus, as long as thermal imaging is done at the appropriate time, shade should not affect the results of the infrared evaluation.

Regarding wind, Strahan has shown that a "one size fits all" correction factor for wind speed does not work (*25*). However, his research shows that by characterizing wind speed versus temperature rise for the material in the laboratory, wind can be appropriately accounted for. Most importantly, though, is that as long as the wind has the same velocity at two different points on a like material, the temperature difference between the two points will be the same even though their surface temperatures will be lower (*24*). Since the objective in thermal imaging of freshly placed HMA is to find temperature differences, the infrared survey will be valid as long as wind conditions are the same at points compared on the freshly placed mat. It is reasonable to believe that wind conditions will be the same at points being compared, as the images of the mat will likely be taken approximately every 30 feet, which is the suggested interval by Gardiner and Brown (*1*).

The further development of infrared technology is occurring at a rapid rate. New models with more features are costing about the same or less than much less sophisticated models from a few years back. A representative lineup of the current infrared cameras, their features, and their cost, is in Table 3.

Table 3. Current Available Infrared Cameras and Their Features.

Camera	Temperature Range	# Spot Temp. Locations	Field of View	Real Time or Scanning	Cost (Approximate)
FLIR ThermaCAM PM 545[1]	-40 °F to 2732 °F	-	24° X 18°	Real Time	$28,000
FLIR ThermaCAM PM 675	-40 °F to 932 °F	5	24° X 18°	Real Time	$47,000
FLIR ThermaCAM PM 695[2]	-40 °F to 932 °F	5	24° X 18°	Real Time	$56,000
Mikron MiKroScan 5104[3]	14 °F to 1472 °F	10	21.5° X 21.5°	Real Time	$19,500
Mikron MiKroScan 7200	-40 °F to 932 °F	10	29° X 22°	Real Time	$40,000
Infrared Solutions IR Snapshot[4]	32 °F to 662 °F	1	18.9°	Scanning	< $15,000

[1] Does not provide actual temperature data, only image.
[2] Same as PM 675 except includes auto focus and built in digital camera.
[3] This camera's technology is rather dated and bulky.
[4] This camera is virtually identical to TxDOT's ThermaSNAP.

IX. GROUND-PENETRATING RADAR

Radar is an electro-magnetic wave and thus obeys the laws governing the transmission and reflection of such waves. The radar system sends discrete pulses of energy into the pavement and captures the reflections from each layer interface within the pavement structure. The amplitude of radar reflections and the time delay between reflections are used to calculate layer thicknesses and layer dielectrics (*26*). For purposes of this study, the surface layer dielectric is of most interest. As will be described, the surface dielectric is the parameter that will be used as an indicator of segregation. The surface dielectric is calculated as follows (*26*):

$$\varepsilon_a = \left[\frac{1 + A_1/A_m}{1 - A_1/A_m}\right]^2$$

where ε_a = dielectric of the surface layer
A_1 = amplitude of the surface reflection in volts
A_m = amplitude of the reflection from a large metal plate in volts (this represents the 100% reflection case)

Work done by Saarenketo and Roimela in Finland spurred on the development of using GPR for detecting segregation. The Finnish researchers studied the relationship between the HMA surface dielectric and air void content. Based upon both laboratory prepared and field samples, the researchers found that the following relationship was reasonable for relating the measured HMA surface dielectric value to air voids (*6*, *27*):

$$\% \text{ Air Voids} = A * e^{B * \text{Surface Dielectric}}$$

where A and B are laboratory-determined constants.

In Finland, this relationship is used with GPR to assess the percent of the pavement and base that has air voids outside of set specification limits. The proportion of air voids out of specifications is determined by dividing the length of measurements with air voids outside of the specifications by the total length of measurement. Pay adjustments from the contract amount are then made from the pay adjustment scales shown in Tables 4 and 5. The schedule in Table 4 applies for air voids higher than specifications; the penalty schedule in Table 5 applies when there are air voids both above and below the specification limits.

Table 4. Finland Penalty Schedule for Air Voids Higher Than Specifications (*28*).

Percent of Air Voids Higher than Specification	Percent Reduction of Contract Sum	
	Surface Layer	Asphalt Base Layer
<=5	0	0
10	-5	0
15	-10	-5
20	-15	-10
25	-20	-15
>=30	-25	-20
*Penalties between points are interpolated.		

Table 5. Finland Penalty Schedule for Air Voids Out of Specification Limits (*28*).

Percent of Air Voids out of Specification Limits	Percent Reduction of Contract Sum	
	Surface Layer	Asphalt Base Layer
<=10	0	0
20	-5	-2.5
25	-10	-5
>=30	-15	-10
*Penalties between points are interpolated.		

Another useful analysis tool adopted for use in this project has been used by the Finnish researchers. Eight longitudinal GPR runs were performed on a new airport runway. Cores were taken to calibrate the relationship between dielectric from the GPR and air void content (*29*). Air voids were then predicted from the surface dielectrics and this information plotted as a contour map displaying the predicted air voids of the entire runway, as shown in Figure 5. Surfer Version 6.04 can be used to perform this function through the following steps:

- GPR data are collected in multiple passes at known transverse offsets from the pavement edge.
- A text file containing GPR trace number, location (in feet), and layer dielectrics is generated in Colormap, TTI's GPR processing software.
- The text file is opened in Excel. The surface air voids are predicted by using the determined relationship between surface dielectric and air voids.
- A three-column text file is created with the first column being the longitudinal distance, the second column transverse distance, and the third column the predicted air void content for that location. This format is necessary for use in Surfer to create the surface plot.
- The text file is opened in Surfer, converted into a data file (*.DAT), which then must be converted into a grid file (*.GRD).
- The surface plot is then generated from the grid file by using the Map function in Surfer.

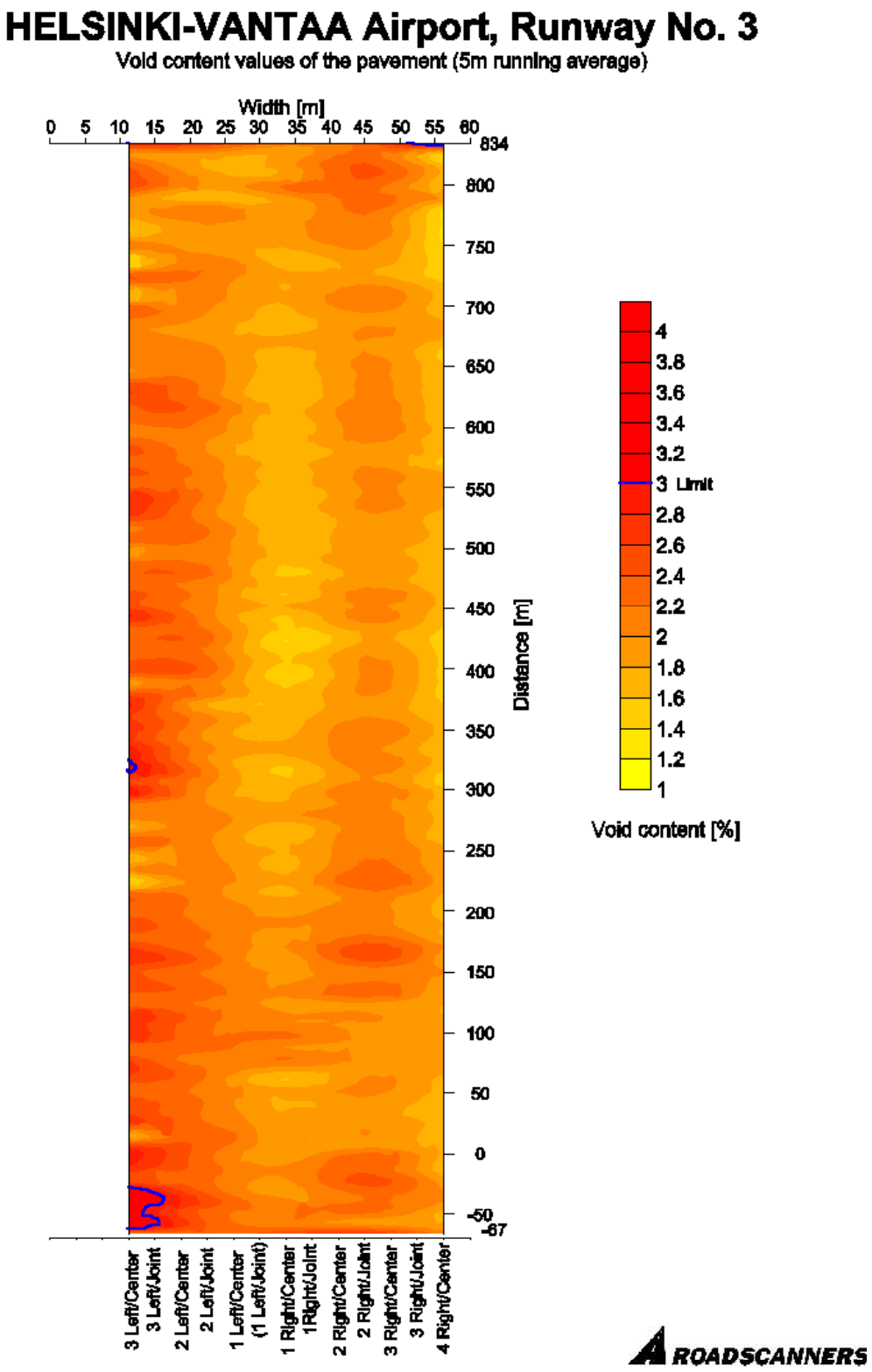

Figure 5. Surface Plot of Voids for Airport Survey from Roadscanners Oy (*29*).

Scullion and Chen adopted the exponential relationship between dielectric constant and air voids for use in the Radar 2000 GPR data acquisition software. This software will process and display the first and second layer dielectric values or the first layer air voids and the second layer moisture content (which is based upon a calibration curve of base dielectric vs. base moisture content), along with the first layer thickness, in real time while data is collected (*5*). GPR is used to compute the dielectric value, and then the specified calibration curve is used to calculate the air void content of the hot mix.

In practice, it has been found that the first layer dielectric value can be quite reliable for detecting segregation. Since the dielectric value of air is 1 and segregation results in higher air voids, the surface dielectric value will dip at segregated locations. This technique was used successfully by Scullion and Chen to locate segregated areas on IH 20 (*5*). Areas where the HMA dielectric value dropped dramatically had visually identifiable segregation. In El Paso, GPR was used as part of the evaluation of five material transfer devices. The HMA dielectric value was monitored with distance to evaluate pavement uniformity and identify areas of low dielectric value. Field cores were taken at locations with dielectric variations and tested in the lab for density. It was shown that a curvilinear relationship existed between HMA dielectric value and density. These data are displayed in Figure 6. From this study, it was concluded that (*14*):

- GPR, with its ability to rapidly scan a pavement and provide continuous results, provides a very promising tool for quality control evaluations of new HMA surfaces.
- The quality of the HMA mat can be related to the uniformity of the surface dielectric plot, and the number of segregated areas can be estimated from the number of sudden localized dips in the surface dielectric.

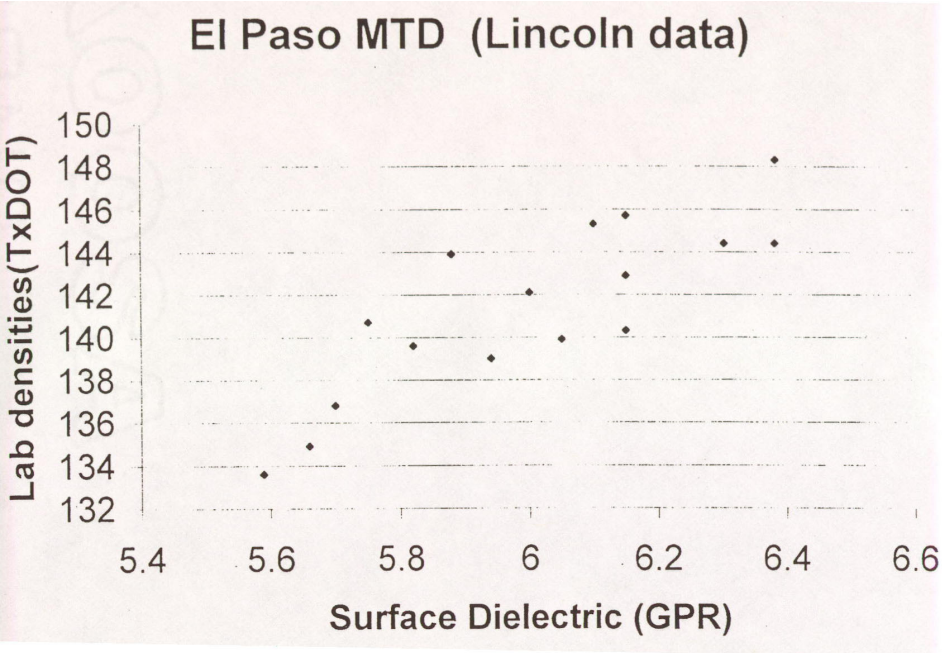

Figure 6. Relationship between Surface Dielectric from GPR and Lab Density (*14*).

CHAPTER 3

LABORATORY VERIFICATION OF INFRARED EQUIPMENT

I. SUMMARY

Before using the infrared imaging equipment in the field, researchers performed a laboratory check of the equipment using an aluminum hotplate, an aluminum plate painted black to go on top of the hot plate and represent HMA, a calibrated surface thermocouple, and the infrared camera. Figure 7 shows the equipment used.

Figure 7. Equipment for Lab Verification of Infrared Equipment.

At temperatures representative of freshly placed HMA and under windless conditions, the accuracy of temperatures provided by the camera was evaluated by comparison to thermocouple-measured temperatures. Researchers performed this evaluation at an angle to the hot plate of 90°, 60°, 45°, and 30° with a camera vertical height of 6 feet and 8 feet. Following this testing, the surface temperature of two hot plates set at different temperatures was measured under windless conditions. A three-speed fan was then used to blow air over the two hot plates, an anemometer used to record wind speed, and temperature measurements with the infrared camera compared to those measured with the calibrated thermocouple.

Under windless conditions, the camera-calculated temperatures were consistently accurate at angles of greater than 45°. Under these circumstances the temperatures based on infrared imaging were within 3 °F of the temperature based on the thermocouple. However, at

angles of 45° and less to the hot plate, the difference between the camera-calculated temperatures and the surface temperature according to the thermocouple was right at or beyond the camera's stated accuracy range, even after considering the accuracy of the thermocouple. The discrepancy between surface temperatures provided by the camera and thermocouple-measured temperatures was greater at a 30° angle than at a 45° angle.

With two hot plates and average wind speeds between 0 and 8 mph, the camera temperatures were likewise accurate as long as the angle from the camera to the hot plates was greater than around 45°. The camera temperatures were within 3 °F of the thermocouple temperatures for both hot plates.

The inaccuracy in temperatures from the camera when the angle is 45° or less is attributable to the fact that when emissivity is determined perpendicularly to the target's surface, the emissivity typically changes when sightings are made at angles greater than 30° to 40° from the normal (*30*). If emissivity is determined from a 90° angle, the emissivity may need to be re-determined for angles below 70° or 60°. Thus, emissivity should be determined at the angle from which the testing will actually take place.

II. EMISSIVITY DETERMINATION OF HOT PLATE SURFACE

The procedure used to determine the emissivity was that described in the camera's user's manual, and is as follows (*31*):

1. Black electrical tape has a known emissivity of 0.95. Place black electrical tape on or next to the target of unknown emissivity.
2. Allow time for both targets to reach the same temperature.
3. Set the emissivity on the camera to 0.95. Acquire the thermal image, and then in the SPOT mode read the temperature of the black electrical tape.
4. Move the cursor onto the target of unknown emissivity.
5. Adjust the emissivity on the camera until the temperature shown for the target of unknown emissivity is the same temperature that was determined for the black electrical tape in step 3.

At first, lab verification of the infrared equipment was going to be performed with the aluminum surface then with the painted aluminum representing HMA. The emissivity of the bare aluminum hot plate immediately surrounding the black electrical tape was found to be 0.26. This emissivity was determined with the camera at a 90^{o} angle to the plate and a distance of 3.3 feet, the image of which is shown in Figure 8. When determining the emissivity of the bare aluminum, it was found that at distances less than infinity on the camera's lens, the accuracy of camera-calculated temperatures was very dependent upon accurately setting the distance on the camera lens. Being that distance increments shown on the lens are only 1.6 feet, 3.3 feet, 6.5 feet, and infinity, this dependency on accurately setting the distance was thought to be a major drawback in using the equipment. However, when testing the aluminum painted black to represent HMA, the focus setting on the camera made little impact. In addition, for road surveys, the distance to the mat will be far enough to where the infinity setting will always be used, so

problems with accurately focusing the camera should not be an issue in the field. It was determined, however, that slight variations in the finish of the bare aluminum hot plate surface caused small variations in emissivity (ε ranged from 0.24 to 0.27) that, at temperatures representative of freshly placed HMA, made multiple spot infrared temperature measurements unreliable because of the varying emissivity. For this reason, further testing was only carried out on the painted plate representing HMA.

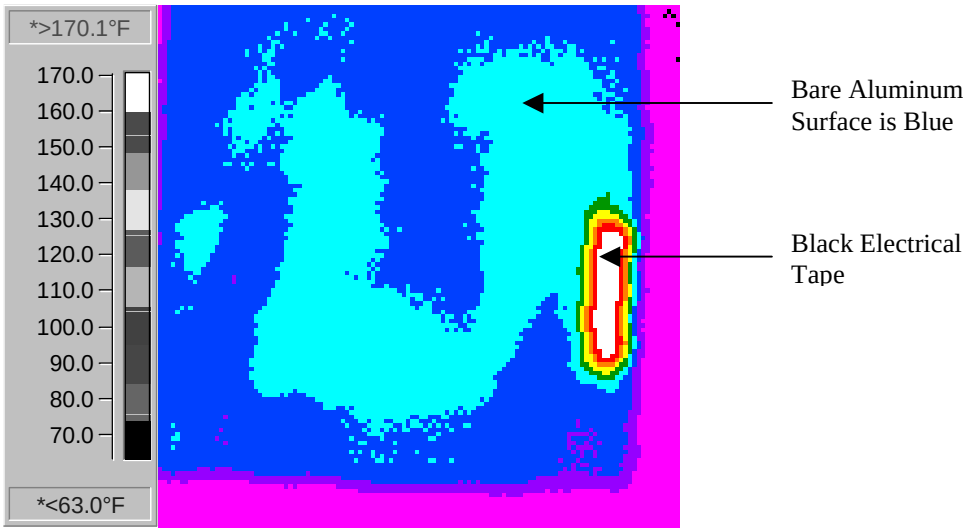

Figure 8. Thermal Image for Emissivity Determination of Aluminum Hot Plate.
Note: Both Aluminum and Electrical Tape are at 175 °F.

The emissivity of the aluminum painted black to represent HMA was determined to be 0.95. Figure 9 is the thermal image that was used in determining the emissivity of the black aluminum. After given time to reach the same temperature, the black electrical tape does not even show up on the thermal image, which means the emissivity of the tape and the plate are the same.

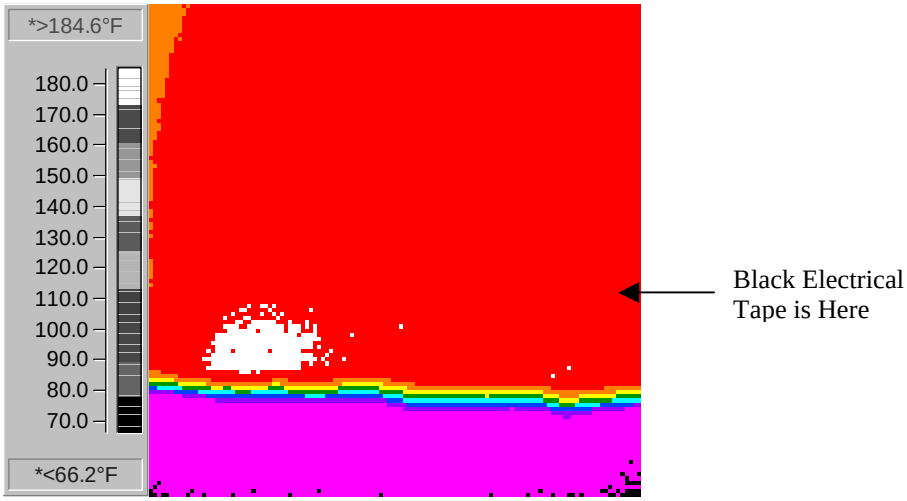

Figure 9. Thermal Image for Emissivity Determination of Painted Aluminum Surface.

As a check on the emissivity, one more image, shown in Figure 10, was taken at an angle and farther away from the hot plate. The camera focus was set to infinity, and a temperature reading of the pad made with the thermocouple, immediately followed by infrared imaging. The thermocouple and infrared temperatures were within 1°F of each other.

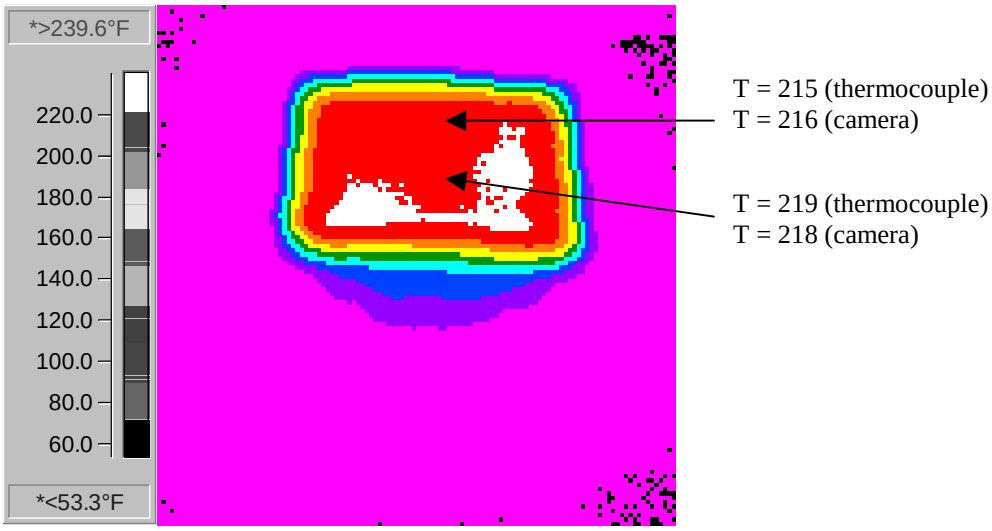

Figure 10. Thermal Image to Verify Emissivity of Painted Aluminum Surface.

III. LABORATORY VERIFICATION OF INFRARED CAMERA TEMPERATURES UNDER WINDLESS CONDITIONS

The setup used to test the camera under windless conditions was to first let the hot plate heat to a temperature representative of freshly placed HMA then take an infrared image of the plate, immediately followed by measuring the temperature of the plate with the thermocouple. Angles of 90°, 60°, 45°, and 30° from the hot plate to the camera were evaluated. In addition, images were taken with a camera height of 6 feet and 8 feet. From the testing researchers concluded that the height of the camera did not affect the accuracy of temperatures. However, at angles of 45° and less to the hot plate, the difference between the camera-calculated temperatures and the surface temperature according to the thermocouple was right at or beyond the camera's stated accuracy range, even after considering the accuracy of the thermocouple. The discrepancy between surface temperatures provided by the camera and thermocouple-measure temperatures was greater at 30° than at a 45° angle.

A. Images with Camera Height of 6 Feet

For images taken from a camera height of 6 feet, the hot plate was set to be between 260 °F and 290 °F. Figure 11 shows the image taken from a 90° angle. At the location shown (Point A), the thermocouple showed the temperature to be 266 °F. The camera showed the temperature at this location to be 268 °F. The white area in the lower left was 280 °F according to the camera. The surface thermocouple verified this temperature.

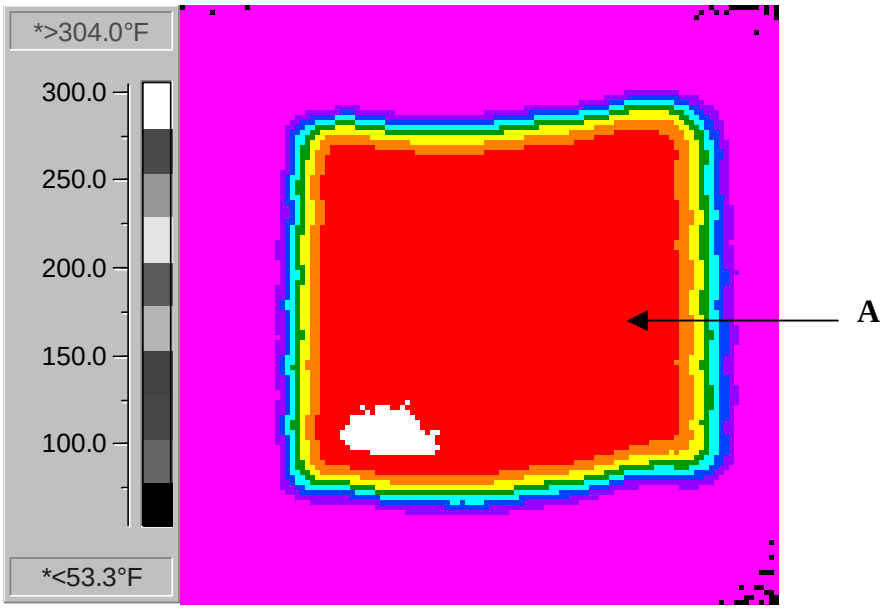

Figure 11. Hot Plate from 90° with Camera Height of 6 Feet.
Note: At point A, thermocouple shows temperature of 266 °F; camera shows 268 °F. Both show temperature of white area to be 280 °F.

Figure 12 is the hot plate from a 60° angle. The temperature at point B is 274 °F according to the thermocouple and 273 °F according to the infrared camera. Again, the hot spot in white in the lower left was verified with the thermocouple. This portion of the hot plate is right at 280 °F.

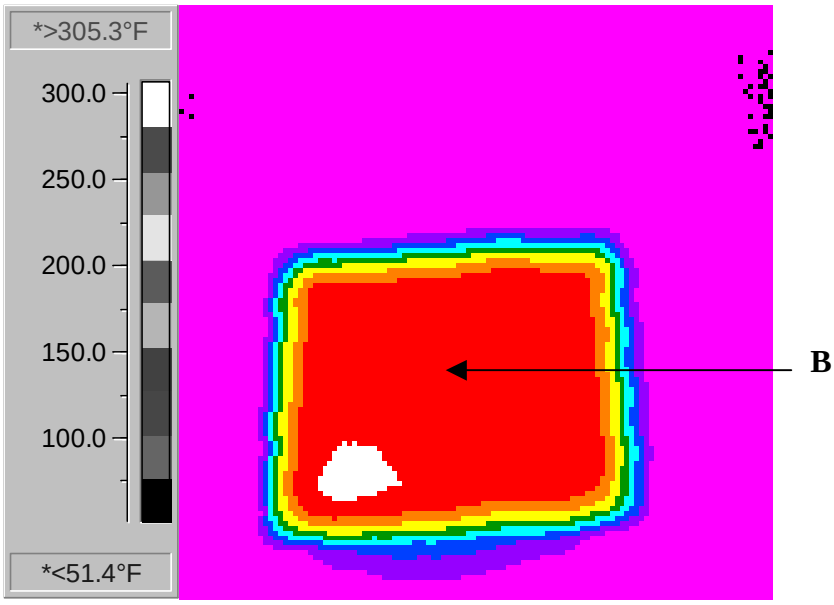

Figure 12. Hot Plate from 60° with Camera Height of 6 Feet.
Note: At point B, thermocouple shows temperature of 274 °F; camera shows 273 °F. Both show temperature of white area to be 280 °F.

Figure 13 shows the infrared image of the hot plate from a 45° angle. At point B, the thermocouple-measured temperature was 290 °F. At this spot, the camera showed the temperature to be 286 °F. With the settings used to acquire this image, this discrepancy is right at the limit of the camera's stated accuracy.

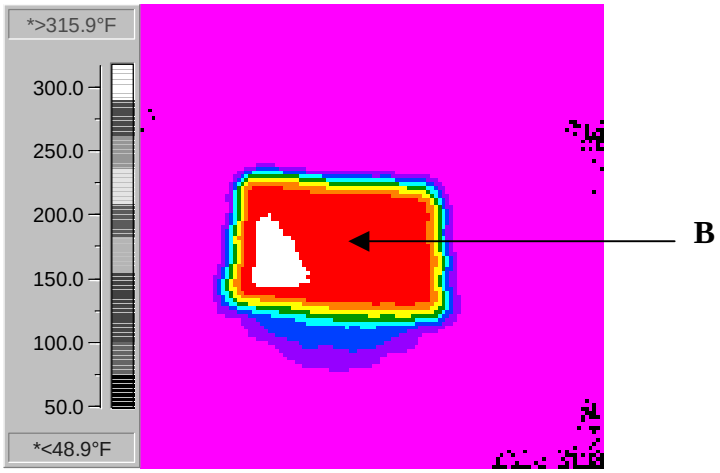

Figure 13. Hot Plate from 45° with Camera Height of Six Feet.
Note: At point B, thermocouple shows temperature of 290 °F; camera shows 286 °F. This discrepancy is right at the limit of the camera's stated accuracy. At this angle a new emissivity determination should probably be performed.

Figure 14 is the hot plate from a 30° angle. From this angle, the difference between the camera-calculated temperature and the temperature from the thermocouple is 8 °F, which is beyond the stated accuracy of the camera. The temperature at point B is 261 °F according to the thermocouple and 253 °F according to the infrared camera.

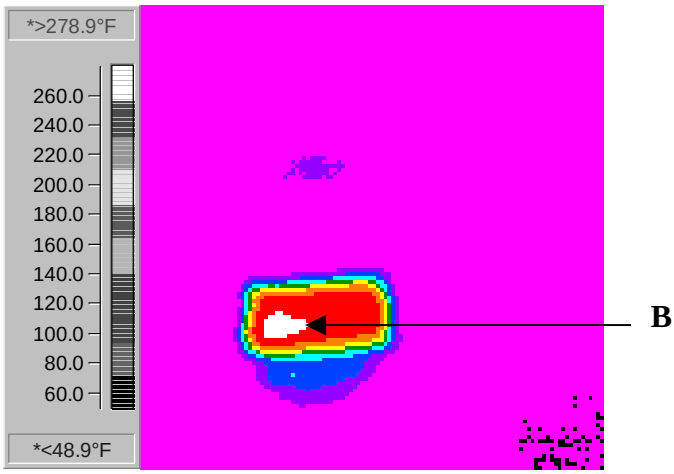

Figure 14. Hot Plate from 30° with Camera Height of 6 Feet.
Note: At point B, thermocouple shows temperature of 261 °F; camera shows 253 °F. This discrepancy is beyond the limit of the camera's stated accuracy. At this angle a new emissivity determination would need to be performed.

B. Images with Camera Height of 8 Feet

For images taken from a camera height of 8 feet, the hot plate was set to be around 325 °F. Figure 15 shows the image taken from a 90° angle. At the location shown (Point B), both the thermocouple and the camera showed the temperature to be 321 °F.

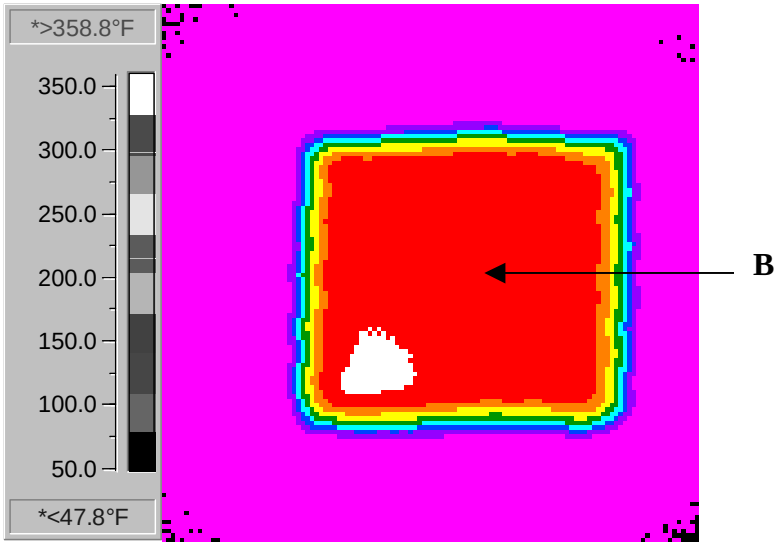

Figure 15. Hot Plate from 90° with Camera Height of 8 Feet.
Note: At point B, both thermocouple and camera show temperature of 321 °F.
Hot spot in white was verified with the thermocouple.

Figure 16 is the hot plate from a 60° angle. At point A, the discrepancy between the thermocouple and the camera was 5° F. At point B, the discrepancy between the two devices was 3 °F. Both of these differences are within the stated accuracy range of the camera.

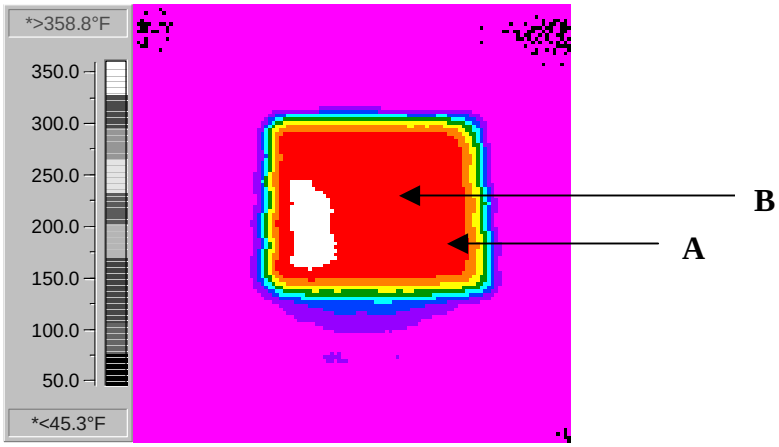

Figure 16. Hot Plate from 60° with Camera Height of 8 Feet.
Note: At point A, thermocouple shows temperature of 325 °F; camera shows 320 °F.
At point B, thermocouple shows temperature of 325 °F; camera shows 322 °F.
Camera temperatures are within its stated accuracy range.

Figure 17 shows the infrared image of the hot plate from a 45° angle. At these temperatures and from this angle, the camera-calculated temperatures are outside of the camera's stated accuracy. There is an 11 °F difference between the thermocouple and camera temperatures at both points A and B.

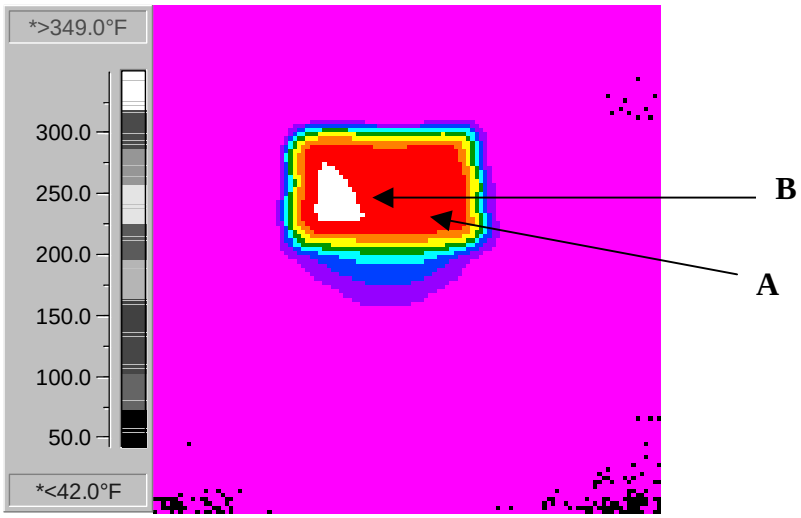

Figure 17. Hot Plate from 45° with Camera Height of 8 Feet.
Note: At point A and B, thermocouple shows temperatures of 324 °F; camera shows 313 °F. These discrepancies are greater than the limit of the camera's stated accuracy. At this angle a new emissivity determination would need to be performed.

Figure 18 shows the hot plate from a 30° angle with a camera height of 8 feet. The accuracy of the camera diminishes as the angle from the camera to the object is reduced. The camera shows a temperature 24 °F cooler than the surface thermocouple. Surface temperatures from the thermocouple are between 321 °F and 324 °F. The camera shows temperatures to be between 297 °F and 300 °F. This is well outside of the stated accuracy of the camera.

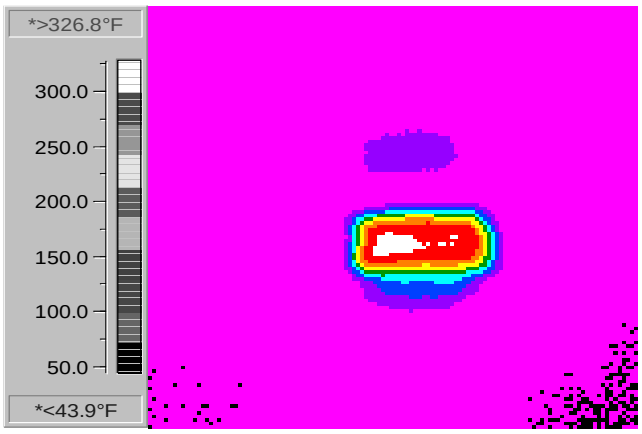

Figure 18. Hot Plate from 30° with Camera Height of 8 Feet.
Note: Thermocouple shows temperatures between 321 °F and 324 °F; camera shows 297 °F to 300 °F. Discrepancies are well outside of the stated accuracy range of the camera. At this angle a new emissivity determination would need to be performed.

IV. LABORATORY INVESTIGATION OF WIND EFFECTS ON INFRARED-DETERMINED TEMPERATURES

For the laboratory testing with wind effects, two hot plates were set at different temperatures and placed side by side. With no wind, one plate was set to have a surface temperature of approximately 315 °F. The other plate had a surface temperature around 280 °F. A camera height of 6 feet was used, and the images presented below are from a 60° angle. At this angle, camera temperatures were within the camera's accuracy range and usually varied from thermocouple temperatures by no more than 2 °F. At a 45° angle and less, the camera temperatures typically were not accurate for reasons previously presented. Figure 19 shows the basic setup and the wind speed being measured over one of the hot plates. It was not possible to get uniform wind speed over both of the plates; the wind speed actually varied even as the anemometer was moved across each plate. For this reason, the wind speed was determined by holding the anemometer in the center of each plate, which is where temperature measurements were taken with the thermocouple for comparison with the infrared camera.

Figure 19. Setup and Wind Speed Being Measured for Lab Testing with Wind.

A. Two Hot Plates with No Wind

Before performing any thermal imaging with wind, the two hot plates were imaged with no wind and the camera temperatures verified with the thermocouple. The camera temperatures were within 3 °F of the thermocouple temperatures. This image is shown in Figure 20. Also noted were significant temperature differentials on one of the plates. These differentials were likely the result of the second hot plate being much smaller than the plate to represent HMA that

was placed on top of it. Plates to represent the HMA were prepared to go on a 12-inch hot plate; however, only one 12-inch plate was available, and an 8-inch plate had to be used for the second test pad. The temperature differences on the second plate were verified with the thermocouple, as is shown in Figure 21.

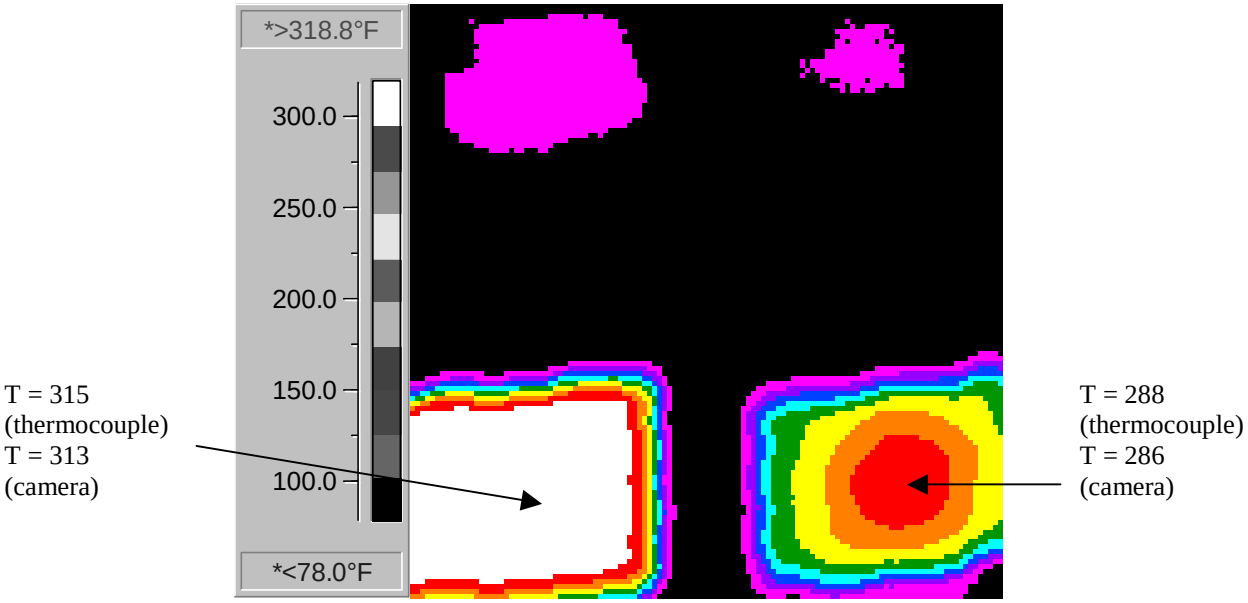

Figure 20. Two Hot Plates with No Wind.

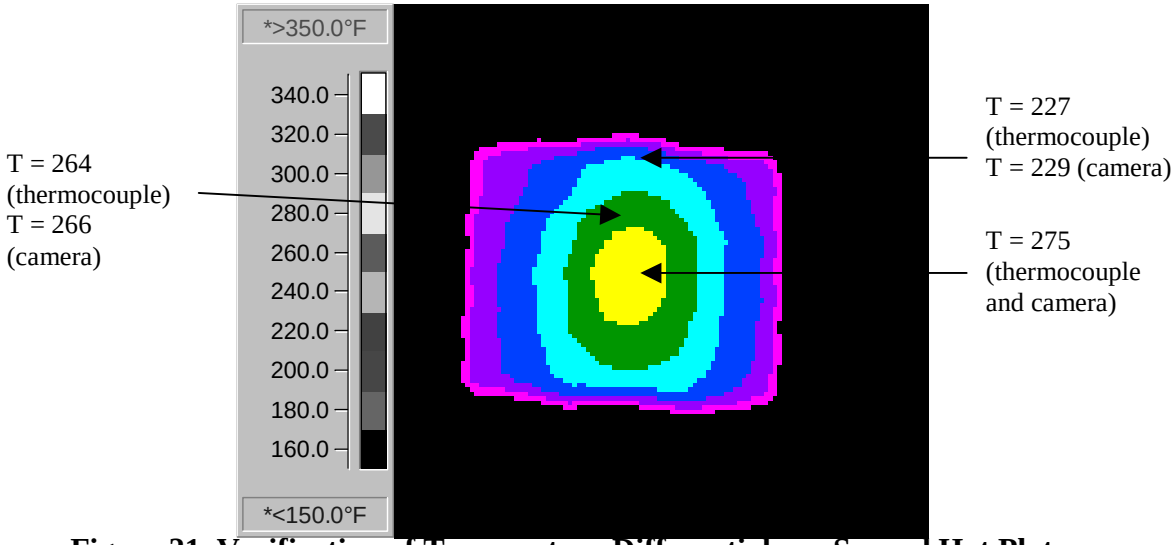

Figure 21. Verification of Temperature Differentials on Second Hot Plate.

B. Hot Plates with Wind Effects

Figure 22 shows the image of the two hot plates with the fan on low speed. The camera's temperatures were within 1 °F of the temperatures from the thermocouple. The average wind speed (averaged over 1 minute with the anemometer) over the plate on the left was 2.5 mph. The average wind speed over the plate to the right was 5.7 mph.

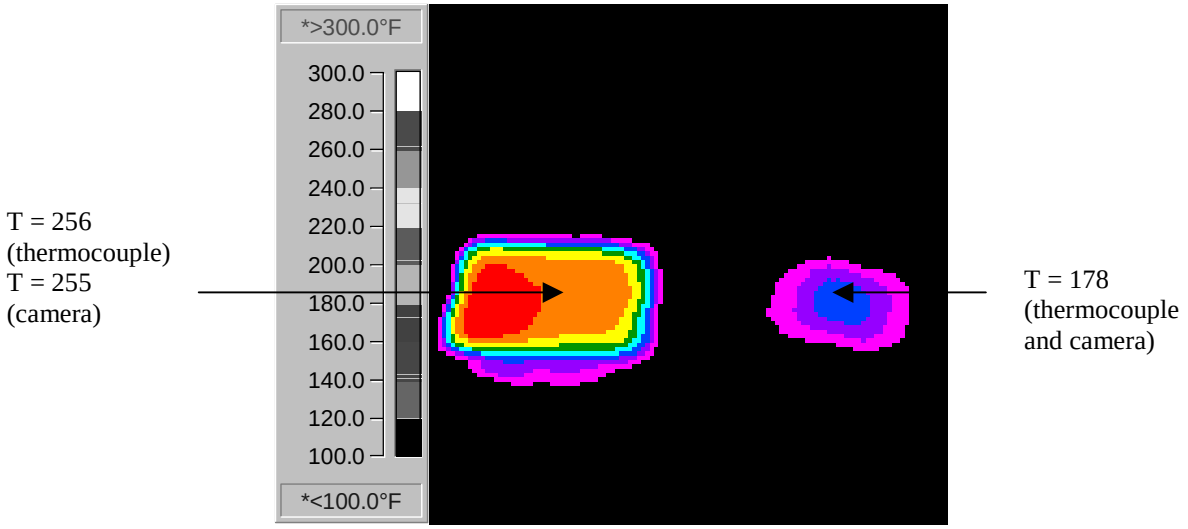

Figure 22. Image of Hot Plates with Low Wind Speed.
Note: Wind speed was lower on the left side of the plate on the left, which is where the red (hotter) strip is located.

With the fan on its medium setting, the average wind speed over the plate on the left was 6.1 mph; the average wind speed over the other plate was 7.1 mph. Camera temperatures were within 3 °F of the thermocouple temperatures, which is within the accuracy of the camera. Figure 23 is an image with medium wind speed.

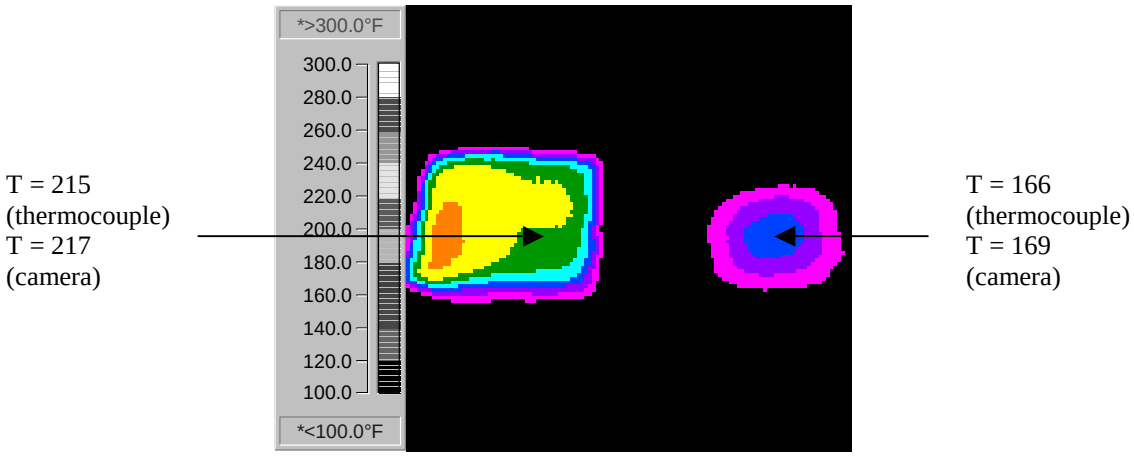

Figure 23. Image of Hot Plates with Medium Wind Speed.
Note: Wind speed was lower on the left side of the plate on the left, which is where the orange (hotter) strip is located.

With the fan on its highest setting, infrared temperatures were likewise within the stated accuracy of the camera. The wind over the center of the plate on the left was 6.4 mph; the right plate saw an average wind speed of 8.1 mph. Figure 24 shows the two plates when the fan was set on high.

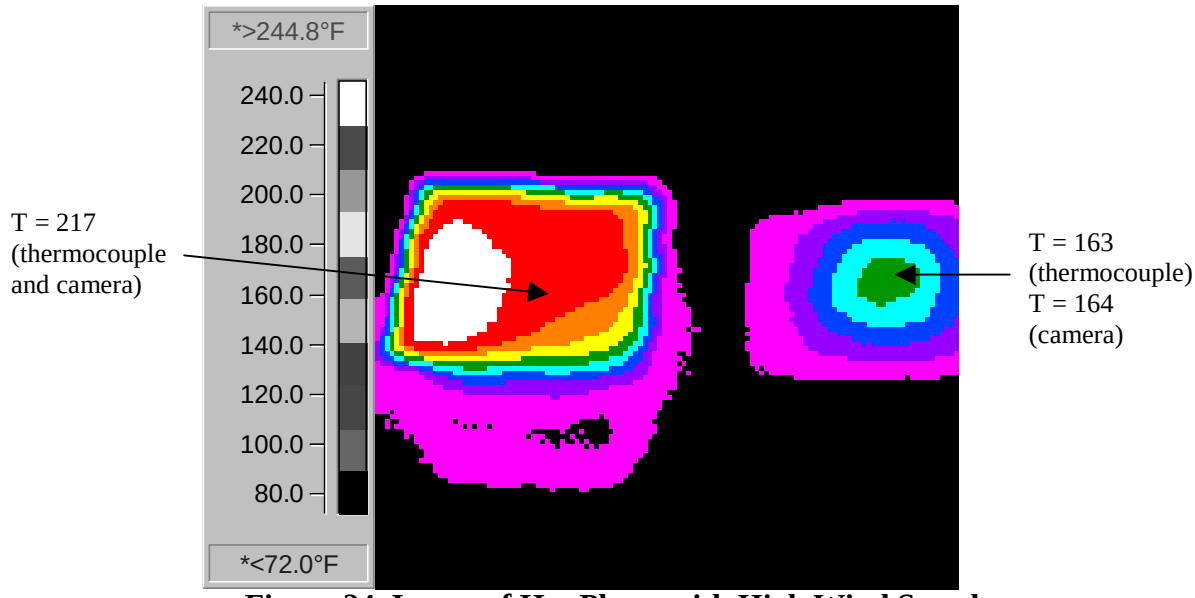

Figure 24. Image of Hot Plates with High Wind Speed.

V. IMPLICATIONS FOR FIELD TESTING

Based upon the controlled laboratory testing with infrared imaging, this technology is adequately accurate for use in the field as long as the necessary parameters (ambient air temperature and emissivity) are set correctly. Whether under windless conditions or with wind, the temperatures based on infrared imaging were generally within 3 °F of the temperatures from the thermocouple, as long as the limits of the technology were not exceeded. However, as was shown in the lab, temperatures based on infrared imaging are influenced by the angle of the camera to the target. Some practical implications from these experiments are:

- The emissivity of the target should be determined with the camera at the angle that will be used for testing. This determination can be performed by using a calibrated thermocouple to measure the temperature of the mix at the surface, taking an infrared image of this location, then adjusting the emittance setting on the camera until the temperature from the camera matches the temperature from the thermocouple.
- It is likely not wise to perform imaging of HMA from the paver looking back, as is sometimes suggested. In the image, the angle from the camera to the mat will gradually decrease as the distance to the mat increases, likely resulting in increasing errors in temperatures at spots farther away in the image.
- The emittance of a material increases as the texture becomes rougher; thus, freshly placed HMA should be somewhat forgiving as to changes in camera angle. However,

avoid angles of less than 45° unless the emissivity is checked and adjusted as necessary.

CHAPTER 4

FIELD DATA COLLECTION AND ANALYSIS PROCEDURES

I. PROTOCOL DEVELOPMENT

In order to efficiently examine the overlays being placed, a test protocol was needed so all members of the research team would be familiar with the process before arriving at the field. As such, a testing protocol was outlined based upon the practices of Washington state, recommendations from the NCAT study, findings from testing the accuracy and limitations of the infrared imaging technology in the laboratory, and the data requirements needed to produce two-dimensional surface plots of the predicted air voids of the mat from GPR data.

II. FIELD TESTING PROTOCOL FOR DATA COLLECTION

1) Note the contractor, location, mix type, approximate overlay thickness, and equipment being used (take photos if possible). Also if possible find out how far the mix is being hauled. Note the method being used to place the mix (belly dump, end dump, windrows, dump directly into hopper, material transfer vehicles (MTVs), etc.).
2) Choose a 1000-foot test strip. Also choose a location far enough ahead of the paving train to allow at least one hour of setup time.
3) With a survey wheel, mark every 100 feet of the test strip. Place the marks in a location on the pavement such that they will not be paved over and covered when the section is imaged.
4) With the thermocouple, spot radiometer, and infrared camera, determine the emissivity setting necessary for the IR devices. Do this test by measuring the mat temperature with a calibrated surface thermocouple, then quickly measure the temperature of that same spot with the IR devices and adjust the emissivity setting until the IR temperature is the same as the temperature measured with the surface thermocouple. Typically for hot mix, a setting between 0.90 and 0.98 is appropriate. Also note the placement temperature of the mix. Knowing the typical placement temperature will aid in deciding upon a temperature span to use on the IR camera.
5) When the paving train is approximately 15 minutes from reaching the start of the test strip, note:

    - sky conditions,
    - ambient air temperature,
    - average wind speed (averaged over about three to five minutes), and
    - double check temperature of mix being placed.

6) Set the necessary parameters on the IR camera (ambient air temp, desired color scheme, desired span, emissivity) and radiometer (emissivity).
7) If desired, start imaging approximately 50 feet before the start of the test section so the imaging crew can get synchronized with each other. Imaging is done with three people (a driver, infrared imager, and radiometer operator). A suggested sequence is as follows:

i. The imager is positioned in the back of a pickup truck to yield an angle from the IR camera to the mat of approximately 45°. The radiometer operator walks alongside the mat being placed between the truck and the mat.

ii. The truck is driven alongside the mat being placed. The IR images are acquired transversely to the mat (with the truck stationary) just as the screed passes and before any rollers have been on the mat. With the camera in the spot mode, the imager examines for temperature anomalies. The radiometer operator simultaneously scans the mat to investigate for temperature anomalies. Infrared imaging is shown in Figure 25.

iii. The imager and radiometer operator discuss their findings and concur on where, if at all, any significant temperature differentials exist. If they do, the radiometer operator marks the location with paint and the driver makes a note of the location number, approximately how many feet into the test section the location is located, the area of the mat with the anomaly (centerline, left wheel path, etc.), and the approximate temperature differential in the anomalous area from the "normal" temperature.

Figure 25. Infrared Imaging in Progress.

8) Imaging is continued throughout the entire test section as described in step 7. In addition to anomalous areas, at least two uniform "normal" areas of the mat should be marked. The imager should periodically check the ambient air temperature during imaging and readjust the camera setting if necessary.
9) After the test section is completed, take another three to five minute average wind speed measurement. Note the final ambient air temperature and weather conditions.
10) Allow the test strip to cool approximately two hours. During this waiting period, the following activities should be performed:

- Review the IR data.
- Set up the GPR van.
- If available, anomalous areas can be investigated with density measuring devices.

11) At the start of the test strip, mark starting locations with paint for the GPR antenna above the "zero" point at locations 1 foot from the outer edge, right wheel path, centerline, left wheel path, and 1 foot from the inner edge of the mat.
12) Take GPR data at intervals of 1 foot per trace at each of the above referenced locations longitudinally through the test strip.
13) Collect the metal plate file.
14) Play back the GPR data and review it for anomalies in surface dielectric. Check to see if areas where the IR data showed anomalies are likewise anomalous in the GPR data.
15) With the GPR in real-time measurement mode, examine the potential problem areas identified in step 14 for abrupt drops in surface dielectric. When and if such locations are found, mark them with paint. At least three areas of low dielectric and three areas of normal dielectric should be marked. Ideally, the low dielectric areas will correspond with low temperature areas from the IR data.
16) Collect a stationary GPR reading (collected in time mode) above each of the marked locations.
17) Collect density data on each marked location with the nuclear density gauge (three one-minute readings) and/or any other density measurement device available.
18) Take at least two 6-inch cores from both normal (good) and low (bad) dielectric/temperature locations. Return these cores to the lab for testing.
19) As a minimum, test the cores for the following: bulk density, Rice gravity, percent asphalt, and gradation. Surface texture, permeability, and rutting with the asphalt pavement analyzer (APA) were also conducted in this project. Resilient modulus testing was planned but was found infeasible due to the size of the cores. Determine the air void content of each core. The core data can then be used to examine for relationships between changes in NDT data and changes in mix properties.
20) Using the stationary GPR readings, determine the surface dielectric of each core with Colormap.
21) Determine the relationship between surface dielectric and air void content from the data in step 19 and step 20. The natural log of the air void content is the dependent variable, and the corresponding dielectric value is the independent variable. Regress the natural log of the air voids on a constant and the dielectric value. This will yield the relationship:

    ln(Air Voids) = constant + slope*dielectric, which transforms to:

    $\%\ \text{Air Voids} = A * e^{B * \text{Surface Dielectric}}$ (*6*, *21*)

22) Using Colormap, generate a text file of the summary statistics for each GPR pass. Insert a column into each of these files with the appropriate transverse offset for that pass.
23) Combine the summary statistics files from all the GPR passes to yield a file with three columns. Column one should be the longitudinal distance of the GPR trace. Column two

should be the transverse offset for that trace. Column three should be the surface dielectric for that trace.

24) Using the relationship developed in step 21, predict the air void content for each trace. Save this data as a text file.
25) Reopen the file saved in step 24 and delete column 3 (the column with surface dielectrics), replacing it with the column of predicted air voids. Save this file as a text file. It will be used in Surfer Version 6.04 to develop a surface plot of the predicted voids in the hot-mix mat.
26) Open Surfer and go to the worksheet view by selecting FILE \ NEW \ WORKSHEET. Open the file created in step 25 by selecting FILE \ OPEN. Save this file in *.DAT format by selecting FILE \ SAVE AS then enter a file name. Return to the Plot View by clicking on WINDOW \ PLOT 1.
27) In Plot View, use the GRID command to generate a *.GRD file from the file created in step 26. Do this by selecting GRID \ DATA; then select the appropriate file. The file created in this step is called a grid file and is necessary for Surfer to generate the surface plot.
28) Generate the surface plot of the predicted air voids of the map by using the PLOT \ CONTOUR command, and select the file generated in step 27.

CHAPTER 5

SH 6 INVESTIGATION

I. SUMMARY

Starting at Texas Reference Marker 602, a 1000 foot test strip in the southbound inside lane was tested with the procedure outlined in Chapter 4. Infrared data was collected on May 16, 2001, and GPR testing and coring was conducted on June 18, 2001. From the IR data, the maximum observed temperature differentials were 25 °F. This differential would be in NCAT's low level of segregation. From the GPR data and relationship developed between GPR dielectric and mat air voids, the test section air voids had a minimum of 7.7 percent, maximum of 9.3 percent, and an average of 8.7 percent. Figure 26 shows the site location.

Important findings from this job include:

- Changes in temperature were significantly correlated to changes in GPR ε, density, texture depth, Rice gravity, air voids, asphalt content, changes in the percent passing of three sieve sizes, and changes in the percent retained on three sieve screens.
- Changes in GPR ε were significantly correlated to changes in temperature, density, permeability, Rice gravity, air voids, asphalt content, changes in the percent passing of six sieve sizes, and changes in the percent retained on six sieve screens.
- In general this mat was placed at a uniform temperature and density.
- A new joint construction method used at this job worked well. The maximum void differential between the joint core and the main lane cores was 1.5 percent.

Figure 26. SH 6 Test Site Starting at RM 602.

II. PAVING PARAMETERS AND ENVIRONMENTAL CONDITIONS

The overlay being placed was a CMHB-C and was approximately 2 inches thick. This is the final surfacing on this portion of SH 6. The mix was placed by first being dumped into a Roadtec Shuttle Buggy 2500, which then remixed and transferred the mix to a Caterpillar AP 1000 B paver. At the time the test section was placed, skies were partly cloudy, the ambient air temperature was 81 °F, and the average wind speed was 3.7 mph.

III. INFRARED IMAGING SETTINGS

The ambient air temperature of 81 °F was input into the camera's settings. The Rainbow 10 color scheme was used, and a temperature span of 200 °F to 350 °F was set to provide 10 colors each representing a 15 °F range. Using the surface thermocouple to measure temperature, it was found that an emissivity setting of 0.97 was appropriate for obtaining accurate infrared temperature measurements with the camera and radiometer.

IV. RESULTS FROM INFRARED IMAGING

In the 1000 foot section tested, three locations were identified with infrared imaging that showed temperature segregation. All of the observed temperature differentials would be in NCAT's low level category of segregation. Figure 27 is 319 feet into the test section. In the left wheel path is a hot spot with a temperature of approximately 277 °F. The rest of the mat has temperatures of approximately 257 °F. At 679 feet into the test section a temperature differential of approximately 20 °F was observed in the centerline. The majority of the mat was 287 °F, while the centerline was approximately 267 °F. The infrared image of this location is in Figure 28. Temperature segregation of 25 °F was seen at 797 feet into the test section. The cold area was again in the centerline of the pavement mat. The centerline temperature was generally around 284 °F, while part of the mat at the right wheel path showed temperatures of 308 °F to 310 °F. Figure 29 shows the temperature differentials at this location. In all other images of the test section, no temperature differentials of significance were observed. Figure 30 shows a representative image for such sections. This image was taken 100 feet into the pavement test section. The maximum temperature difference in this image is 16 °F. In this image the mean temperature is 257 °F, the minimum temperature is 247 °F, and the maximum temperature is 263 °F.

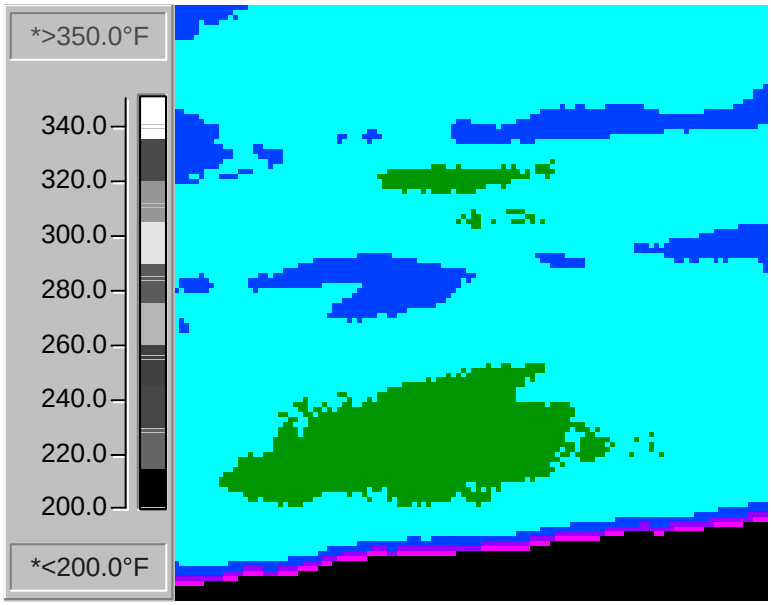

Figure 27. Temperature Differentials of 20 °F 319 Feet into SH 6 Test Site.

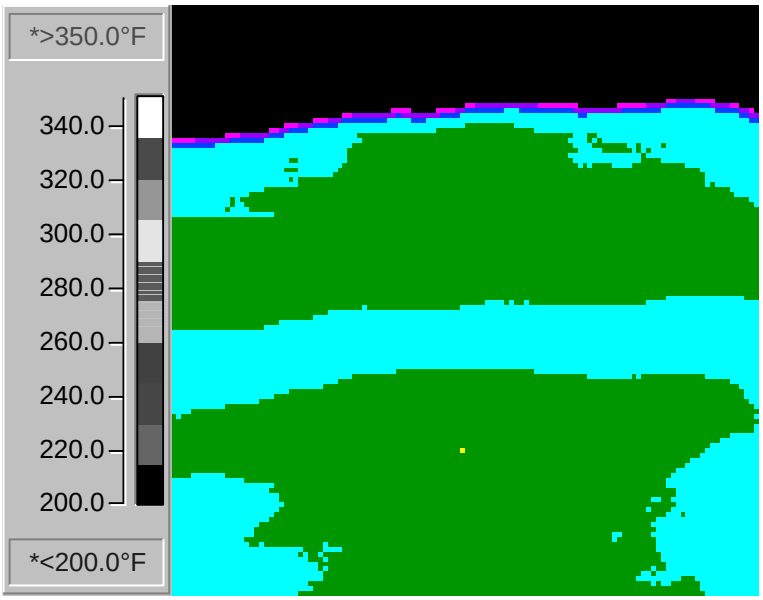

Figure 28. Temperature Differentials of 20 °F in Centerline at 679 Feet in SH 6 Test Section.

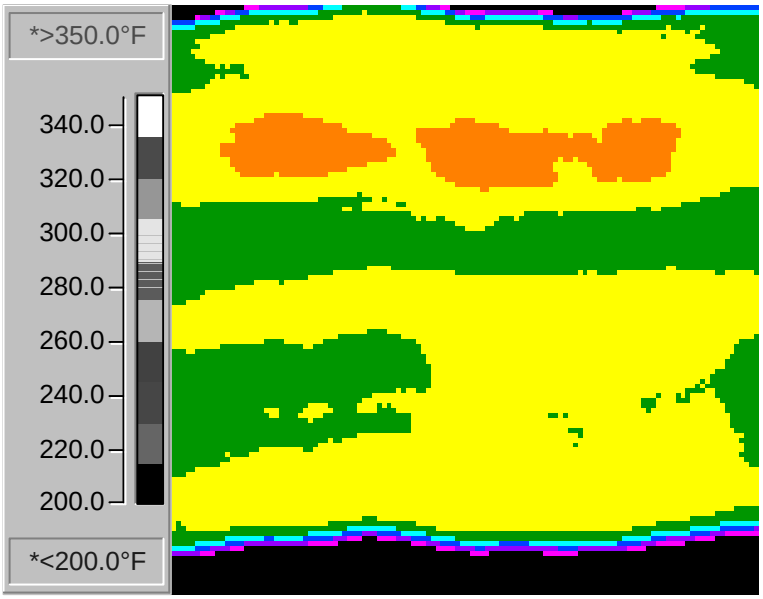

Figure 29. Temperature Differentials of 25 °F at 797 Feet into SH 6 Test Site.

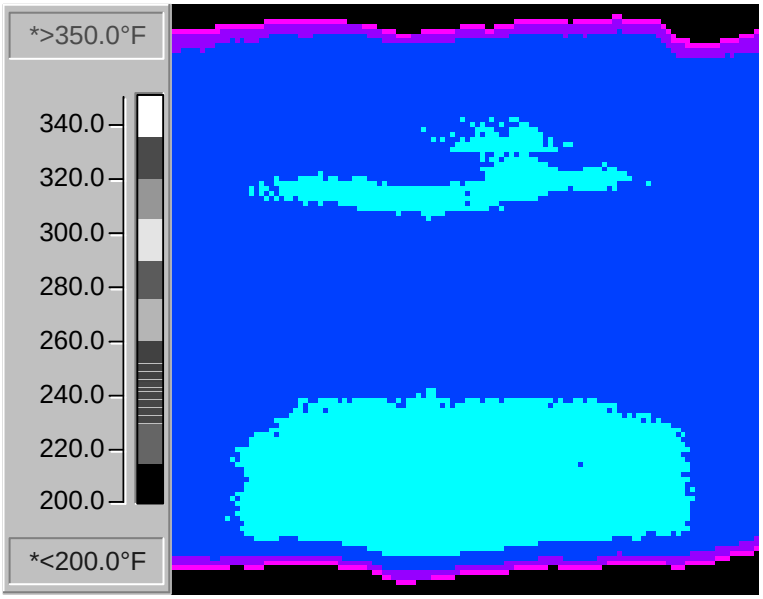

Figure 30. Representative Image of Uniform Pavement Mat on SH 6.

V. RESULTS FROM GROUND-PENETRATING RADAR

Five ground-penetrating radar passes were performed on June 18, 2001. The GPR showed the cooler centerline previously shown in Figure 29 to be lower than the typically observed dielectric for this job. Thus, coring was conducted at this location, with "normal" cores taken a short distance further down the test strip. From laboratory analysis of cores where stationary GPR readings were taken, the following relationship between air voids and GPR dielectric was estimated for the overlay on SH 6:

$$\ln(\text{Air Voids}) = 2.9948 - 0.14454\varepsilon \qquad R^2 = 0.8694$$
$$(0.2312) \quad (0.03962) \qquad \text{(s.e)} \qquad \hat{\sigma} = 0.0282$$

which transforms to:

$$\% \text{ Air Voids} = 19.982 * e^{(-0.1445\varepsilon)}$$

Based upon this relationship, predictions of air voids and density (based on average Rice gravity) were made for each of the approximately 5,000 GPR readings, resulting in the statistics shown in Table 6.

Table 6. Predicted Mat Statistics for SH 6 from GPR Data.

Parameter	Average	Minimum	Maximum	Standard Deviation
Density	139.1 lb/cf	138.2 lb/cf	140.6 lb/cf	0.437
% Density	91.3	90.7	92.3	0.287
% Air Voids	8.68	7.70	9.29	0.287

From the standpoint of assessing mat uniformity, a simple and appealing approach is to create a graph of the probability distribution of parameters of interest. For example, the distribution of percent air voids, based upon the above model, for the test section on SH 6 is shown in Figure 31. An example of how this would be useful is in determining bonuses or penalties. If bonus starts at air voids of 8 percent or less, it is easy to read off the graph that approximately 1 to 2 percent of the section had voids less than or equal to 8 percent. This approach is also more appropriate than using the mean and standard deviation for statistical inferences because the cumulative probability distribution is generated solely from data collected, whereas using the mean and standard deviation to make statistical inferences assumes the distribution is normal. The data set of predicted air voids was tested for normality, and at the 95 percent confidence level the null hypothesis that the distribution was normal was rejected.

Data collected from the five passes with GPR also make it possible to create a two-dimensional surface plot of the estimated air voids for the overlay. For this particular job, the range of air voids was quite small (7.7 percent to 9.3 percent). Regardless, the surface plot is useful for rapidly being able to locate areas of differences in the mat. The surface plot of predicted air voids for the SH6 test section is shown in Figure 32.

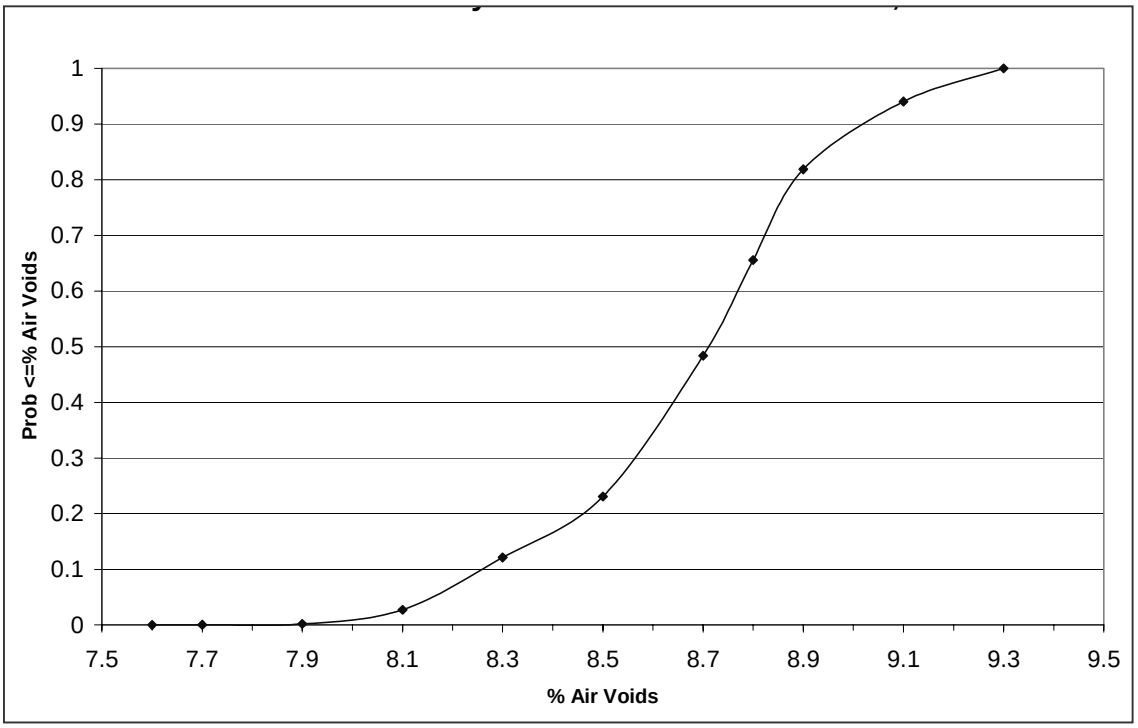

Figure 31. Distribution of Air Voids for SH 6 Test Section.

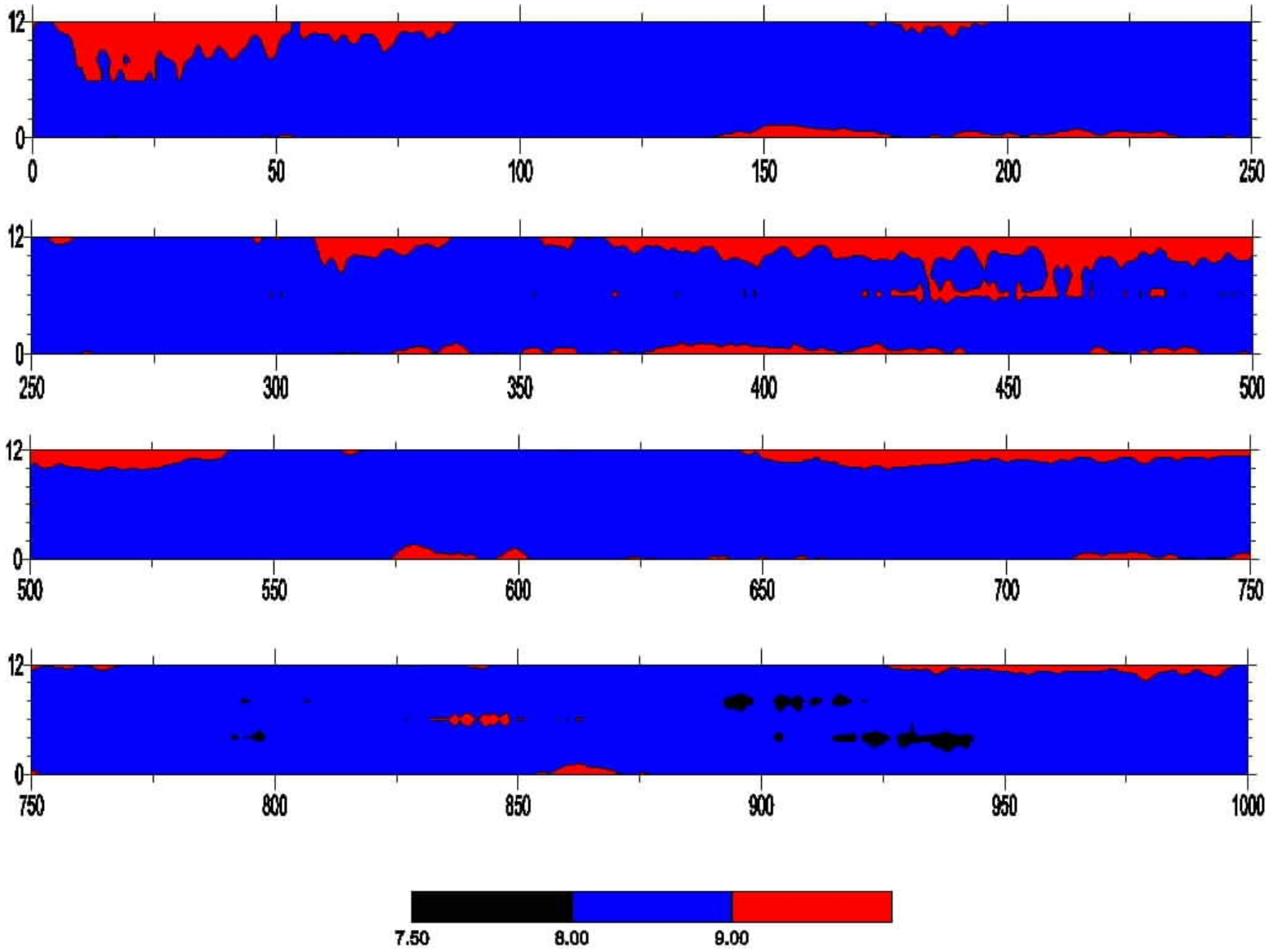

Figure 32. Surface Plot of Air Voids for SH 6 Test Section.

VI. RESULTS FROM CORES

Cores were taken from the test section based upon the locations of the most significant changes in temperature and surface dielectric. A laboratory test sequence was performed which included bulk density, surface texture depth, permeability, rut depth after 8000 passes of the Asphalt Pavement Analyzer, Rice gravity, percent air voids, percent asphalt, and gradation. All results except for gradation are presented in Table 7, with gradation results shown in Table 8 and Figure 33.

Core H3 was an 8 inch diameter core for trial in TTI's overlay tester. However, this testing was found infeasible, as the surface area of the core available for gluing to the testing frame was not adequate. A new joint construction method was used at this job. The joint core gives evidence to the effectiveness of this new construction technique, as the joint core did not have significantly higher voids than any of the other cores taken.

Table 7. Core Results from SH 6 Test Section.

Core	Temp (F)	GPR ε	Bulk Density (pcf)	Texture Depth (in)	Permeability (cm/s)	Rut Depth (8000 passes, mm)	Rice Gravity (pcf)	Air Voids (%)	Asphalt Content (%)
H1	292	6.1	139.28	0.038	0.001667	5.507	152.214	8.49725	4.46
H2	294	6.2	139.53	0.019	0.001634	2.675	151.549	7.93077	4.34
H3	*	6.1	138.78	0.041					
L1	283	5.7	139.21	0.041	0.001649	4.73	152.643	8.80027	3.52
L2	*	5.3	138.71	0.036	0.001749	2.881	152.864	9.25921	3.33
Joint	*	**	137.84	0.044	0.002102	6.132	152.265	9.47362	3.14

Note: Design asphalt content was 4.2%

*Core location selected solely from GPR. No temperature data available.

**GPR data not available due to close proximity to lane under traffic.

Table 8. Gradations for SH 6 Cores.

Core	H1	H2	L1	L2	Joint	JMF
Passing 3/4	100	100	100	100	100	100 (7/8 inch)
Passing 1/2	89.3	85.6	85.6	86.9	86.3	98.6 (5/8 inch)
Passing 3/8	77.4	74.9	71.9	73	73.6	68
Passing #4	48.8	47.7	44	46.2	45.1	40.3
Passing #10	22.8	22.5	22.6	21.8	22.5	20
Passing #40	13.9	13.9	14	13.7	14.7	12.8
Passing #80	8.9	9	9	9.3	10	7.7
Passing #200	6.7	6.9	6.9	7.3	7.9	6.1

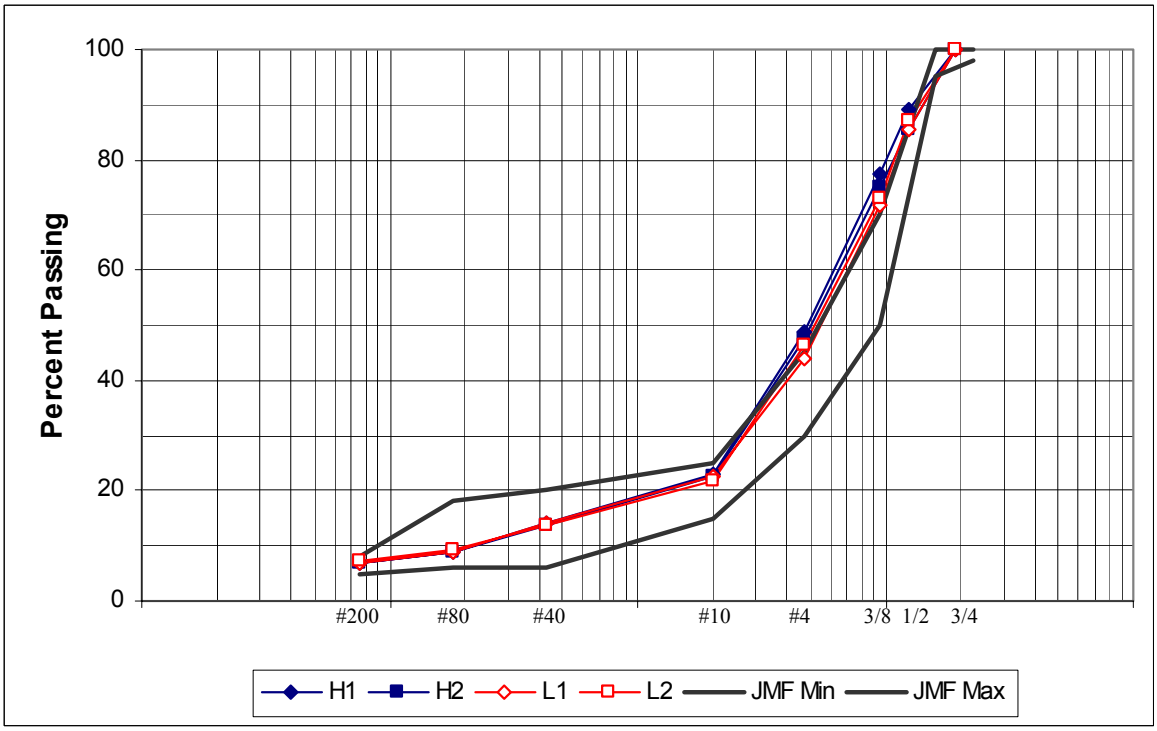

Figure 33. Gradation Results from SH 6 Test Section.

Based upon the values and narrow range of observed and predicted air voids at this job, it appears compaction was adequately taking place. Also of significance is the effectiveness of the new joint construction design used. The joints were only about 1 pound per cubic foot less than the typical mat densities, easily passing TxDOT's SS3146 joint specification of a maximum drop in density at the joint of 3 pounds per cubic foot. However, the mix was running on the fine side beyond the grading limits on the 1/2 and 3/8 inch sieves and was substantially finer than the job mix formula (JMF). Three out of four cores were out of the grading limits on the #4 sieve, again on the fine side. The asphalt content of the low temperature/low dielectric cores was more than the ± 0.3 percent tolerance from JMF allowed by SS 3146. Thus, even though the range of air voids was quite small, there were some quality control issues observed at this job, namely changes in asphalt content, as previously discussed, and to some extent gradation, as shown in Figure 34, where the number of sieves with a change of greater than 3 percent retained are graphed against change in temperature. Figure 34 illustrates that with greater temperature changes, there was a greater change in gradation.

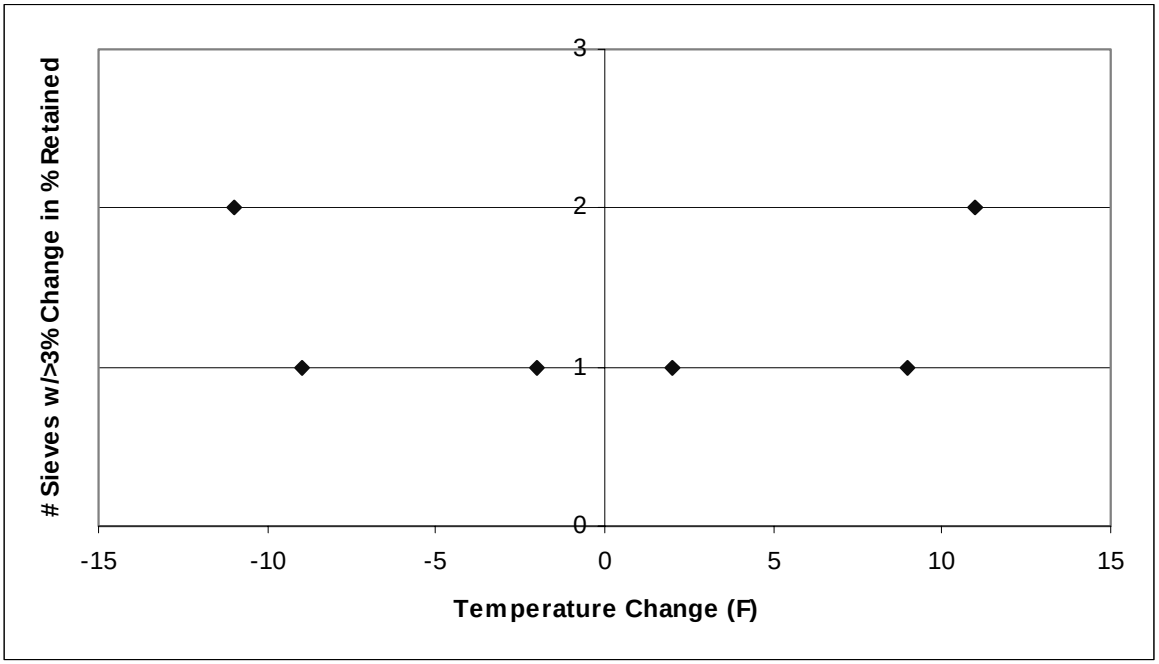

Figure 34. Number of Sieves with Greater than 3% Change in Percent Retained for SH 6.

VII. RELATIONSHIPS BETWEEN CHANGES IN TEMPERATURE AND DIELECTRIC AND CHANGES IN MIX PARAMETERS

The first step in assessing the ability of the NDT devices to indicate significant changes in HMA properties is to determine if a significant correlation exists between changes in the NDT data and changes in important HMA properties. To accomplish this, researchers first differenced the NDT and laboratory data between cores. For example, subtracting the temperature of Core 2 from the temperature of Core 1 results in a temperature differential between these two cores. Then, subtracting the void content of Core 2 from the void content of Core 1 yields the corresponding air void differential. Data for all combinations of cores from the job were differenced in this manner to yield a matrix of temperature differentials, dielectric differentials, and the corresponding differentials of the HMA properties. Researchers then determined the correlation value between changes in the NDT data and changes in each HMA property measured (for example, the correlation between temperature differentials and air void differentials). Researchers only considered those correlations that were statistically different from zero (at the 95 percent confidence level) as significant.

Some of the more noteworthy non-zero correlations are presented in Table 9. The complete correlation matrices are presented in Appendix A. Since SS 3146 tolerances are based on density (if the density profile is in effect), asphalt content, and gradation, some items are of particular note:

- Changes in both temperature and dielectric are highly correlated with changes in air voids.
- Correlations between changes in NDT data and changes in percent asphalt were high.

- Correlations between changes in NDT data and changes in the individual percent retained on certain sieve sizes were high.

In addition, it is noteworthy that changes in temperature and changes in GPR dielectric correlated perfectly.

Table 9. Selected Significant Correlations between Data for SH 6.

	ΔTemp (F)	**Δ GPR ε**
Δ Temp (F)	1.00	1.00
Δ GPR ε	1.00	1.00
Δ Bulk Density (pcf)	0.79	0.60
Δ Air Voids (%)	-0.87	-0.95
Δ Asphalt Content	0.96	0.95
Δ Permeability (cm/s)		-0.84
Δ % Retained on 3/8	-0.97	-0.91
Δ % Retained on #4		0.57
Δ % Retained on #10	0.94	0.45
Δ % Retained on #40		0.83
Δ % Retained on #80	-0.64	0.69
Δ % Retained on #200		0.79

Based upon SS 3146, the maximum change in temperature and dielectric before the mix could be out of specification was investigated by regressing the observed changes in each mix parameter on the observed change in temperature or dielectric, as appropriate, for each instance that showed a significantly different from zero correlation. The independent variables in all instances were change in temperature and change in dielectric. These regressions are presented in Appendix A. The value of the temperature or dielectric change that would result in a change in hot-mix parameters equal to the allowable tolerance from SS 3146 was then calculated from the regression slope.

For the tolerance on air voids, the high to low density range of 8.0 lb/cf was translated into percent voids based upon cores' average Rice gravity. Table 10 shows the results of this analysis. Although SS 3146 specifies gradation tolerances as deviations from individual percent retained, limits are also presented for changes in percent passing (based upon Item 340 tolerances) since most previous work (namely the NCAT study) on identifying segregation has focused on changes in percent passing.

Table 10. Limits on Changes in Temperature and Dielectric before Mix Parameter Changes Are at Tolerance Limit.

Mix Parameter	Tolerance	ΔTemp Limit (F)	Δ GPR ε Limit
Δ Air Voids (%)	Range of 5.2*	80	4.0
Δ Asphalt Content	± 0.3	3.6	0.22
Δ % Passing 3/8	± 5	13	1.2
Δ% Passing #4	± 5	13	1.6
Δ % Passing #10	± 5		5.8
Δ % Passing #40	± 3	309	16.5
Δ % Passing #80	± 3		8.2
Δ % Passing #200	± 3		5.7
Δ % Retained on 3/8	± 5	19.5	1.4
Δ % Retained on #4	± 5		4.6
Δ % Retained on #10	± 5	12.6	2.3
Δ % Retained on #40	± 3		4.2
Δ % Retained on #80	± 3		6.3
Δ %Retained on #200	± 3		19

*Based on Cores' Average Rice Gravity and SS 3146 Density Profile Specifications

Clearly, some of these limits in Table 10 are quite unrealistic, indicating that although a statistically significant relationship did exist, the magnitude of the relationship (i.e., the slope of the regression line) was quite small. Furthermore, the maximum observed temperature differential where cores were taken was 11 °F, and the maximum change in dielectric of cores was 0.9. Thus, any limits beyond these values are essentially out of sample and subject to much higher uncertainty. Nevertheless, the data indicates a very real relationship between the NDT data, changes in asphalt content, and changes in certain gradation parameters. The data further supports the theory that the segregation at this job was primarily asphalt content and gradation changes. The asphalt content of the low temperature/low dielectric cores was out of the allowable tolerance from SS 3146.

Based upon the results presented in Table 10, the following limits for changes in temperature and GPR dielectric appear reasonable from this job:

Temperature: All values within ±12.5 °F of the mean; maximum range of 25 °F. Clearly, despite the significant changes in asphalt content with only a slight change in temperature, a range limit of 3.6 °F is quite unrealistic from a specification standpoint. In addition, since specifications are based on changes from JMF, this limit would assume that either the highest or lowest temperature spot was at JMF asphalt content, which is an unlikely scenario. The limited number of cores at this job would make such a limit even more questionable. However, the limits in Table 5 for changes in percent retained are reasonable. Although this job was running on the fine side outside of specification tolerances on several sieve sizes, for development of general specifications on NDT data it should be assumed that average NDT readings are representative of JMF hot mix. Thus, the tolerance is based upon the relationship between changes in temperature and changes in the percent retained on the #10 sieve.

GPR ε: All values within ± 0.25 of the mean; maximum range of 0.5. The GPR dielectric was most highly correlated to air voids and asphalt content. From Table 5 it can be seen that this parameter was much more responsive, as far as specification limits go, to changes in asphalt content on this job. However, a limit of 0.2 on the dielectric range is quite stringent. This would assume either the high or low dielectric is at JMF asphalt content, which is unlikely. The high dielectric cores at this job had asphalt contents above JMF, and the low dielectric core had an asphalt content below JMF. A tolerance of ± 0.25 of the mean is reasonable because, assuming the mean dielectric is representative of JMF asphalt content, data from this job indicates changes in dielectrics of more than 0.25 would be expected to indicate a change in asphalt content that is beyond the allowable tolerance of SS 3146. A maximum range of 0.5 is consistent with other studies that have indicated a change of 0.5 can be significant and reinforces the tolerance limit.

VIII. CONCLUSIONS

The paving job on SH 6 SB appeared quite uniform when inspected, both with the infrared and GPR. However, core testing revealed that significant changes were likely occurring in the mat, particularly with the asphalt content of the mix. With the limited number of cores, it is unknown if such drastic changes in asphalt content would likely be observed at every location where temperature drops were observed.

Despite the appearance of uniformity with NDT, significant changes in mix parameters are possible. In addition, it is important to note that significant changes in asphalt content were observed, even though drastic changes in gradation were not seen. Thus, the following conclusions from this job are made:

- NDT tools were effective at finding mat irregularities.
- Changes in NDT data thought to be negligible based upon previous work actually revealed significant changes in asphalt content. Thus, NDT limits could be job-specific.
- The appearance of homogeneity from the use of MTVs may be misleading, as substantial changes in hot-mix asphalt content were observed despite the original belief that the job was uniform.
- Substantial changes in asphalt content can exist without substantial changes in gradation. This contrasts the NCAT study where a decrease in asphalt content of 0.75 percent to 1.3 percent is expected to be accompanied by at least two sieve sizes being at least 10 percent coarser.

CHAPTER 6

US 79 INVESTIGATION

I. SUMMARY

A CMHB-C overlay being placed on the northbound lane of US 79 was imaged on August 7, 2001. The 1000 foot test section was marked off starting just north of Cal Davis Road. Figure 35 shows the site. The shoulder was being placed simultaneously with the main lane, yielding a mat approximately 21 feet wide. Research efforts were focused on the main lane.

From the IR data, the maximum observed temperature differentials of the operation were 25 °F. In addition, there were two locations where the paver stopped, one of which exhibited mix temperatures as much as 80 °F below the temperature the mix was normally placed. However, the voids in these areas did not appear to be significantly different than the mat as a whole. GPR and coring was conducted on September 13, 2001. From the GPR data and relationship developed between GPR dielectric and mat air voids, the test section air voids in the main lane had a minimum of 6.5 percent, maximum of 13.4 percent, and an average of 10.4 percent.

Important findings from this job include:

- Changes in temperature were significantly correlated to changes in GPR ε, density, permeability, Rice gravity, air voids, changes in percent passing of four sieve sizes, and changes in percent retained on two sieve sizes.
- Changes in GPR ε were significantly correlated to changes in temperature, density, permeability, Rice gravity, air voids, changes in percent passing of four sieve sizes, and changes in percent retained on one sieve size.

Figure 35. US 79 Test Site Location.

II. PAVING PARAMETERS AND ENVIRONMENTAL CONDITIONS

The overlay being placed on US 79 was a CMHB mix and was approximately 2 inches thick. The mix was dumped directly into a Roadtech Shuttle Buggy 2500, which then remixed and transferred the mix to a Caterpillar AP 1000B paver. A mat 21 feet wide was being placed, as the shoulder was being pulled with the main lane. The same paving crew and equipment used on the SH 6 job placed this job. At the time of testing, skies were clear, the ambient air temperature was 101 °F, and the average wind speed was 0.6 mph. The paving train is shown in Figure 36.

Figure 36. Paving Train on US 79.

III. INFRARED IMAGING SETTINGS

The ambient air temperature of 101 °F was set in the camera. The Rainbow 10 color scheme was used with a temperature span from 200 °F to 350 °F. An emissivity setting of 0.95 on the camera was determined appropriate to match camera temperatures to mat surface temperatures measured with the thermocouple.

IV. RESULTS FROM INFRARED IMAGING

In the 1000 foot test section, five locations were observed to have temperature drops that would be considered significant under the NCAT developed recommendations. All of these locations would be in the NCAT low level of segregation category. In addition, the paver stopped two times in the test section. These sites were marked for further investigation.

Figure 37 is at 200 feet into the test section. The centerline shows to be approximately 20 °F cooler than the rest of the mat. Figure 38, at 220 feet, shows a maximum temperature drop of 25 °F from the right edge of the lane to the left wheelpath. At 360 feet, the paver stopped. When started again, the mix that had been under the paver had cooled to between 226 °F to 242 °F. This location is shown in Figure 39 and passed a density profile test that was subsequently performed with an average to low density range of 2.9 lb/cf and a high to low density range of 4.7 lb/cf. Four cores were eventually taken from the location shown in Figure 40, with low dielectric cores coming from the cool centerline and high dielectric cores coming from the hotter area on the right edge of the main lane. Figure 41 is at 790 feet into the test section and shows a maximum temperature change of 25 °F from the aqua areas to the areas that are yellow. In the left side of Figure 42 is a region of the mat where the paver had been stopped (860 feet), which is 25 °F to 30 °F cooler than the temperature the mix is at after the paver started moving again. Temperature differentials of 25 °F were observed at 895 feet, shown in Figure 43. Figure 44 is at 500 feet and is where "normal" cores were taken.

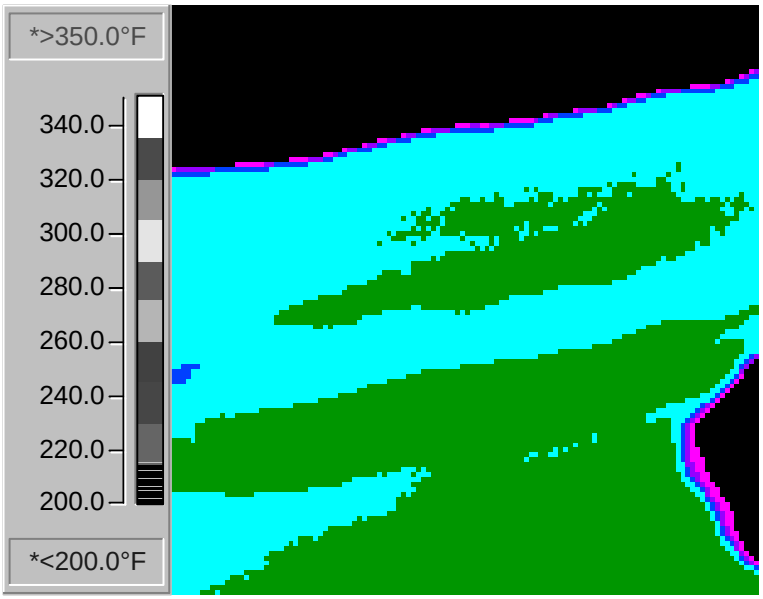

Figure 37. Cool Centerline at 200 Feet on US 79 with Temperature Drop of 20 °F.

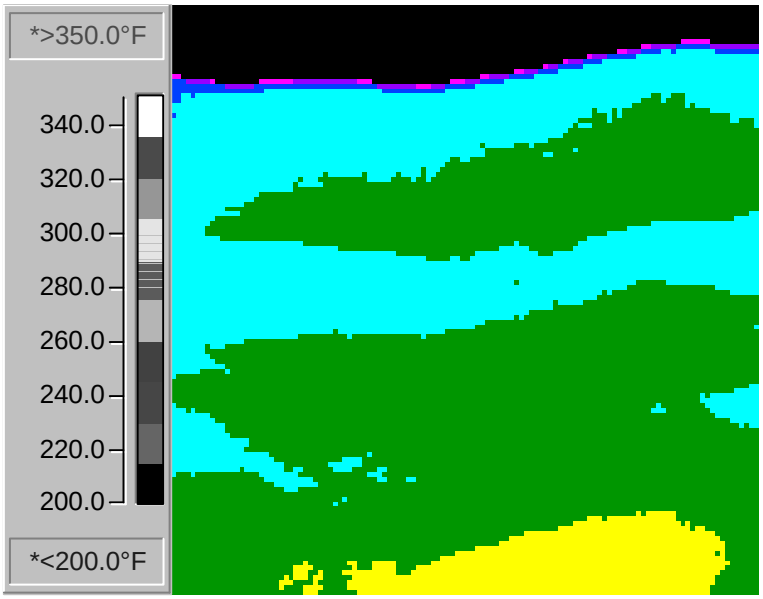

Figure 38. Temperature Drop of 27 °F 220 Feet into US 79 Test Section.

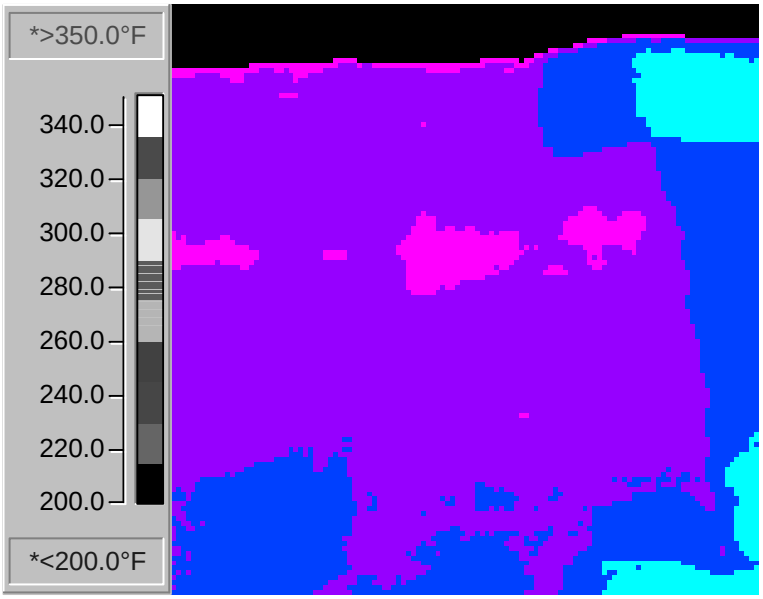

Figure 39. Location of Paver Being Stopped at 360 Feet on US 79.

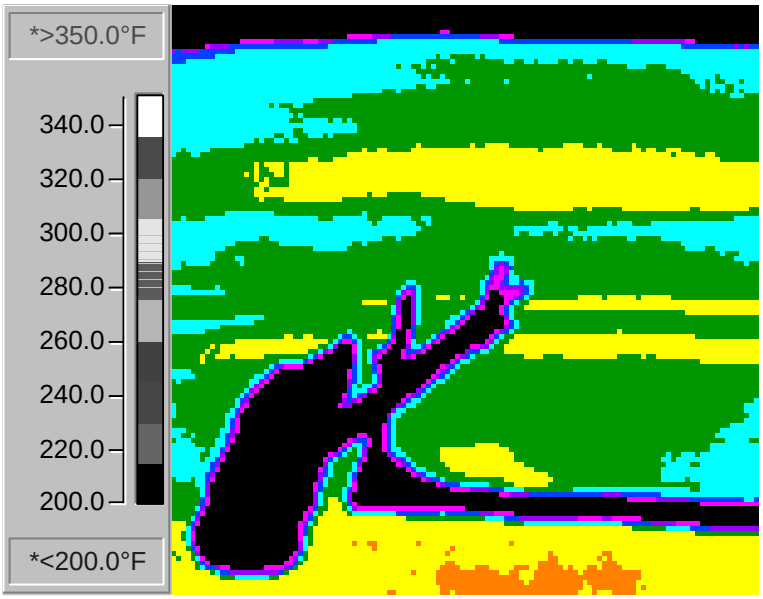

Figure 40. IR Image at 620 Feet into US 79 Test Section.

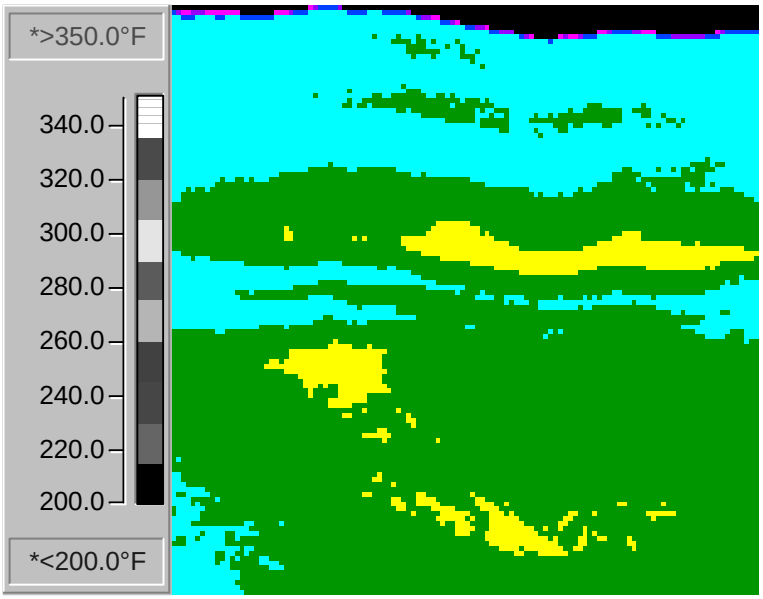

Figure 41. Temperatures from 270 °F to 295 °F at 790 Feet on US 79.

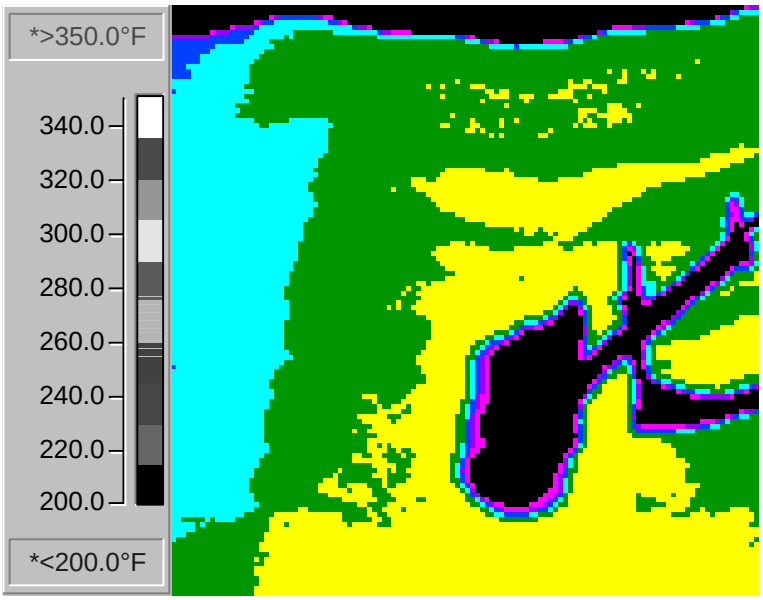

Figure 42. Contrast in Mat Temperatures Where Paver Stopped (Aqua Region) and Typical Mat on US 79.

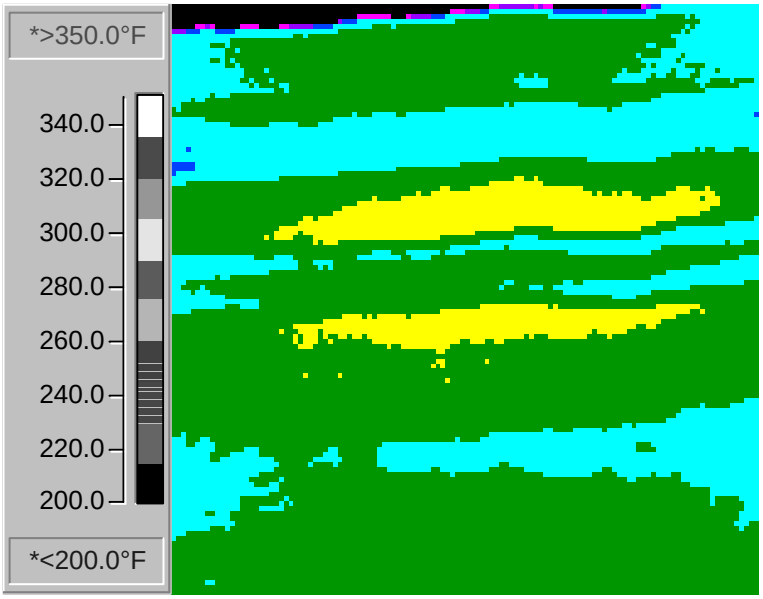

Figure 43. Temperature Drops of 25 °F at 895 Feet on US 79.

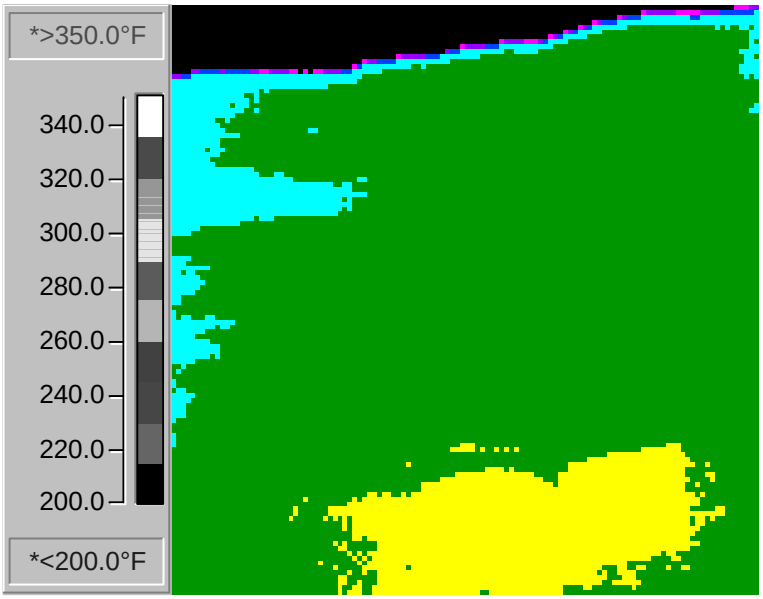

Figure 44. Normal Section at 500 Feet into US 79 Test Section.

V. RESULTS FROM GROUND-PENETRATING RADAR

On September 13, 2001, GPR and coring was conducted on US 79. Since the shoulder was being placed with the main lane, one GPR pass was conducted one foot outside the shoulder line, then four GPR passes were made in the main lane at locations of 1, 3, 6, and 9.5 feet inside the shoulder line. Some of the most dramatic changes in dielectric were detected at the location previously shown in Figure 40; thus four cores were taken here. Two "normal" cores were taken at 500 feet, as the IR showed this area to be uniform, and GPR showed this area to be representative of the typical observed dielectric values of the test section. From stationary GPR readings and laboratory analysis of cores, the relationship between air voids and GPR dielectric for the overlay on US 79 was estimated as:

$$\ln(\text{Air Voids}) = 4.4510 - 0.34355\varepsilon \qquad R^2 = 0.9852$$
$$(0.1226)\ \ (0.02106) \qquad (\text{s.e.})\ \ \hat{\sigma} = 0.0265$$

which transforms to:

$$\%\ \text{Air Voids} = 85.713 * e^{(-0.3435\varepsilon)}$$

Based upon this relationship, predictions of air voids and density (based upon cores' average Rice gravity) were made for each of the GPR readings made over the test section. Table 11 presents summary statistics for the main lane and all collected data. The main lane has lower average voids than the entire mat as a whole, probably due to compaction efforts being focused on this portion of the mat. The lower compaction in the shoulder is more evident in Figure 45, where the distribution of air voids for all data is further to the right than the distribution for only the main lanes. For example, with all data approximately 20 percent of observations have air voids of 12 percent or more. With just the main lane data only 9 percent of observations have

voids of 12 percent or more. The cumulative distribution frequency graph would be more appropriate to use for statistical inferences, as the hypothesis that the distributions were normal was rejected at the 95 percent confidence level for both all the air void data and the air void data for the main lane.

Table 11. Predicted Mat Statistics for US 79 from GPR.

Parameter	Average	Minimum	Maximum	Standard Deviation
Density (all data)	135.2	129.8	141.7	2.19
% Density (all data)	89.2	85.6	93.5	1.44
% Voids (all data)	10.8	6.5	14.4	1.44
Density (main lane)	135.8	131.3	141.7	1.91
% Density (main lane)	89.6	86.6	93.5	1.26
% Voids (main lane)	10.4	6.5	13.4	1.26

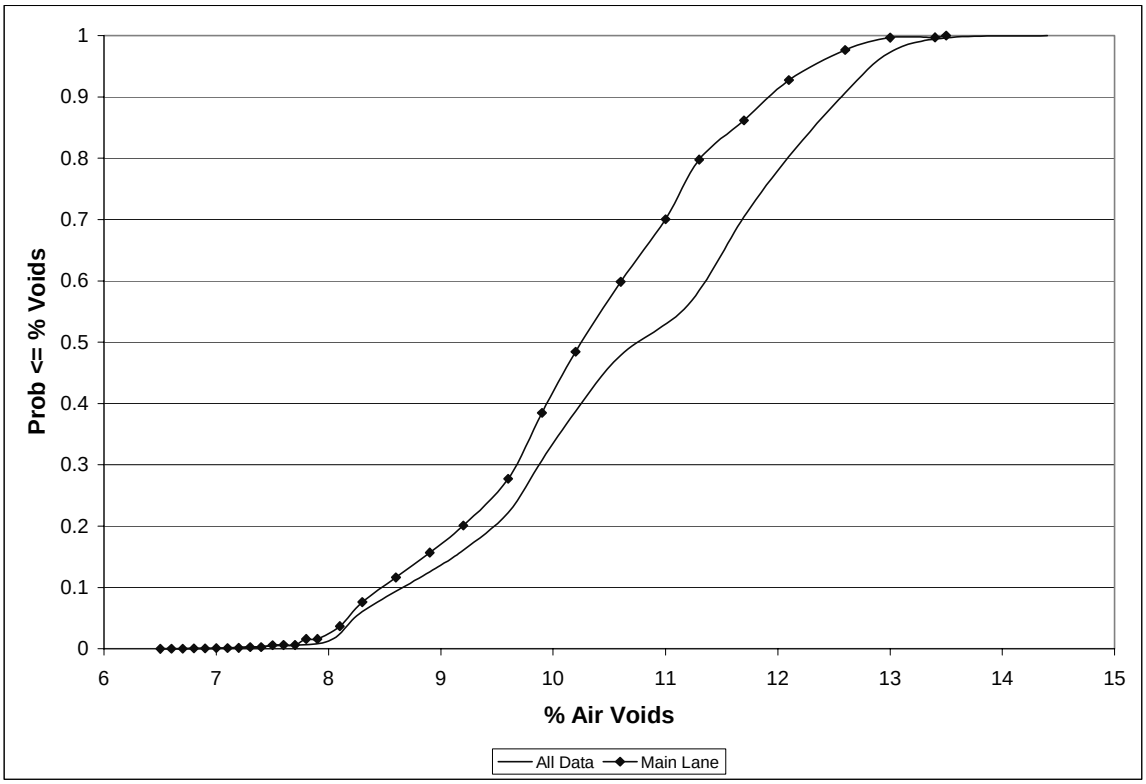

Figure 45. Air Voids Cumulative Probability Distribution for US 79.

Figure 46 shows the surface plot of the predicted air voids for the US 79 test section. The longitudinal zero point is at the shoulder stripe. Interestingly, the patterns at locations where the paver was stopped (360 and 860 feet) do not appear to stand out from the rest of the mat, even though at 360 feet the mix was 35 °F to 80 °F cooler than the typical mix temperatures.

In the main lane of the test section, approximately 60 percent of the voids would be expected to be greater than or equal to 10 percent. Approximately 10 percent of the main lane of the test section is predicted to have voids greater than or equal to 12 percent. Since the ambient air temperature was above 100 °F, the mix was typically going down at temperatures between 260 °F and 300 °F, the asphalt content of all cores was higher than JMF, and in general the cores were in specification on gradation, the relatively high voids were likely due to rolling problems and the paver stops that occurred.

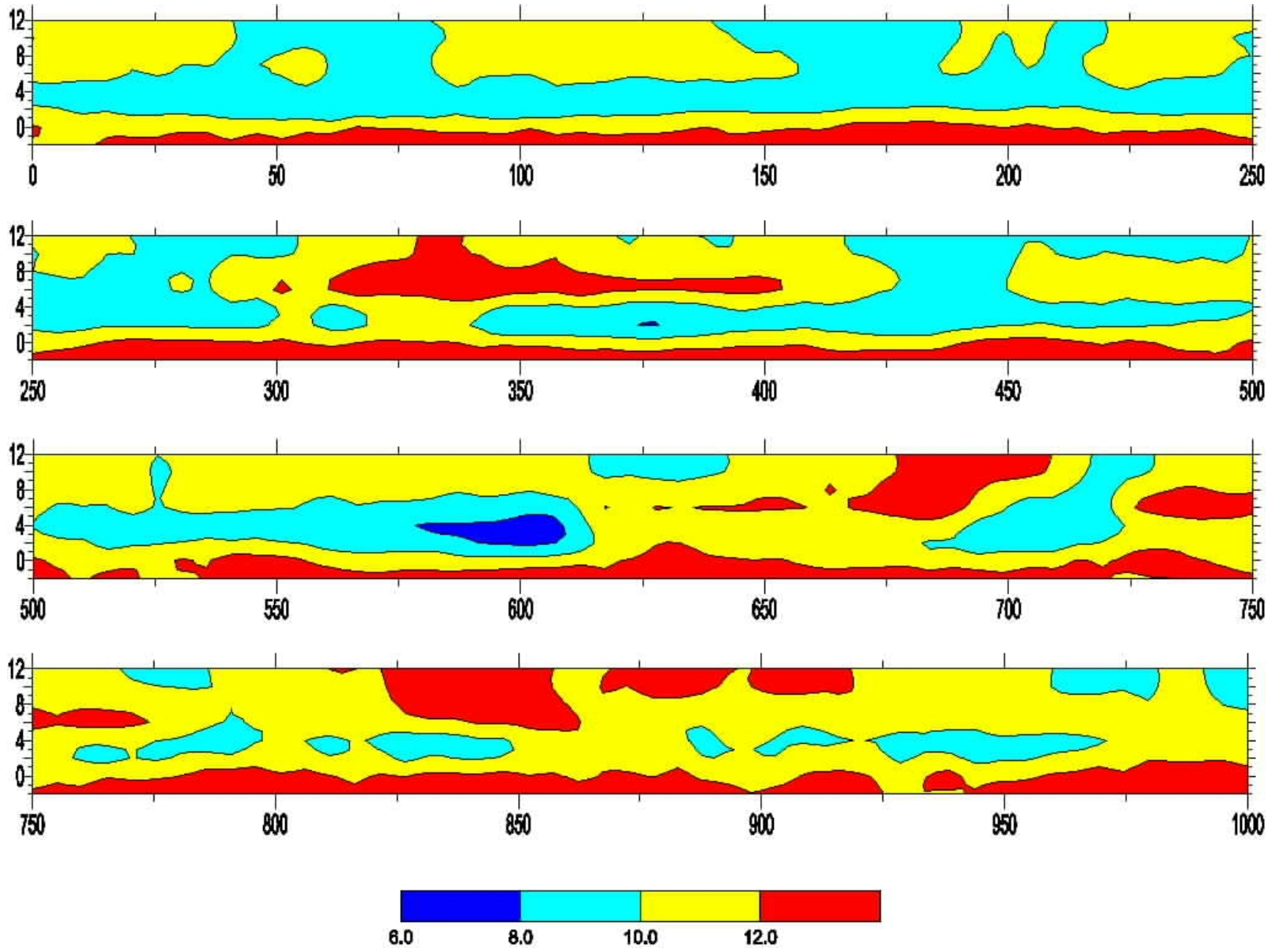

Figure 46. Surface Plot of US 79 Air Voids.

VI. RESULTS FROM CORES

Four 6-inch diameter cores were taken from the location shown previously in Figure 40 (620 feet), where low dielectric readings corresponded to the cooler centerline, and high dielectric readings corresponded with the hotter area on the right edge of the main lane. Two cores representative of a uniform temperature area that appeared to be of normal dielectric value were taken from the location shown in Figure 44 (500 feet). All cores were tested for bulk density, surface texture depth, permeability, rut depth after 8000 passes of the Asphalt Pavement Analyzer, Rice gravity, air voids, asphalt content, and gradation. All results except for gradation are presented in Table 12, with gradation results shown in Table 13 and Figure 47. All cores taken at this job had gradations very close to each other and were all within specification limits.

Table 12. Core Results from US 79 Test Section.

Core	Temp (F)	GPR ε	Bulk Density (pcf)	Texture Depth (in)	Permeability (cm/s)	Rut Depth (8000 passes, mm)	Rice Gravity (pcf)	Air Voids (%)	Asphalt Content (%)
N1	277	5.4	131.0	0.2594	0.0007285	5.402	151.37	13.48	5.01
N2	282	5.7	133.5	0.0697	0.0007579	4.588	152.43	12.39	4.66
L1	273	5.4	131.8	0.0737	0.0009551	5.055	151.52	12.99	4.99
L2	275	5.3	131.2	0.0429	0.001051	4.358	152.47	13.92	4.85
X1	290	6.4	136.9	0.0747	0.0009211	8.973	151.61	9.74	4.84
X2	290	6.6	137.3	0.051	0.00001689	2.499	150.29	8.66	5.00

Note: Design Asphalt Content was 4.6%

Table 13. Gradations for US 79 Cores.

Core	N1	N2	L1	L2	X1	X2	JMF
Passing 5/8	100	100	100	100	100	100	100
Passing 3/8	69.1	67.7	70.7	65.1	67.9	68.5	69.8
Passing #4	37.4	36.3	38.2	35.3	38.5	36.6	37.1
Passing #10	20.9	20.9	21.3	20	22.6	20.7	18.8
Passing #40	13	12.9	13	12.7	13.9	13	11.3
Passing #80	10.9	10.9	10.5	9.9	11.6	10.5	8.7
Passing #200	8.6	9	8	7.1	9.4	8.1	5.7

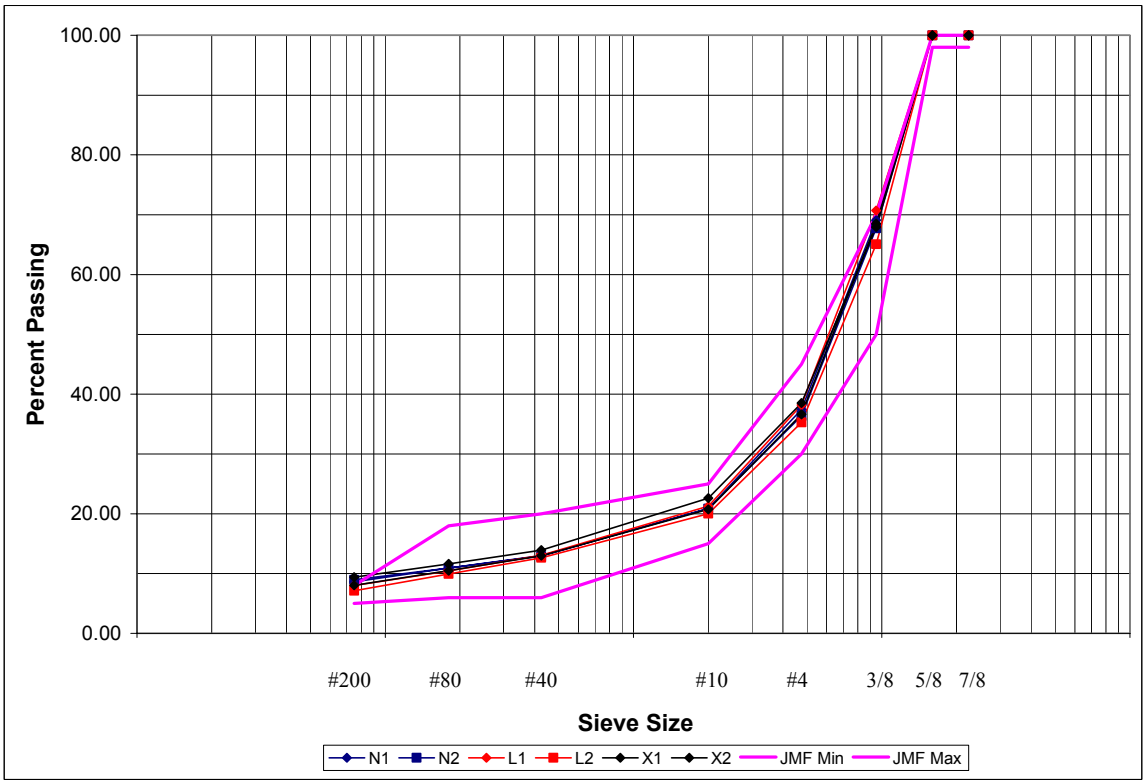

Figure 47. Gradation Results from US 79 Test Section.

VII. RELATIONSHIPS BETWEEN CHANGES IN TEMPERATURE AND DIELECTRIC AND CHANGES IN MIX PARAMETERS

Using the methods described on page 50 (Chapter 5 Section VII), researchers determined the significant correlations between changes in the NDT data and changes in the measured HMA properties. Appendix B presents the complete matrix of all significant correlations. Table 14 presents the correlation values between key variables for US 79. Key points are:

- NDT data were highly correlated to changes in density and air voids.
- Correlation values between NDT data and mix parameters not related to density were relatively low.
- Changes in temperature and changes in dielectric were highly correlated to one another.

Table 14. Selected Significant Correlations between Data for US 79.

	ΔTemp (F)	Δ GPR ε
Δ Temp (F)	1.00	0.97
Δ GPR ε	0.97	1.00
Δ Bulk Density (pcf)	0.96	0.99
Δ Air Voids (%)	-0.94	-0.99

For relationships with non-zero correlations, the maximum change in NDT data before mix parameters may be out of tolerances specified in SS 3146 was investigated by regressing the observed changes in each mix parameter on the observed change in temperature and dielectric from GPR. Changes in temperature (or dielectric as appropriate) were the independent variable in all cases. These regressions are presented in Appendix B. The value of the change in temperature or dielectric that would indicate an expected change in a mix parameter beyond the allowable operational tolerance was then calculated from the regression slope. These results are presented in Table 15.

Table 15. Limits on Changes of NDT Data before Mix Parameter Changes Are at Tolerance Limit for US 79.

Mix Parameter	Tolerance	Δ Temp Limit (F)	Δ GPR ε Limit
Δ Air Voids (%)	Range of 5.3; AVG to low of 3.3*	Range: 20; AVG to low: 12	Range: 1.4; AVG to low: 0.8
Δ % Passing #10	± 5	90	6.9
Δ % Passing #40	± 3	86	6.8
Δ % Passing #80	± 3	69	6.23
Δ % Passing #200	± 3	49	4.6
Δ % Retained on #40	± 3	126	9.7
Δ %Retained on #200	± 3	201	

*Based on cores' average Rice Gravity and SS 3146 Density Profile Specifications

Tables 12 and 13 show that the asphalt content and gradation of the hot mix were relatively uniform for this project. The main parameter that varied was the air void content; thus, the changes in NDT data are primarily attributed to changes in air void content. The correlations between parameters and the NDT limits in Table 15 also clearly indicate that changes in NDT data were primarily due to density variations. Correlation values were much higher and NDT limits much lower for the relationship between the NDT data and air voids than for any other mix parameter. Figures 48 and 49 further show that segregation was not of the gradation variety, as there was no trend in the number of sieves with significant changes with increasing temperature and dielectric changes. In only one instance was a change in individual percent retained of greater than 5 percent observed. This change was on the 3/8 sieve between cores L1 and L2.

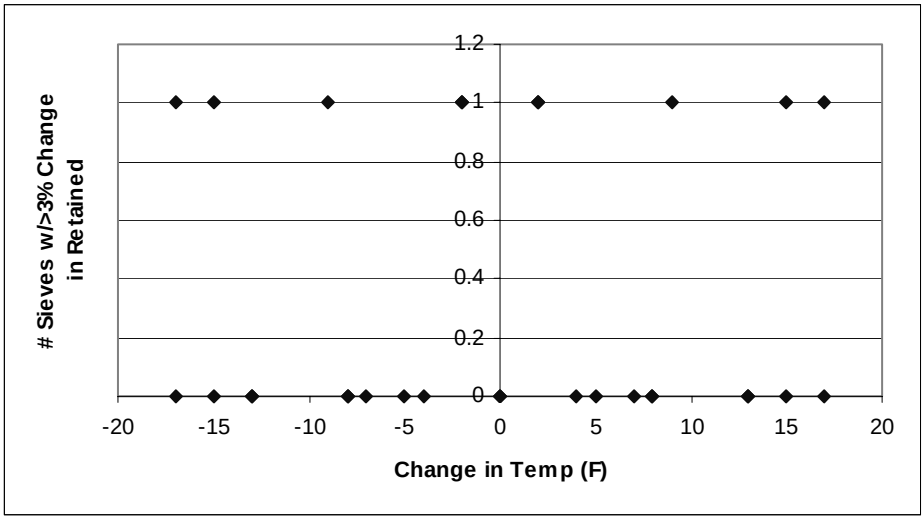

Figure 48. Number of Sieves with Greater than 3% Change in Percent Retained vs. Change in Temperature for US 79.

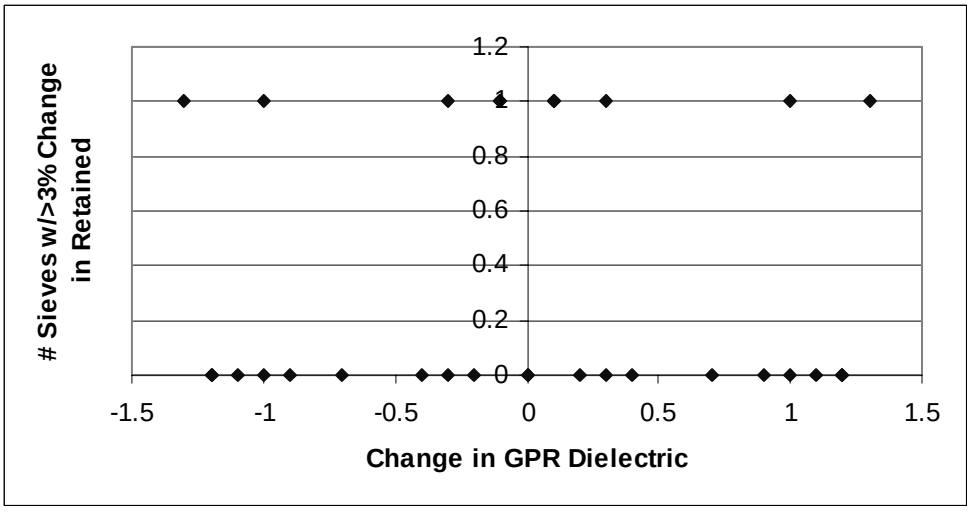

Figure 49. Number of Sieves with Greater than 3% Change in Percent Retained vs. Change in GPR Dielectric for US 79.

The closeness of cores' gradations, lack of any trend in the number of sieves with significant changes with changes in NDT data, and cores' wide range of air voids further support the observation that major differences in NDT data on this job were not due to gradation changes. Thus, it appears that non-uniformity at this job was primarily density variations, and the following limits on NDT data are reasonable from data collected at this paving operation:

Temperature: No values more than 12 °F below the mean; maximum range of 20 °F. The data indicate changes in temperature were classic temperature segregation in which lower temperature areas did not compact as well. The higher values in Table 15 are all from parameters in which correlation values were significant, but relatively low, and changes between cores were quite small. Thus, the temperature limit is based upon the high to low air void tolerance.

GPR ε: No values more than 0.8 below the mean; maximum range of 1.4. Based upon SS 3146 density profile criteria and cores' average Rice gravity, a maximum allowable range (average to low void content) of 3.3 percent and a high to low air void range of 5.3 percent would be allowed on this job. The relationship between GPR dielectric and air voids on this job indicates a change in dielectric of 0.8 would indicate a 3.3 percent change in voids, and a change in dielectric of 1.4 would be indicative of a 5.3 percent change in voids. These limits reasonably assume that the average dielectric is indicative of the average air voids of the mat. This assumption is reasonable because it has already been discussed that changes in NDT were primarily indicative of density variations, and the GPR data were nearly perfectly related to changes in air voids.

VIII. CONCLUSIONS

The US 79 job is another case in which an MTV was used and relatively few locations of temperature differentials were seen that would be considered substantial under the proposed limits on current studies on this topic. NDT data also indicated that locations where the paver stopped still passed SS 3146 density profile criteria. This finding may be due to the fact that the entire job had relatively high void contents. Changes in data from both NDT devices were most highly related to changes in air voids, with substantially lower correlations to other mix parameters. The GPR dielectric was a better predictor of air voids than the temperature data. The relationship predicting changes in voids from changes in dielectric has a higher R^2 (0.99) and a lower standard error (0.33) than the relationship between changes in temperature and changes in voids (R^2=0.88, $\hat{\sigma}$ =1.1). In addition, examination of the temperature photos with the air void surface plot reveals that in many instances where temperature data showed a cold spot, predicted voids were actually lower, not higher as would ordinarily be expected. Thus, the following conclusions are made from this job:

- NDT tools were effective at identifying anomalous areas of the mat. However, if density changes are the primary irregularities occurring in the mat, GPR is a much better tool for investigation.
- Changes in temperature are less reliable for finding mat irregularities if little asphalt content or gradation changes are occurring. Imaging is performed before any rolling, so rolling patterns and effort will impact whether or not significant density changes occur over the cold areas.
- The major variations in density on this job are thought to be primarily due to rolling efforts. Air voids at locations where the paver stopped and the mix cooled before it was rolled were not noticeably different than the overall pattern of voids in the mat.

CHAPTER 7

IH 10 INVESTIGATION

I. SUMMARY

Infrared imaging was performed on a section of the IH 10 westbound inside lane starting just west of Texas Reference Marker 659 on September 12, 2001. GPR was conducted on September 27, 2001. Three locations chosen from the infrared data were investigated. Core testing revealed that one location had primarily density changes, and the other two locations exhibited both gradation and density irregularities. Overall, however, temperature and GPR measurements were both most relatable to mat air voids. The data indicate approximately 75 percent of the test location is expected to have air voids greater than 12 percent.

Many cores were taken at this job, and analysis revealed that better relationships between NDT data and mix changes were obtained by grouping the cores together according to where they were taken. This finding is reasonable as different types of mix anomalies (asphalt content, gradation, density, etc.) may be occurring at locations several stations apart. However, limits on NDT data were based upon the entire pooled data set to avoid specifications based upon potentially biased relationships. Regardless, the following relationships were significant:

- Changes in temperature were significantly correlated to changes in GPR ε, density, texture depth, permeability, rut depth after 8000 passes of the APA, air voids, asphalt content, and changes in both percent passing and percent retained on numerous sieve sizes.

- Changes in GPR ε were significantly correlated to changes in temperature, density, texture depth, permeability, rut depth, air voids, and changes in both percent passing and percent retained on numerous sieve sizes.

II. PAVING PARAMETERS AND ENVIRONMENTAL CONDITIONS

The mix being placed was a 1 inch lift of Superpave with a nominal max aggregate size of 0.5 inch. A 1 inch Type D level up had been previously placed in some locations. The mix was being placed by belly dump trucks into windrows. A windrow pickup device transferred the mix into a BG 260C paver to place the mix. The design air voids was 7.2 percent. At the time of testing, skies were clear, the ambient air temperature was 92 °F, and the average wind speed was 0.5 mph. The paving operation is shown in Figure 50.

Figure 50. Paving Operation on IH 10 WB.

III. INFRARED IMAGING SETTINGS

The ambient air temperature of 92 °F was input into the camera's settings. The Rainbow 10 color scheme was used with a temperature span of 200 °F to 350 °F. An emissivity setting of 0.95 reconciled camera-calculated surface temperatures to temperatures measured with a surface thermocouple.

IV. RESULTS FROM INFRARED IMAGING

With such a thin lift going down (1 inch), variations in temperature were expected. In the test strip, four locations were observed to have significant temperature differentials. Following rolling and cooling, core locations were marked at three of the locations of observed significant temperature differentials. Figure 51 shows the location of the first four cores, at which a maximum temperature drop of 45 °F was observed. The right wheel path appeared moderately segregated at the location shown in Figure 52, in which a maximum temperature drop of 52 °F was observed. Figure 53 is a close-up view of the streak shown in Figure 52. Figure 54 is the IR image of the location where cores 5 through 10 were taken. The maximum temperature differential here was 33 °F. Cores 11 and 12 were taken at the location shown in Figure 55, which had a maximum temperature differential of 40 °F.

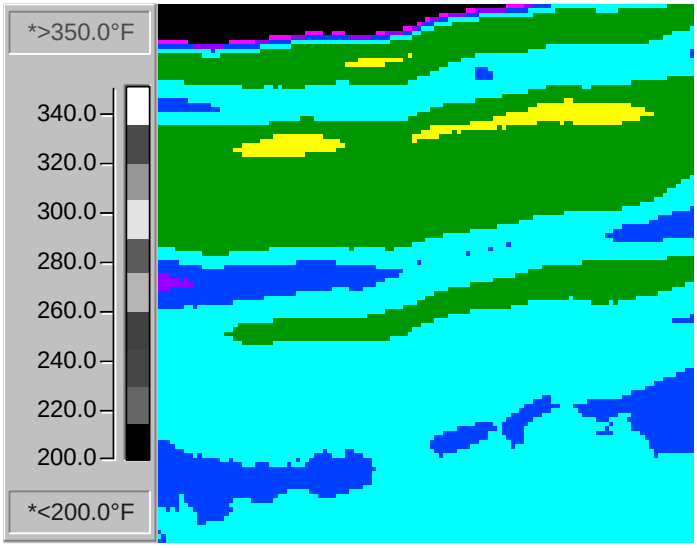

Figure 51. IR Image of Core Locations 1-4 on IH 10.

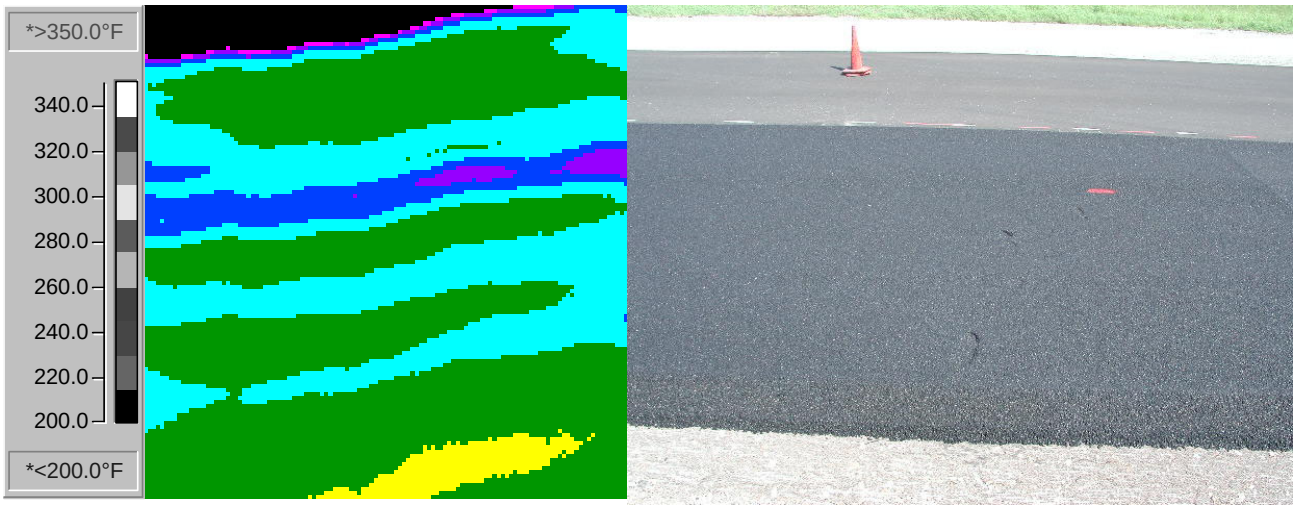

Figure 52. Temperature Drop of 52 °F on IH 10.

Figure 53. Close-up of Cold Streak Shown in Figure 52.

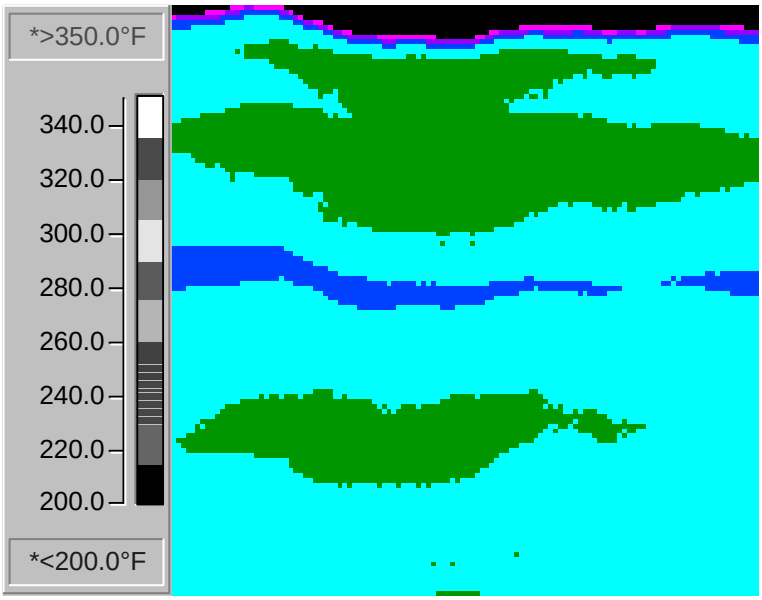

Figure 54. IR Image of Core Locations 5-10 on IH 10.

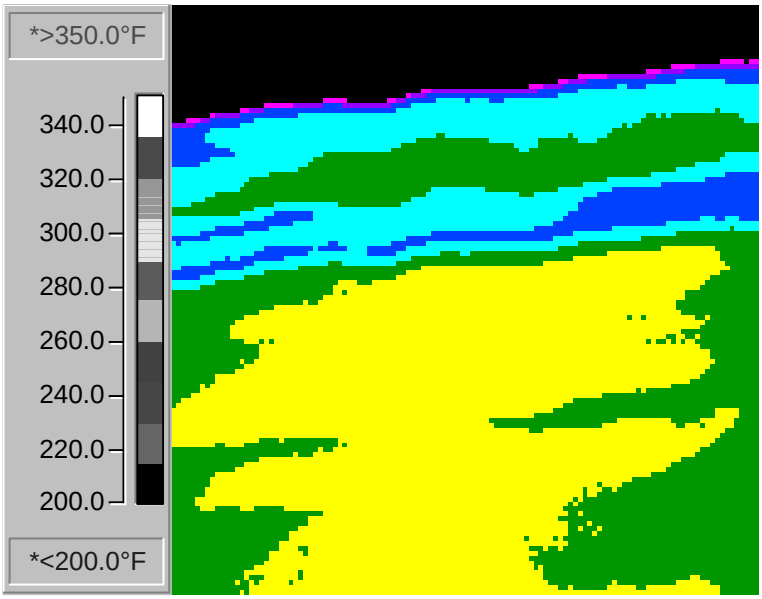

Figure 55. IR Image of Core Locations 11 and 12 on IH 10.

V. RESULTS FROM GROUND-PENETRATING RADAR

GPR and coring was conducted on September 27, 2001. Typically, these data are used to predict air voids based upon the relationship: % Air Voids = $ae^{b\varepsilon}$. However, as Figure 56 shows, the data contain an outlier that does not fit the trend at all. However, if discarded, the three points at a dielectric value of 6.0 result in a constant "a" of 30,233 (constants from other jobs investigated in this project ranged from 20 to 367). Compounding the problem is the fact that the data file has dielectric values as low as 4.8, whereas the minimum dielectric of cores was 5.6. The net effect is that discarding the outlier results in predictions of air voids as high as 60+ percent at the lower dielectric values, clearly unrealistic, and using the outlier in the analysis would clearly skew the result away from the true relationship. Thus, the predicted air void distribution in Figure 57 and the air void plot, shown in Figure 58, were generated by discarding the outlier and only making predictions for the range of dielectric values used in the regression. Observed dielectrics of less than the minimum in the data set of cores (6.0) were assumed to have greater air voids than the void content prediction for a dielectric of 6.0, which is 13.9 percent. Figure 57 shows that 75 percent of the mat is expected to have voids greater than 12 percent, and 45 percent of GPR observations had dielectrics less than the minimum dielectric of cores taken. Figure 58 further illustrates that most of the mat is expected to have high void contents. The relationship developed and used is as follows:

$$\ln(\text{Air Voids}) = 10.32 - 1.2798\varepsilon \qquad R^2 = 0.7991$$
$$(1.32) \quad (0.2138) \qquad \text{(s.e.)} \quad \hat{\sigma} = 0.120$$

which transforms to:

$$\% \text{ Air Voids} = 30233 * e^{(-1.2798\varepsilon)}$$

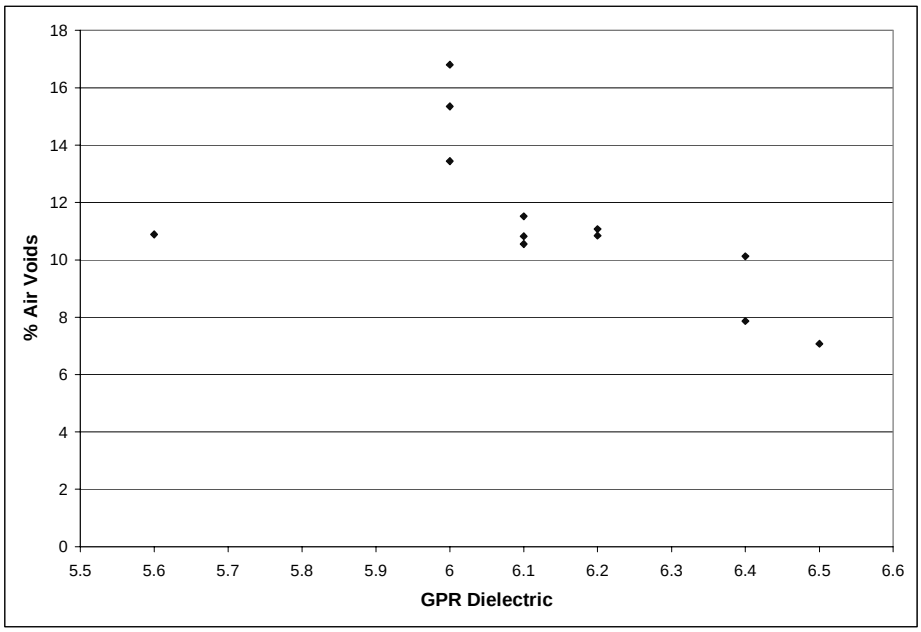

Figure 56. Percent Voids vs. GPR Dielectric for IH 10.

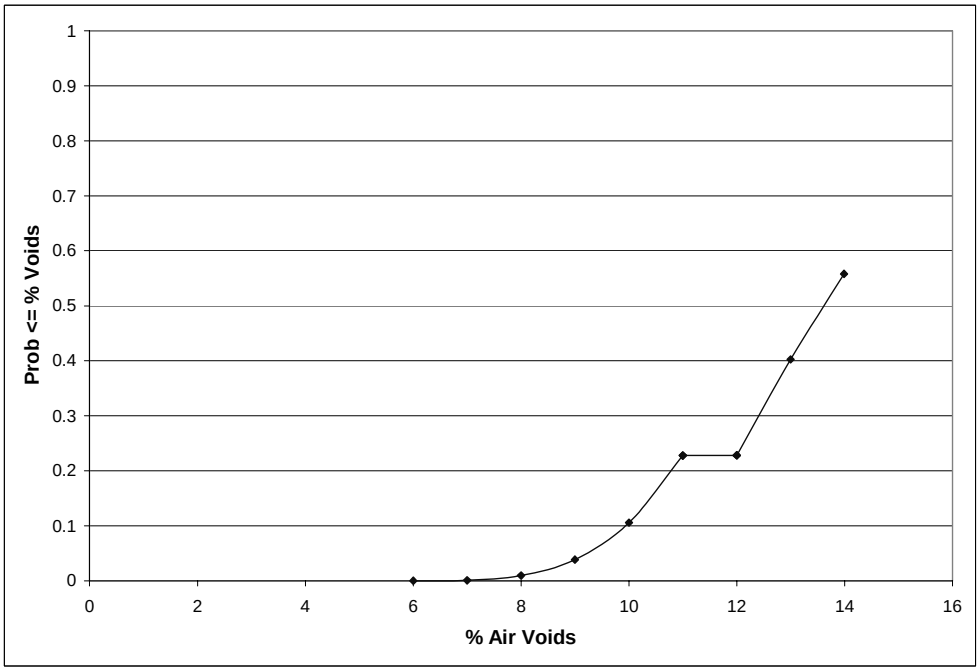

Figure 57. Predicted Air Void Distribution for IH 10 Test Section.

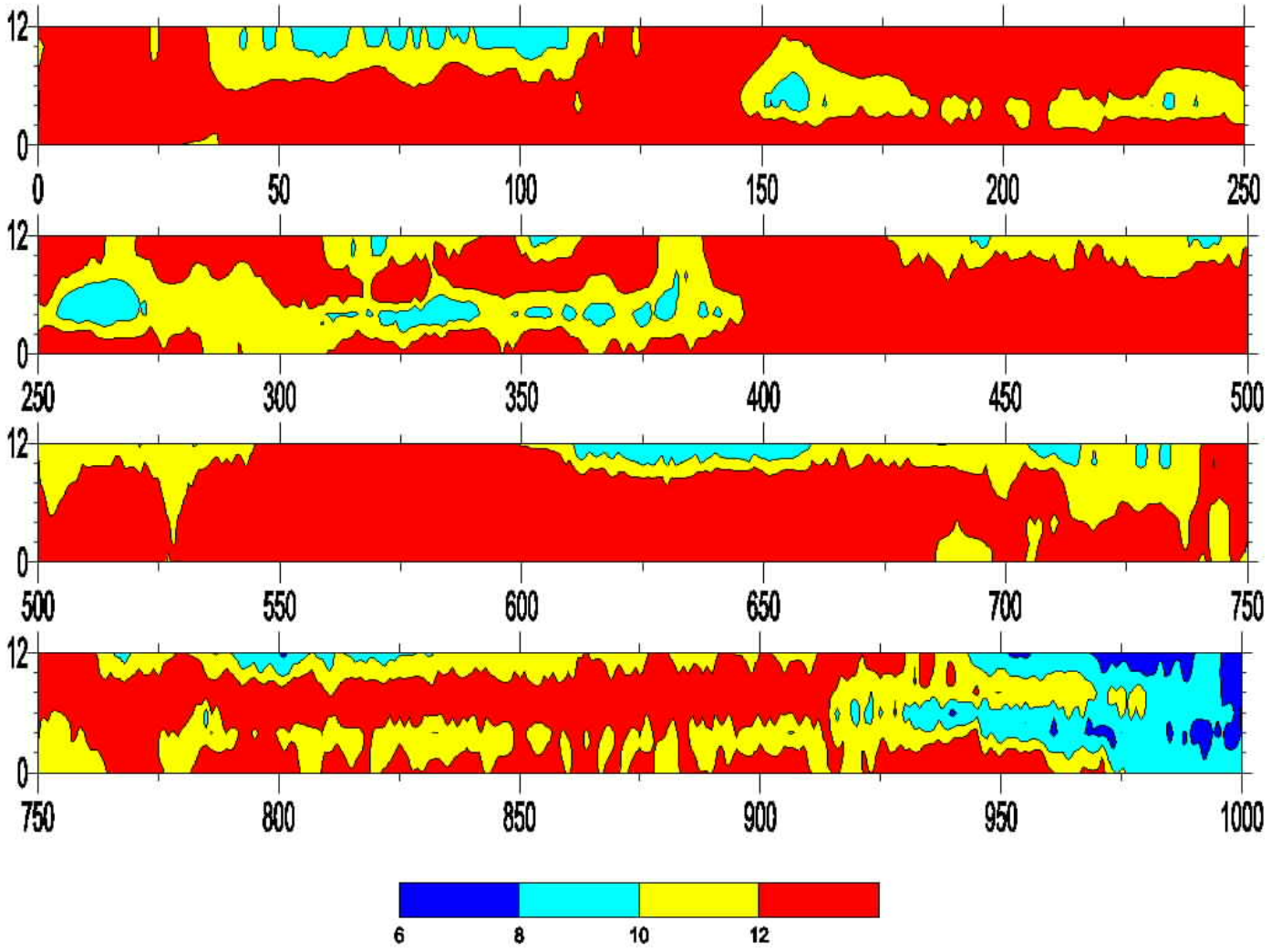

Figure 58. Surface Plot of IH 10 Predicted Air Voids.

VI. RESULTS FROM CORES

Cores were taken from the locations shown previously in Figures 51, 54, and 55. Figures 59, 60, and 61 show the core locations. A laboratory test sequence was performed which included bulk density, surface texture depth, permeability, rut depth after 8000 passes of the Asphalt Pavement Analyzer, Rice gravity, percent air voids, percent asphalt, and gradation. Table 16 presents all results except for gradation. Table 17 contains all the cores' gradations. Due to the large number of cores, gradation graphs are presented for each group of cores. Figure 62 shows the gradations for cores 1 through 4. Figure 63 shows gradations for cores 5 through 10, and Figure 64 shows gradations for cores 11 and 12.

In Figure 62, the colder temperature cores (cores 2 and 3) were as much as 5 percent coarser on a sieve size and had 1.5 times the air void content as cores 1 and 4. Thus, this location had both temperature and gradation segregation. This same trend is not seen in Figure 63. The cooler temperatures here were cores 5 and 9, which had gradations in between the "normal" temperature cores 7, 8, and 10. Core 6, which had the highest temperature, had essentially a gradation identical to the coldest cores. However, from density data it was discovered that core 6 had air voids of 7 percent, whereas the cooler cores 5 and 9 had voids of 13 and 11.5 percent, respectively. Cores 7, 8, and 10 had voids between 10.5 and 11 percent. Thus, this location was true temperature segregation, resulting in low density, with minimal gradation segregation.

Figure 64 shows that core 12, the hotter of cores 11 and 12, had 3 to 4 percent more passing on three sieve sizes. The air void content of core 12 was also approximately 2 percent below the void content of core 11. This would indicate some gradation and temperature segregation occurring.

Figure 59. Locations of Cores 1-4 on IH 10 Test Section.

Figure 60. Locations of Cores 5-10 on IH 10 Test Section.

Figure 61. Locations of Cores 11 and 12 on IH 10 Test Section.

Table 16. Core Results from IH 10 Test Section.

Core	Temp (F)	GPR ε	Bulk Density (pcf)	Texture Depth (in)	Permeability (cm/s)	Rut Depth (8000 passes, mm)	Rice Gravity (pcf)	Air Voids (%)	Asphalt Content (%)
1	291	6.4	137.1	0.029	0.0006432	3.077	152.54	10.12	4.87
2	248	6	125.8	0.034	0.00076	5.722	151.22	16.80	4.68
3	253	6	128.7	0.029	0.001102	3.96	152.01	15.34	4.72
4	291	6.2	135.9	0.029	0.0006178	5.327	152.38	10.85	4.96
5	257	6	131.7	0.032	0.0003948	3.995	152.20	13.44	4.95
6	279	6.5	139.3	0.023	0.000299	3.103	149.95	7.08	4.95
7	270	6.1	133.6	0.025	0.0002375	3.509	149.37	10.55	5.19
8	270	6.1	134.7	0.026	0.0006392	2.735	151.08	10.82	4.84
9	260	6.1	133.3	0.031	0.001068	2.896	150.65	11.52	5.15
10	270	5.6	134.5	0.03	0.001263	4.134	150.98	10.89	4.92
11	278	6.2	134.9	0.029	0.0004296	5.133	151.72	11.08	4.92
12	295	6.4	137.9	0.025	0.0003528	2.876	149.68	7.87	4.93

Note: Design Asphalt Content was 4.8%

Table 17. Gradations for IH 10 Cores.

Core	1	2	3	4	5	6	7	8	9	10	11	12	JMF
Passing 3/4	100	100	100	100	100	100	100	100	100	100	100	100	100
Passing 1/2	100	100	100	100	100	100	100	100	100	100	100	100	99
Passing 3/8	89	85.6	84.8	89.1	88.4	91.1	91.8	93	90	88.2	86.7	90.4	87
Passing #4	55.3	48.4	49.8	55.8	57.6	56.8	59.2	60.4	57.7	53.1	54.5	58.4	51
Passing #8	34.3	31	31.9	34.4	35.8	36.5	38.5	36.5	36.5	34.2	35.1	36.9	31
Passing #16	24.8	22.7	23.8	24.4	25.6	25.4	27.4	26.1	25.9	24.7	25	26.2	21
Passing #30	18	16.3	17.3	17.6	18.2	18.1	10	18.8	18.7	18	17.9	18.8	15
Passing #50	12.4	10.8	11.9	11.9	12.4	12.3	13.9	13	13.1	12.8	12.2	12.9	10
Passing #100	10.1	8.5	9.8	9.5	10.3	8.6	9.6	10.8	9.7	9.5	8.8	10.4	7
Passing #200	7.7	6.2	7.3	7.1	7.5	6.3	7.1	7.9	7.8	7.4	6.6	7.9	5

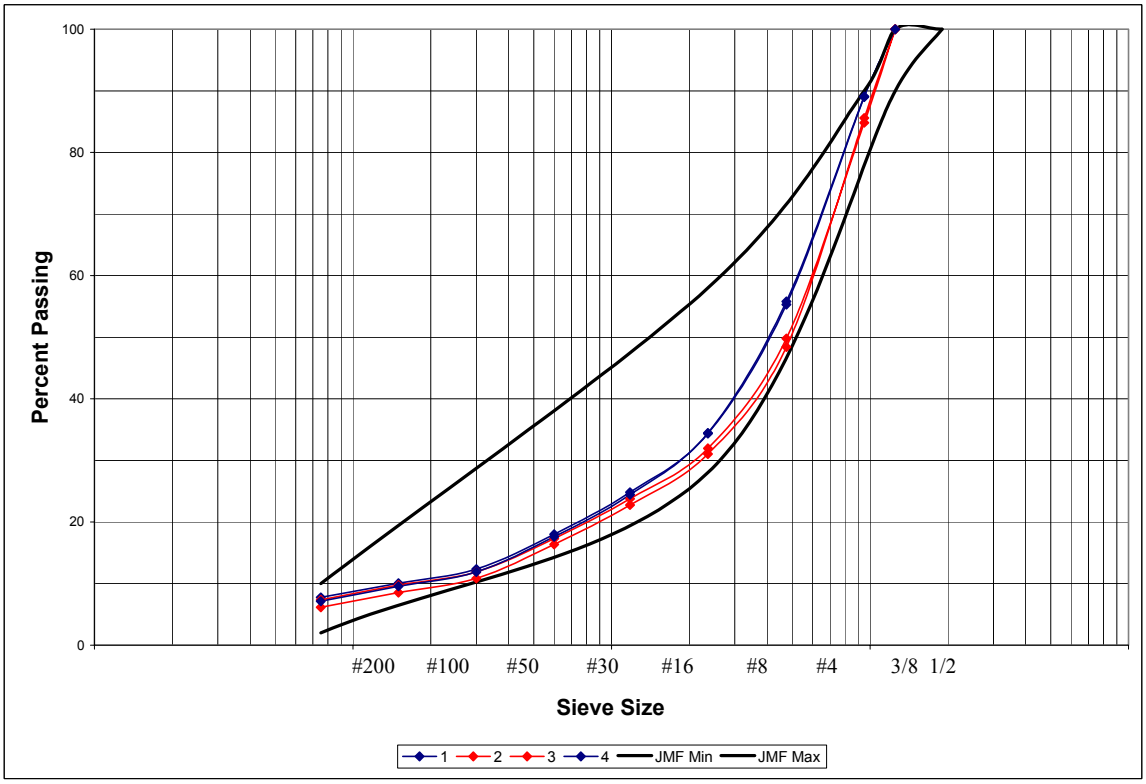

Figure 62. Gradation Graph for IH 10 Cores 1 through 4.

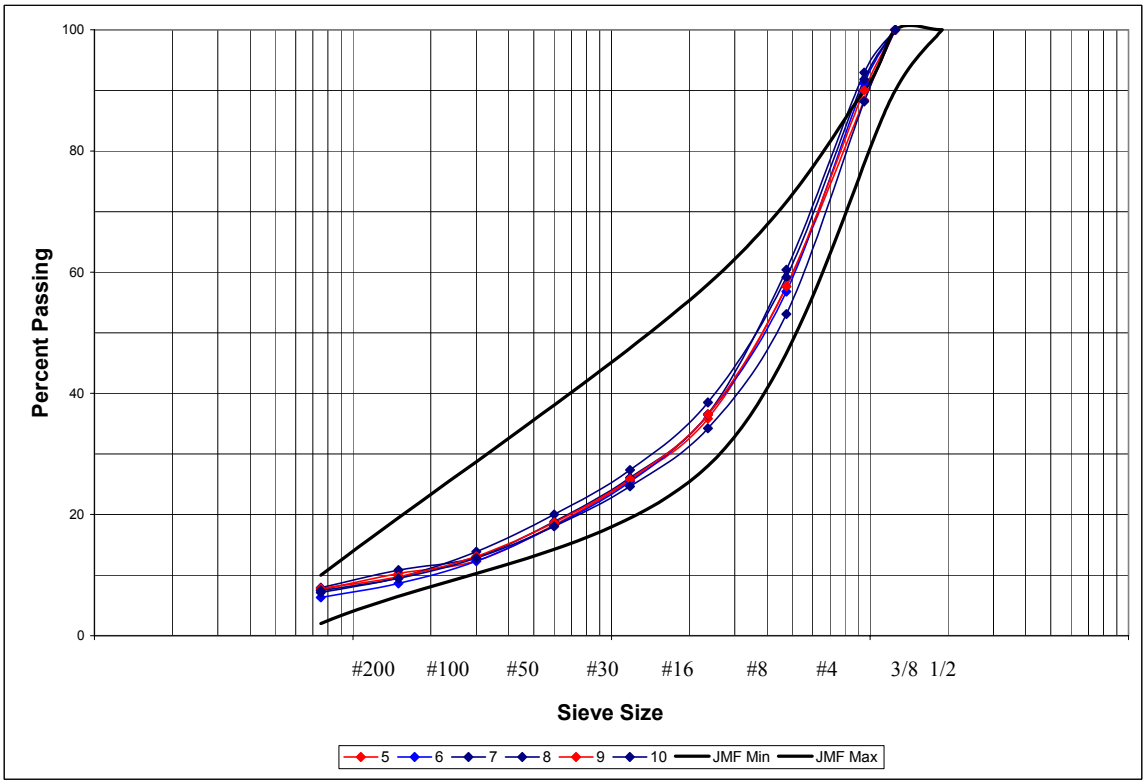

Figure 63. Gradation Graph for IH 10 Cores 5 through 10.

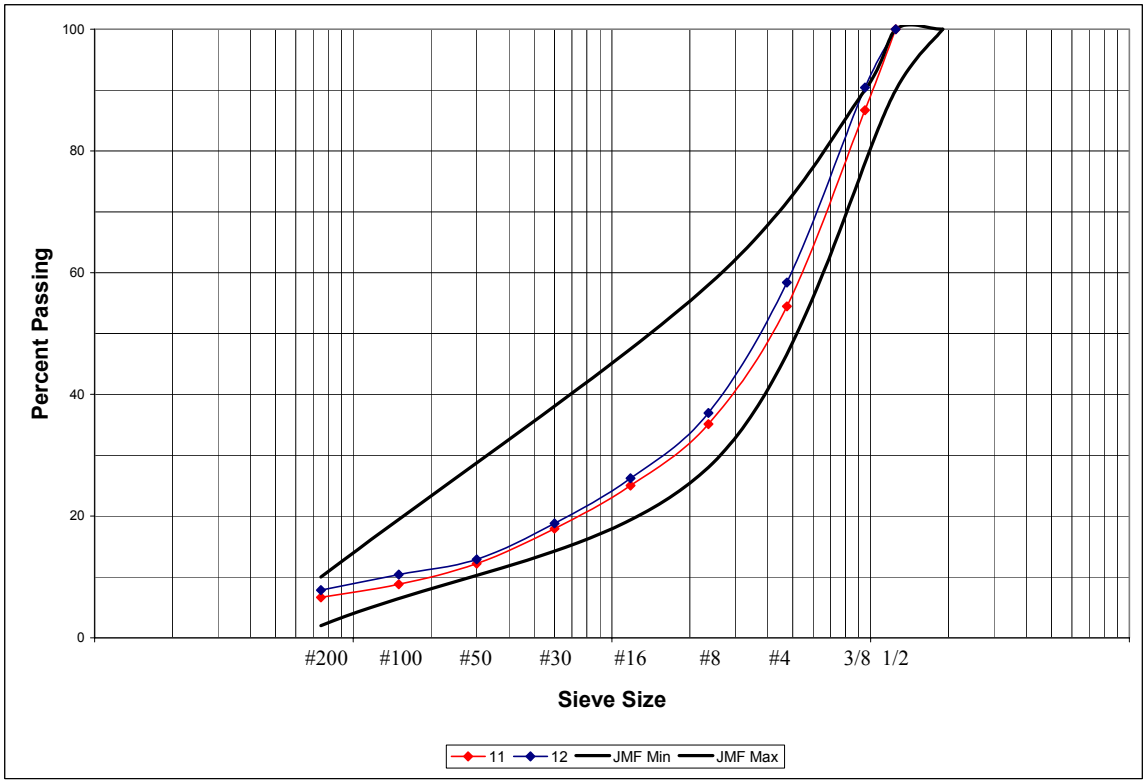

Figure 64. Gradation Graph for IH 10 Cores 11 and 12.

VII. RELATIONSHIPS BETWEEN CHANGES IN TEMPERATURE AND DIELECTRIC AND CHANGES IN MIX PARAMETERS

Using the methods described on page 50 (Chapter 5 Section VII), researchers determined the significant correlations between changes in the NDT data and changes in the measured HMA properties. For GPR, core 10 was discarded since it was clearly an outlier. In addition, since numerous cores were taken in groups over a large area, data were analyzed both as a whole, and with differences only between cores that were in the same group (i.e., from the same general location). This was done to evaluate whether the relationships between NDT and mix parameters improved with the grouped analysis, which would indicate that changes in NDT data on areas far apart do not necessarily indicate the same thing as changes in NDT within a localized area. This hypothesis was made because, especially with temperature data, trucks could be arriving at different temperatures, and slight changes at the plant may have occurred, etc. The correlation matrices and regressions of changes in mix parameters on changes of NDT data are presented in Appendix C.

Table 18 shows the non-zero correlations between key variables for the IH 10 job (complete correlation matrices are in Appendix C). Of particular note is that correlation values increased for nearly all cases when the grouped data set was compared to the entire pooled data set. Essentially this means that by grouping the data, scatter was reduced, which supports the

hypothesis that the same change in NDT data does not imply the same change in mix properties when comparing a localized area to locations many stations apart. Figures 65 and 66 illustrate this finding, where Figure 65 is generated from all possible differences in data collected, and Figure 66 is from differences only between cores that were taken from the same area. Note the steeper slope, increased R^2, and reduced standard error in Figure 66 (grouped) versus Figure 65 (pooled).

Table 18. Selected Significant Correlations between Data for IH 10.

	Δ Temp	Δ Temp (Grouped)	Δ GPR ε	Δ GPR ε (Grouped)
Δ Temp	1.00	1.00	0.62	0.79
Δ GPR ε	0.62	0.79	1.00	1.00
Δ Density	0.88	0.95	0.87	0.90
Δ % Voids	-0.82	-0.93	-0.86	-0.93

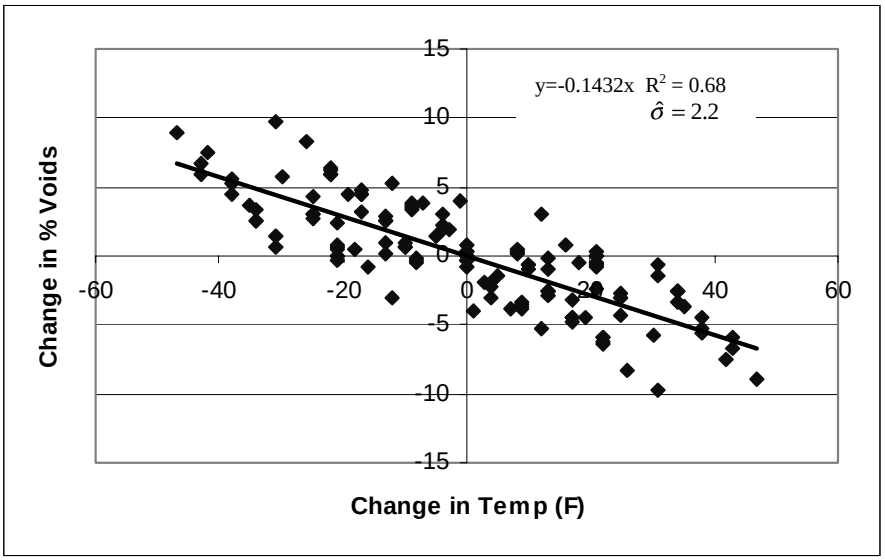

Figure 65. Change in Voids vs. Change in Temp for All IH 10 Data.

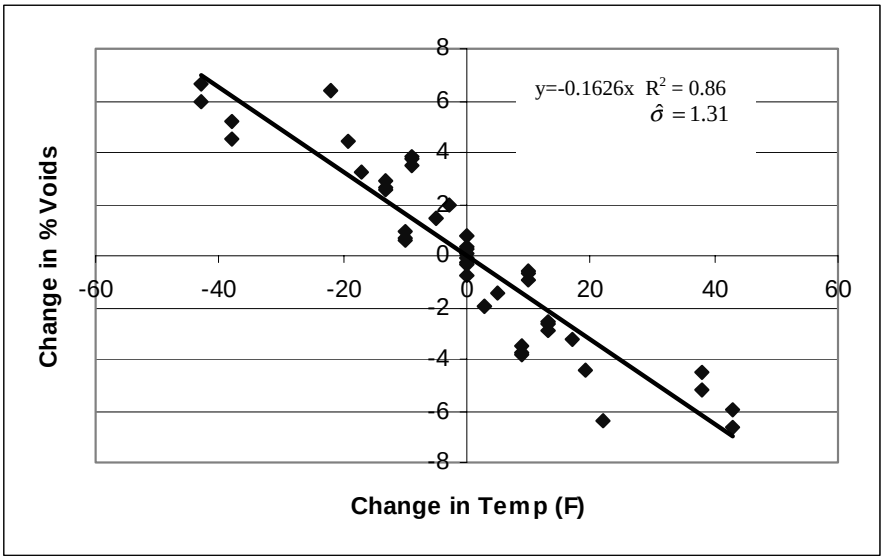

Figure 66. Change in Voids vs. Change in Temp for Grouped IH 10 Data.

For changes in temperature, the highest correlations to mix measurements were to density parameters, texture depth, and the 3/8-inch sieve. Changes in dielectrics were most highly correlated to changes in density parameters and texture depth. The limits on NDT changes, the complete results of which are presented in Appendix C, indicate changes in NDT were mostly indicative of density changes. Also important is the fact that the majority of NDT limits decreased when the relationship between NDT changes and mix changes was based upon the grouped data. This implies the magnitude of the relationship between changes in NDT data and changes in mix parameters was greater for the grouped data (see previous Figures 65 and 66), which essentially means that different types of segregation may be occurring at different locations, and thus when examining for segregation it is likely more meaningful to compare NDT data within smaller areas, rather than many stations apart. For example, a temperature drop of 30 °F within a 20 foot area is likely much more relatable to a change in a specific mix parameter than a temperature difference of 30 °F between two points that are 500 feet apart.

The data from this job indicate NDT data were primarily an indicator of density variations in the mat. As such, the NDT limits presented in Table 19 are the most appropriate for this job. These limits are based upon the SS 3146 density profile criterion.

Table 19. Limits on Changes of NDT Data before Mix Parameter Changes Are at Tolerance Limit for IH 10.

Mix Parameter	Tolerance	Δ Temp Limit	Δ Temp Limit (Grouped)	Δ GPR ε Limit	Δ GPR ε Limit (Grouped)
Δ Air Voids (%)	Range of 4; AVG to low of 2*	Range: 28; AVG to low: 14	Range: 25; AVG to low: 12.5	Range: 0.3; AVG to low: 0.15	Range: 0.3; AVG to low: 0.15

*Based on Cores' average Rice Gravity and SS 3146 Density Profile Specifications

Based upon the results presented above, the following limits on NDT data are reasonable from this job:

Temperature: No values more than 14 °F below the mean; maximum range of 28 °F. From Table 4 it is clear that changes in temperature were mostly indicative of changes in density. Although analyzing data with cores grouped according to their location results in better relationships between NDT data and mix parameters (and a lower NDT limit), the temperature limit is based upon the entire data set for two reasons: a) although when examining for segregation it is likely more meaningful to compare NDT data within smaller areas, rather than many stations apart, partitioning the analysis into small sections would be time consuming and impractical from an implementation standpoint, and b) specifically selecting data points for use in development of general specification limits could result in biased limits.

GPR ε: All values within ±0.15 of the mean; maximum range of 0.3. The analysis shows the tightest limits on dielectric to be from the density specification. Of all mix parameters, the dielectric was most highly related to changes in air voids. The dielectric limits are thus based upon the relationship between dielectric and air voids and the density criteria of SS 3146.

VIII. CONCLUSIONS

Despite the many differences in gradation between cores, the NDT data were still most indicative of density variations at this job, and no trend existed between NDT changes and the number of sieve sizes with significant changes. This observation substantiates the notion of previous studies that NDT devices such as infrared imaging cannot distinguish between types of segregation; however, the NDT data again worked well in identifying anomalous areas of the mat. From the IH 10 testing, the following conclusions are made:

- NDT tools were effective at identifying areas of the mat with non-uniformity.
- Changes in NDT data within a short distance are likely more meaningful than differences at locations many stations apart. However, singling out small locations for analysis, although improving the relationships between NDT data and mix parameters, would be time-consuming from an implementation standpoint and could result in bias in the development of general specifications.
- Many irregularities were occurring at the IH 10 job. The void content of cores ranged from 7 to 17 percent, and of the possible combinations of cores to compare, 20 percent of observations had two or more sieve sizes with a change in percent passing of more than 5 percent. However, there were relatively few occurrences (9 percent) of only one sieve size with a change in percent retained greater than 5 percent. The large differences in percent passing were the result of the cumulative effect of smaller changes in percent retained. No cores had sieve sizes that were beyond the operational tolerances allowed from JMF.
- Placement of such a thin layer (1 inch) likely contributed to the temperature variations seen at this job.

CHAPTER 8

US 290 INVESTIGATION

I. SUMMARY

On September 19 and 20, 2001, researchers examined a hot in place recycling job (HIPR) on US 290 in the eastbound inside lane. The test strip began just east of the Brazos River. Infrared data were collected on the 19th, with GPR and coring taking place on the 20th. From the infrared data, the maximum observed temperature differentials were 40 °F. From the GPR data and the relationship developed between air voids and GPR dielectric, the air voids in the test section had a minimum of 3.1, maximum of 16.3, and average of 7.7.

Important findings from this job include:

- Changes in temperature were significantly correlated to changes in bulk density, permeability, Rice gravity, air voids, percent asphalt, changes in percent passing every sieve size of the JMF, and changes in the percent retained on every sieve size of the JMF.
- Changes in GPR ε were significantly correlated to changes in temperature, changes bulk density, permeability, Rice gravity, air voids, percent asphalt, changes in percent passing every sieve size of the JMF, and changes in the percent retained on every sieve size of the JMF.

II. PAVING PARAMETERS AND ENVIRONMENTAL CONDITIONS

The existing mix was a Type D, and an additional 1-inch of Type D was being added. The new Type D layer on top was the one being investigated. Cutler RePaving performed the recycling operation. A pre-heater went ahead of the recycling machine to heat the existing mix. The recycler then had another set of heaters, followed by knives to scarify the existing mix. Augers then carried the old mix to where a rejuvenating agent was added. The 1-inch lift of recycled mix was then placed with the first screed on the machine. New Type D mix was dumped into a hopper at the front of the machine, conveyed to the second screed, and placed in a 1-inch lift on top of the recycled mix. The recycler is shown in Figure 67. At the time the section was placed, skies were partly cloudy, the ambient air temperature was 90 °F, and the average wind speed was 0.3 mph.

Figure 67. Recycling Machine on US 290.

III. INFRARED IMAGING SETTINGS

The ambient air temperature of 90 °F was input into the camera's settings, and the Rainbow 10 color scheme was used. With the surface thermocouple, it was found that an emissivity setting of 0.97 was appropriate for obtaining accurate infrared temperatures. TxDOT's ThermaSNAP camera was used to image approximately half of the test section. The last half of the test strip was imaged with FLIR Systems' ThermaCam PM 695 real-time infrared/digital camera.

IV. RESULTS FROM INFRARED IMAGING

In the 1000 foot test section, five areas exhibiting temperature segregation were seen. These areas had temperature differentials between 20 °F and 40 °F. Figure 68 is at 130 feet into the test section and shows the center portion of the mat is approximately 20 °F cooler than the mix around it. Figure 69 shows a section at 530 feet where the middle portion of the mat is as much as 25 °F hotter. Temperature drops of 40 °F are seen in Figure 70, taken at 850 feet into the test section. At this location the supply of trucks ran out, which is probably why the temperatures are so low, as colder mix from the sides of the hopper was likely conveyed back. Figure 71 is at 900 feet into the test section and again shows a temperature drop of 40 °F. The cold spot is an isolated area in the centerline. Figure 72, taken at 980 feet, shows the centerline being as much as 30 °F cooler than the rest of the mat.

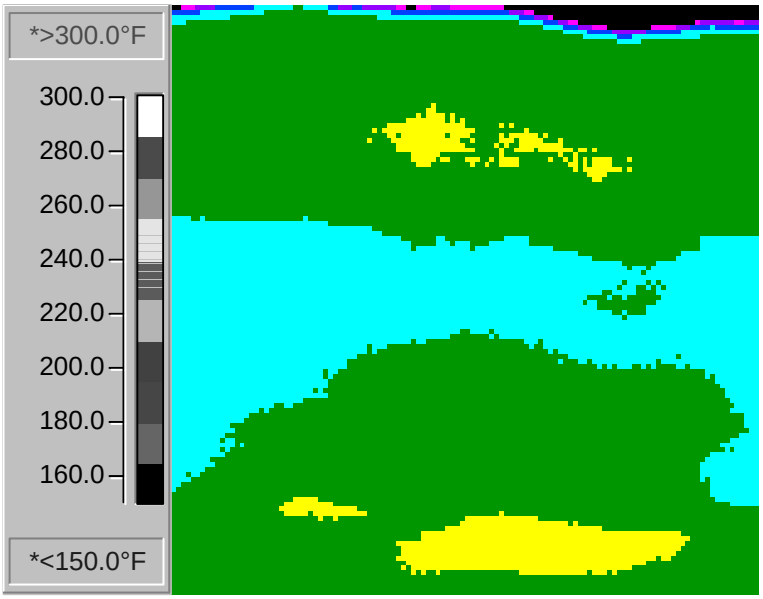

Figure 68. Temp Drop of 20 °F at 130 Feet into US 290 Test Section.

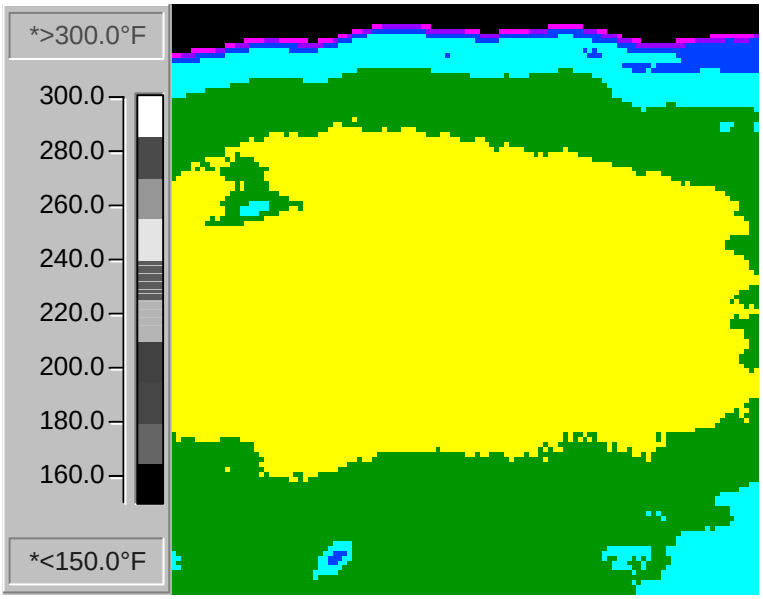

Figure 69. Center of Mat 25 °F Hotter at 530 Feet into US 290 Test Section.

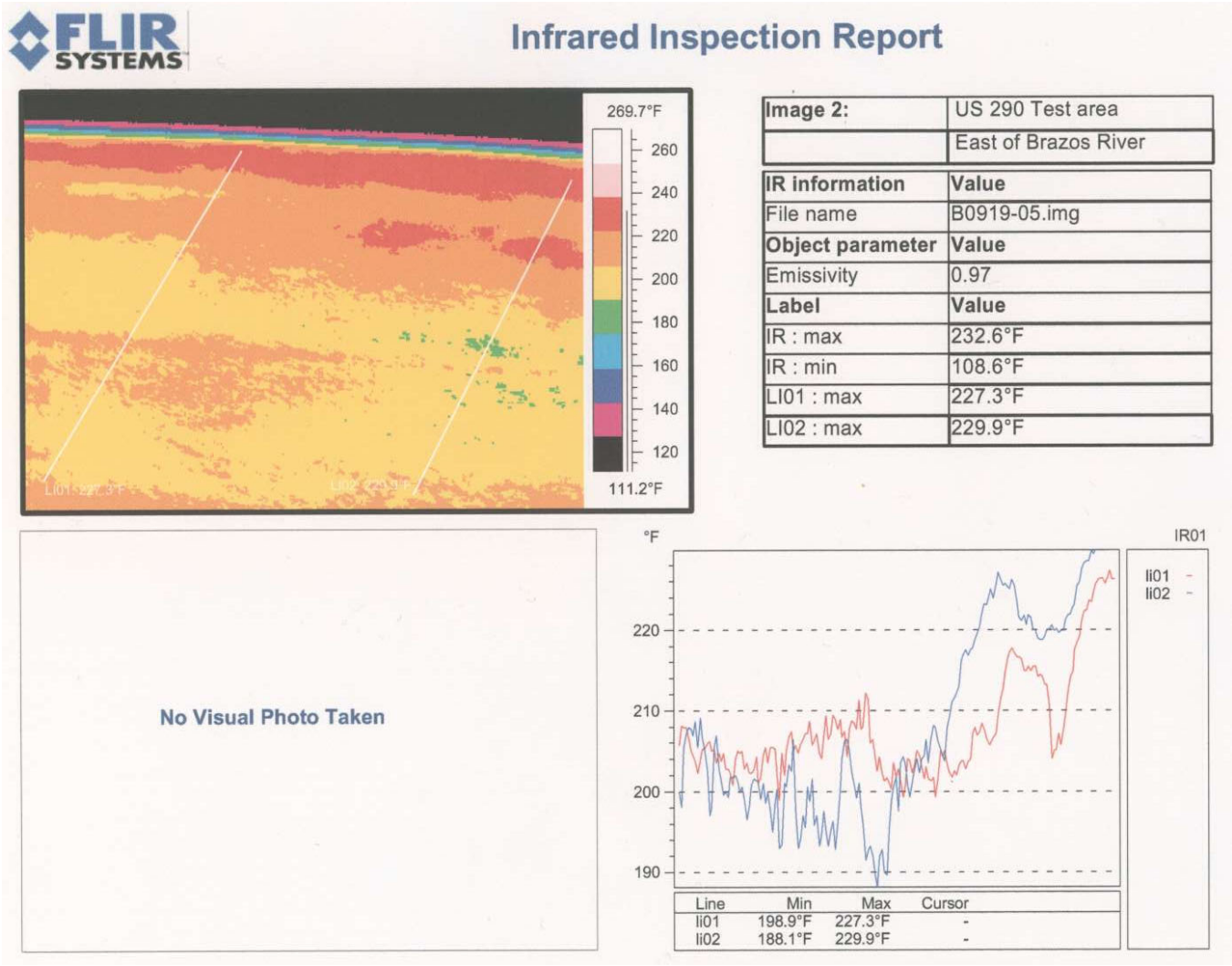

Figure 70. Temperature Drops of 40 °F at 850 Feet into US 290 Test Section.

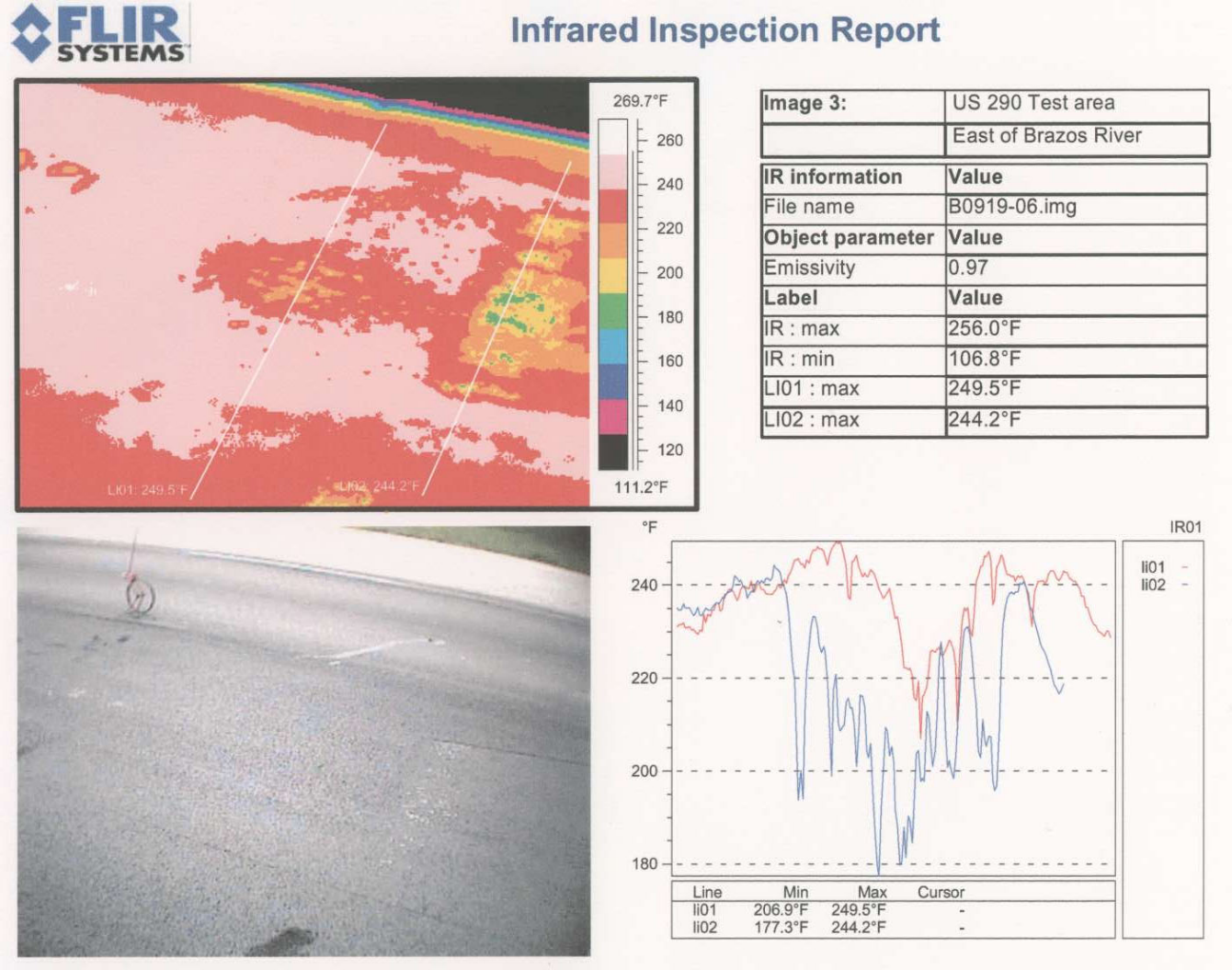

Figure 71. Temperature Drops of 40 °F at 900 Feet into US 290 Test Section.

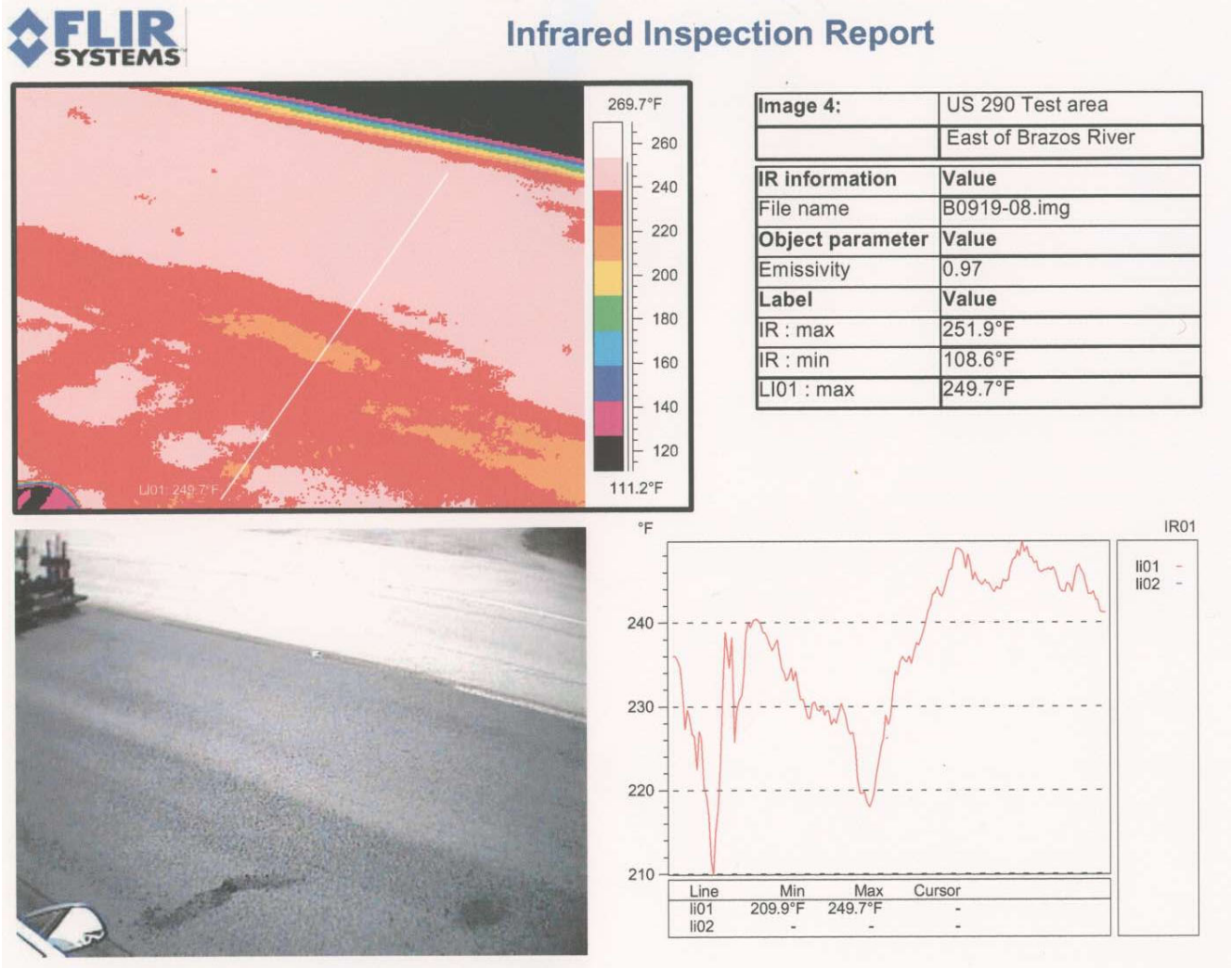

Figure 72. Temperature Drop of 30 °F at 980 feet into US 290 Test Section.

V. RESULTS FROM GROUND-PENETRATING RADAR

Five passes of GPR were performed on September 20, 2001. The location shown previously in Figure 70 had the lowest dielectric readings of the entire section, so anomalous cores were taken here. Normal cores were taken at 800 feet into the test strip. From laboratory analysis of cores where stationary GPR readings were taken, the following relationship between air voids and GPR dielectric was estimated for the mat on US 290:

$$\ln(\text{Air Voids}) = 5.9048 - 0.6354\varepsilon \qquad R^2 = 0.9147$$
$$(0.4870)\ \ (0.0868) \qquad \text{(s.e.)} \qquad \hat{\sigma} = 0.1283$$

which transforms to:

$$\%\ \text{Air Voids} = 366.79 * e^{(-0.6354\varepsilon)}$$

From this relationship, predictions of density and air voids were made for each of the GPR readings. Table 20 shows the resulting summary statistics.

Table 20. Predicted Mat Statistics for US 290 Test Section.

Parameter	Average	Minimum	Maximum	Standard Deviation
Density	144.25	130.85	151.46	2.23
% Density	92.26	83.70	96.88	1.426
% Air Voids	7.74	3.12	16.30	1.43

Although the range of minimum to maximum air voids of this job is wide, Figure 73 shows that approximately 90 percent of the mat had air voids between 5 and 10 percent. Five percent of the section is predicted to have voids over 10 percent, and 5 percent is predicted to have voids less than 5 percent.

Figure 74 shows the surface plot of predicted voids for the US 290 test section. At 530 feet, where the IR showed the center of the mat to be hotter, the voids were likewise predicted lower from the GPR data. At 850 feet, which the IR showed to be about 40 °F cooler than the normal mat temperature, the predicted voids were the highest of the entire test section.

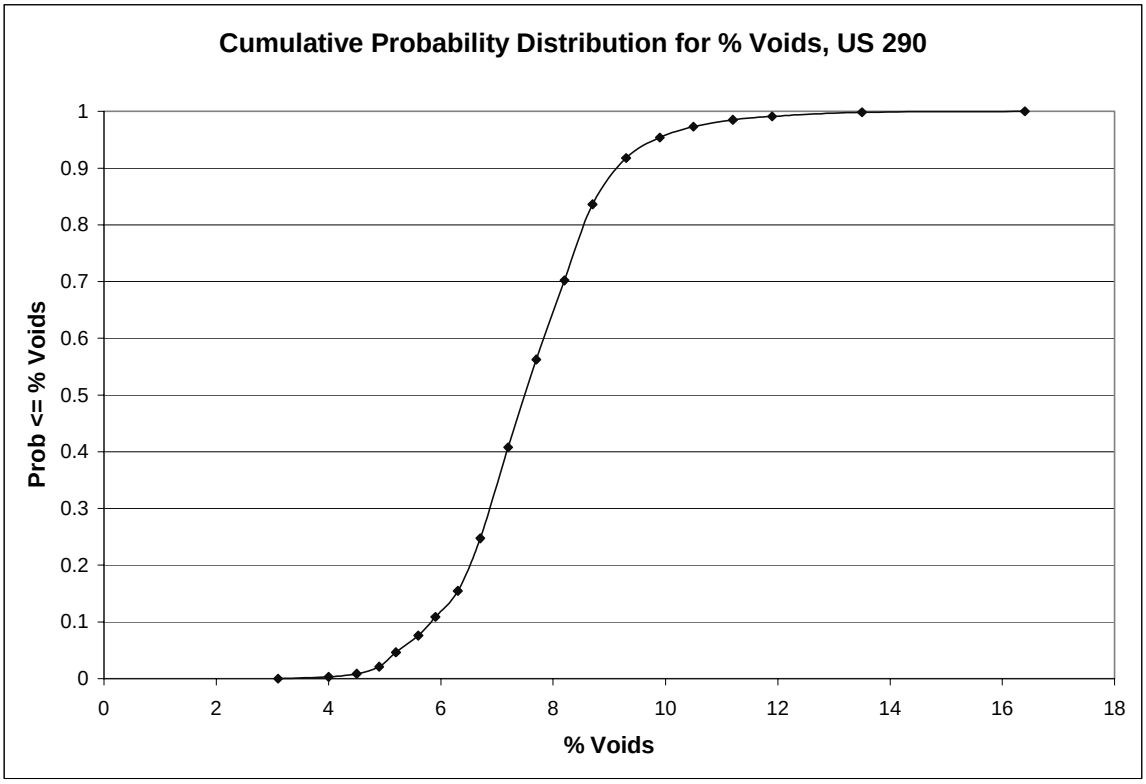

Figure 73. Distribution of Air Voids for US 290 Test Section.

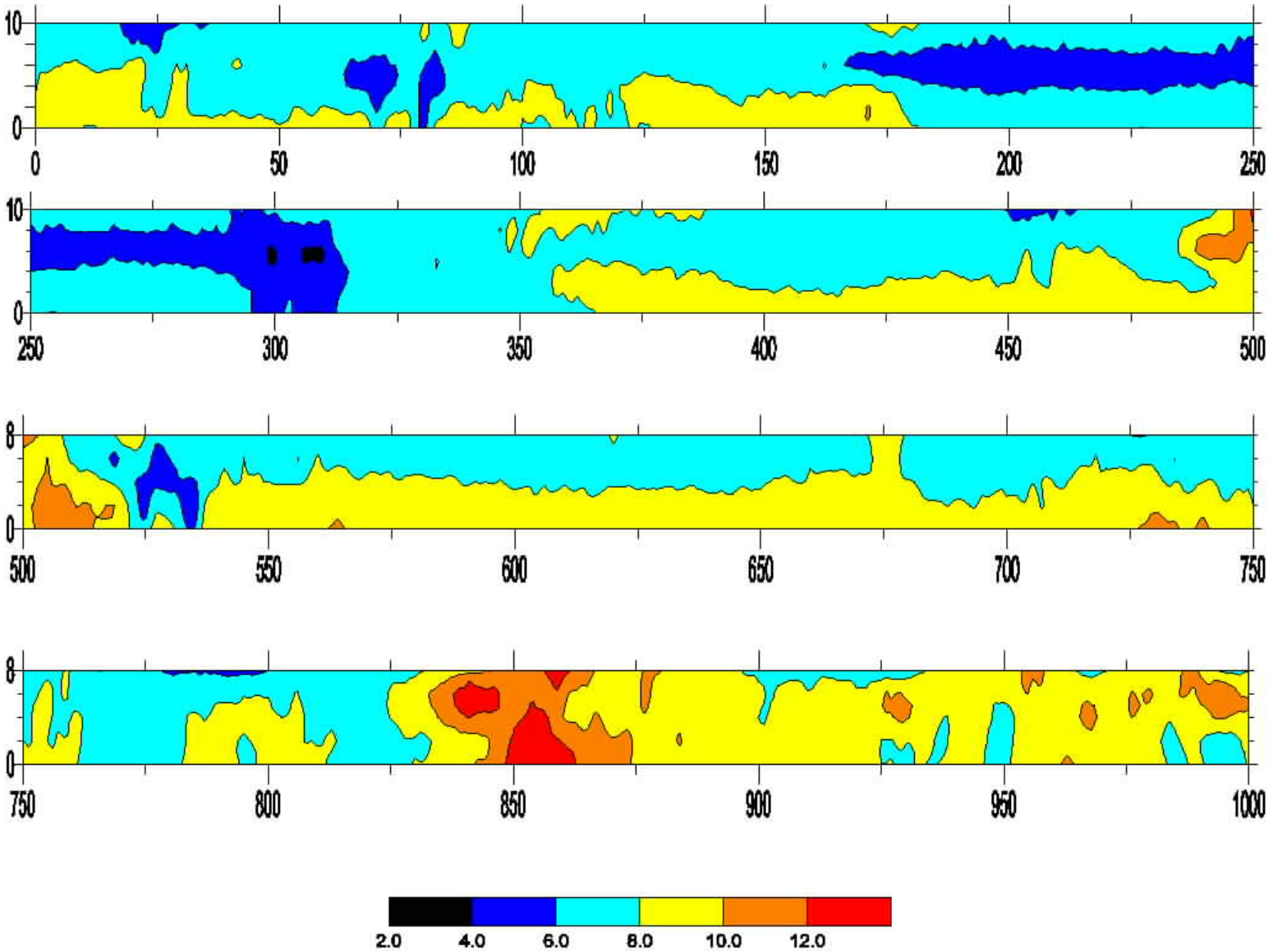

Figure 74. Surface Plot of Air Voids for US 290 Test Section.

VI. RESULTS FROM CORES

Based upon significant differences seen with the infrared and GPR equipment, seven cores were taken for testing in the laboratory. These cores were tested for bulk density, surface texture depth, permeability, rut depth after 8000 passes of the Asphalt Pavement Analyzer, Rice gravity, percent air voids, percent asphalt, and gradation. All results except for gradation are presented in Table 21, with gradation results shown in Table 22 and Figure 75.

The low temperature/low dielectric cores had a permeability rate approximately nine times that of the high dielectric cores, double the air voids of the predicted mat average, and two of these four cores had an asphalt content more than 0.5 percent below the JMF asphalt content of 4.8 percent. The average void content of the high dielectric cores was 10.6 percent less than the predicted mat average, and these cores had asphalt contents approximately 0.9 percent higher than the JMF. The low dielectric cores were coarser than the JMF, with as much as 17 percent less passing on one sieve size (the #4) than JMF, while the high dielectric cores were finer than the JMF, with as much as 5 percent more passing a sieve size (the #10) than the JMF.

Table 21. Core Results from US 290 Test Section.

Core	Temp (F)	GPR ε	Bulk Density (pcf)	Texture Depth (in)	Permeability (cm/s)	Rut Depth (8000 passes, mm)	Rice Gravity (pcf)	Air Voids (%)	Asphalt Content (%)
L1	195	5.1	131.1	0.03145	0.0006105	5.832	156.48	16.21	4.46
L2	200	5.4	135.9	0.030451	0.0003966	4.209	156.82	13.33	4.69
L3	200	5.2	135.6	0.027275	0.0003165	4.656	157.16	13.72	4.31
L4	200	4.8	132.8	0.038281	0.0005276	4.744	155.83	14.80	4.07
N1	245	6.1	145.7	0.048426	0.00006189	4.87	155.79	6.48	5.58
N2	245	6.2	145.2	0.019837	0.00005003	4.644	156.58	7.29	5.66
N3	245	6.3	144.8	0.021882	0.00004227	5.928	155.72	7.00	5.75

Note: Design Asphalt Content was 4.8%

Table 22. Gradations for US 290 Cores.

Core	L1	L3	L4	N1	N2	N3	JMF
Passing 3/4	100	100	100	100	100	100	100
Passing 1/2	97.3	94.8	94.8	98.7	99.4	98.8	99.9
Passing 3/8	86.7	83.4	85.9	94.7	95.3	94.7	93.7
Passing #4	53.1	47.3	51.3	68.7	71.1	70	67.3
Passing #10	31.9	29.4	30.5	43.4	44.7	44.7	39.3
Passing #40	21.4	20	20.7	27.2	27.8	27.9	24.4
Passing #80	10.9	10.1	10.4	11.9	11.6	11.7	10.9
Passing #200	4.4	3.9	4.1	3.7	3.7	3.7	4

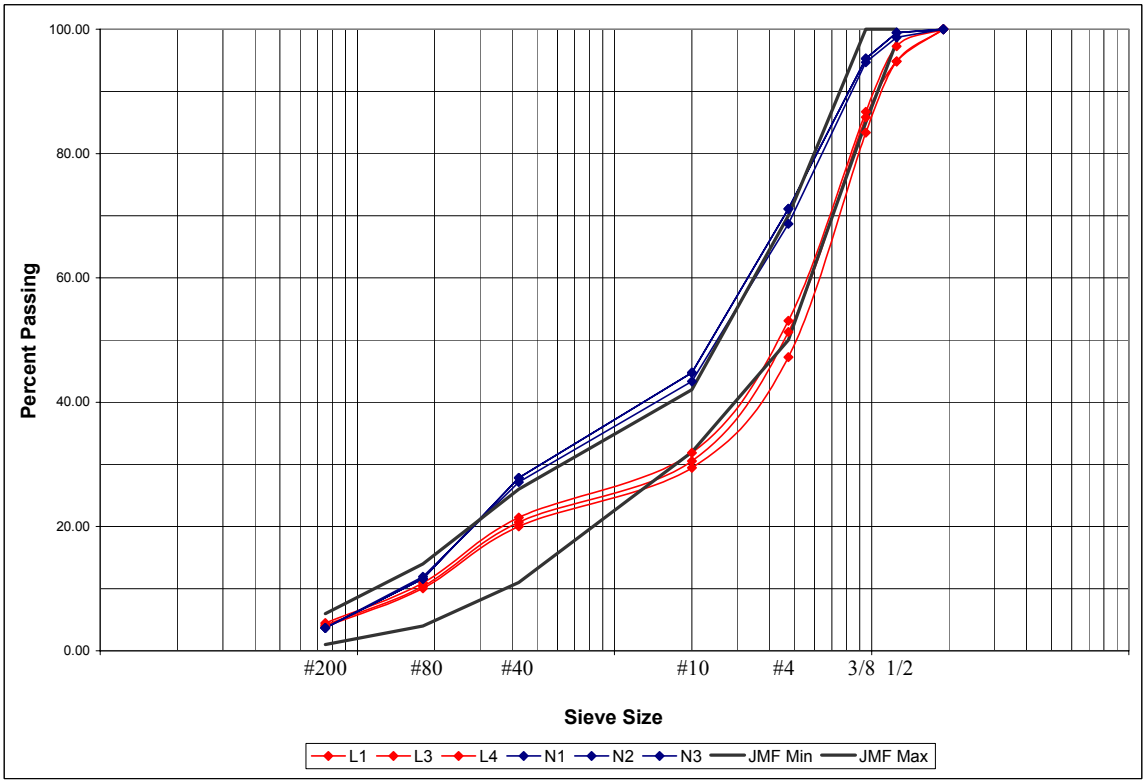

Figure 75. Gradation Results from US 290 Test Section.

VII. RELATIONSHIPS BETWEEN CHANGES IN TEMPERATURE AND DIELECTRIC AND CHANGES IN MIX PARAMETERS

Using the methods described on page 50 (Chapter 5 Section VII), researchers determined the significant correlations between changes in the NDT data and changes in the measured HMA properties. The complete correlation matrices are presented in Appendix D. Table 23 presents the correlations between key variables. Changes in NDT observations on this job showed strong correlations to changes in density, permeability, air voids, asphalt content, and changes in percent passing and percent retained on seven sieve sizes.

For variable combinations with non-zero correlations, changes in each mix parameter were regressed on changes in the NDT data to estimate the magnitude of changes in mix properties indicated by a certain level of change in the NDT data. In this manner, the limit on changes in NDT data before a mix property would be out of specification was examined. The regression equations are in Appendix D. Table 24 shows the level of change in NDT data that would indicate a mix parameter could be out of specification.

Table 23. Selected Significant Correlations between Data for US 290.

	ΔTemp (F)	Δ GPR ε
Δ Temp (F)	1.00	0.95
Δ GPR ε	0.95	1.00
Δ Bulk Density (pcf)	0.98	0.96
Δ Permeability (cm/s)	-0.94	-0.94
Δ Air Voids (%)	-0.99	0.96
Δ % Asphalt	0.96	0.99

Table 24. Limits on Changes of NDT Data before Mix Parameter Changes Are at Tolerance Limit for US 290.

Mix Parameter	Tolerance	ΔTemp Limit (F)	Δ GPR ε Limit
Δ Air Voids (%)	Range of 3.8; AVG to low 1.9	Range: 23; AVG to low: 11.5	Range: 0.6; AVG to low: 0.3
Δ % Asphalt	0.3	10.9	0.3
Δ % Passing #1/2	5	72	1.8
Δ % Passing #3/8	5	25	0.6
Δ % Passing #4	5	12	0.3
Δ % Passing #10	5	17	0.4
Δ % Passing #40	3	20	0.5
Δ % Passing #80	3	114	3.0
Δ % Passing #200	3	312	8.4
Δ % Retained on #1/2	5	73	1.8
Δ % Retained on #3/8	5	38	1.0
Δ % Retained on #4	5	24	0.6
Δ % Retained on #10	5	42	1.1
Δ % Retained on #40	3	21	0.6
Δ % Retained on #80	3	25	0.6
Δ % Retained on #200	3	80	2.1

From Table 24 it is clear that the magnitude of the relationship between changes in NDT data and changes in voids, asphalt content, and gradation, was substantial, as evidenced by the limits on NDT data before mix parameter changes would be at the allowable tolerance levels. The NDT limits based upon this job are:

Temperature: All values within ±11 °F of the mean; maximum range on 22 °F. If the high or low temperature were at JMF asphalt content, a temperature tolerance based upon percent asphalt would be reasonable. However, the data show that the low temperature cores were below JMF asphalt content, and the high temperature cores were well above JMF asphalt content. Thus, it appears reasonable that JMF asphalt content would be at a temperature somewhere in between, presumably at the average temperature, which supports the tolerance of ±11 °F. Furthermore, the tolerance on temperature from the density profile criteria is 11 °F. The

maximum temperature range of 22 °F is consistent with the tolerance from the relationship with changes in asphalt content and the high to low range of air voids limit. Furthermore, this maximum temperature range would capture the possibility of sieve sizes being out of specification based upon the data from this job.

GPR ε: All values within ±0.3 of the mean; maximum range of 0.6. As with the recommended temperature limits, the tolerance is based upon the relationship between the NDT data and changes in asphalt content of the mix and is likewise consistent with tolerances from the density specifications. A maximum range of 0.6 is consistent with the recommended tolerance and would capture the possibility of density and/or as many as three sieve sizes being out of allowable operational tolerances.

VIII. CONCLUSIONS

Data collected at the hot in place recycling job on US 290 showed strong relationships between changes in NDT data and changes in hot-mix parameters. Locations tested had significant changes in density, asphalt content, and gradation. Of the four jobs examined, this job is the only one where the NDT changes were indicative of changes in all three of these important parameters. However, this is likely due to the fact that the bad cores were taken from an area where the supply of trucks with fresh mix ran out. Data from other jobs indicate that, in general, the changes in NDT data were either primarily indicative of changes in asphalt content and gradation or changes in density.

The temperature differential between the high and low areas tested on this mat would be in the NCAT proposed high level of segregation. The differences seen in the analysis of cores were consistent with the expected changes from the NCAT study at this level of segregation. Fortunately, this drastic of a change was only seen at the isolated location where the supply of mix ran out.

Based upon the US 290 testing, the following conclusions are made:

- NDT tools were effective at locating anomalous areas of the pavement mat.
- Changes in NDT data at locations where mix supplies run low are likely indicative of more severe segregation issues.

CHAPTER 9

CONCLUSIONS AND RECOMMENDATIONS

I. SUMMARY

This project has focused on using two non-destructive testing technologies: infrared imaging and ground-penetrating radar, to evaluate the uniformity of newly placed hot mix overlays. Four sections were tested, and cores were taken where anomalies were identified in either of the NDT readings. The cores were returned to TTI laboratories and a range of tests conducted to measure important materials properties such as air void content, percentage asphalt, and gradation.

On each 1000 foot test section, GPR data were collected in five passes at different lateral offsets (outer edge, outer wheel path, mid lane, inside wheel path and inside edge). In each pass 1000 GPR reflections were taken (1 per foot); therefore, a total of 5000 GPR traces were collected in each section. The laboratory cores were used to develop a relationship between the measured field dielectric and core air voids. The 5000 data points were therefore converted into 5000 estimates of mat air voids. Using a software package, these data points were displayed as a contour map for each project. It was therefore possible to compare the temperature contour maps recorded during mat placement with those computed from the GPR data. The contour plot also makes it simple to examine a section and more accurately identify high void locations that may be prone to premature distress.

The important conclusions from this study are:

- With the four projects tested, significant changes in air voids were measured on two projects. Variations in asphalt content were the primary changes found on one project, and significant changes in both voids and gradation changes were found on one project.
- Both IR and GPR were found to be good indicators of mat uniformity. Both provide a comprehensive picture of the new surface.
- Surface temperature, as measured by an IR camera, is a good indicator of surface quality. Large changes in surface temperature were strongly correlated to large changes in either voids, asphalt content, or gradation.
- From the data it is proposed that variations in surface temperature of greater than 25 °F indicate significant changes in mat quality. This is similar to recommendations from other agencies that have investigated the use of thermal imaging for quality control of hot-mix overlays.
- Surface dielectric is perhaps the best indicator of mix density. This is a non-contact measurement, so it is not impacted by surface texture.
- Variations in surface dielectric, as measured by the GPR, are highly correlated to changes in mat properties. The variations were primarily attributed to changes in air void content.

- The problem areas detected by the IR (cold spots) typically were found to be lower density areas with the GPR.
- It is proposed that for CMHB and SMA type mixes, variations of surface dielectric of greater than 0.8 from the mean will indicate a mat that is out of specifications. For dense-graded mixes, the max allowable dielectric variation should be ± 0.4.
- Density profiling is quite time-consuming and thus seems only reasonable if one suspects problems. Even still, the location of the highest temperature differentials observed during this project (approximately 80 °F cooler than typical laydown temperatures at a location where the paver stopped on US 79) passed the density profile test.
- There was no significant relationship observed between changes in the NDT data and rutting depth as measured by the Asphalt Pavement Analyzer.
- Of the four jobs, only two jobs showed a significant relationship between changes in texture depth and changes in air voids.
- The temperature uniformity of the mat was strongly related to the continuity of the lay down operation. Locations where the paver stopped resulted in surface temperature variations of 30 to 80 °F.
- Both IR and GPR could be considered as effective quality control or quality assurance methods. Infrared imaging provides a means of assessing mat quality and identifying potential problems as placement is taking place, thus allowing the opportunity for corrective action. GPR provides a rapid and reliable means of obtaining density data and should be considered as a replacement for nuclear density techniques. TxDOT should consider future implementation of these technologies. Ideas on how this can be achieved are presented below.

Table 25 shows a summary of each job. The computed distribution of air void contents for each of the four jobs is shown in Figure 76.

Table 25. Summary of Test Sites Investigated.

Test Site	Mix Type	Operation	Problems Noted	Comments
SH 6	CMHB-C	MTV	Asphalt content; gradations on the fine side	Uniform job; air voids uniform; joints good
US 79	CMHB-C	MTV	Air voids	Gradations and asphalt content uniform; void problems
IH 10	Superpave ½”	Windrow Elevator	Compaction problems	Voids high
US 290	Type D	HIPR	Air voids and gradation; supply of trucks ran out	Generally acceptable; isolated bad spot

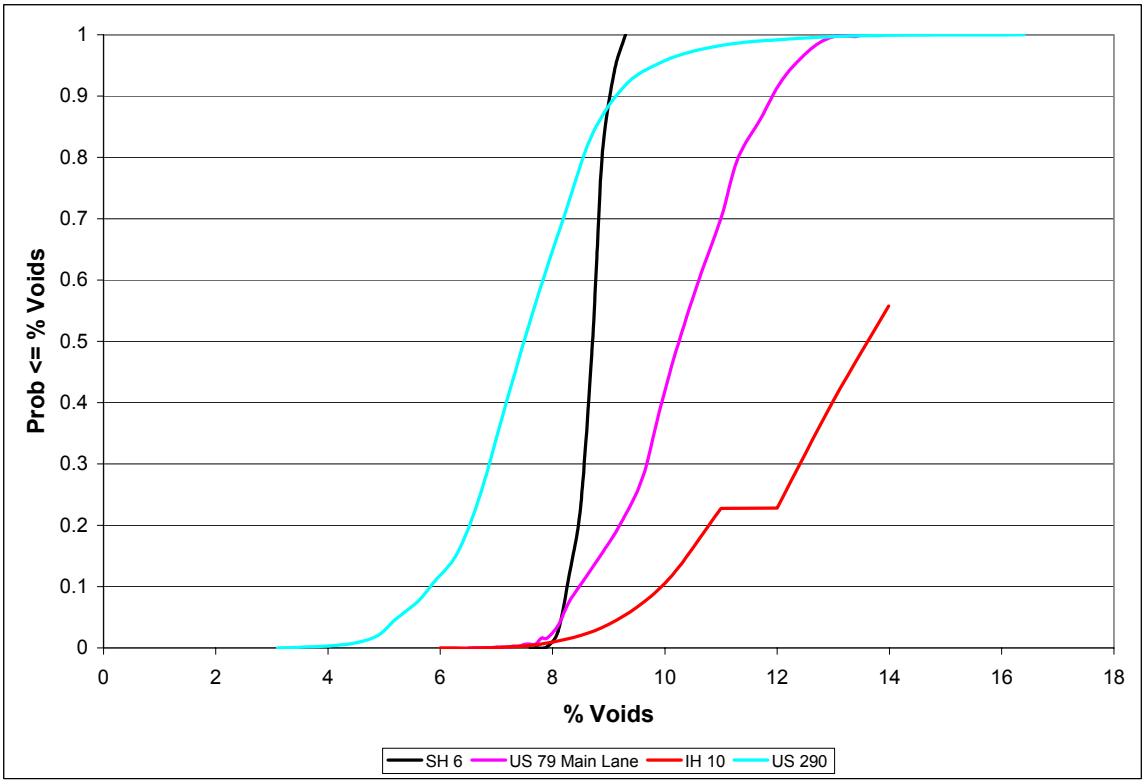

Figure 76. Expected Distributions of Mat Air Voids for Test Locations.

Figure 76 illustrates that the SH 6 job, by far, had the most uniform mat air voids. Although as a whole the US 79 job has greater voids than the US 290 job, the US 79 site is more uniform since the tails of the US 290 distribution (especially the upper tail) are so broad. Interestingly, both the SH 6 and US 79 jobs were using a MTV. However, although not as uniform as the US 79 job, the distribution of the US 290 job is clearly more desirable since, except for the extreme upper one-percentile, the US 290 distribution of voids is approximately 3 percent less for any given probability. Due to reasons previously discussed, the entire distribution (and thus overall variability) could not be developed for the IH 10 job, but it is clearly shown that the IH 10 job was the worst of the four, as 75 percent of this mat is expected to have voids greater than 12 percent, and 45 percent of the mat is expected to have voids greater than 14 percent.

For most of the cases reported in this project there is a strong correlation between the IR and GPR results. Anomalous locations identified with the IR camera often were found to be areas where the surface dielectric changed substantially. Figure 77 shows such an area. The coldest area in the IR image is the green areas. This area likewise was predicted to have high air voids. Directly above this location in both images is a hotter area, which from the GPR data was predicted to have less air voids.

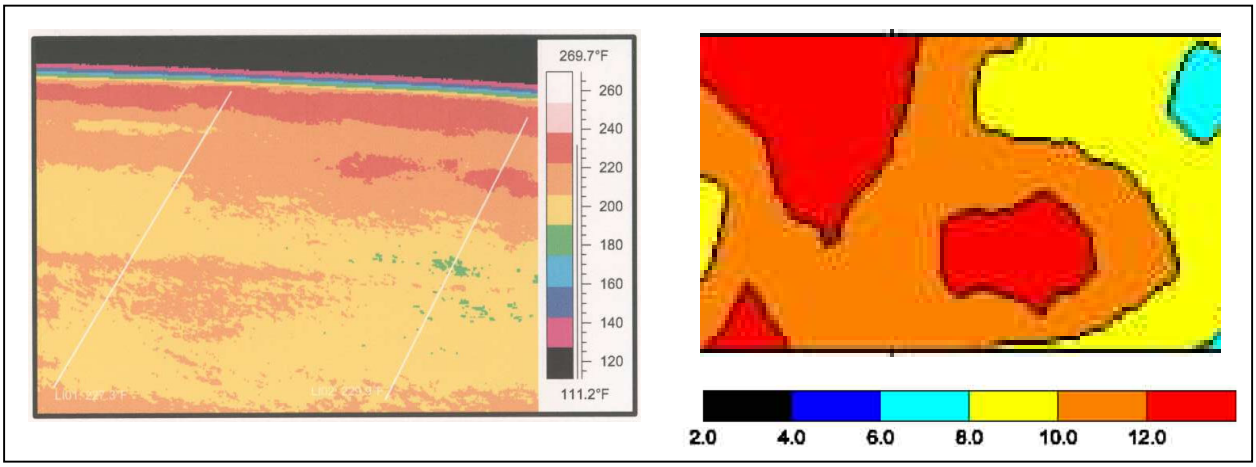

Figure 77. IR Image with Corresponding Void Predictions.

In some cases there is not a strong correlation between variations in surface temperature and changes in air voids. Since imaging is performed before rolling, such occurrences would be expected. As noted in previous studies, rolling patterns could help minimize compaction problems that may occur within lower temperature areas. Furthermore, it has been observed that temperature differentials could be indicative of a change in other mix properties such as asphalt content or gradation, or a combination of small changes in several parameters, and thus temperature differentials may or may not translate into a density problem.

II. RECOMMENDATION FOR CALIBRATION TESTS AND ACCURACY OF NDT EQUIPMENT

Calibration of the infrared devices requires a blackbody source and other specialized equipment and expertise. It would be cost-prohibitive for the user to procure the hardware necessary for calibration of an IR camera. As such, calibration of these devices is best left to manufacturers of the equipment. The IR camera provided measurements well within its stated accuracy limits of ±2 percent as long as the emissivity setting was appropriately set. Thus, the real issue with IR devices is determining the proper emittance value of the target. Also important is to determine the emissivity from approximately the same angle that will be used for data collection. In general, an emissivity setting of 0.95 is appropriate for hot-mix asphalt. However, two appropriate methods of determining the emissivity of a material are:

- Use black electrical tape (emissivity = 0.95). Complete details of this procedure are in Chapter 4. Since the emissivity of the tape is so close to that of HMA, it would be reasonable to simply use a value of 0.95 rather than use this method.
- Use a calibrated surface thermocouple. The surface temperature is measured with the thermocouple and an IR image is simultaneously acquired. The emissivity on the IR device is adjusted until the temperature of the test spot matches the measured temperature from the thermocouple. Although reasonable for use with HMA, one must be cautious to ensure good coupling between the surface probe and the hot-mix

surface to avoid errors in the thermocouple reading. The determined emittance should be between 0.90 and 0.98.

Methods for calibrating a GPR system should include the signal to noise ratio, signal stability, time calibration, end reflection, and symmetry of the metal plate reflection. These methods are in Appendix E. Antenna bounce and especially the metal plate reading affect the accuracy of GPR data. Software used for processing the GPR data includes a bounce compensation function. However, variability in metal plate readings remains an issue that requires further investigation.

III. RECOMMENDATION ON EFFECTIVENESS OF INFRARED EQUIPMENT FOR DETECTING SEGREGATION

Calibration studies indicated that the IR camera is highly accurate at measuring the surface temperature providing that the emissivity is appropriately set. The emissivity is a measure of the percentage of energy transmitted from the surface of an object. For materials such as HMA, an emisivity of 0.95 is reasonable. From laboratory studies it is recommended that the data be collected with the camera operating at an angle of no less than 45°. For normal paving operations the camera should stand in the back of a pickup truck. Operating under the assumption that wind speeds will be the same at all points within each thermal image, wind effects should not be a concern since temperature differences are what is being investigated. As long as the wind has the same velocity at points being examined, the temperature difference will be the same even though their surface temperatures will be lower (*19*). During this project no winds greater than 4 mph were encountered.

The data collected showed that changes in temperature were significantly correlated to changes in:

- surface dielectric (all test sites),
- air voids (three test sites),
- asphalt content (two test sites), and
- gradation (two test sites).

With regard to an acceptance limit on the maximum allowable temperature differential, the IR data was found to be an effective device that yielded results relatable to changes in hot-mix properties. The following changes in surface temperature were found to give changes in properties that exceed current limits from TxDOT's current density profiling specification:

- US 79..... 20 °F
- IH 10..... 25 °F
- US 290..... 23 °F

Based on these results TxDOT should adopt the recommendations from both Washington State and NCAT. The maximum temperature variation permitted should be less than 25 °F.

IV. RECOMMENDATION ON EFFECTIVENESS OF GPR FOR DETECTING SEGREGATION

Ground-penetrating radar was found to be an effective tool for locating anomalous areas of the pavement mat. This technology is especially well suited to measuring air voids, but GPR data also were relatable to changes in other mix parameters. GPR provides a rapid, simple means of examining an entire project. The amplitude of reflection from the HMA surface is used to compute the surface dielectric of the new hot-mix mat. These values are independent of wind speed, surface temperature, or surface texture. The only limitation on GPR testing is that the data should not be collected after significant rainfall. Changes in surface dielectric were found to be strongly related to changes in:

- air void content (all test sites),
- asphalt content (one test site), and
- gradation (one test site).

Based on TxDOT's specifications, the following changes in surface dielectric were found to indicate problems in hot-mix properties:

- US 79..... Max range of 1.4; no values more than 0.8 from the mean
- IH 10..... Max range of 0.3
- US 290..... Max range of 0.6; no values more than 0.4 from the mean

The simplest way of using GPR is to graph surface dielectric for any run over a project and flag areas with reductions in dielectric of 0.8 (for coarse mixes) and 0.4 (for dense mixes) from the mean. This technique is illustrated in Figure 78.

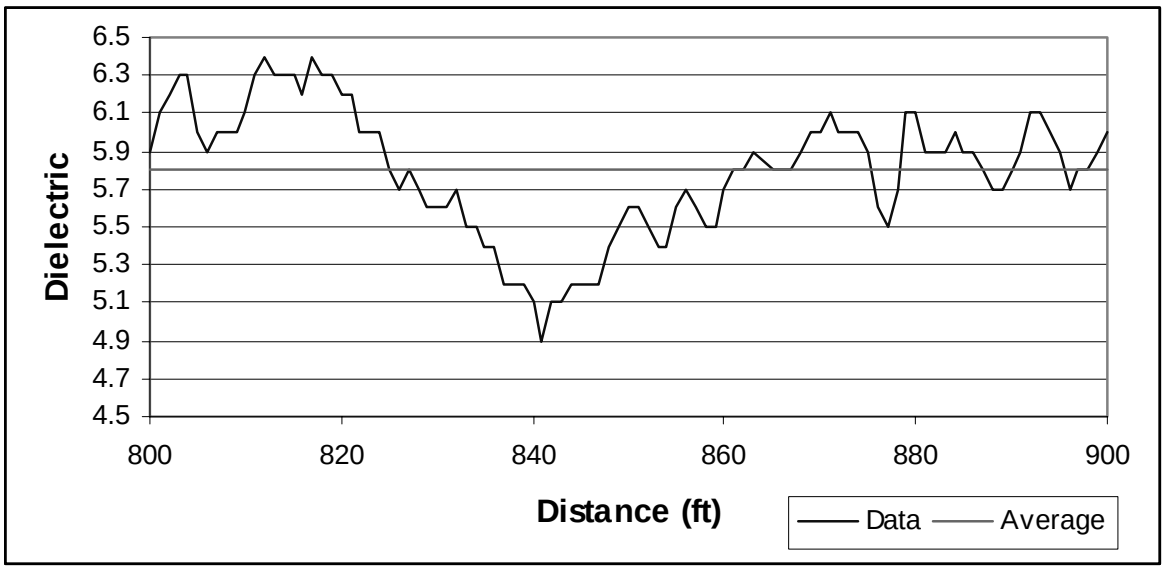

Figure 78. Example GPR Data Showing Significant Drop in Dielectric.

The best use of GPR is to adopt the methodology proposed in Finland and demonstrated in this project. A minimum of three calibration cores for each project should be used to develop the relationship between field dielectric and air voids. Using the methods developed in this project it is then possible to generate a contour map of air voids for any project. A sample of an air void contour plot is demonstrated in Figure 79.

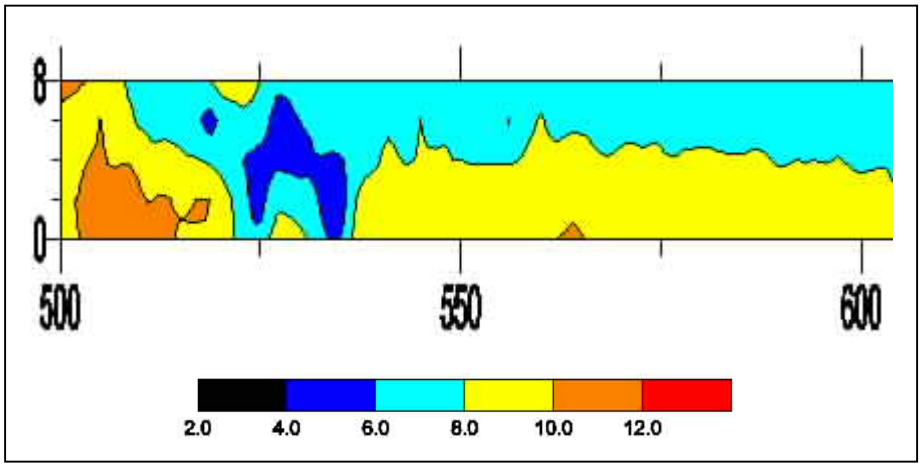

Figure 79. Example Surface Plot of Air Voids from GPR Data.

V. RECOMMENDATIONS ON MATERIAL ACCEPTABILITY LIMITS

Based on the results in Chapters 5 through 8 the following criteria are proposed:

- Significant changes in mix properties will occur if changes in surface temperature of more than 25 °F are measured in the field.
- Significant changes in mix properties will occur if the surface dielectric changes by more than 0.8 for coarse-graded CHMB mixes and 0.4 for dense-graded materials. The US 79 job was a CMHB while US 290 was a dense-graded surface. From previous experience the normal variation in surface dielectric is higher with the coarser mixes, and thus a separate limit is recommended for coarse mixes and dense-graded mixes.

VI. RECOMMENDATIONS FOR USE OF NDT DEVICES AS QC/QA

Although both IR and GPR proved to be effective measures of mat uniformity, neither of the two devices used in this project were thought optimum for full implementation. The IR cameras are expensive, in the range of $20,000 to $50,000. The angle of operation and limited field of view make development of a field test and acceptance protocol difficult. A typical image covers about 20 to 30 feet of pavement; therefore, multiple images need to be collected and merged as the paving train passes along the highway. Coming back to an exact location is nearly impossible unless the area is marked immediately upon imaging. However, the infrared imaging technology appears well suited as a quality control device. There is now substantial evidence

that temperature differentials of greater than 25 °F are indicative of some type of significant change in the hot-mix properties. Infrared imaging could be used during laydown to identify if problems are occurring and therefore provide the opportunity to become aware of problems while they are occurring and take corrective action. However, ideas for a more effective approach utilizing infrared technology are discussed in the next section.

The 1 GHz GPR system used is relatively large and bulky. The existing antenna has an effective depth of penetration of over 20 inches. A slightly higher operating frequency system, such as 2 GHz, would have the advantages of smaller size (factor of 2) and greater near-surface accuracy. Furthermore, the GPR systems in use are all vehicle mounted. With recent advances in GPR systems it should be possible to build a handheld unit for spot-specific measurement. This system could potentially replace the nuclear density gauge and would have significant advances over alternative density measurement systems in that it would be non-contact and therefore not impacted by surface texture.

For the Texas materials tested in this project no significant correlations were developed between surface texture and engineering properties. Surface texture was only relatable to density on two of the jobs tested. Texture-measuring systems may not be optimal for Texas materials.

VII. RECOMMENDATION FOR IMPLEMENTATION

Both ground-penetrating radar and infrared imaging can be used as TxDOT quality control (IR) and quality assurance (GPR) systems. However, some implementation work should be undertaken to optimize field operations. The following ideas are proposed for TxDOT consideration.

A development concept for implementing IR technology is shown in Figure 80. In recent years, low-cost infrared sensors for spot measurements have become available. These sensors cost in the order of $250 to $400 each. The rolling beam, shown in Figure 81, would have between six and 10 sensors spread out at regular intervals. A distance-measuring instrument (DMI) would be included in a wheel so data could be collected at known regular intervals as the mat is being placed. The information could be summarized in regular intervals, such as every 100 feet.

The control box at the end of the sensor bar would house the data collection and processing system. The surface mapping system developed in this project for processing GPR could be used to print out color contours similar to that produced by infrared cameras. The advantages of this system are many:

- It is expected a system could be developed for less than the price of a full-featured infrared camera.
- Accurately locating anomalous locations would be possible with this system since the data would be tied in to a DMI and each sensor would be at a known transverse offset. Accurately locating areas on a hot-mix mat from an infrared image is virtually infeasible unless the location is immediately marked, and even then there is guesswork involved.

- Labor involved would be reduced with this system. Potentially only one person would be needed. Using the infrared camera typically required three people: a driver, an imager, and a person to mark locations so they could be found later on.

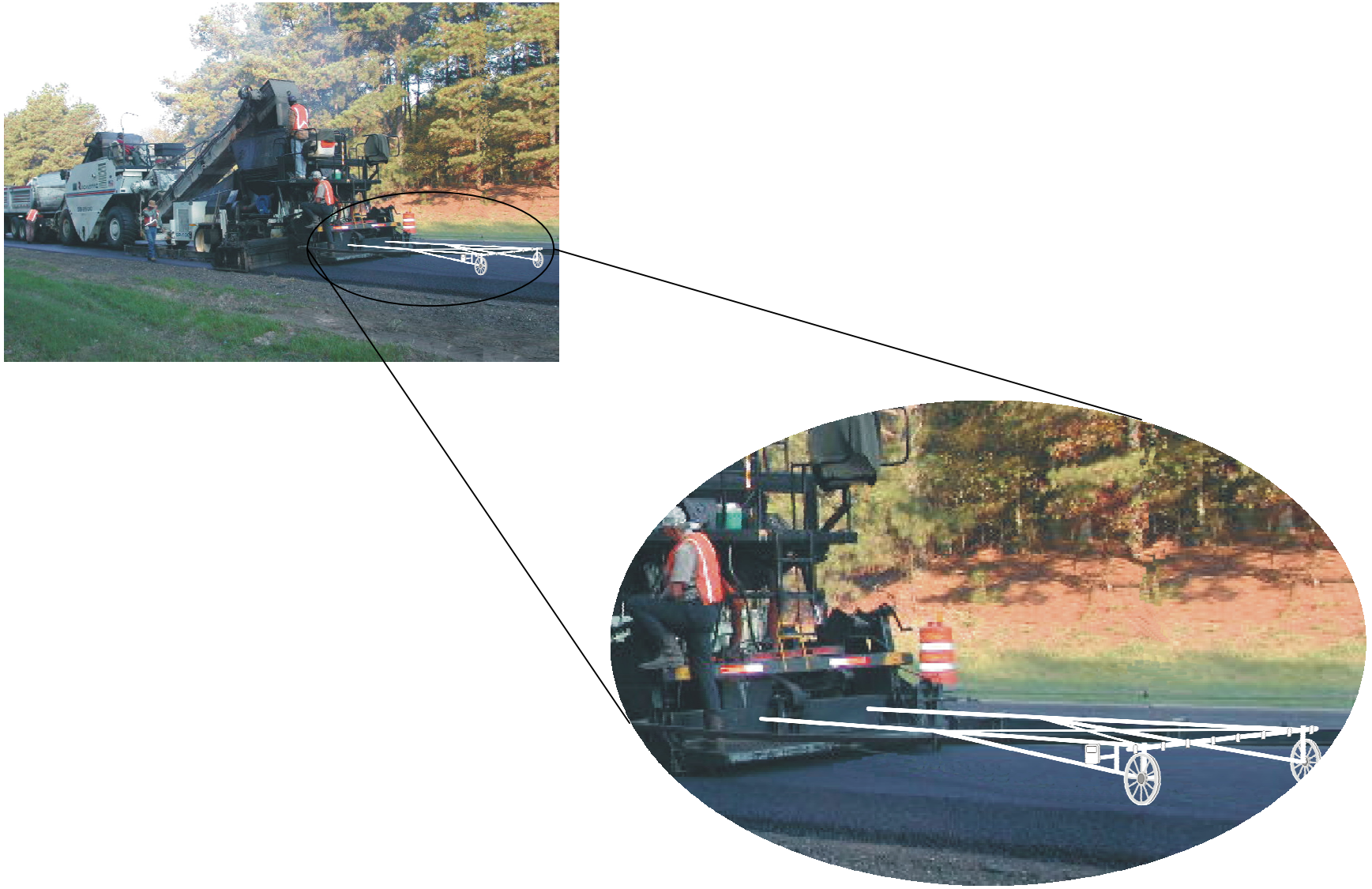

Figure 80. Concept Infrared Sensor Bar for Quality Control.

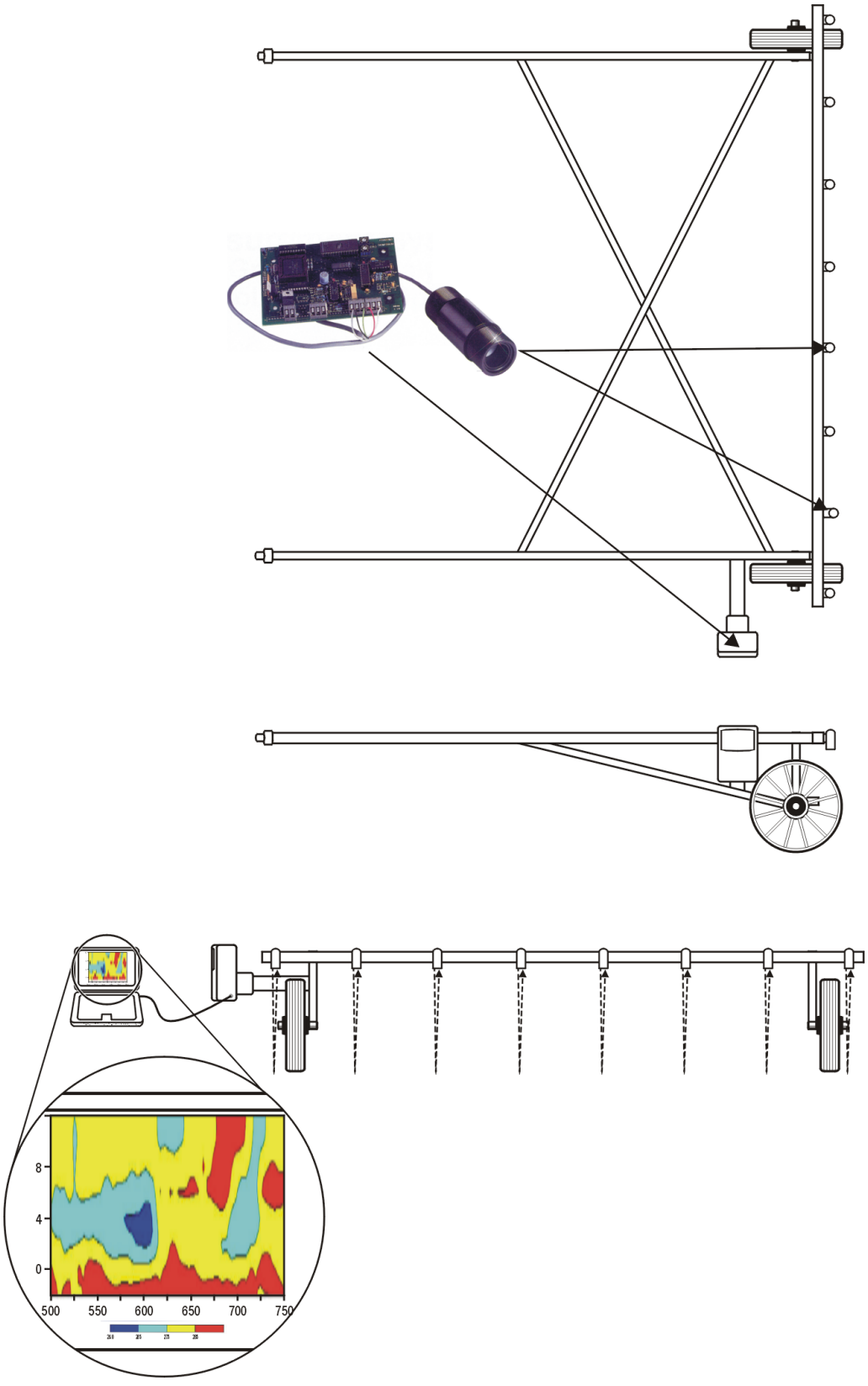

Figure 81. Schematic of Concept Infrared Sensor Bar.

Similar concepts could be developed for GPR systems. The advantage of GPR is that data can be collected anytime after placement and GPR can be used to get an air void profile of the entire mat. Development concepts could include multiple antennas fixed on a vehicle, or small handheld units that could be placed on top of the pavement. These concepts are illustrated in Figure 82 and would provide several advantages over existing density measurement techniques:

- The system would be non-contact and thus not susceptible to problems from surface texture as is the case with other density-measuring units, whether they are nuclear or capacitance based.
- The system is non-nuclear and thus would not be subject to the hazards, permits, and paperwork required with the use of nuclear devices.
- The system would provide virtually instantaneous readings, as opposed to having to wait several minutes with nuclear devices

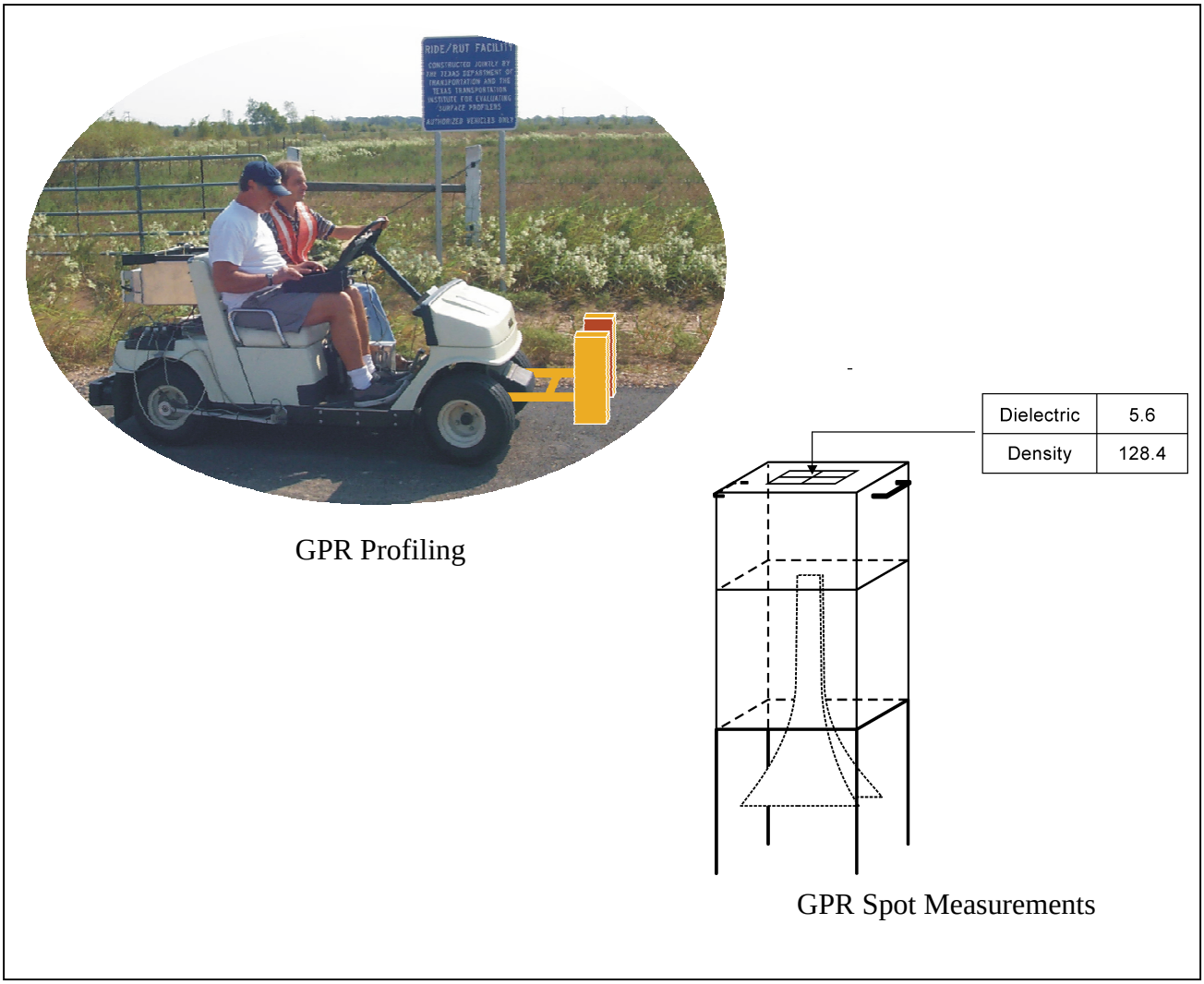

Figure 82. Concept GPR Systems for Quality Assurance and Rapid Non-Contact Density Measurement.

REFERENCES

1. M. Stroup-Gardiner and E. R. Brown. *Segregation in Hot-Mix Asphalt Pavements*, NCHRP Report 441, Transportation Research Board, National Research Council, Washington, D.C., 2000.
2. S. Read. *Construction Related Temperature Differential Damage in Asphalt Concrete Pavements*, University of Washington, 1996.
3. Segregation: Causes and Cures for Hot Mix Asphalt, AASHTO, 1997.
4. R. Wilson. *Special Provision and/or Specification Change Memorandum 58-99*, Texas Department of Transportation, December 20, 1999.
5. T. Scullion and Y. Chen. *Using Ground-Penetrating Radar for Real-Time Quality Control Measurements on New HMA Surfaces*, Report 1702-5, Texas Transportation Institute, 1999.
6. T. Saarenketo. Using GPR and Dielectric Probe Measurements in Pavement Density Quality Control, Tranportation Research Board Record, 1997, pp. 34-41.
7. S. Cross, M. Hainin, and A. Ado-Osei. *Effects of Segregation on Mix Properties of Hot Mix Asphalt*, Report KU-96-6, University of Kansas, 1998.
8. *Segregation Check Points*, Kansas Department of Transportation.
9. *Segregation Check Using the Nuclear Density Gauge*, Kansas Department of Transportation, 1999.
10. *Special Provision to the Standard Specifications*, 90p-198-R3, Kansas Department of Transportation.
11. *Special Provision to Special Specification 3146-017*, Texas Department of Transportation, September 2001.
12. *Test Method Tex*-207F – *Part V*, Texas Department of Transportation.
13. *Special Provision to Item 340, 340-005*, Texas Department of Transportation.
14. M. Tahmoressi, D. Head, T. Saenz, and S. Rebala. *Material Transfer Device Showcase in El Paso, Texas*, Texas Department of Transportation, 1999.
15. J. W. Henault. *Development of Guidelines for Reduction of Temperature Differential Damage (TDD) for Hot Mix Asphalt Pavement Projects in Connecticut*, Report 2222-1-99-5, Connecticut Department of Transportation, 1999.
16. Washington Department of Transportation [online]. Available *http://pavements.ce.washington.edu/sptc/search.asp*.
17. K. Willoughby, et al. *Construction-Related Asphalt Concrete Pavement Temperature Differentials and the Corresponding Density Differentials*, Report WA-RD 476.1, Washington Department of Transportation, July 2001.
18. *Tech Notes*, Washington Department of Transportation, September 2001.
19. K. Willoughby (personal correspondence). March 25, 2002.
20. *Cyclic Density Special Provision*, Washington Department of Transportation.
21. C. Chang, G. Baladi, and T. Wolff. *Detecting Segregation in Bituminous Pavements*, 81st Transportation Research Board Annual Meeting, Washington, D.C., January 2002.
22. Ircon Inc. Introduction to Infrared Thermometry, Technical Solution TS104 [online]. Available *http://www.ircon.com/techsolution.html#5.*
23. Mikron Instrument Company, Inc., Table of Emissivity of Various Surfaces.
24. G. Strahan (personal correspondence). February 9, 2001.

25. G. Strahan. Wind Effects on Electrical Hot Spots-Some Experimental IR Data, Texas Infrared.
26. T. Scullion. *Development and Implementation of the Texas Ground Penetrating Radar System.*
27. T. Saarenketo and P. Roimela. Ground Penetrating Radar Techniques in Asphalt Pavement Density Control, Proceedings of the Seventh International Conference on Ground Penetrating Radar, May 27-30, 1998, Lawrence, Kansas, Vol 2, pp. 461-46.
28. Finland GPR Specs (Paallystetutka tiiviyden lasdunvalvonnassa).
29. *Measurements at Helsinki-Vantaa Airport, Runway No. 3*. Roadscanners Oy Survey Report 01/2001.
30. Omega Engineering, Inc. Transactions in Measurement and Control – Volume 1- Non-Contact Temperature Measurement [online]. Available *http://www.omega.com/literature/transactions/volume1/trantocvol1.html*.
31. Inframetrics, Inc. Thermasnap Operating Instructions, Inframetrics, Inc., 1997.

APPENDIX A

SH 6 CORRELATION MATRICES AND REGRESSION EQUATIONS

Table A1. Significant Correlations between Data for SH 6.

	ΔTemp (F)	Δ GPR ε
Δ Temp (F)	1.00	1.00
Δ Lab ε	1.00	
Δ GPR ε	1.00	1.00
Δ Bulk Density (pcf)	0.79	0.60
Δ Texture Depth (in)	-0.73	
Δ Permeability (cm/s)		-0.84
Δ Rice Gravity (pcf)	-0.89	-0.90
Δ Air Voids (%)	-0.87	-0.95
Δ Asphalt Content	0.96	0.95
Δ % Passing 3/8	0.80	0.69
Δ% Passing #4	0.92	0.61
Δ % Passing #10		0.82
Δ % Passing #40	-0.99	0.60
Δ % Passing #80		-0.87
Δ % Passing #200		-0.85
Δ % Retained on 3/8	-0.97	-0.91
Δ % Retained on #4		0.57
Δ % Retained on #10	0.94	0.45
Δ % Retained on #40		0.83
Δ % Retained on #80	-0.64	0.69
Δ % Retained on #200		0.79

Table A2. Complete Correlation Matrix between Differences of Data for SH 6.

	Temp	Lab e	GPR E	Bulk Density	Texture Depth (in)	Permeability (cm/s)	Rut Depth (8000 passes, mm)	Rice Gravity	% Density	Air Voids (%)	Asphalt Content
Temp	1	1.00	1.00	0.79	-0.73	-0.12	-0.41	-0.89	0.87	-0.87	0.96
Lab e		1	0.09	0.85	-0.72	-0.90	-0.63	-0.31	0.80	-0.80	0.82
GPR E			1	0.60	-0.35	-0.84	0.24	-0.90	0.95	-0.95	0.95
Bulk Density				1	-0.64	-0.97	-0.51	-0.35	0.89	-0.89	0.80
Texture Depth (in)					1	0.54	0.78	0.72	-0.81	0.81	-0.62
Permeability (cm/s)						1	0.56	0.12	-0.75	0.75	-0.67
Rut Depth (8000 passes, mm)							1	0.13	-0.43	0.43	-0.19
Rice Gravity								1	-0.74	0.74	-0.66
% Density									1	-1.00	0.90
Air Voids (%)										1	-0.90
Asphalt Content											1

	Passing 3/4	Passing 1/2	Passing 3/8	Passing #4	Passing #10	Passing #40	Passing #80	Passing #200	Retained 3/4	Retained 1/2	Retained 3/8	Retained #4	Retained #10	Retained #40	Retained #80	Retained #200
Temp	#DIV/0!	0.34	0.80	0.92	0.02	-0.99	-0.34	-0.34	#DIV/0!	-0.34	-0.97	-0.13	0.94	0.34	-0.64	0.34
Lab e	#DIV/0!	0.30	0.49	0.71	0.03	-0.88	-0.90	-0.87	#DIV/0!	-0.30	-0.47	-0.35	0.72	0.83	0.18	0.18
GPR E	#DIV/0!	0.16	0.69	0.61	0.82	0.60	-0.87	-0.85	#DIV/0!	-0.16	-0.91	0.57	0.45	0.83	0.69	0.79
Bulk Density	#DIV/0!	0.08	0.32	0.46	0.28	-0.76	-0.97	-0.96	#DIV/0!	-0.08	-0.45	-0.21	0.42	0.92	0.48	0.30
Texture Depth (in)	#DIV/0!	0.26	-0.27	-0.53	0.07	0.48	0.47	0.43	#DIV/0!	-0.26	0.75	0.52	-0.55	-0.37	0.06	0.07
Permeability (cm/s)	#DIV/0!	-0.10	-0.19	-0.37	-0.11	0.88	0.98	0.95	#DIV/0!	0.10	0.23	0.33	-0.36	-0.89	-0.36	-0.15
Rut Depth	#DIV/0!	0.36	0.18	-0.19	0.61	0.73	0.42	0.31	#DIV/0!	-0.36	0.17	0.93	-0.32	-0.17	0.47	0.60
Rice Gravity	#DIV/0!	0.11	-0.53	-0.53	-0.51	-0.14	0.15	0.21	#DIV/0!	-0.11	0.97	-0.16	-0.44	-0.25	-0.34	-0.46
% Density	#DIV/0!	0.00	0.49	0.59	0.45	-0.48	-0.77	-0.79	#DIV/0!	0.00	-0.80	-0.07	0.52	0.78	0.51	0.44
Air Voids (%)	#DIV/0!	0.00	-0.49	-0.59	-0.45	0.48	0.77	0.79	#DIV/0!	0.00	0.80	0.07	-0.52	-0.78	-0.51	-0.44
Asphalt Content	#DIV/0!	0.44	0.80	0.84	0.53	-0.47	-0.75	-0.81	#DIV/0!	-0.44	-0.79	0.17	0.75	0.85	0.54	0.66
Passing 3/4	#DIV/0!	#DIV/0!	#DIV/0!	#DIV/0!	#DIV/0!	#DIV/0!	#DIV/0!	#DIV/0!	#DIV/0!	#DIV/0!	#DIV/0!	#DIV/0!	#DIV/0!	#DIV/0!	#DIV/0!	#DIV/0!
Passing 1/2		1.00	0.78	0.67	0.23	-0.21	-0.23	-0.30	#DIV/0!	-1.00	-0.08	0.45	0.64	0.40	0.17	0.55
Passing 3/8			1.00	0.93	0.49	-0.14	-0.32	-0.41	#DIV/0!	-0.78	-0.68	0.44	0.85	0.52	0.34	0.74
Passing #4				1.00	0.21	-0.41	-0.45	-0.49	#DIV/0!	-0.67	-0.71	0.08	0.98	0.55	0.11	0.48
Passing #10					1.00	0.33	-0.25	-0.37	#DIV/0!	-0.23	-0.49	0.84	0.01	0.49	0.94	0.93
Passing #40						1.00	0.83	0.75	#DIV/0!	0.21	0.01	0.60	-0.48	-0.66	0.09	0.18
Passing #80							1.00	0.99	#DIV/0!	0.23	0.28	0.16	-0.41	-0.95	-0.48	-0.31
Passing #200								1.00	#DIV/0!	0.30	0.34	0.03	-0.43	-0.99	-0.58	-0.44
Retained 3/4									#DIV/0!	#DIV/0!	#DIV/0!	#DIV/0!	#DIV/0!	#DIV/0!	#DIV/0!	#DIV/0!
Retained 1/2										1.00	0.08	-0.45	-0.64	-0.40	-0.17	-0.55
Retained 3/8											1.00	-0.15	-0.62	-0.39	-0.34	-0.52
Retained #4												1.00	-0.09	0.12	0.69	0.85
Retained #10													1.00	0.46	-0.08	0.30
Retained #40														1.00	0.66	0.58
Retained #80															1.00	0.85
Retained #200																1.00

Table A3. Correlation Coefficient t-values for SH 6.

Note: Bold values indicate significance at 95% confidence level.

	Temp	Lab e	GPR E	Bulk Density	Texture Depth (in)	Permeability (cm/s)	Rut Depth (8000 passes, mm)	Rice Gravity	% Density	Air Voids (%)	Asphalt Content
Temp		**109.22**	**227.80**	**6.73**	**5.68**	0.51	1.93	**8.23**	**7.32**	**7.32**	**14.27**
Lab e			0.40	**8.46**	**5.48**	**8.86**	**3.43**	1.37	**5.68**	**5.68**	**6.10**
GPR E				**3.94**	1.95	**6.57**	1.05	**8.85**	**12.38**	**12.38**	**12.38**
Bulk Density					**4.46**	**16.67**	**2.50**	1.58	**8.20**	**8.20**	**5.70**
Texture Depth (in)						**2.72**	**5.23**	**4.36**	**5.95**	**5.95**	**3.36**
Permeability (cm/s)							**2.90**	0.50	**4.85**	**4.85**	**3.87**
Rut Depth (8000 passes, mm)								0.54	2.01	2.01	0.84
Rice Gravity									**4.68**	**4.68**	**3.73**
% Density										**284,718,796.87**	**8.67**
Air Voids (%)											**8.67**
Asphalt Content											

	Passing 3/4	Passing 1/2	Passing 3/8	Passing #4	Passing #10	Passing #40	Passing #80	Passing #200	Retained 3/4	Retained 1/2	Retained 3/8	Retained #4	Retained #10	Retained #40
Temp	#DIV/0!	1.56	**5.67**	**10.26**	0.08	**24.49**	1.56	1.56	#DIV/0!	1.56	**16.00**	0.54	**12.19**	1.56
Lab e	#DIV/0!	1.36	**2.41**	**4.26**	0.12	**7.87**	**8.66**	**7.64**	#DIV/0!	1.36	**2.24**	1.60	**4.39**	**6.37**
GPR E	#DIV/0!	0.67	**4.08**	**3.23**	**5.97**	**3.15**	**7.34**	**6.95**	#DIV/0!	0.67	**9.40**	**2.93**	**2.14**	**6.20**
Bulk Density	#DIV/0!	0.35	1.43	**2.23**	1.23	**5.04**	**17.02**	**14.57**	#DIV/0!	0.35	**2.14**	0.92	1.96	**9.87**
Texture Depth (in)	#DIV/0!	1.12	1.17	**2.63**	0.28	**2.31**	**2.26**	2.04	#DIV/0!	1.12	**4.74**	**2.61**	**2.81**	1.69
Permeability (cm/s)	#DIV/0!	0.43	0.84	1.70	0.45	**7.72**	**23.17**	**12.91**	#DIV/0!	0.43	1.02	1.48	1.63	**8.15**
Rut Depth	#DIV/0!	1.64	0.78	0.84	**3.24**	**4.48**	1.98	1.39	#DIV/0!	1.64	0.72	**10.81**	1.43	0.75
Rice Gravity	#DIV/0!	0.49	**2.65**	**2.68**	**2.49**	0.62	0.64	0.90	#DIV/0!	0.49	**18.38**	0.69	**2.11**	1.11
% Density	#DIV/0!	0.01	**2.38**	**3.14**	**2.11**	**2.31**	**5.09**	**5.46**	#DIV/0!	0.01	**5.66**	0.32	**2.58**	**5.32**
Air Voids (%)	#DIV/0!	0.01	**2.38**	**3.14**	**2.11**	**2.31**	**5.09**	**5.46**	#DIV/0!	0.01	**5.66**	0.32	**2.58**	**5.32**
Asphalt Content	#DIV/0!	**2.05**	**5.72**	**6.50**	**2.68**	**2.24**	**4.84**	**5.81**	#DIV/0!	**2.05**	**5.48**	0.72	**4.80**	**6.90**
Passing 3/4		#DIV/0!	#DIV/0!	#DIV/0!	#DIV/0!	#DIV/0!	#DIV/0!	#DIV/0!	#DIV/0!	#DIV/0!	#DIV/0!	#DIV/0!	#DIV/0!	#DIV/0!
Passing 1/2			**5.30**	**3.84**	1.02	0.92	1.03	1.35	#DIV/0!	#NUM!	0.33	**2.15**	**3.53**	1.88
Passing 3/8				**10.51**	**2.37**	0.58	1.45	1.93	#DIV/0!	**5.30**	**3.97**	**2.11**	**6.85**	**2.60**
Passing #4					0.90	1.89	**2.11**	**2.39**	#DIV/0!	**3.84**	**4.24**	0.33	**21.26**	**2.77**
Passing #10						1.48	1.08	1.70	#DIV/0!	1.02	**2.40**	**6.45**	0.05	**2.38**
Passing #40							**6.19**	**4.83**	#DIV/0!	0.92	0.05	**3.15**	**2.34**	**3.74**
Passing #80								**29.87**	#DIV/0!	1.03	1.23	0.70	1.89	**13.61**
Passing #200									#DIV/0!	1.35	1.53	0.12	2.01	**25.77**
Retained 3/4										#DIV/0!	#DIV/0!	#DIV/0!	#DIV/0!	#DIV/0!
Retained 1/2											0.33	**2.15**	**3.53**	1.88
Retained 3/8												0.66	**3.39**	1.80
Retained #4													0.37	0.53
Retained #10														**2.21**
Retained #40														
Retained #80														
Retained #200														

Table A4. Regressions between Changes in NDT Data and Changes in Mix Parameters for SH 6.

	Lab ε	GPR E	Bulk Density	Texture Depth (in)	Permeability (cm/s)	Rice Gravity	% Density	Air Voids (%)	Asphalt Content
Delta Temp Regressions									
Intercept	0	0	0	0		0	0	0	-1.85E-17
Slope	0.013883	0.045146	0.022573	-0.00149		-0.083617	0.065169	-0.065169	0.083689
R-Square	0.997658	0.999653	0.61816	0.535737		0.790024	0.748546	0.748546	0.918749
S.E.	0.000336	0.00042	0.00887	0.000694		0.021554	0.018885	0.018885	0.012444
T-Test	41.28054	107.3872	2.544719	-2.148443		-3.879406	3.450722	-3.450722	6.72535
Prob(T)	1.57E-07	1.33E-09	0.051597	0.084411		0.011649	0.018223	0.018223	0.001102
Delta GPR ε Regressions									
Intercept			-1.53E-17		0	0	0	0	1.39E-17
Slope			0.551408		-0.000104778	-1.269458	1.281455	-1.281455	1.311823
R-Square			0.356909		0.705554492	0.813038	0.894969	0.894969	0.894936
S.E.			0.17446		2.14047E-05	0.192504	0.138822	0.138822	0.142136
T-Test			3.160667		-4.895114047	-6.594445	9.230919	-9.230919	9.229319
Prob(T)			0.005148		0.000475301	3.89E-05	1.63E-06	1.63E-06	1.64E-06

	Passing 3/8	Passing #4	Passing #10	Passing #40	Passing #80	Passing #200	Retained 3/8	Retained #4	Retained #10	Retained #40	Retained #80	Retained #200
Delta Temp Regressions												
Intercept	0	0		0			-7.4E-17		-1.48E-16		0	
Slope	0.376214	0.396602		-0.009709			-0.256796		0.396117		-0.012621	
R-Square	0.640803	0.854043		0.970874			0.934286		0.891918		0.410194	
S.E.	0.140834	0.081978		0.000841			0.034052		0.068946		0.007567	
T-Test	2.671322	4.837899		-11.54701			-7.541192		5.745339		-1.667901	
Prob(T)	0.044278	0.004724		8.54E-05			0.000649		0.00224		0.156209	
Delta GPR ε Regressions												
Intercept	0	7.4E-17	0	0	9.25E-18	-9.25E-18	1.11E-16	-5.55E-17	3.7E-17	-1.85E-17	2.78E-17	0
Slope	4.059113	3.059113	0.862069	0.182266	-0.364532	-0.522167	-3.472906	1.073892	2.197044	0.576355	0.472906	0.157635
R-Square	0.48001	0.36681	0.664591	0.354939	0.749316	0.728286	0.830811	0.323354	0.202288	0.681146	0.472906	0.630542
S.E.	1.335991	1.270989	0.193666	0.077701	0.066676	0.100859	0.495597	0.491249	1.379676	0.1247	0.157882	0.038157
T-Test	3.038279	2.406876	4.451327	2.345722	-5.467251	-5.177203	-7.007523	2.186042	1.592435	4.621943	2.995323	4.131182
Prob(T)	0.011281	0.034806	0.000977	0.038779	0.000196	0.000305	2.25E-05	0.051321	0.139594	0.000738	0.012181	0.001669

APPENDIX B

US 79 CORRELATION MATRICES AND REGRESSIONS

Table B1. Significant Correlations between Data for US 79.

	ΔTemp (F)	Δ GPR ε
Δ Temp (F)	1.00	0.97
Δ GPR ε	0.97	1.00
Δ Bulk Density (pcf)	0.96	0.99
Δ Permeability (cm/s)	-0.60	-0.67
Δ Rice Gravity (pcf)	-0.49	-0.64
Δ Air Voids (%)	-0.94	-0.99
Δ % Passing #10	0.48	0.47
Δ % Passing #40	0.62	0.60
Δ % Passing #80	0.57	0.48
Δ % Passing #200	0.56	0.45
Δ % Retained on #40	0.38	0.37
Δ %Retained on #200	-0.42	

Table B2. Complete Correlation Matrix between Differences of Data for US 79.

	Temp (F)	Lab E	GPR E	Bulk Density	Texture Depth (in)	Permeability (cm/s)	Rut Depth (8000 passes, mm)	Max theoretical sp. Gravity (lb/cf)	% Density	Air Voids (%)	Asphalt Content
Temp (F)	1	0.64	0.97	0.96	-0.26	-0.60	0.18	-0.49	0.94	-0.94	-0.13
Lab E		1	0.50	0.43	0.35	-0.61	-0.10	-0.30	0.44	-0.44	-0.14
GPR E			1	0.99	-0.33	-0.67	0.09	-0.64	0.99	-0.99	0.05
Bulk Density				1	-0.43	-0.60	0.14	-0.54	0.98	-0.98	-0.06
Texture Depth (in)					1	0.03	0.16	-0.14	-0.35	0.35	0.38
Permeability (cm/s)						1	0.59	0.81	-0.70	0.70	-0.35
Rut Depth (8000 passes, mm)							1	0.27	0.06	-0.06	-0.22
Max theoretical sp. Gravity (lb/cf)								1	-0.69	0.69	-0.75
% Density									1	-1.00	0.11
Air Voids (%)										1	-0.11
Asphalt Content											1

	Passing 5/8	Passing 3/8	Passing #4	Passing #10	Passing #40	Passing #80	Passing #200	Retained 3/8	Retained #4	Retained #10	Retained #40	Retained #80	Retained #200
Temp (F)	#DIV/0!	-0.08	0.18	0.48	0.62	0.57	0.56	0.08	-0.29	-0.33	0.38	-0.25	-0.42
Lab E	#DIV/0!	-0.20	-0.20	-0.01	0.13	0.38	0.46	0.20	-0.12	-0.34	-0.06	-0.65	-0.42
GPR E	#DIV/0!	0.06	0.25	0.47	0.60	0.48	0.45	-0.06	-0.15	-0.19	0.37	-0.06	-0.32
Bulk Density	#DIV/0!	0.03	0.25	0.51	0.62	0.49	0.47	-0.03	-0.19	-0.25	0.41	-0.05	-0.35
Texture Depth (in)	#DIV/0!	0.35	0.27	0.04	0.00	0.28	0.26	-0.35	0.22	0.53	0.08	-0.54	-0.21
Permeability (cm/s)	#DIV/0!	-0.21	0.12	0.16	0.09	0.02	-0.06	0.21	-0.43	0.01	0.19	0.08	0.16
Rut Depth	#DIV/0!	0.04	0.66	0.84	0.84	0.76	0.62	-0.04	-0.59	0.12	0.79	-0.25	-0.31
Rice Gravity	#DIV/0!	-0.53	-0.35	-0.16	-0.20	-0.13	-0.07	0.53	-0.44	-0.44	-0.11	-0.13	0.04
% Density	#DIV/0!	0.13	0.29	0.47	0.58	0.44	0.42	-0.13	-0.07	-0.12	0.37	-0.01	-0.31
Air Voids (%)	#DIV/0!	-0.13	-0.29	-0.47	-0.58	-0.44	-0.42	0.13	0.07	0.12	-0.37	0.01	0.31
Asphalt Content	#DIV/0!	0.50	0.32	-0.06	-0.04	-0.21	-0.34	-0.50	0.42	0.69	-0.11	0.43	0.41
Passing 5/8	#DIV/0!	#DIV/0!	#DIV/0!	#DIV/0!	#DIV/0!	#DIV/0!	#DIV/0!	#DIV/0!	#DIV/0!	#DIV/0!	#DIV/0!	#DIV/0!	#DIV/0!
Passing 3/8		1	0.75	0.41	0.19	0.33	0.33	-1.00	0.76	0.91	0.52	-0.17	-0.44
Passing #4			1	0.87	0.75	0.72	0.61	-0.75	0.14	0.73	0.90	-0.17	-0.45
Passing #10				1	0.95	0.90	0.79	-0.41	-0.25	0.31	0.98	-0.29	-0.56
Passing #40					1	0.86	0.73	-0.19	-0.46	0.12	0.87	-0.21	-0.42
Passing #80						1	0.97	-0.33	-0.22	0.19	0.89	-0.66	-0.79
Passing #200							1	-0.33	-0.11	0.12	0.83	-0.79	-0.91
Retained 3/8								1	-0.76	-0.91	-0.52	0.17	0.44
Retained #4									1	0.63	-0.10	-0.08	-0.21
Retained #10										1	0.39	-0.01	-0.14
Retained #40											1	-0.37	-0.67
Retained #80												1	0.86
Retained #200													1

Table B3. Correlation Coefficient t-values for US 79.

Note: Bold values indicate significance at 95% confidence level.

	Temp (F)	Lab E	GPR E	Bulk Density	Texture Depth (in)	Permeability (cm/s)	Rut Depth (8000 passes, mm)	Max theoretical sp. Gravity (lb/cf)	% Density	Air Voids (%)	Asphalt Content
Temp (F)		**4.45**	**20.13**	**18.30**	1.40	**3.99**	0.98	**2.94**	**14.11**	**14.11**	0.70
Lab E			**3.05**	**2.51**	1.95	**4.02**	0.52	1.66	**2.57**	**2.57**	0.72
GPR E				**36.09**	1.86	**4.83**	0.50	**4.37**	**49.79**	**49.79**	0.25
Bulk Density					**2.56**	**3.96**	0.72	**3.42**	**28.38**	**28.38**	0.33
Texture Depth (in)						0.17	0.85	0.74	1.97	1.97	**2.17**
Permeability (cm/s)							**3.82**	**7.39**	**5.14**	**5.14**	1.96
Rut Depth (8000 passes, mm)								1.48	0.29	0.29	1.18
Max theoretical sp. Gravity (lb/cf)									**5.01**	**5.01**	**5.97**
% Density										#DIV/0!	0.58
Air Voids (%)											0.58
Asphalt Content											

	Passing 5/8	Passing 3/8	Passing #4	Passing #10	Passing #40	Passing #80	Passing #200	Retained 3/8	Retained #4	Retained #10	Retained #40	Retained #80	Retained #200
Temp (F)	#DIV/0!	0.42	0.97	**2.91**	**4.23**	**3.68**	**3.60**	0.42	1.59	1.87	**2.15**	1.34	**2.43**
Lab E	#DIV/0!	1.11	1.09	0.04	0.72	**2.16**	**2.72**	1.11	0.65	1.92	0.32	**4.50**	**2.48**
GPR E	#DIV/0!	0.31	1.38	**2.84**	**3.94**	**2.87**	**2.66**	0.31	0.81	1.05	**2.10**	0.34	1.79
Bulk Density	#DIV/0!	0.14	1.36	**3.12**	**4.16**	**2.94**	**2.78**	0.14	1.04	1.37	**2.39**	0.27	1.95
Texture Depth (in)	#DIV/0!	1.96	1.48	0.19	0.01	1.53	1.43	1.96	1.22	**3.34**	0.41	**3.37**	1.15
Permeability (cm/s)	#DIV/0!	1.12	0.64	0.86	0.47	0.09	0.29	1.12	**2.53**	0.07	1.04	0.42	0.88
Rut Depth	#DIV/0!	0.21	**4.64**	**8.13**	**8.27**	**6.11**	**4.19**	0.21	**3.92**	0.63	**6.88**	1.38	1.73
Rice Gravity	#DIV/0!	**3.28**	1.99	0.85	1.11	0.68	0.39	**3.28**	**2.61**	**2.62**	0.56	0.70	0.21
% Density	#DIV/0!	0.72	1.59	**2.82**	**3.73**	**2.63**	**2.42**	0.72	0.37	0.65	**2.14**	0.07	1.70
Air Voids (%)	#DIV/0!	0.72	1.59	**2.82**	**3.73**	**2.63**	**2.42**	0.72	0.37	0.65	**2.14**	0.07	1.70
Asphalt Content	#DIV/0!	**3.06**	1.80	0.33	0.22	1.11	1.89	**3.06**	**2.45**	**5.06**	0.57	**2.49**	**2.41**
Passing 5/8		#DIV/0!	#DIV/0!	#DIV/0!	#DIV/0!	#DIV/0!	#DIV/0!	#DIV/0!	#DIV/0!	#DIV/0!	#DIV/0!	#DIV/0!	#DIV/0!
Passing 3/8			**6.00**	**2.36**	1.02	1.85	1.87	**251,098,376.70**	**6.13**	**11.47**	**3.23**	0.93	**2.58**
Passing #4				**9.55**	**6.05**	**5.51**	**4.06**	**6.00**	0.72	**5.62**	**10.73**	0.91	**2.65**
Passing #10					**16.73**	**10.62**	**6.93**	**2.36**	1.36	1.71	**24.65**	1.58	**3.62**
Passing #40						**9.10**	**5.70**	1.02	**2.73**	0.67	**9.39**	1.14	**2.47**
Passing #80							**20.71**	1.85	1.20	1.00	**10.43**	**4.68**	**6.76**
Passing #200								1.87	0.56	0.64	**7.79**	**6.86**	**11.62**
Retained 3/8									**6.13**	**11.47**	**3.23**	0.93	**2.58**
Retained #4										**4.33**	0.53	0.40	1.16
Retained #10											**2.25**	0.04	0.74
Retained #40												**2.13**	**4.75**
Retained #80													**8.78**
Retained #200													

Table B4. Regressions between Changes in NDT Data and Changes in Mix Parameters for US 79.

	Temp (F)	Lab E	GPR E	Bulk Density	Permeability (cm/s)	Max theoretical sp. Gravity (lb/cf)	% Density	Air Voids (%)
Delta Temp regressions								
Intercept		5.92E-17	0	0	-3.61401E-21	0	0	0
Slope		0.186844	0.072803	0.3628452	-3.01234E-05	-0.052163778	0.270345	-0.27034531
R-Square		0.413821	0.935385	0.9228568	0.361914241	0.235631654	0.876776	0.87677614
S.E.		0.042025	0.003616	0.0198255	7.55895E-06	0.017755158	0.019153	0.01915327
T-Test		4.446006	20.13292	18.301943	-3.985128468	-2.937950574	14.11484	-14.1148404
Prob(T)		0.000118	1.37E-18	1.792E-17	0.000416544	0.006416113	1.6E-14	1.5955E-14
Delta GRP ε regressions								
Intercept	0	5.92E-17		0	-3.61401E-21	0	0	0
Slope	12.848101	1.925316		4.964557	-0.000448454	-0.908860759	3.813989	-3.81398866
R-Square	0.9353848	0.248984		0.97896	0.454513768	0.405324322	0.988831	0.98883134
S.E.	0.6381639	0.63192		0.1375441	9.28448E-05	0.208044909	0.076602	0.07660194
T-Test	20.132919	3.04677		36.094305	-4.830150252	-4.368579666	49.78971	-49.7897106
Prob(T)	1.372E-18	0.004892		1.18E-25	4.06662E-05	0.000145911	1.21E-29	1.213E-29

	Passing #10	Passing #40	Passing #80	Passing #200	Retained #40	Retained #200
Delta Temp regressions						
Intercept	0	0	0	0	0	0
Slope	0.055708	0.034848	0.043335	0.061447	0.02379	-0.014883
R-Square	0.231786	0.389945	0.325576	0.315835	0.14174	0.17399
S.E.	0.019166	0.008237	0.011787	0.017091	0.011063	0.006129
T-Test	2.906578	4.230545	3.676537	3.595247	2.150387	-2.428554
Prob(T)	0.006933	0.000213	0.000955	0.001186	0.039995	0.021591
Delta GRP ε regressions						
Intercept	0	0	0	0	0	
Slope	0.727848	0.443038	0.481013	0.651899	0.310127	
R-Square	0.224203	0.357152	0.227297	0.201437	0.136493	
S.E.	0.255867	0.112329	0.167605	0.245294	0.147414	
T-Test	2.844631	3.944128	2.86992	2.657625	2.103783	
Prob(T)	0.008071	0.000466	0.007587	0.012667	0.044185	

APPENDIX C

IH 10 CORRELATION MATRICES AND REGRESSIONS

Table C1. Significant Correlations between Data from IH 10.

	Δ Temp	Δ Temp (Grouped)	Δ GPR ε	Δ GPR ε (Grouped)
Δ Temp	1.00	1.00	0.62	0.79
Δ GPR ε	0.62	0.79	1.00	1.00
Δ Density	0.88	0.95	0.87	0.90
Δ Texture Depth	-0.59	-0.62	-0.64	-0.67
Δ Permeability	-0.41	-0.31	-0.44	-0.40
Δ Rut Depth	-0.23	-0.36	-0.36	-0.47
Δ % Voids	-0.82	-0.93	-0.86	-0.93
Δ % Asphalt	0.25	0.34		
Δ % Passing 3/8	0.43	0.71	0.39	0.54
Δ % Passing #4	0.44	0.59	0.30	
Δ % Passing #8	0.39	0.60	0.32	0.44
Δ % Passing #16	0.30	0.43	0.20	
Δ % Passing #30			0.25	
Δ % Passing #50	0.25	0.40		
Δ % Passing #200	0.20			
Δ % Retained 3/8	-0.43	-0.71	0.23	-0.54
Δ % Retained #4	-0.31			
Δ % Retained #8	0.42	0.47	0.35	
Δ % Retained #16	0.47	0.73	0.43	0.66
Δ % Retained #30	0.28	0.31	0.25	0.42
Δ % Retained #50	0.26			
Δ % Retained #100			0.23	

Table C2. Limits on Changes of NDT Data before Mix Parameter Changes Are at Tolerance Limit for IH 10.

Mix Parameter	Tolerance	Δ Temp Limit	Δ Temp Limit (Grouped)	Δ GPR ε Limit	Δ GPR ε Limit (Grouped)
Δ Air Voids (%)	Range of 4; AVG to low of 2*	Range: 28; AVG to low: 14	Range: 25; AVG to low: 12.5	Range: 0.3; AVG to low: 0.15	Range: 0.3; AVG to low: 0.15
Δ % Asphalt	± 0.3	125	94		
Δ % Passing 3/8	± 5	74	49	0.89	0.88
Δ % Passing #4	± 5	50	41	0.78	
Δ % Passing #8	± 5	94	81	1.23	1.65
Δ % Passing #16	± 3	126	109	2.07	
Δ % Passing #30	± 3			0.84	
Δ % Passing #50	± 3	244	178		
Δ % Passing #200	± 3	394			
Δ % Retained 3/8	± 5	74	49	0.89	0.88
Δ % Retained #4	± 5	146			
Δ % Retained #8	± 5	105	86	2.08	
Δ % Retained #16	± 3	107	89	1.24	1.4
Δ % Retained #30	± 3	454	502	5.66	0.42
Δ % Retained #50	± 3	714			
Δ % Retained #100	± 3			3.03	

*Based on Cores' Average Rice Gravity and SS 3146 Density Profile Specifications

Table C3. Complete Correlation Matrix between Differences of Data for IH 10 Pooled Data.

	Temp (F)	Lab E	GPR E	Bulk Density (lb/cf)	Texture Depth (in)	Permeability (cm/s)	Rut Depth (8000 passes, mm)	Max Theoretical Density	% Density	Air Voids	Asphalt Content
Temp (F)	1	0.60	0.62	0.88	-0.59	-0.41	-0.23	-0.08	0.82	-0.82	0.25
Lab E		1	0.71	0.73	-0.69	-0.49	-0.31	-0.05	0.69	-0.69	0.06
GPR E			1	0.58	-0.55	-0.66	-0.31	-0.14	0.57	-0.57	0.12
Bulk Density (lb/cf)				1	-0.72	-0.40	-0.49	-0.25	0.98	-0.98	0.45
Texture Depth (in)					1	0.51	0.56	0.58	-0.80	0.80	-0.33
Permeability (cm/s)						1	0.09	0.30	-0.44	0.44	-0.29
Rut Depth (8000 passes, mm)							1	0.41	-0.55	0.55	-0.38
Max Theoretical Density								1	-0.45	0.45	-0.48
% Density									1	-1.00	0.52
Air Voids										1	-0.52
Asphalt Content											1

	Passing 1/2	Passing 3/8	Passing #4	Passing #8	Passing #16	Passing #30	Passing #50	Passing #100	Passing #200	Retained on 3/8	Retained on #4	Retained on #8	Retained on #16	Retained on #30	Retained on #50	Retained on #100	Retained on #200
Temp (F)	#DIV/0!	0.43	0.44	0.39	0.30	0.16	0.25	0.16	0.20	-0.43	-0.31	0.42	0.47	0.28	0.26	0.09	0.02
Lab E	#DIV/0!	0.41	0.39	0.33	0.20	0.31	0.03	0.03	-0.07	-0.41	-0.25	0.40	0.45	0.39	0.35	-0.02	0.24
GPR E	#DIV/0!	0.34	0.36	0.32	0.23	0.11	0.00	-0.02	-0.07	-0.34	-0.27	0.35	0.40	0.42	0.53	0.02	0.20
Bulk Density (lb/cf)	#DIV/0!	0.65	0.65	0.64	0.53	0.22	0.47	0.18	0.24	-0.65	-0.45	0.56	0.72	0.52	0.33	0.30	-0.05
Texture Depth (in)	#DIV/0!	-0.68	-0.59	-0.65	-0.62	0.19	-0.54	-0.16	-0.09	0.68	0.27	-0.42	-0.65	-0.55	-0.53	-0.39	-0.27
Permeability (cm/s)	#DIV/0!	-0.43	-0.52	-0.56	-0.49	0.31	-0.19	0.00	0.22	0.43	0.49	-0.41	-0.59	-0.68	-0.88	-0.20	-0.54
Rut Depth	#DIV/0!	-0.68	-0.67	-0.63	-0.69	-0.13	-0.71	-0.65	-0.69	0.68	0.44	-0.62	-0.54	-0.59	-0.35	-0.11	-0.17
Rice Gravity	#DIV/0!	-0.54	-0.40	-0.60	-0.59	0.42	-0.55	0.08	0.03	0.54	0.07	-0.11	-0.58	-0.49	-0.41	-0.66	-0.01
% Density	#DIV/0!	0.72	0.69	0.72	0.62	0.11	0.56	0.15	0.22	-0.72	-0.43	0.54	0.79	0.59	0.40	0.43	-0.04
Air Voids	#DIV/0!	-0.72	-0.69	-0.72	-0.62	-0.11	-0.56	-0.15	-0.22	0.72	0.43	-0.54	-0.79	-0.59	-0.40	-0.43	0.04
Asphalt Content	#DIV/0!	0.61	0.71	0.83	0.80	-0.39	0.79	0.11	0.25	-0.61	-0.61	0.45	0.81	0.67	0.49	0.71	-0.24
Passing 1/2	#DIV/0!	#DIV/0!	#DIV/0!	#DIV/0!	#DIV/0!	#DIV/0!	#DIV/0!	#DIV/0!	#DIV/0!	#DIV/0!	#DIV/0!	#DIV/0!	#DIV/0!	#DIV/0!	#DIV/0!	#DIV/0!	#DIV/0!
Passing 3/8		1	0.91	0.85	0.81	-0.13	0.73	0.43	0.39	-1.00	-0.49	0.84	0.86	0.74	0.66	0.32	0.32
Passing #4			1	0.94	0.91	-0.05	0.79	0.56	0.52	-0.91	-0.81	0.92	0.92	0.91	0.77	0.26	0.36
Passing #8				1	0.97	-0.24	0.87	0.37	0.37	-0.85	-0.76	0.73	0.97	0.92	0.76	0.54	0.19
Passing #16					1	-0.31	0.94	0.49	0.48	-0.81	-0.76	0.70	0.89	0.89	0.74	0.49	0.25
Passing #30						1	-0.33	0.21	0.28	0.13	-0.10	0.19	-0.13	-0.08	-0.36	-0.55	-0.09
Passing #50							1	0.52	0.58	-0.73	-0.61	0.58	0.75	0.69	0.48	0.54	0.05
Passing #100								1	0.93	-0.43	-0.57	0.71	0.22	0.40	0.31	-0.45	0.54
Passing #200									1	-0.39	-0.53	0.63	0.24	0.32	0.11	-0.30	0.20
Retained on 3/8										1	0.49	-0.84	-0.86	-0.74	-0.66	-0.32	-0.32
Retained on #4											1	-0.75	-0.71	-0.85	-0.67	-0.08	-0.30
Retained on #8												1	0.72	0.75	0.66	-0.11	0.49
Retained on #16													1	0.90	0.72	0.55	0.12
Retained on #30														1	0.85	0.33	0.38
Retained on #50															1	0.19	0.64
Retained on #100																1	-0.49
Retained on #200																	1

Table C4. Correlation Coefficient t-values for IH 10 Pooled Data.

Note: Bold values indicate significance at 95% confidence level.

	Temp (F)	Lab E	GPR E	Bulk Density (lb/cf)	Texture Depth (in)	Permeability (cm/s)	Rut Depth (8000 passes, mm)	Max Theoretical Density	% Density	Air Voids	Asphalt Content
Temp (F)		**8.60**	**9.03**	**20.76**	**8.40**	**5.07**	**2.66**	0.92	**16.56**	**16.56**	**3.00**
Lab E			**11.37**	**12.22**	**10.92**	**6.33**	**3.72**	0.59	**10.76**	**10.76**	0.65
GPR E				**8.18**	**7.59**	**9.96**	**3.73**	1.56	**7.87**	**7.87**	1.40
Bulk Density (lb/cf)					**11.98**	**4.98**	**6.49**	**2.90**	**50.40**	**50.40**	**5.78**
Texture Depth (in)						**6.72**	**7.66**	**8.21**	**15.20**	**15.20**	**4.02**
Permeability (cm/s)							1.02	**3.58**	**5.54**	**5.54**	**3.51**
Rut Depth (8000 passes, mm)								**5.13**	**7.48**	**7.48**	**4.69**
Max Theoretical Density									**5.82**	**5.82**	**6.26**
% Density										#NUM!	**7.01**
Air Voids											**7.01**
Asphalt Content											

	Passing 1/2	Passing 3/8	Passing #4	Passing #8	Passing #16	Passing #30	Passing #50	Passing #100	Passing #200	Retained on 3/8	Retained on #4	Retained on #8	Retained on #16	Retained on #30	Retained on #50	Retained on #100	Retained on #200
Temp (F)	#DIV/0!	**5.50**	**5.51**	**4.86**	**3.64**	1.81	**2.96**	1.83	**2.35**	**5.50**	**3.70**	**5.23**	**6.07**	**3.27**	**3.10**	1.06	0.22
Lab E	#DIV/0!	**5.14**	**4.86**	**3.93**	**2.33**	**3.69**	0.33	0.38	0.83	**5.14**	**2.95**	**5.04**	**5.67**	**4.76**	**4.30**	0.21	**2.82**
GPR E	#DIV/0!	**4.19**	**4.40**	**3.92**	**2.65**	1.28	0.03	0.21	0.81	**4.19**	**3.21**	**4.20**	**4.91**	**5.22**	**7.12**	0.18	**2.29**
Bulk Density (lb/cf)	#DIV/0!	**9.66**	**9.71**	**9.40**	**7.14**	**2.62**	**6.14**	**2.12**	**2.87**	**9.66**	**5.80**	**7.77**	**11.87**	**7.02**	**3.99**	**3.63**	0.53
Texture Depth (in)	#DIV/0!	**10.51**	**8.23**	**9.74**	**8.94**	**2.15**	**7.39**	1.91	1.05	**10.51**	**3.19**	**5.21**	**9.69**	**7.45**	**7.15**	**4.86**	**3.24**
Permeability (cm/s)	#DIV/0!	**5.50**	**7.03**	**7.68**	**6.36**	**3.75**	**2.19**	0.04	**2.52**	**5.50**	**6.44**	**5.07**	**8.24**	**10.69**	**20.87**	**2.27**	**7.35**
Rut Depth	#DIV/0!	**10.54**	**10.31**	**9.35**	**10.78**	1.45	**11.51**	**9.67**	**10.80**	**10.54**	**5.60**	**8.97**	**7.26**	**8.29**	**4.21**	1.31	1.95
Rice Gravity	#DIV/0!	**7.38**	**4.98**	**8.64**	**8.30**	**5.20**	**7.55**	0.90	0.40	**7.38**	0.75	1.26	**8.13**	**6.41**	**5.12**	**9.93**	0.11
% Density	#DIV/0!	**11.72**	**10.76**	**11.89**	**9.03**	1.29	**7.72**	1.73	**2.52**	**11.72**	**5.47**	**7.35**	**14.92**	**8.41**	**4.93**	**5.38**	0.44
Air Voids	#DIV/0!	**11.72**	**10.76**	**11.89**	**9.03**	1.29	**7.72**	1.73	**2.52**	**11.72**	**5.47**	**7.35**	**14.92**	**8.41**	**4.93**	**5.38**	0.44
Asphalt Content	#DIV/0!	**8.77**	**11.37**	**17.23**	**15.37**	**4.79**	**14.72**	1.30	**2.96**	**8.77**	**8.72**	**5.82**	**15.96**	**10.17**	**6.44**	**11.50**	**2.81**
Passing 1/2		#DIV/0!	#DIV/0!	#DIV/0!	#DIV/0!	#DIV/0!	#DIV/0!	#DIV/0!	#DIV/0!	#DIV/0!	#DIV/0!	#DIV/0!	#DIV/0!	#DIV/0!	#DIV/0!	#DIV/0!	#DIV/0!
Passing 3/8			**24.77**	**18.67**	**15.78**	1.49	**12.29**	**5.46**	**4.90**	#NUM!	**6.46**	**17.43**	**19.00**	**12.59**	**10.13**	**3.85**	**3.90**
Passing #4				**31.30**	**25.56**	0.53	**14.81**	**7.78**	**7.01**	**24.77**	**15.83**	**26.56**	**26.29**	**24.59**	**13.70**	**3.05**	**4.39**
Passing #8					**49.73**	**2.84**	**20.26**	**4.51**	**4.53**	**18.67**	**13.28**	**12.13**	**43.71**	**27.66**	**13.28**	**7.34**	**2.25**
Passing #16						**3.75**	**30.24**	**6.37**	**6.23**	**15.78**	**13.37**	**11.32**	**21.95**	**22.47**	**12.50**	**6.49**	**2.89**
Passing #30							**4.01**	**2.39**	**3.31**	1.49	1.12	**2.17**	1.52	0.92	**4.45**	**7.48**	0.99
Passing #50								**6.85**	**8.21**	**12.29**	**8.87**	**8.15**	**13.04**	**10.88**	**6.22**	**7.26**	0.57
Passing #100									**28.49**	**5.46**	**7.88**	**11.36**	**2.62**	**4.95**	**3.70**	**5.67**	**7.23**
Passing #200										**4.90**	**7.20**	**9.15**	**2.78**	**3.90**	1.31	**3.57**	**2.29**
Retained on 3/8											**6.46**	**17.43**	**19.00**	**12.59**	**10.13**	**3.85**	**3.90**
Retained on #4												**12.81**	**11.53**	**18.51**	**10.31**	0.94	**3.62**
Retained on #8													**11.88**	**12.97**	**10.09**	1.22	**6.48**
Retained on #16														**23.65**	**11.92**	**7.59**	1.42
Retained on #30															**18.62**	**3.95**	**4.69**
Retained on #50																**2.17**	**9.48**
Retained on #100																	**6.32**

Table C5. Regressions between Changes in Temperature and Changes in Mix Parameters for IH 10 Pooled Data.

	Lab E	GPR E	Bulk Density (lb/cf)	Texture Depth (in)	Permeability (cm/s)	Rut Depth (8000 passes, mm)	% Density	Air Voids	Asphalt Content
Delta Temp Regressions									
Intercept	-2.36E-17	0	0	-5.26E-20	3.16E-20	2.36E-17	0	0	0
Slope	0.023243	0.009362	0.211767	-0.000119	-8.71E-06	-0.014742	0.143244	-0.143244	0.002368
R-Square	0.362599	0.385512	0.768284	0.351552	0.164816	0.051521	0.678461	0.678461	0.064677
S.E.	0.002703	0.001037	0.0102	1.42E-05	1.72E-06	0.005548	0.008649	0.008649	0.00079
T-Test	8.599614	9.030951	20.76127	-8.395153	-5.065002	-2.657365	16.56217	-16.56217	2.998242
Prob(T)	2.12E-14	1.89E-15	2.96E-43	6.59E-14	1.36E-06	0.008855	6.27E-34	6.27E-34	0.00325

	Passing 3/8	Passing #4	Passing #8	Passing #16	Passing #50	Passing #200	Retained on 3/8	Retained on #4	Retained on #8	Retained on #16	Retained on #30	Retained on #50
Delta Temp Regressions												
Intercept	0	-1.1E-16	-2.2E-16	1.3E-16	-5.4E-17	-3.4E-17	0	-1.6E-16	-5.4E-17	1.35E-16	0	0
Slope	0.06771	0.10086	0.05296	0.02372	0.01231	0.00757	-0.06771	-0.03434	0.047669	0.028123	0.006586	0.00417
R-Square	0.18902	0.18957	0.15376	0.09241	0.06316	0.0406	0.189021	0.095435	0.173815	0.220589	0.075853	0.068825
S.E.	0.0123	0.01829	0.0109	0.00652	0.00416	0.00323	0.012301	0.009272	0.009115	0.004636	0.002016	0.001345
T-Test	5.50454	5.51432	4.86004	3.6383	2.96037	2.34562	-5.50454	-3.70344	5.229691	6.065693	3.266538	3.099776
Prob(T)	1.9E-07	1.8E-07	3.3E-06	0.00039	0.00365	0.0205	1.88E-07	0.000312	6.54E-07	1.32E-08	0.00139	0.002371

Table C6. Complete Correlation Matrix between Differences of Data for IH 10 Pooled Data without Core 10.

	Temp (F)	Lab E	GPR E	Bulk Density (lb/cf)	Texture Depth (in)	Permeability (cm/s)	Rut Depth (8000 passes, mm)	Max Theoretical Density	% Density	Air Voids	Asphalt Content
Temp (F)	1	0.62	0.84	0.88	-0.60	-0.47	-0.22	-0.08	0.83	-0.83	0.25
Lab E		1	0.75	0.78	-0.68	-0.41	-0.30	-0.07	0.73	-0.73	0.05
GPR E			1	0.87	-0.64	-0.44	-0.36	-0.24	0.86	-0.86	0.16
Bulk Density (lb/cf)				1	-0.74	-0.52	-0.50	-0.24	0.98	-0.98	0.45
Texture Depth (in)					1	0.52	0.55	0.60	-0.82	0.82	-0.33
Permeability (cm/s)						1	0.05	0.40	-0.57	0.57	-0.35
Rut Depth (8000 passes, mm)							1	0.41	-0.55	0.55	-0.38
Max Theoretical Density								1	-0.45	0.45	-0.48
% Density									1	-1.00	0.53
Air Voids										1	-0.53
Asphalt Content											1

	Passing 1/2	Passing 3/8	Passing #4	Passing #8	Passing #16	Passing #30	Passing #50	Passing #100	Passing #200	Retained on 3/8	Retained on #4	Retained on #8	Retained on #16	Retained on #30	Retained on #50	Retained on #100	Retained on #200
Temp (F)	#DIV/0!	0.43	0.44	0.39	0.30	0.16	0.26	0.15	0.20	-0.43	-0.31	0.42	0.47	0.28	0.30	0.10	0.00
Lab E	#DIV/0!	0.40	0.35	0.30	0.17	0.35	0.07	0.02	-0.05	-0.40	-0.18	0.36	0.43	0.32	0.23	0.04	0.14
GPR E	#DIV/0!	0.39	0.30	0.32	0.20	0.25	0.14	-0.08	-0.01	-0.39	-0.09	0.23	0.43	0.25	0.17	0.23	-0.17
Bulk Density (lb/cf)	#DIV/0!	0.66	0.67	0.65	0.54	0.22	0.47	0.19	0.24	-0.66	-0.49	0.60	0.73	0.58	0.46	0.30	-0.03
Texture Depth (in)	#DIV/0!	-0.67	-0.57	-0.64	-0.61	0.17	-0.58	-0.16	-0.11	0.67	0.24	-0.40	-0.64	-0.53	-0.56	-0.43	-0.23
Permeability (cm/s)	#DIV/0!	-0.46	-0.50	-0.59	-0.51	0.32	-0.33	0.04	0.20	0.46	0.41	-0.32	-0.63	-0.63	-0.81	-0.39	-0.40
Rut Depth	#DIV/0!	-0.68	-0.67	-0.63	-0.68	-0.13	-0.73	-0.65	-0.70	0.68	0.44	-0.62	-0.53	-0.60	-0.38	-0.13	-0.15
Rice Gravity	#DIV/0!	-0.55	-0.42	-0.62	-0.60	0.42	-0.55	0.07	0.04	0.55	0.09	-0.13	-0.59	-0.54	-0.56	-0.66	-0.04
% Density	#DIV/0!	0.73	0.72	0.74	0.63	0.11	0.56	0.15	0.21	-0.73	-0.47	0.58	0.81	0.65	0.55	0.42	-0.02
Air Voids	#DIV/0!	-0.73	-0.72	-0.74	-0.63	-0.11	-0.56	-0.15	-0.21	0.73	0.47	-0.58	-0.81	-0.65	-0.55	-0.42	0.02
Asphalt Content	#DIV/0!	0.61	0.72	0.84	0.81	-0.39	0.80	0.11	0.25	-0.61	-0.63	0.47	0.82	0.70	0.61	0.73	-0.27
Passing 1/2	#DIV/0!	#DIV/0!	#DIV/0!	#DIV/0!	#DIV/0!	#DIV/0!	#DIV/0!	#DIV/0!	#DIV/0!	#DIV/0!	#DIV/0!	#DIV/0!	#DIV/0!	#DIV/0!	#DIV/0!	#DIV/0!	#DIV/0!
Passing 3/8		1	0.91	0.85	0.81	-0.12	0.76	0.43	0.41	-1.00	-0.49	0.84	0.86	0.76	0.77	0.35	0.31
Passing #4			1	0.94	0.92	-0.03	0.85	0.57	0.56	-0.91	-0.80	0.92	0.92	0.91	0.83	0.32	0.30
Passing #8				1	0.97	-0.23	0.91	0.37	0.39	-0.85	-0.76	0.73	0.97	0.94	0.86	0.59	0.15
Passing #16					1	-0.31	0.97	0.49	0.50	-0.81	-0.77	0.70	0.89	0.91	0.85	0.53	0.22
Passing #30						1	-0.35	0.21	0.27	0.12	-0.13	0.22	-0.12	-0.05	-0.39	-0.58	-0.05
Passing #50							1	0.53	0.58	-0.76	-0.69	0.65	0.78	0.79	0.72	0.52	0.12
Passing #100								1	0.94	-0.43	-0.58	0.72	0.22	0.41	0.35	-0.44	0.57
Passing #200									1	-0.41	-0.59	0.68	0.25	0.38	0.22	-0.32	0.26
Retained on 3/8										1	0.49	-0.84	-0.86	-0.76	-0.77	-0.35	-0.31
Retained on #4											1	-0.73	-0.71	-0.84	-0.65	-0.15	-0.20
Retained on #8												1	0.72	0.73	0.66	-0.06	0.44
Retained on #16													1	0.92	0.83	0.60	0.08
Retained on #30														1	0.87	0.43	0.27
Retained on #50															1	0.41	0.53
Retained on #100																1	-0.45
Retained on #200																	1

Table C7. Correlation Coefficient t-values for IH 10 Pooled Data without Core 10.

Note: Bold values indicate significance at 95% confidence level.

	Temp (F)	Lab E	GPR E	Bulk Density (lb/cf)	Texture Depth (in)	Permeability (cm/s)	Rut Depth (8000 passes, mm)	Max Theoretical Density	% Density	Air Voids
Temp (F)		**8.19**	**16.28**	**19.32**	**7.73**	**5.50**	**2.39**	0.87	**15.39**	**15.39**
Lab E			**11.61**	**12.85**	**9.75**	**4.67**	**3.25**	0.69	**11.18**	**11.18**
GPR E				**18.56**	**8.67**	**5.06**	**3.96**	**2.56**	**17.33**	**17.33**
Bulk Density (lb/cf)					**11.46**	**6.33**	**5.98**	**2.61**	**45.96**	**45.96**
Texture Depth (in)						**6.32**	**6.86**	**7.75**	**14.79**	**14.79**
Permeability (cm/s)							0.54	**4.52**	**7.20**	**7.20**
Rut Depth (8000 passes, mm)								**4.72**	**6.90**	**6.90**
Max Theoretical Density									**5.26**	**5.26**
% Density										**493,147,422.05**
Air Voids										

	Asphalt Content	Passing 1/2	Passing 3/8	Passing #4	Passing #8	Passing #16	Passing #30	Passing #50	Passing #100	Passing #200	Retained on 3/8	Retained on #4	Retained on #8	Retained on #16	Retained on #30	Retained on #50	Retained on #100	Retained on #200
Temp (F)	**2.72**	#DIV/0!	**5.01**	**5.05**	**4.40**	**3.27**	1.69	**2.77**	1.62	**2.16**	**5.01**	**3.38**	**4.83**	**5.52**	**3.01**	**3.31**	1.08	0.02
Lab E	0.57	#DIV/0!	**4.53**	**3.92**	**3.28**	1.83	**3.87**	0.73	0.19	0.51	**4.53**	1.92	**3.97**	**4.94**	**3.47**	**2.51**	0.41	1.43
GPR E	1.65	#DIV/0!	**4.34**	**3.28**	**3.54**	**2.12**	**2.67**	1.46	0.87	0.11	**4.34**	0.95	**2.48**	**5.01**	**2.73**	1.76	**2.44**	1.78
Bulk Density (lb/cf)	**5.29**	#DIV/0!	**9.02**	**9.49**	**8.86**	**6.66**	**2.35**	**5.56**	1.97	**2.58**	**9.02**	**5.83**	**7.75**	**11.22**	**7.30**	**5.34**	**3.26**	0.30
Texture Depth (in)	**3.69**	#DIV/0!	**9.46**	**7.26**	**8.68**	**7.98**	1.85	**7.31**	1.68	1.13	**9.46**	**2.55**	**4.48**	**8.66**	**6.52**	**7.10**	**5.01**	**2.51**
Permeability (cm/s)	**3.85**	#DIV/0!	**5.37**	**6.03**	**7.58**	**6.22**	**3.50**	**3.59**	0.45	**2.13**	**5.37**	**4.71**	**3.54**	**8.41**	**8.44**	**14.53**	**4.35**	**4.54**
Rut Depth	**4.28**	#DIV/0!	**9.52**	**9.43**	**8.45**	**9.77**	1.41	**11.14**	**8.87**	**10.28**	**9.52**	**5.10**	**8.27**	**6.53**	**7.77**	**4.25**	1.37	1.58
Rice Gravity	**5.74**	#DIV/0!	**6.88**	**4.84**	**8.15**	**7.78**	**4.85**	**6.87**	0.77	0.39	**6.88**	0.90	1.35	**7.64**	**6.68**	**7.05**	**9.14**	0.37
% Density	**6.42**	#DIV/0!	**11.01**	**10.64**	**11.31**	**8.47**	1.13	**6.99**	1.63	**2.27**	**11.01**	**5.53**	**7.37**	**14.30**	**8.94**	**6.80**	**4.87**	0.18
Air Voids	**6.42**	#DIV/0!	**11.01**	**10.64**	**11.31**	**8.47**	1.13	**6.99**	1.63	**2.27**	**11.01**	**5.53**	**7.37**	**14.30**	**8.94**	**6.80**	**4.87**	0.18
Asphalt Content		#DIV/0!	**8.04**	**10.77**	**16.10**	**14.20**	**4.37**	**13.87**	1.18	**2.73**	**8.04**	**8.45**	**5.49**	**14.83**	**10.30**	**8.05**	**11.09**	**2.94**
Passing 1/2			#DIV/0!	#DIV/0!	#DIV/0!	#DIV/0!	#DIV/0!	#DIV/0!	#DIV/0!	#DIV/0!	#DIV/0!	#DIV/0!	#DIV/0!	#DIV/0!	#DIV/0!	#DIV/0!	#DIV/0!	#DIV/0!
Passing 3/8				**23.11**	**16.88**	**14.24**	1.27	**12.07**	**4.94**	**4.65**	#NUM!	**5.79**	**16.39**	**17.18**	**11.97**	**12.41**	**3.88**	**3.40**
Passing #4					**28.85**	**23.62**	0.29	**16.68**	**7.13**	**7.00**	**23.11**	**13.95**	**23.66**	**24.20**	**22.71**	**15.38**	**3.46**	**3.31**
Passing #8						**45.07**	**2.48**	**22.42**	**4.08**	**4.38**	**16.88**	**12.14**	**10.95**	**39.44**	**29.63**	**17.88**	**7.52**	1.58
Passing #16							**3.33**	**39.90**	**5.79**	**5.95**	**14.24**	**12.38**	**10.29**	**19.81**	**23.31**	**16.89**	**6.55**	**2.32**
Passing #30								**3.87**	**2.26**	**2.95**	1.27	1.37	**2.34**	1.28	0.54	**4.44**	**7.45**	0.54
Passing #50									**6.49**	**7.42**	**12.07**	**9.96**	**8.81**	**13.12**	**13.57**	**10.86**	**6.41**	1.28
Passing #100										**28.31**	**4.94**	**7.37**	**10.69**	**2.34**	**4.62**	**3.87**	**5.13**	**7.15**
Passing #200											**4.65**	**7.57**	**9.53**	**2.71**	**4.29**	**2.30**	**3.55**	**2.82**
Retained on 3/8												**5.79**	**16.39**	**17.18**	**11.97**	**12.41**	**3.88**	**3.40**
Retained on #4													**10.95**	**10.51**	**15.91**	**8.89**	1.60	**2.16**
Retained on #8														**10.78**	**11.09**	**9.10**	0.58	**5.05**
Retained on #16															**24.43**	**15.18**	**7.73**	0.80
Retained on #30																**17.95**	**4.98**	**2.96**
Retained on #50																	**4.61**	**6.44**
Retained on #100																		**5.24**
Retained on #200																		

Table C8. Regressions between Changes in GPR Dielectric and Changes in Mix Parameters for IH 10 Pooled Data without Core 10.

	Temp (F)	Lab E	Bulk Density (lb/cf)	Texture Depth (in)	Permeability (cm/s)	Rut Depth (8000 passes, mm)	Max Theoretical Density	% Density	Air Voids
Delta GPR E Regressions									
Intercept	0	-2.83E-17	0	9.46E-20	4.78035E-20	2.02E-17	0	0	0
Slope	79.0379	2.583175	19.73251	-0.011924	-0.000722219	-2.159388	-1.49037901	13.94918	-13.94918
R-Square	0.710403	0.555226	0.761278	0.410176	0.191436025	0.12698	0.05721676	0.735418	0.735418
S.E.	4.855882	0.222473	1.063272	0.001376	0.000142824	0.544833	0.58214229	0.805101	0.805101
T-Test	16.27673	11.61121	18.55828	-8.666348	-5.056692188	-3.963396	-2.56016273	17.32601	-17.32601
Prob(T)	6E-31	8.96E-21	1.59E-35	4.62E-14	1.73596E-06	0.000132	0.01183155	4.34E-33	4.34E-33

	Passing 1/2	Passing 3/8	Passing #4	Passing #8	Passing #16	Passing #30	Retained on 3/8	Retained on #8	Retained on #16	Retained on #30	Retained on #100
Delta GPR E Regressions											
Intercept	0	0	8.4E-16	5.2E-16	0	6.5E-17	9.69E-17	-6.5E-17	-6.5E-17	-4.8E-17	8.07E-18
Slope	0	5.59475	6.38776	4.04373	1.4519	3.54227	-5.59475	2.402332	2.413994	0.533528	0.994169
R-Square	#DIV/0!	0.14861	0.09073	0.10411	0.04001	0.06199	0.14861	0.054075	0.188316	0.064446	0.052172
S.E.	0	1.28857	1.94585	1.14142	0.68435	1.32591	1.288574	0.966833	0.482252	0.195606	0.407752
T-Test	#DIV/0!	4.34182	3.28276	3.54272	2.12157	2.67157	-4.34182	2.484744	5.005669	2.727565	2.438173
Prob(T)	#DIV/0!	3.2E-05	0.00138	0.00058	0.03614	0.00871	3.18E-05	0.014485	2.15E-06	0.007438	0.016378

Table C9. Complete Correlation Matrix between Differences of Data for IH 10 Grouped Data.

	Temp (F)	Lab E	GPR E	Bulk Density (lb/cf)	Texture Depth (in)	Permeability (cm/s)	Rut Depth (8000 passes, mm)	Max Theoretical Density	% Density	Air Voids	Asphalt Content
Temp (F)	1	0.60	0.49	0.95	-0.62	-0.31	-0.36	-0.08	0.93	-0.93	0.34
Lab E		1	0.76	0.75	-0.69	-0.51	-0.32	-0.02	0.73	-0.73	-0.11
GPR E			1	0.62	-0.64	-0.68	-0.54	-0.27	0.66	-0.66	0.25
Bulk Density (lb/cf)				1	-0.67	-0.27	-0.45	-0.06	0.98	-0.98	0.24
Texture Depth (in)					1	0.49	0.48	0.53	-0.76	0.76	-0.10
Permeability (cm/s)						1	0.04	0.21	-0.31	0.31	-0.21
Rut Depth (8000 passes, mm)							1	0.13	-0.46	0.46	-0.09
Max Theoretical Density								1	-0.28	0.28	-0.28
% Density									1	-1.00	0.29
Air Voids										1	-0.29
Asphalt Content											1

	Passing 1/2	Passing 3/8	Passing #4	Passing #8	Passing #16	Passing #30	Passing #50	Passing #100	Passing #200	Retained on 3/8	Retained on #4	Retained on #8	Retained on #16	Retained on #30	Retained on #50	Retained on #100	Retained on #200
Temp (F)	#DIV/0!	0.71	0.59	0.60	0.43	0.03	0.40	0.09	0.11	-0.71	-0.18	0.47	0.73	0.31	0.21	0.21	-0.01
Lab E	#DIV/0!	0.43	0.36	0.32	0.09	0.29	-0.19	-0.13	-0.28	-0.43	-0.12	0.32	0.54	0.46	0.32	-0.04	0.23
GPR E	#DIV/0!	0.64	0.59	0.65	0.44	0.01	0.07	-0.12	-0.21	-0.64	-0.28	0.44	0.77	0.76	0.62	0.17	0.20
Bulk Density (lb/cf)	#DIV/0!	0.62	0.49	0.50	0.30	0.19	0.24	-0.02	0.02	-0.62	-0.12	0.39	0.68	0.29	0.13	0.20	-0.10
Texture Depth (in)	#DIV/0!	-0.68	-0.43	-0.58	-0.49	0.28	-0.37	0.07	0.21	0.68	-0.08	-0.22	-0.60	-0.39	-0.43	-0.35	-0.26
Permeability (cm/s)	#DIV/0!	-0.50	-0.54	-0.64	-0.51	0.44	-0.06	0.07	0.38	0.50	0.37	-0.37	-0.66	-0.80	-0.89	-0.11	-0.60
Rut Depth	#DIV/0!	-0.53	-0.51	-0.45	-0.50	-0.18	-0.49	-0.48	-0.52	0.53	0.25	-0.46	-0.34	-0.41	-0.20	0.09	-0.10
Rice Gravity	#DIV/0!	-0.31	0.05	-0.31	-0.27	0.61	-0.27	0.47	0.43	0.31	-0.51	0.33	-0.29	-0.03	-0.19	-0.71	0.15
% Density	#DIV/0!	0.66	0.46	0.55	0.35	0.05	0.29	-0.12	-0.08	-0.66	0.00	0.30	0.72	0.29	0.17	0.35	-0.12
Air Voids	#DIV/0!	-0.66	-0.46	-0.55	-0.35	-0.05	-0.29	0.12	0.08	0.66	0.00	-0.30	-0.72	-0.29	-0.17	-0.35	0.12
Asphalt Content	#DIV/0!	0.30	0.45	0.73	0.68	-0.51	0.66	-0.06	0.12	-0.30	-0.43	0.14	0.66	0.41	0.34	0.60	-0.34
Passing 1/2	#DIV/0!	#DIV/0!	#DIV/0!	#DIV/0!	#DIV/0!	#DIV/0!	#DIV/0!	#DIV/0!	#DIV/0!	#DIV/0!	#DIV/0!	#DIV/0!	#DIV/0!	#DIV/0!	#DIV/0!	#DIV/0!	#DIV/0!
Passing 3/8		1	0.86	0.79	0.70	-0.16	0.50	0.31	0.21	-1.00	-0.30	0.75	0.81	0.62	0.63	0.06	0.40
Passing #4			1	0.87	0.82	-0.10	0.56	0.56	0.44	-0.86	-0.74	0.92	0.82	0.84	0.76	-0.15	0.49
Passing #8				1	0.94	-0.47	0.71	0.24	0.18	-0.79	-0.58	0.60	0.92	0.81	0.78	0.32	0.26
Passing #16					1	-0.57	0.86	0.43	0.36	-0.70	-0.60	0.56	0.73	0.73	0.74	0.25	0.32
Passing #30						1	-0.54	0.20	0.28	0.16	-0.04	0.23	-0.27	-0.20	-0.46	-0.65	-0.11
Passing #50							1	0.45	0.53	-0.50	-0.36	0.32	0.45	0.30	0.30	0.35	0.00
Passing #100								1	0.91	-0.31	-0.65	0.71	0.02	0.32	0.23	-0.68	0.53
Passing #200									1	-0.21	-0.55	0.57	-0.03	0.12	-0.05	-0.51	0.13
Retained on 3/8										1	0.30	-0.75	-0.81	-0.62	-0.63	-0.06	-0.40
Retained on #4											1	-0.74	-0.46	-0.75	-0.58	0.38	-0.40
Retained on #8												1	0.58	0.71	0.59	-0.51	0.58
Retained on #16													1	0.77	0.70	0.33	0.15
Retained on #30														1	0.92	-0.10	0.55
Retained on #50															1	-0.01	0.70
Retained on #100																1	-0.57
Retained on #200																	1

Table C10. Correlation Coefficient t-values for IH 10 Grouped Data.

Note: Bold values indicate significance at 95% confidence level.

	Temp (F)	Lab E	GPR E	Bulk Density (lb/cf)	Texture Depth (in)	Permeability (cm/s)	Rut Depth (8000 passes, mm)	Max Theoretical Density	% Density	Air Voids	Asphalt Content
Temp (F)		**4.83**	**3.61**	**19.74**	**5.18**	**2.08**	**2.46**	0.50	**16.46**	**16.46**	**2.32**
Lab E			**7.58**	**7.44**	**6.24**	**3.83**	**2.22**	0.11	**6.97**	**6.97**	0.72
GPR E				**5.10**	**5.39**	**6.07**	**4.21**	1.84	**5.64**	**5.64**	1.66
Bulk Density (lb/cf)					**5.78**	1.83	**3.29**	0.38	**28.77**	**28.77**	1.58
Texture Depth (in)						**3.64**	**3.59**	**4.09**	**7.56**	**7.56**	0.67
Permeability (cm/s)							0.25	1.39	**2.10**	**2.10**	1.42
Rut Depth (8000 passes, mm)								0.86	**3.40**	**3.40**	0.58
Max Theoretical Density									1.87	1.87	1.89
% Density										#DIV/0!	1.94
Air Voids											1.94
Asphalt Content											

	Passing 1/2	Passing 3/8	Passing #4	Passing #8	Passing #16	Passing #30	Passing #50	Passing #100	Passing #200	Retained on 3/8	Retained on #4	Retained on #8	Retained on #16	Retained on #30	Retained on #50	Retained on #100	Retained on #200
Temp (F)	#DIV/0!	**6.47**	**4.70**	**4.83**	**3.10**	0.18	**2.79**	0.60	0.71	**6.47**	1.21	**3.44**	**6.83**	**2.08**	1.37	1.36	0.05
Lab E	#DIV/0!	**3.08**	**2.50**	**2.18**	0.59	1.98	1.28	0.84	1.91	**3.08**	0.81	**2.21**	**4.14**	**3.33**	**2.17**	0.26	1.55
GPR E	#DIV/0!	**5.34**	**4.78**	**5.50**	**3.18**	0.08	0.45	0.75	1.42	**5.34**	1.88	**3.19**	**7.91**	**7.60**	**5.16**	1.11	1.30
Bulk Density (lb/cf)	#DIV/0!	**5.11**	**3.66**	**3.78**	**2.06**	1.26	1.63	0.12	0.10	**5.11**	0.78	**2.75**	**6.00**	2.00	0.83	1.34	0.63
Texture Depth (in)	#DIV/0!	**6.00**	**3.11**	**4.64**	**3.68**	1.91	**2.55**	0.47	1.38	**6.00**	0.54	1.47	**4.91**	**2.75**	**3.09**	**2.46**	1.74
Permeability (cm/s)	#DIV/0!	**3.72**	**4.20**	**5.34**	**3.88**	**3.15**	0.37	0.45	**2.63**	**3.72**	**2.58**	**2.57**	**5.69**	**8.58**	**12.89**	0.72	**4.85**
Rut Depth	#DIV/0!	**4.03**	**3.85**	**3.28**	**3.71**	1.21	**3.63**	**3.51**	**3.96**	**4.03**	1.70	**3.39**	**2.31**	**2.89**	1.31	0.59	0.65
Rice Gravity	#DIV/0!	**2.13**	0.31	**2.12**	1.85	**4.96**	1.83	**3.48**	**3.10**	**2.13**	**3.86**	**2.27**	1.98	0.17	1.29	**6.58**	0.96
% Density	#DIV/0!	**5.75**	**3.38**	**4.29**	**2.42**	0.33	1.98	0.80	0.53	**5.75**	0.01	**2.05**	**6.68**	1.97	1.08	**2.43**	0.81
Air Voids	#DIV/0!	**5.75**	**3.38**	**4.29**	**2.42**	0.33	1.98	0.80	0.53	**5.75**	0.01	**2.05**	**6.68**	1.97	1.08	**2.43**	0.81
Asphalt Content	#DIV/0!	**2.07**	**3.28**	**6.86**	**6.01**	**3.86**	**5.65**	0.41	0.77	**2.07**	**3.07**	0.94	**5.75**	**2.93**	**2.33**	**4.90**	**2.38**
Passing 1/2		#DIV/0!	#DIV/0!	#DIV/0!	#DIV/0!	#DIV/0!	#DIV/0!	#DIV/0!	#DIV/0!	#DIV/0!	#DIV/0!	#DIV/0!	#DIV/0!	#DIV/0!	#DIV/0!	#DIV/0!	#DIV/0!
Passing 3/8			**10.84**	**8.48**	**6.30**	1.04	**3.79**	**2.08**	1.37	*******	2.01	**7.26**	**9.02**	**5.19**	**5.27**	0.40	**2.82**
Passing #4				**11.47**	**9.20**	0.65	**4.35**	**4.40**	**3.21**	**10.84**	**7.22**	**14.75**	**9.26**	**10.10**	**7.48**	1.01	**3.62**
Passing #8					**18.07**	**3.48**	**6.61**	1.62	1.20	**8.48**	**4.58**	**4.85**	**15.08**	**9.06**	**8.04**	**2.16**	1.72
Passing #16						**4.48**	**10.88**	**3.09**	**2.52**	**6.30**	**4.87**	**4.38**	**6.99**	**7.00**	**7.05**	1.64	**2.22**
Passing #30							**4.11**	1.33	1.91	1.04	0.24	1.51	1.83	1.32	**3.40**	**5.54**	0.74
Passing #50								**3.24**	**4.07**	**3.79**	**2.52**	**2.18**	**3.28**	**2.05**	**2.06**	**2.42**	0.02
Passing #100									**13.79**	**2.08**	**5.52**	**6.61**	0.10	**2.21**	1.56	**6.03**	**4.10**
Passing #200										1.37	**4.31**	**4.55**	0.17	0.80	0.30	**3.81**	0.87
Retained on 3/8											2.01	**7.26**	**9.02**	**5.19**	**5.27**	0.40	**2.82**
Retained on #4												**7.15**	**3.40**	**7.37**	**4.66**	**2.69**	**2.81**
Retained on #8													**4.65**	**6.48**	**4.78**	**3.83**	**4.61**
Retained on #16														**7.85**	**6.34**	**2.27**	0.97
Retained on #30															**15.17**	0.64	**4.27**
Retained on #50																0.07	**6.27**
Retained on #100																	**4.49**

Table C11. Regressions between Changes in Temperature and Changes in Mix Parameters for IH 10 Grouped Data.

	Lab E	GPR E	Bulk Density (lb/cf)	Texture Depth (in)	Permeability (cm/s)	Rut Depth (8000 passes, mm)	% Density	Air Voids	Asphalt Content
Delta Temperature Regressions									
Intercept	2.02E-17	0	0	7.89E-20	-3.08E-20	-1.01E-17	0	0	0
Slope	0.029783	0.008928	0.24151	-0.000148	-8.03E-06	-0.02182	0.162603	-0.162603	0.003197
R-Square	0.357466	0.237068	0.902734	0.389559	0.093668	0.126278	0.865808	0.865808	0.114002
S.E.	0.006161	0.002471	0.012232	2.85E-05	3.85E-06	0.008856	0.009878	0.009878	0.001375
T-Test	4.833857	3.612588	19.74347	-5.177133	-2.083417	-2.463777	16.46163	-16.46163	2.324683
Prob(T)	1.74E-05	0.000788	3.5E-23	5.66E-06	0.043193	0.017825	3.54E-20	3.54E-20	0.024879

	Passing 3/8	Passing #4	Passing #8	Passing #16	Passing #50	Retained on 3/8	Retained on #8	Retained on #16	Retained on #30
Delta Temperature Regressions									
Intercept	0	0	0	0	0	0	0	0	0
Slope	0.101976	0.120945	0.062472	0.027522	0.016867	-0.101976	0.058394	0.033689	0.005975
R-Square	0.498852	0.345076	0.357166	0.18627	0.156746	0.498852	0.220219	0.525907	0.09353
S.E.	0.015771	0.02571	0.012932	0.008876	0.006037	0.015771	0.016955	0.004936	0.00287
T-Test	6.465884	4.704206	4.830704	3.100677	2.79411	-6.465884	3.444025	6.825698	2.081728
Prob(T)	7.67E-08	2.65E-05	1.76E-05	0.003402	0.007742	7.67E-08	0.00129	2.3E-08	0.043355

Table C12. Complete Correlation Matrix between Differences of Data for IH 10 Grouped Data without Core 10.

	Temp (F)	Lab E	GPR E	Bulk Density (lb/cf)	Texture Depth (in)	Permeability (cm/s)	Rut Depth (8000 passes, mm)	Max Theoretical Density	% Density	Air Voids	Asphalt Content
Temp (F)	1	0.66	0.79	0.96	-0.66	-0.48	-0.40	-0.04	0.94	-0.94	0.41
Lab E		1	0.79	0.80	-0.68	-0.41	-0.25	0.05	0.77	-0.77	-0.16
GPR E			1	0.90	-0.67	-0.40	-0.47	-0.24	0.93	-0.93	0.14
Bulk Density (lb/cf)				1	-0.68	-0.38	-0.48	-0.02	0.98	-0.98	0.30
Texture Depth (in)					1	0.42	0.45	0.49	-0.77	0.77	-0.07
Permeability (cm/s)						1	-0.26	0.16	-0.40	0.40	-0.09
Rut Depth (8000 passes, mm)							1	0.08	-0.49	0.49	-0.01
Max Theoretical Density								1	-0.23	0.23	-0.22
% Density									1	-1.00	0.33
Air Voids										1	-0.33
Asphalt Content											1

	Passing 1/2	Passing 3/8	Passing #4	Passing #8	Passing #16	Passing #30	Passing #50	Passing #100	Passing #200	Retained on 3/8	Retained on #4	Retained on #8	Retained on #16	Retained on #30	Retained on #50	Retained on #100	Retained on #200
Temp (F)	#DIV/0!	0.83	0.82	0.81	0.58	0.04	0.43	0.15	0.16	-0.83	-0.33	0.63	0.92	0.79	0.49	0.19	0.02
Lab E	#DIV/0!	0.36	0.26	0.22	-0.04	0.37	-0.17	-0.14	-0.23	-0.36	0.01	0.23	0.48	0.41	0.11	-0.02	0.09
GPR E	#DIV/0!	0.54	0.33	0.44	0.17	0.18	0.07	-0.25	-0.20	-0.54	0.14	0.18	0.66	0.42	0.09	0.32	-0.23
Bulk Density (lb/cf)	#DIV/0!	0.71	0.66	0.66	0.41	0.20	0.30	0.04	0.08	-0.71	-0.22	0.51	0.83	0.66	0.26	0.19	-0.11
Texture Depth (in)	#DIV/0!	-0.64	-0.38	-0.56	-0.46	0.24	-0.39	0.06	0.14	0.64	-0.21	-0.14	-0.56	-0.37	-0.39	-0.37	-0.16
Permeability (cm/s)	#DIV/0!	-0.33	-0.26	-0.42	-0.27	0.45	-0.01	0.20	0.44	0.33	0.03	-0.08	-0.48	-0.59	-0.82	-0.22	-0.42
Rut Depth	#DIV/0!	-0.44	-0.41	-0.35	-0.43	-0.25	-0.52	-0.50	-0.60	0.44	0.12	-0.36	-0.18	-0.27	0.14	0.08	0.06
Rice Gravity	#DIV/0!	-0.26	0.17	-0.25	-0.21	0.59	-0.22	0.48	0.42	0.26	-0.69	0.45	-0.22	0.18	-0.16	-0.70	0.21
% Density	#DIV/0!	0.74	0.61	0.69	0.44	0.07	0.33	-0.06	-0.01	-0.74	-0.07	0.40	0.85	0.60	0.29	0.33	-0.15
Air Voids	#DIV/0!	-0.74	-0.61	-0.69	-0.44	-0.07	-0.33	0.06	0.01	0.74	0.07	-0.40	-0.85	-0.60	-0.29	-0.33	0.15
Asphalt Content	#DIV/0!	0.27	0.43	0.75	0.67	-0.47	0.66	-0.07	0.16	-0.27	-0.40	0.09	0.67	0.45	0.27	0.63	-0.53
Passing 1/2	#DIV/0!	#DIV/0!	#DIV/0!	#DIV/0!	#DIV/0!	#DIV/0!	#DIV/0!	#DIV/0!	#DIV/0!	#DIV/0!	#DIV/0!	#DIV/0!	#DIV/0!	#DIV/0!	#DIV/0!	#DIV/0!	#DIV/0!
Passing 3/8		1	0.84	0.76	0.63	-0.09	0.53	0.30	0.28	-1.00	-0.13	0.70	0.78	0.60	0.55	0.10	0.24
Passing #4			1	0.82	0.76	0.01	0.65	0.61	0.60	-0.84	-0.65	0.90	0.76	0.84	0.58	-0.12	0.27
Passing #8				1	0.92	-0.44	0.82	0.25	0.30	-0.76	-0.43	0.49	0.89	0.80	0.65	0.42	-0.02
Passing #16					1	-0.54	0.96	0.46	0.49	-0.63	-0.48	0.45	0.64	0.71	0.64	0.31	0.11
Passing #30						1	-0.49	0.23	0.29	0.09	-0.15	0.35	-0.20	-0.12	-0.59	-0.67	-0.05
Passing #50							1	0.47	0.57	-0.53	-0.42	0.36	0.50	0.52	0.42	0.34	-0.04
Passing #100								1	0.92	-0.30	-0.69	0.75	-0.02	0.46	0.23	-0.67	0.53
Passing #200									1	-0.28	-0.69	0.69	0.05	0.38	0.00	-0.50	0.17
Retained on 3/8										1	0.13	-0.70	-0.78	-0.60	-0.55	-0.10	-0.24
Retained on #4											1	-0.66	-0.30	-0.69	-0.29	0.39	-0.18
Retained on #8												1	0.48	0.67	0.39	-0.52	0.42
Retained on #16													1	0.74	0.54	0.42	-0.14
Retained on #30														1	0.72	-0.06	0.31
Retained on #50															1	0.10	0.61
Retained on #100																1	-0.61
Retained on #200																	1

Table C13. Correlation Coefficient t-values for IH 10 Grouped Data without Core 10.

Note: Bold values indicate significance at 95% confidence level.

	Temp (F)	Lab E	GPR E	Bulk Density (lb/cf)	Texture Depth (in)	Permeability (cm/s)	Rut Depth (8000 passes, mm)	Max Theoretical Density	% Density	Air Voids	Asphalt Content
Temp (F)		**5.03**	**7.24**	**18.44**	**4.90**	**3.10**	**2.49**	0.24	**15.45**	**15.45**	**2.57**
Lab E			**7.39**	**7.47**	**5.18**	**2.52**	1.46	0.26	**6.81**	**6.81**	0.90
GPR E				**11.61**	**5.13**	**2.46**	**3.01**	1.39	**13.97**	**13.97**	0.77
Bulk Density (lb/cf)					**5.31**	**2.30**	**3.13**	0.09	**25.99**	**25.99**	1.75
Texture Depth (in)						**2.63**	**2.84**	**3.19**	**6.86**	**6.86**	0.37
Permeability (cm/s)							1.50	0.93	**2.48**	**2.48**	0.51
Rut Depth (8000 passes, mm)								0.47	**3.17**	**3.17**	0.08
Max Theoretical Density									1.33	1.33	1.28
% Density										#NUM!	2.00
Air Voids											2.00
Asphalt Content											

	Passing 1/2	Passing 3/8	Passing #4	Passing #8	Passing #16	Passing #30	Passing #50	Passing #100	Passing #200	Retained on 3/8	Retained on #4	Retained on #8	Retained on #16	Retained on #30	Retained on #50	Retained on #100	Retained on #200
Temp (F)	#DIV/0!	**8.51**	**8.07**	**7.80**	**4.02**	0.20	**2.73**	0.85	0.92	**8.51**	2.00	**4.62**	**13.67**	**7.36**	**3.16**	1.07	0.14
Lab E	#DIV/0!	**2.17**	1.54	1.25	0.22	**2.24**	0.99	0.77	1.31	**2.17**	0.04	1.36	**3.06**	**2.51**	0.63	0.10	0.53
GPR E	#DIV/0!	**3.65**	2.00	**2.76**	0.95	1.05	0.39	1.46	1.14	**3.65**	0.81	1.04	**4.93**	**2.60**	0.54	1.91	1.35
Bulk Density (lb/cf)	#DIV/0!	**5.70**	**5.02**	**4.98**	**2.53**	1.16	1.76	0.23	0.46	**5.70**	1.29	**3.35**	**8.36**	**4.97**	1.52	1.10	0.61
Texture Depth (in)	#DIV/0!	**4.73**	**2.31**	**3.78**	**2.92**	1.39	**2.38**	0.34	0.82	**4.73**	1.24	0.80	**3.83**	**2.28**	**2.41**	**2.28**	0.92
Permeability (cm/s)	#DIV/0!	2.00	1.53	**2.59**	1.58	**2.85**	0.07	1.18	**2.76**	2.00	0.14	0.47	**3.12**	**4.09**	**7.96**	1.28	**2.64**
Rut Depth	#DIV/0!	**2.74**	**2.52**	**2.09**	**2.69**	1.47	**3.47**	**3.26**	**4.27**	**2.74**	0.70	**2.19**	1.05	1.60	0.79	0.45	0.36
Rice Gravity	#DIV/0!	1.53	0.98	1.44	1.21	**4.15**	1.30	**3.08**	**2.59**	1.53	**5.43**	**2.86**	1.27	1.02	0.91	**5.53**	1.21
% Density	#DIV/0!	**6.31**	**4.33**	**5.45**	**2.77**	0.40	2.01	0.36	0.06	**6.31**	0.39	**2.45**	**9.18**	**4.29**	1.68	2.00	0.84
Air Voids	#DIV/0!	**6.31**	**4.33**	**5.45**	**2.77**	0.40	2.01	0.36	0.06	**6.31**	0.39	**2.45**	**9.18**	**4.29**	1.68	2.00	0.84
Asphalt Content	#DIV/0!	1.57	**2.71**	**6.40**	**5.11**	**3.02**	**4.95**	0.39	0.89	1.57	**2.44**	0.49	**5.13**	**2.84**	1.58	**4.58**	**3.50**
Passing 1/2		#DIV/0!	#DIV/0!	#DIV/0!	#DIV/0!	#DIV/0!	#DIV/0!	#DIV/0!	#DIV/0!	#DIV/0!	#DIV/0!	#DIV/0!	#DIV/0!	#DIV/0!	#DIV/0!	#DIV/0!	#DIV/0!
Passing 3/8			**8.76**	**6.55**	**4.56**	0.49	**3.55**	1.77	1.65	#NUM!	0.76	**5.60**	**7.03**	**4.24**	**3.75**	0.56	1.38
Passing #4				**8.21**	**6.54**	0.04	**4.87**	**4.35**	**4.24**	**8.76**	**4.82**	**11.54**	**6.63**	**8.65**	**4.06**	0.71	1.58
Passing #8					**13.37**	**2.75**	**8.20**	1.44	1.77	**6.55**	**2.70**	**3.18**	**10.91**	**7.55**	**4.90**	**2.61**	0.12
Passing #16						**3.62**	**19.11**	**2.92**	**3.15**	**4.56**	**3.12**	**2.82**	**4.71**	**5.70**	**4.68**	1.88	0.60
Passing #30							**3.22**	1.35	1.68	0.49	0.87	**2.13**	1.15	0.68	**4.16**	**5.09**	0.29
Passing #50								**3.05**	**3.91**	**3.55**	**2.62**	**2.18**	**3.25**	**3.42**	**2.61**	2.02	0.20
Passing #100									**13.77**	1.77	**5.45**	**6.33**	0.14	**2.91**	1.32	**5.07**	**3.51**
Passing #200										1.65	**5.46**	**5.41**	0.26	**2.31**	0.02	**3.31**	1.00
Retained on 3/8											0.76	**5.60**	**7.03**	**4.24**	**3.75**	0.56	1.38
Retained on #4												**5.02**	1.75	**5.44**	1.75	**2.37**	1.01
Retained on #8													**3.12**	**5.12**	**2.39**	**3.43**	**2.66**
Retained on #16														**6.28**	**3.63**	**2.63**	0.80
Retained on #30															**5.92**	0.34	1.83
Retained on #50																0.54	**4.31**
Retained on #100																	**4.32**

Table C14. Regressions between Changes in GPR Dielectric and Changes in Mix Parameters for IH 10 Grouped Data without Core 10.

	Temp (F)	Lab E	Bulk Density (lb/cf)	Texture Depth (in)	Permeability (cm/s)	Rut Depth (8000 passes, mm)	% Density	Air Voids
Delta GPR E Regressions								
Intercept	0	-1.31E-17	0	0	1.75386E-20	0	0	0
Slope	65.08065	2.939172	18.68002	-0.012016	-0.000610282	-2.242823	13.08905	-13.08905
R-Square	0.621245	0.630735	0.808024	0.450983	0.159526601	0.220932	0.859151	0.859151
S.E.	8.98306	0.397553	1.609583	0.002344	0.000247629	0.744524	0.936863	0.936863
T-Test	7.244819	7.393151	11.6055	-5.126988	-2.464504178	-3.012426	13.97115	-13.97115
Prob(T)	2.61E-08	1.71E-08	3.43E-13	1.27E-05	0.019097982	0.004946	2.06E-15	2.06E-15

	Passing 3/8	Passing #8	Retained on 3/8	Retained on #16	Retained on #30
Delta GPR E Regressions					
Intercept	0	0	-1.04E-16	0	0
Slope	5.669355	3.032258	-5.669355	2.096774	0.322581
R-Square	0.293401	0.192329	0.293401	0.431982	0.174368
S.E.	1.555301	1.098463	1.555301	0.425035	0.124086
T-Test	3.645181	2.760456	-3.645181	4.933178	2.599651
Prob(T)	0.00091	0.00935	0.00091	2.25E-05	0.01385

APPENDIX D

US 290 CORRELATION MATRICES AND REGRESSIONS

Table D1. Significant Correlations between Data for US 290.

	ΔTemp (F)	**Δ GPR ε**
Δ Temp (F)	1.00	0.95
Δ GPR ε	0.95	1.00
Δ Bulk Density (pcf)	0.98	0.96
Δ Permeability (cm/s)	-0.94	-0.94
Δ Rice Gravity (pcf)	-0.50	-0.32
Δ Air Voids (%)	-0.99	0.96
Δ % Asphalt	0.96	0.99
Δ % Passing #1/2	0.85	0.89
Δ % Passing #3/8	0.97	0.93
Δ % Passing #4	0.97	0.95
Δ % Passing #10	0.98	0.97
Δ % Passing #40	0.98	0.97
Δ % Passing #80	0.91	0.89
Δ % Passing #200	-0.86	-0.82
Δ % Retained on #1/2	-0.85	-0.89
Δ % Retained on #3/8	-0.98	-0.91
Δ % Retained on #4	-0.97	-0.96
Δ % Retained on #10	0.91	0.87
Δ % Retained on #40	0.99	0.97
Δ % Retained on #80	0.99	0.97
Δ % Retained on #200	0.97	0.96

Table D2. Complete Correlation Matrix between Differences of Data for US 290.

	Change T	Change Lab E	Change E	Change Density	Change Texture Depth	Change Perm	Change Rut Depth	Change Rice Gravity	Change % Density	Change % AV	Change % AC
Change T	1	-0.26	0.95	0.98	-0.10	-0.94	0.19	-0.50	0.99	-0.99	0.96
Change Lab E		1	-0.09	-0.22	0.28	0.21	0.38	0.03	-0.21	0.21	-0.10
Change E			1	0.96	-0.25	-0.94	0.19	-0.32	0.96	-0.96	0.99
Change Density				1	-0.11	-0.98	0.04	-0.37	1.00	-1.00	0.95
Change Texture Depth					1	0.19	-0.17	-0.41	-0.07	0.07	-0.20
Change Perm						1	0.00	0.27	-0.97	0.97	-0.91
Change Rut Depth							1	-0.46	0.07	-0.07	0.23
Change Rice Gravity								1	-0.44	0.44	-0.39
Change % Density									1	-1.00	0.95
Change % AV										1	-0.95
Change % AC											1

	Passing 3/4	Passing 1/2	Passing 3/8	Passing #4	Passing #10	Passing #40	Passing #80	Passing #200	Retained 1/2	Retained 3/8	Retained #4	Retained #10	Retained #40	Retained #80	Retained #200
Change T	#DIV/0!	0.85	0.97	0.97	0.98	0.98	0.91	-0.86	-0.85	-0.98	-0.97	0.91	0.99	0.99	0.97
Change Lab E	#DIV/0!	-0.04	-0.18	-0.19	-0.16	-0.16	0.02	0.27	0.04	0.25	0.20	-0.24	-0.17	-0.20	-0.03
Change E	#DIV/0!	0.89	0.93	0.95	0.97	0.97	0.89	-0.82	-0.89	-0.91	-0.96	0.87	0.97	0.97	0.96
Change Density	#DIV/0!	0.79	0.91	0.92	0.94	0.94	0.84	-0.92	-0.79	-0.93	-0.93	0.83	0.95	0.95	0.95
Change Texture Depth	#DIV/0!	-0.20	-0.09	-0.14	-0.16	-0.16	0.04	0.15	0.20	0.03	0.19	-0.09	-0.16	-0.21	0.00
Change Perm	#DIV/0!	-0.70	-0.83	-0.85	-0.88	-0.88	-0.74	0.96	0.70	0.86	0.86	-0.73	-0.89	-0.90	-0.88
Change Rut Depth	#DIV/0!	0.32	0.15	0.15	0.15	0.16	0.28	0.31	-0.32	-0.05	-0.15	0.18	0.12	0.13	0.13
Change Rice Gravity	#DIV/0!	-0.33	-0.52	-0.49	-0.45	-0.47	-0.55	0.20	0.33	0.59	0.46	-0.55	-0.44	-0.44	-0.48
Change % Density	#DIV/0!	0.80	0.93	0.93	0.95	0.95	0.86	-0.91	-0.80	-0.95	-0.93	0.85	0.96	0.96	0.96
Change % AV	#DIV/0!	-0.80	-0.93	-0.93	-0.95	-0.95	-0.86	0.91	0.80	0.95	0.93	-0.85	-0.96	-0.96	-0.96
Change % AC	#DIV/0!	0.93	0.97	0.97	0.99	0.99	0.94	-0.78	-0.93	-0.93	-0.98	0.92	0.99	0.98	0.98
Passing 3/4	#DIV/0!	#DIV/0!	#DIV/0!	#DIV/0!	#DIV/0!	#DIV/0!	#DIV/0!	#DIV/0!	#DIV/0!	#DIV/0!	#DIV/0!	#DIV/0!	#DIV/0!	#DIV/0!	#DIV/0!
Passing 1/2		1	0.94	0.94	0.93	0.93	0.96	-0.51	-1.00	-0.85	-0.94	0.94	0.92	0.91	0.91
Passing 3/8			1	1.00	0.99	0.99	0.97	-0.71	-0.94	-0.98	-0.99	0.99	0.99	0.98	0.98
Passing #4				1	1.00	1.00	0.96	-0.72	-0.94	-0.98	-1.00	0.98	1.00	0.99	0.97
Passing #10					1	1.00	0.95	-0.77	-0.93	-0.97	-1.00	0.96	1.00	1.00	0.98
Passing #40						1	0.95	-0.76	-0.93	-0.98	-1.00	0.96	1.00	1.00	0.98
Passing #80							1	-0.58	-0.96	-0.93	-0.95	0.96	0.95	0.93	0.97
Passing #200								1	0.51	0.78	0.74	-0.60	-0.78	-0.79	-0.76
Retained 1/2									1	0.85	0.94	-0.94	-0.92	-0.91	-0.91
Retained 3/8										1	0.97	-0.96	-0.97	-0.97	-0.96
Retained #4											1	-0.97	-1.00	-1.00	-0.97
Retained #10												1	0.96	0.95	0.93
Retained #40													1	1.00	0.98
Retained #80														1	0.97
Retained #200															1

Table D3. Correlation Coefficient t-values for US 290.

Note: Bold values indicate significance at 95% confidence level.

	Change T	Change Lab E	Change E	Change Density	Change Texture Depth	Change Perm	Change Rut Depth	Change Rice Gravity	Change % Density	Change % AV	Change % AC
Change T		1.71	**19.32**	**29.10**	0.62	**17.32**	1.20	**3.70**	**36.47**	**36.47**	**21.02**
Change Lab E			0.58	1.41	1.81	1.38	**2.60**	0.22	1.36	1.36	0.63
Change E				**22.72**	1.62	**17.54**	1.25	**2.11**	**21.08**	**21.08**	**52.04**
Change Density					0.68	**34.66**	0.25	**2.55**	**88.44**	**88.44**	**19.49**
Change Texture Depth						1.23	1.10	**2.81**	0.45	0.45	1.28
Change Perm							0.02	1.76	**27.06**	**27.06**	**13.69**
Change Rut Depth								**3.25**	0.47	0.47	1.52
Change Rice Gravity									**3.09**	**3.09**	**2.68**
Change % Density										#DIV/0!	**19.57**
Change % AV											**19.57**
Change % AC											

	Passing 3/4	Passing 1/2	Passing 3/8	Passing #4	Passing #10	Passing #40	Passing #80	Passing #200	Retained 1/2	Retained 3/8	Retained #4	Retained #10	Retained #40	Retained #80	Retained #200
Change T	#DIV/0!	**8.70**	**19.72**	**21.34**	**28.52**	**27.26**	**11.28**	**9.12**	**8.70**	**23.41**	**22.14**	**11.71**	**31.60**	**30.51**	**22.86**
Change Lab E	#DIV/0!	0.21	0.99	1.04	0.86	0.84	0.11	1.50	0.21	1.36	1.10	1.32	0.93	1.08	0.18
Change E	#DIV/0!	**10.45**	**13.72**	**15.41**	**20.80**	**19.90**	**10.44**	**7.69**	**10.45**	**11.37**	**17.08**	**9.16**	**21.62**	**21.42**	**17.42**
Change Density	#DIV/0!	**6.88**	**11.79**	**12.46**	**15.28**	**14.75**	**8.29**	**12.87**	**6.88**	**13.33**	**12.98**	**8.00**	**16.35**	**16.13**	**15.67**
Change Texture Depth	#DIV/0!	1.06	0.50	0.76	0.88	0.85	0.19	0.78	1.06	0.17	1.01	0.46	0.88	1.16	0.02
Change Perm	#DIV/0!	**5.26**	**7.90**	**8.42**	**10.01**	**9.73**	**5.85**	**19.44**	**5.26**	**8.76**	**8.89**	**5.67**	**10.49**	**10.81**	**9.82**
Change Rut Depth	#DIV/0!	1.77	0.78	0.81	0.78	0.84	1.55	1.72	1.77	0.25	0.80	0.94	0.65	0.68	0.69
Change Rice Gravity	#DIV/0!	1.87	**3.19**	**2.95**	**2.70**	**2.79**	**3.49**	1.06	1.87	**3.84**	**2.71**	**3.50**	**2.59**	**2.57**	**2.87**
Change % Density	#DIV/0!	**6.96**	**12.93**	**13.53**	**16.63**	**16.14**	**8.95**	**11.98**	**6.96**	**15.66**	**13.89**	**8.60**	**17.70**	**17.39**	**17.52**
Change % AV	#DIV/0!	**6.96**	**12.93**	**13.53**	**16.63**	**16.14**	**8.95**	**11.98**	**6.96**	**15.66**	**13.89**	**8.60**	**17.70**	**17.39**	**17.52**
Change % AC	#DIV/0!	**13.54**	**19.85**	**22.91**	**34.32**	**32.52**	**14.34**	**6.49**	**13.54**	**13.93**	**25.56**	**12.09**	**34.72**	**29.97**	**24.39**
Passing 3/4		#DIV/0!	#DIV/0!	#DIV/0!	#DIV/0!	#DIV/0!	#DIV/0!	#DIV/0!	#DIV/0!	#DIV/0!	#DIV/0!	#DIV/0!	#DIV/0!	#DIV/0!	#DIV/0!
Passing 1/2			**14.05**	**14.20**	**13.19**	**13.26**	**17.10**	**3.14**	#NUM!	**8.61**	**14.10**	**14.22**	**12.80**	**11.59**	**11.77**
Passing 3/8				**98.95**	**42.10**	**45.41**	**20.92**	**5.31**	**14.05**	**27.40**	**51.17**	**30.40**	**38.43**	**29.77**	**23.26**
Passing #4					**61.57**	**67.88**	**18.31**	**5.56**	**14.20**	**25.45**	**106.15**	**26.09**	**53.38**	**40.79**	**22.04**
Passing #10						**342.43**	**16.39**	**6.30**	**13.19**	**23.07**	**75.12**	**18.04**	**200.17**	**72.94**	**25.81**
Passing #40							**16.91**	**6.18**	**13.26**	**23.68**	**77.96**	**18.67**	**129.27**	**66.77**	**25.74**
Passing #80								**3.79**	**17.10**	**13.05**	**16.06**	**18.11**	**15.55**	**13.17**	**20.74**
Passing #200									**3.14**	**6.56**	**5.78**	**3.94**	**6.55**	**6.82**	**6.20**
Retained 1/2										**8.61**	**14.10**	**14.22**	**12.80**	**11.59**	**11.77**
Retained 3/8											**22.62**	**17.80**	**22.98**	**22.36**	**17.81**
Retained #4												**22.26**	**65.53**	**56.55**	**20.18**
Retained #10													**17.24**	**15.96**	**13.39**
Retained #40														**76.66**	**25.89**
Retained #80															**19.76**

Table D4. Regressions between Changes in NDT Data and Changes in Mix Parameters for US 290.

	Temp (F)	GPR E	Bulk Density	Permeability (cm/s)	Rice Gravity (lb/cf)	% Density	Air Voids (%)	Asphalt Content
Delta T Regressions								
Intercept		2.11E-17	0	-1.03257E-20	0	0	0	-4.23E-17
Slope		0.023159	0.248525	-9.05032E-06	-0.011545	0.165648	-0.165648	0.027511
R-Square		0.903228	0.954898	0.882352138	0.254915	0.970802	0.970802	0.91696
S.E.		0.001199	0.00854	5.22523E-07	0.003121	0.004542	0.004542	0.001309
T-Test		19.32207	29.10101	-17.32044108	-3.699347	36.46866	-36.46866	21.01656
Prob(T)		3.32E-22	5.29E-29	1.81975E-20	0.000635	7.12E-33	7.12E-33	1.44E-23
Delta GPR Dielectric Regressions								
Intercept	-8.25E-16		-2.13E-16	-2.45997E-21	6.29E-18	-1.4E-16	1.4E-16	-6.7E-17
Slope	39.00131		10.05449	-0.000371955	-0.297454	6.60812	-6.60812	1.170392
R-Square	0.903228		0.928062	0.884979142	0.100489	0.917388	0.917388	0.985443
S.E.	2.018485		0.44261	2.12022E-05	0.140713	0.31354	0.31354	0.022492
T-Test	19.32207		22.7164	-17.54317567	-2.11391	21.07582	-21.07582	52.0369
Prob(T)	3.32E-22		7.59E-25	1.14529E-20	0.040651	1.29E-23	1.29E-23	4.52E-39

	Passing 1/2	Passing 3/8	Passing #4	Passing #10	Passing #40	Passing #80	Passing #200	Retained 1/2	Retained 3/8	Retained #4	Retained #10	Retained #40	Retained #80	Retained #200
Delta T Regressions														
Intercept	0	1.2E-16	-1E-16	-1E-15	3.3E-16	-1E-17	-7E-18	9.62E-17	-4.7E-16	-4.1E-16	-1.8E-16	-5.9E-17	5.33E-16	2.59E-17
Slope	0.06853	0.20188	0.40904	0.28939	0.14675	0.02635	-0.0096	-0.06853	-0.1332	-0.20645	0.119442	0.142741	0.119695	0.03736
R-Square	0.73006	0.93282	0.94207	0.96673	0.9637	0.81973	0.74795	0.730056	0.951388	0.945975	0.830392	0.972732	0.970804	0.949163
S.E.	0.00787	0.01024	0.01917	0.01015	0.00538	0.00233	0.00106	0.007875	0.00569	0.009324	0.010201	0.004517	0.003923	0.001634
T-Test	8.70202	19.7179	21.3386	28.5226	27.2632	11.2838	-9.1154	-8.70202	-23.4092	-22.1422	11.70839	31.60434	30.51284	22.86444
Prob(T)	1.4E-09	2.4E-18	2.8E-19	9.1E-23	3.2E-22	4E-12	5.2E-10	1.4E-09	2.21E-20	1.02E-19	1.64E-12	5.07E-24	1.36E-23	4.24E-20
Delta GPR Dielectric Regressions														
Intercept	1.4E-16	5E-16	6.4E-16	-7E-16	6.1E-16	3.6E-17	-3E-17	-4.4E-17	-7.2E-16	-8.1E-16	4.4E-17	2.15E-16	7.63E-16	9.76E-17
Slope	2.79752	7.62374	15.5818	11.1513	5.64779	1.01474	-0.3592	-2.79752	-4.84019	-7.9263	4.436773	5.495733	4.610551	1.434445
R-Square	0.79607	0.87045	0.89451	0.93923	0.93394	0.79573	0.6788	0.796074	0.822003	0.912413	0.749709	0.94348	0.942473	0.91553
S.E.	0.26758	0.55583	1.01124	0.53606	0.28386	0.09716	0.04669	0.26758	0.42565	0.464106	0.484467	0.254203	0.215267	0.082342
T-Test	10.4549	13.716	15.4087	20.8022	19.8966	10.4439	-7.6924	-10.4549	-11.3713	-17.0787	9.158046	21.6195	21.41784	17.4206
Prob(T)	2.4E-11	3.3E-14	1.7E-15	5.6E-19	1.9E-18	2.4E-11	1.8E-08	2.38E-11	3.31E-12	1.13E-16	4.67E-10	1.97E-19	2.54E-19	6.68E-17

APPENDIX E

GROUND-PENETRATING RADAR SPECIFICATIONS

These specifications are based largely on the GPR reflection from a large metal plate. The amplitude of reflection is measured in volts typically from the maximum positive peak to the preceding negative.

Performance Specifications:

1. Noise to Signal Ratio Test: The antenna will be positioned at its recommended operating height above a minimum 16 square foot (4' x 4') metal plate. The radar unit shall be turned on and allowed to operate for a 15 minute warm- up period. After warm-up, the unit shall be operated at maximum pulse rate and 50 radar waveform pulses shall be recorded. The recorded waveforms shall then be evaluated for noise to signal ratio. No averaging or signal cleanup such as sky wave removal (and reflection subtraction) shall be allowed. The noise to signal ratio is described by the following equation:

$$\frac{Noise\ Level\ (A_n)}{Signal\ Level\ (A_{mp})} \leq 0.05\ (5\%)$$

The Signal Level A_{mp} is defined as the average metal plate reflection in volts as measured from the peak to the preceding minimum. The Noise Level (A_n) is defined as the average maximum amplitude in volts occurring between 2 and 10 ns after the surface echo. The Noise Level is measured from any positive peak to either the preceding or trailing negative, whichever is greater. The Noise to Signal Ratio shall be less or equal to 0.05 (5 percent).

2. Signal Stability Test: The same test configuration shall be used as described in the Noise to Signal Ratio test. Fifty traces shall be recorded at the minimum data rate of 25 traces/second. The signal stability shall be evaluated using the following equation:

$$\frac{A_{max} - A_{min}}{A_{AVG}} \leq 0.01(1\%)$$

where:

A_{max} is defined as the maximum amplitude for all 50 traces.
A_{min} is defined as the minimum amplitude for all 50 traces.
A_{AVG} is defined as the average trace amplitude of all 50 traces.

The signal stability test results for the GPR shall be less than or equal to 1 percent.

3. Long-Term Signal Stability: The same test configuration shall be used as described in the Noise to Signal Ratio test. The Radar shall be switched on with no warm-up and allowed to operate for two hours continuously. As a minimum, a single waveform shall be captured every two minutes, 60 in total. The amplitude of reflection shall be calculated and plotted against time. For the system to be performing adequately the amplitude should remain constant after a short warm-up period. The stability criteria is as follows:

$$\frac{A_{any} - A_{20}}{A_{20}} \leq 0.03\,(3\%)$$

where:

A_{20} is the amplitude measured at 20 minutes.
A_{any} is the any amplitude measured after 20 minutes.

4. Variations in Time Calibration Factor: The same test configuration shall be used as described in the Noise to Signal Ratio test, 50 traces are collected and the height of the antenna is measured. The test is repeated at two other heights. Typically heights of approximately 15 inches, 20 inches, and 25 inches are used. The time delay from the end reflection at the tip of the antenna to the metal plate reflection is measured for each trace and their mean is time t_i (where the subscript represents height position at i). The difference between t_2 and t_1 represents the time to travel a fixed distance in air. For bistatic antennas the travel distance must be calculated based on the system geometry. The factor C_1 is calculated by dividing the distance by the time difference (inches per nanosecond). The factor C_2 represents the same between heights 2 and 3. The variation in time calibration factor is as shown below:

$$\frac{C_1 - C_2}{\text{Mean of } C_1 \text{ and } C_2} \leq 0.02\,(2\%)$$

The variation in time calibration factor shall be less than or equal 2 pecent.

5. End Reflection Test: The same test configuration and results from the Noise to Signal Ratio test shall be used. The amplitude of the end reflection directly preceding the metal plate reflection shall be measured. The size of the end reflection shall be:

$$\frac{A_E}{A_{mp}} < 0.15\,(15\%)$$

where:

A_E is the mean of the amplitude of end reflection defined as any peak occurring from 1 to 5 nanoseconds before the metal plate reflection.
A_{mp} is the mean of the amplitude of reflection from the metal plate.

The end reflection in the metal plate test shall be less than 15 percent the amplitude of metal plate reflection.

6. Symmetry of Metal Plate Reflection: The same test configuration as used in the Signal to Noise Ratio test shall be used. Two different criteria have been established for symmetry as described below:

6.1 The first criteria is the time from the maximum negative peak following the surface reflection to the zero crossing point shall be measured. The required specification is:

$$t_f \leq 0.7ns$$

6.2 The second criteria is based on the symmetry of the "legs" of the metal plate reflection. The amplitude is measured from the positive peak to both the preceding and trailing negative. The specification is:

$$A_{min}/A_{max} > .95\ (95\%)$$

Where A_{min} and A_{max} are the minimum and maximum metal plate reflections measured using the preceding or trailing negatives. The ratio should be at least 95 percent.

7. Concrete Penetration Test: The antenna shall be placed at its recommended operating height above a 6-inch thick concrete block. The concrete block shall be non-reinforced, minimum age of 28 days, and a minimum 3000 psi compressive strength. The block shall be 3 foot x 3 foot or greater to ensure that all the GPR energy enters the concrete. The concrete block shall be placed on top of a metal plate. Two hundred traces shall be recorded. The reflection amplitude from the top and bottom of the concrete block shall be measured. The concrete penetration test is defined by the following equation:

$$\frac{A_{bottom}}{A_{top}} \geq 0.25\ (25\%)$$

where:

A_{top} is defined as the mean of the measured return amplitude from the top of the concrete slab.
A_{bottom} is defined as the mean of the measured return amplitude from the metal plate.

The concrete penetration test results for the GPR shall be greater than or equal to 25 percent.

APPENDIX F

PAVETRACKER EVALUATION

The Pavetracker capacitance-based density device, shown in Figure F1, was tried as part of this project. As evidenced in the photo, the unit is much smaller than a nuclear gauge. Density readings are provided at the rate of about one per second. Under ideal circumstances the error in the gauge reading would be a mix-specific constant that could be determined in the lab via cores. The offset on the gauge could then be adjusted to calibrate it to the mix. This gauge is lightweight, substantially less expensive than a nuclear gauge (costs about $5,000), very simple to operate, and does not require the administrative hassles of using a nuclear device.

Figure F1. Nuclear Gauge (left) vs. Pavetracker (right).

The Pavetracker worked nicely to rapidly scan the pavement for changes, but the readings from the gauge were found to be very sensitive to surface texture. A small stone about the size of a #4 sieve opening on the pavement surface was found to make the density reading drop by almost 10 lb/cf. This problem could probably be addressed through careful operator training, and in fact the manufacturer recommends sweeping the pavement mat before placing the gauge on it. However, a more substantial problem with the gauge is that the errors in the readings often were significantly related to the lab core density. This is a highly undesirable characteristic as it implies the slope factor of the gauge is not appropriate.

Perhaps the best evaluation method of the Pavetracker is with the data provided by Donald J. Giesel & Associates as part of their promotional literature. The company has distributed a spreadsheet with density readings on 32 locations with both the Pavetracker gauge and a nuclear gauge. Lab densities are also presented for all 32 locations. Essentially the gauges are a predictor of true densities, and the accepted true density is the lab density. Thus, the gauges can be evaluated by assessing how well they predict the lab density. Three standard methods used to assess a prediction are the sum of squared errors (SSE), mean squared error (MSE), and mean absolute percent error (MAPE). The higher these statistics are, the worse of a predictor the gauge is. Table F1 presents these results from Giesel & Associates' data. Their data show the nuclear gauge to be a better performer. In addition to the data in Table F1, the mean absolute error for the gauges was 1.6 lb/cf for the Pavetracker and 1.2 lb/cf for the nuclear gauge.

Table F1. Prediction Statistics for Density Gauges.

Gauge	SSE	MSE	MAPE
Pavetracker	156.5	4.9	1.1
Nuke	99.5	3.1	0.8

In addition to the above three measures of gauge performance, there are two other important criteria a gauge should meet: 1)The mean error from the gauge should be zero, and 2) the error should not be correlated to the true lab density. The data provided by Giesel & Associates show both gauges to meet criteria number one. Likewise, the mean error was zero from the Pavetracker on jobs it was used on during this project. However, one of the data sets collected during this study and the extensive data set from Giesel & Associates show a statistically significant relationship between lab density and the error from the Pavetracker gauge reading. Figure F2 illustrates this problem. At low core densities, the Pavetracker reading was generally too low. At high core densities, the Pavetracker reading was too high. This means the Pavetracker exaggerates the outer extreme density ranges. If a specification such as the density profile was being used, the Pavetracker may often fail sections that really should pass. Figure F2 should be contrasted to Figure F3, which illustrates that the errors from the nuclear gauge appear to be randomly distributed around the perfect fit line. Statistical analysis of the data verifies that, indeed, the errors from the nuclear gauge are not correlated to core density.

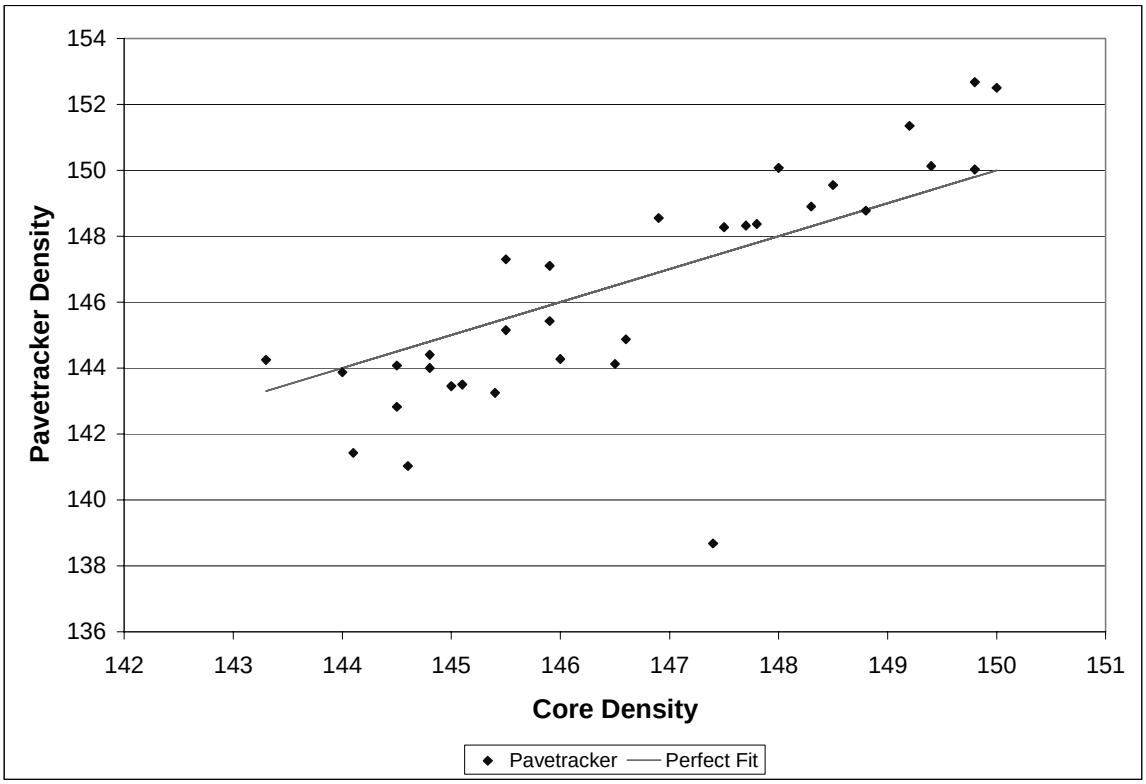

Figure F2. Slope Factor Problems with Pavetracker.

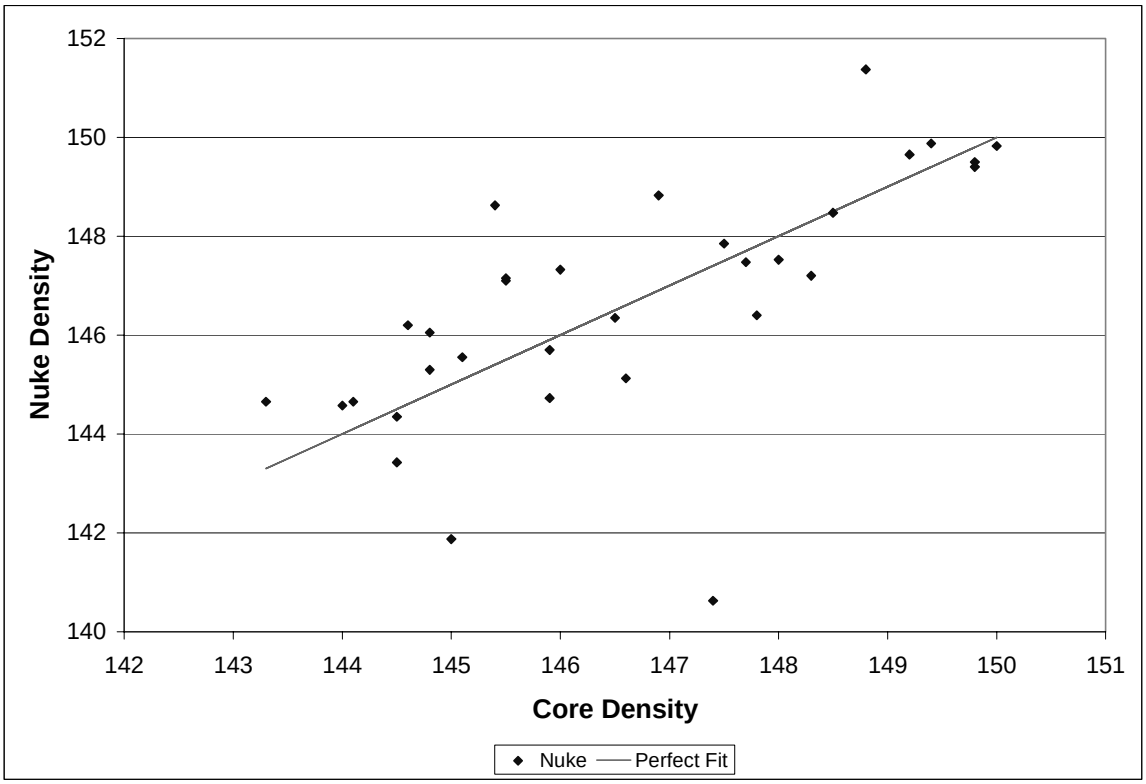

Figure F3. Dispersion of Nuclear Densities around the Perfect Fit Line.

In summary, the Pavetracker in general did work for finding changes in density, but there are some issues that need to be addressed before TxDOT should consider using this unit. From an accuracy standpoint, data indicate the nuclear gauge performs slightly better. The slight decrease in accuracy of the Pavetracker when compared to the nuclear gauge would probably be insignificant in relation to the time and cost savings from such a unit. The real problem with the Pavetracker is the dependency of the errors on the true core density. This is a serious flaw in the unit that results in bias in the readings. At low densities, the unit tends to read too low. At high densities, the unit tends to read too high. The nuclear gauge does not appear to have this problem. As such, TxDOT should continue to investigate non-nuclear density technologies, but should wait for products to develop further before attempting to switch. Transtech Systems has a device called the Pavement Quality Indicator (PQI), which was not evaluated in this project, and Giesel & Associates reportedly is willing to work with TxDOT to tweak the unit for their pavements. A non-contact density device utilizing ground-penetrating radar has also been proposed in this project.